THE UNIVERSITY
of EDINBURGH

Investigating axon-oligodendrocyte interactions during myelinated axon formation in vivo

Sigrid Mensch

PhD

The University of Edinburgh

2014

I have read and understood The University of Edinburgh guidelines on plagiarism and declare that this thesis is the result of my own work except where indicated by references. This thesis has been submitted to The University of Edinburgh for the degree of Doctor of Philosophy only.

Sigrid Mensch

Abstract

Myelin is essential for normal nervous system conduction as well as providing metabolic support for the ensheathed axon and has been implicated to influence axon calibre (diameter of the axon body) growth. In demyelinating diseases, the disruption of these functions causes axon degeneration resulting in neurological impairment. The neurons that are myelinated in the CNS and the axon-oligodendrocyte (axon-OL) interactions that might regulate axon calibre and myelination during myelinated axon formation are still mostly unknown, preventing a deeper understanding of CNS development and repair.

This doctoral thesis identifies a specific subset of interneurons that are myelinated and investigates the axon-oligodendrocyte interactions during axon calibre growth and initial myelination.

In the zebrafish spinal cord, Commisural Primary Ascending interneurons (CoPA), Circumferential Descending interneurons (CiD) and reticulospinal neurons are amongst the first to be myelinated, whereas Commisural Bifurcating Longitudinal interneurons (CoBL) and Circumferential Ascending interneuron (CiA) are not myelinated during early developmental stages. Of the myelinated neurons, axon calibre of reticulo spinal neurons is increased in time with myelin ensheathment, while the axon calibre of CoPA and CiD interneurons is not increased with the onset of myelination. In order to investigate whether there might be a causative relationship between axon calibre increase and myelin ensheathment, the majority of oligodendrocytes were eliminated by olig2 morpholino knockdown. In the absence of oligodendrocytes, the axon calibre of reticulospinal neurons was normal, demonstrating that axon calibre growth is independent of axon-OL interactions and myelin ensheathment. In order to further investigate which aspects of myelinated axon formation might be regulated by axon-OL interactions, axonal activity was reduced through inhibition of synaptic vesicle release by global expression of Tetanus-toxin (TetTx). TetTx treated zebrafish showed a 40% decrease of myelinated axons in the spinal cord. Interestingly, only 10% of this reduction was caused by a decrease in oligodendrocyte number in the spinal cord. Single cell analysis of individual oligodendrocytes revealed a 30% reduction of myelin sheaths

per oligodendrocyte in TetTx treated animals, indicating a positive correlation between synaptic vesicle release and the extent of myelination. Timelapse analysis of the myelinating behaviour of individual oligodendrocytes revealed that the decrease in myelin sheaths per cell in the absence of synaptic vesicle release results from a reduction in the initial formation of sheaths rather than an increased retraction of myelin sheaths. Furthermore, individual myelin sheaths formed by the same oligodendrocyte exhibit a dynamic range of different growth rates in control animals, which was reduced to a more uniform, slow growth of myelin sheaths in the absence of synaptic vesicle release. This suggests that local axon-OL interactions can regulate the dynamic myelin sheath growth through synaptic vesicle release.

The analyses in this doctoral thesis identifies a subset of the neurons that are myelinated during the onset of myelination in the zebrafish spinal cord, demonstrates that axon caliber growth of these neurons is independent of myelin ensheathment and that axon-OL interactions mediated by synaptic vesicle release can regulate the extent of myelination and influence the dynamic myelinating behavior of oligodendrocytes in vivo. These findings begin to elucidate the axon-OL interactions underlying myelinated axon formation during CNS development, from which future studies might derive neuro-regenerative treatments for demyelinating diseases.

Acknowledgements

First and foremost, I would like to thank my PhD supervisor, Dave Lyons, for his guidance and advice, for all the time that he invested in interpreting the data and making sense of it all and most importantly, for being a true “Doktorvater” during my PhD.

I would also like to thank the Lyons group, the members of Lina and the Lyons, for their encouragement and help during the lab work and for cheering me on during the write up. All of this would have been a total eclipse of the heart without you.

Also, I would like to give a special thank you to my family, particularly my parents, who are always with me no matter the geographical distance. To my mother, for reminding me to enjoy the moment, and to my father, for being the voice of reason in my life.

To all my friends, far and near, thank you for being my extended family.

And finally, I would like to thank Juraj, for being the reason I get up in the morning and for his undivided love and support every step of the way.

Table of Contents

1. Introduction

Myelination is essential for neuronal signal conduction as well as providing metabolic support for the ensheathed axon and a disruption of these functions causes axon degeneration in demyelinating diseases. Precise axon-oligodendrocyte interactions are required to ensure the accurate formation of myelinated axons in the central nervous system, e.g. the axon-oligodendrocyte interactions that may regulate axon calibre (the cross-sectional diameter of the axon body) and the precise correlation of the longitudinal length and thickness of myelin sheaths with the axon calibre. These axon-oligodendrocyte interactions, however, are not fully understood and the selection process determining which axons are myelinated and which are not remains unclear. A better understanding of axon-oligodendrocyte interactions during normal CNS development will improve future myelin repair strategies in demyelinating diseases. Using high resolution imaging, I aimed to investigate the properties of myelinated axons in comparison to unmyelinated axons, whether axon-oligodendrocyte interactions during myelin ensheathment can regulate the calibre of the myelinated axons and whether axon-oligodendrocyte interactions, mediated through synaptic vesicle release, can regulate myelin ensheathment of myelinated axons. In this doctoral thesis, 1) I identified 3 spinal cord neurons that are fated for myelination, reticulospinal neurons (RS), commisural primary ascending interneurons (CoPA) and circumferential descending interneurons (CiD, and 3 spinal cord neuron that are not myelinated during the early development of zebrafish larvae, Rohon-Beard sensory neurons (RB), commisural bifurcating longitudinal interneurons (CoBL) and circumferential ascending interneurons (CiA). 2) I characterized the axon calibre of these identified axons under normal conditions and found that while the axon calibre of RS neurons increases concomitant with the onset of myelination, the axon calibre of CoPA and CiD neurons does not increase with the onset of myelination. In order to investigate whether axon calibre increases with oligodendrocyte contact or myelin ensheathment, I measured the axon calibre of the 20 largest calibre axons in the absence of all oligodendrocyte lineage cells and found that axon calibre is regulated independently of oligodendrocyte contact and myelin ensheathment. 3) I investigated the influence of axon calibre and axonal synaptic vesicle release during myelinated axon formation and found that both axon properties

can regulate axonal selection during myelination. 4) I characterized the influence of axonal activity on the behaviour of myelinating oligodendrocytes and found that synaptic vesicle release can regulate the myelinating capacity of oligodendrocytes by regulating the number of myelin sheaths formed per oligodendrocyte. 5) I found that local synaptic vesicle release can influence the dynamic growth rate of individual myelin sheaths.

In the introduction, I will discuss the myelin sheath formation, the importance of myelin for functional nervous system signal conduction and the known axon-oligodendrocyte interactions underlying the axonal selection process during myelination.

1.1 Myelin

Myelin evolved approximately 400 million years ago and is the evolutionary latest addition to the nervous system. Myelin is found in all vertebrate classes with the exception of the evolutionary oldest, such as the jawless fish, although axons in these organisms are surrounded by glial cells and glial ensheathment of axons resembling myelin sheaths has even been found in invertebrates (Baumann and Pham-Dinh; as reviewed in Waehneldt, 1990; Yoshida and Colman, 1996). Myelin research dates back to the early 19^{th} century when it was first described (Virchow, 1854). Myelination is a process that continues from midgestation in humans (Inder and Huppi, 2000), early postnatal life in mammals (Yakovlev and Lecours, 1966; Baumann and Pham-Dinh, 2001) and 3dpf in zebrafish (Almeida et al., 2011) into adult life (Miller et al., 2012). This includes de novo myelination of previously unmyelinated areas in the CNS as well as the remodelling of myelin sheaths on already myelinated axons (Young et al., 2013). Myelin is formed by oligodendrocytes in the central nervous system (CNS) (Rio Hortega, 1921) and by Schwann cells in the peripheral nervous system (PNS) and constitutes of a plasma membrane extension that ensheathes the axon of specific neurons with multiple membrane layers in a spiral fashion (Geren and Schmitt, 1954; Sobottka et al., 2011; Snaidero et al., 2014).

In the PNS, every myelinating Schwann cells only forms one myelin sheath around an axon on a one-to-one ratio and is therefore closely associated with the axon it

myelinates. In the CNS, however, oligodendrocytes can form multiple myelin sheaths around different axons and adjacent myelin sheaths along one axon can be formed by different oligodendrocytes (Rio Hortega, 1928; Bunge et al., 1962; Bunge, 1968). The number of myelin sheaths formed per oligodendrocyte can vary dramatically from cell to cell and according to the area of the CNS and the species studied (Baumann and Pham-Dinh, 2001), e.g. the number of myelin sheaths per oligodendrocytes can range from 80 myelin sheaths per cell in the corpus callosum (Matthews and Duncan, 1971; Snaidero and Simons, 2014), to 40 in the optic nerve of the rat (Peters et al., 1991), to 1 in the spinal cord of the cat (Bunge et al., 1961). The oligodendrocytes with a large number of myelin sheaths in the corpus callosum and cortex have been shown to form sheaths ranging from 20 to 200µm in length around relatively small calibre axons (Matthews and Duncan, 1971; Chong et al., 2012; Snaidero and Simons, 2014), while the oligodendrocytes in the spinal cord with only one sheath per cell have been shown to myelinate relatively thick axons with an internode length of approximately 1500µm (Remahl and Hildebrand, 1990). These observations indicate 1) that there is a linear relationship between axon diameter, myelin thickness and myelin sheath length and 2) that there are intrinsically different subsets of oligodendrocytes, each subset with a predetermined number of myelin sheaths formed per oligodendrocytes. The increase of axon diameter from 1 to 15µm has been shown to increase the myelin sheath length from 100 to 1500µm (Hildebrand and Hahn, 1978; Hildebrand, 1993; Murray and Blakemore, 1980) and myelin thickness has been shown to increase with a rise in axon calibre (Hildebrand and Hahn, 1978), indicating that axonal properties indeed regulate the extent of myelination. A recent in vivo study showed that the number of myelin sheath generated per oligodendrocyte is not predetermined by intrinsic factors as has been suggested (Baumann and Pham-Dinh, 2001), but is plastic and can be increased by experimental introduction of supernumerary large calibre axons into the spinal cord of zebrafish (Almeida et al., 2011). It is unclear, however, what axon properties can influence the myelination of individual oligodendrocytes and how this might occur on a cellular level. Below, I will give a brief overview of oligodendrocyte development, myelin sheath formation and of the mechanisms that might regulate axon selection during myelination.

1.1.1 Oligodendrocyte development

Before cells of the oligodendrocyte lineage mature into myelinating oligodendrocytes, they undergo multiple stages of development, including the oligodendrocyte precursor cell (OPC) specification from neural progenitor cells, OPC differentiation into immature, non-myelinating oligodendrocytes and the maturation into myelinating oligodendrocytes (Pfeiffer et al., 1993; as reviewed in Boulanger and Messier, 2014). OPCs originate from multi-potent neural stem cells in the ventricular neuroepithelium in the neural tube during embryogenesis (Pfeiffer et al., 1993; Levine et al., 1993; Hardy and Reynolds 1993; Warf et al., 1991) and in the subventricular zone of the forebrain during adult life (Lim and Alvarez-Buylla, 1999; Menn et al., 2006; Richardson et al., 2006). The neural progenitor cells in the ventricular neuroepithelium give rise to neurons, astrocytes and oligodendrocytes, of which oligodendrocytes are the last to be specified in their cell fate, largely at postnatal stages in rodents (Altman and Bayer, 1997; as reviewed in Thomas et al., 2000 and Miller, 2002) and at approximately 36 hours post fertilisation (hpf) in zebrafish (Kirby et al., 2006). Multiple factors interact to form the anterior-posterior and dorsal-ventral axis of the neural tube. Amongst other factors, sonic hedgehog (Shh) is a key factor patterning the ventral axis, while bone morphogenic protein (BMP) as well as Wnt are key factors patterning the dorsal axis (as reviewed in Lumsden and Krumlauf, 1996; Puelles and Rubenstein, 2003; Jessel, 2000). The neural tube is patterned by concentration gradients of different signalling molecules that define domains within the neural tube, such as the motor neuron progenitor domain (pMN) and the p0-p2 domains in the ventral neural tube, each of which give rise to distinct cell types (Briscoe et al., 2000; reviewed in Jessel, 2000 and Rowitch, 2004). The pMN domain that gives rise to motor neurons and OPCs, for example, is precisely demarcated by the expression of the transcription factors Olig1 and Olig2 (Lu et al., 2000; Zhou et al., 2000), whereas the p0-p3 domain, that do not express Olig1 or Olig2, give rise to the ventral interneurons (Marti et al., 1995; Poncet et al., 1996; Pringle et al., 1996; Orentas et al., 1999; Briscoe et al., 2000; reviewed in Jessel, 2000, Miller, 2002 and Rowitch, 2004). The different extrinsic and intrinsic factors that regulate oligodendrocyte lineage progression in mammals are extensively summarized in Miller, 2002; Rowitch, 2004; Baumann and Pham-Dinh, 2001 and He

and Lu, 2013. Four of the main transcription factors necessary for oligodendrocyte development in mammals and zebrafish are Olig2, Olig1, Sox10 and Myrf. The basic helix-loop-helix transcription factors Olig1 and Olig2 are expressed in oligodendrocytes lineage cells from early OPC stages through migration, differentiation to myelinating oligodendrocyte stages (Park et al., 2002; Zhou et al., 2001; Zhou and Anderson, 2002). While Olig2 is essential for the earliest stages of motor-neuron and OPC formation, other transcription factors, such as Olig1 (Xin et al., 2005), Nkx2.2 (Qi et al., 2001) and Sox10 (Takada et al.; 2010; Stolt et al., 2002) are, amongst others, subsequently required for OPC differentiation to myelinating oligodendrocytes in mammals (Lu et al., 2000; Zhou et al., 2000; Ligon et al., 2006) and in zebrafish (Park et al., 2002; Lewis et al., 2005; Schebesta and Serluca, 2009; Zhou and Anderson, 2002). The down-regulation of transcription factors important for motor neuron development, such as Pax6, towards the end of motor-neuron generation allows the distribution pattern of the more ventrally located transcription factor, Nkx2.2, to change and overlap with the Olig2 domain (Zhou et al., 2001). Cells expressing both transcription factors subsequently develop into oligodendrocytes so that a subset of spinal cord oligodendrocytes that expresses Nkx2.2, while all oligodendrocytes express Olig2, Olig1 and Sox10.

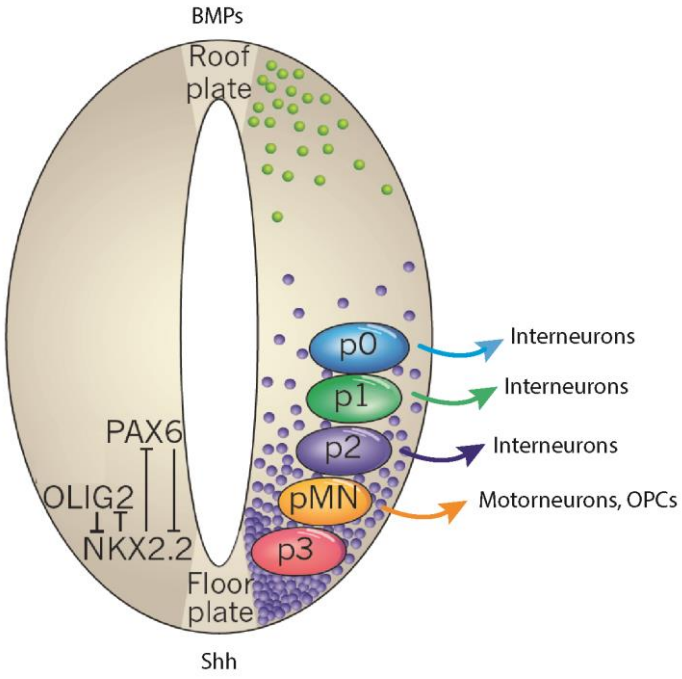

Figure 1.1: Patterning of the neural tube creates unique domains for neuronal and glial progenitors. A schematic cross-sectional view of the neural tube. The morphogens BMP and Shh determine the dorsal to ventral gradient of the neural tube. The interactions of the different transcription factors, such as Olig2, Nkx2.2 and Pax6 shape the regionally restricted p0, p1, p2, pMN, p3 domains. The p0-p2 domains will give rise to interneurons, while the pMN domain will give rise to motorneurons and OPCs. Image adapted from Rowitch and Kriegstein, 2010.

Olig1 and Sox10 act synergistically together to activate the myelin basic protein (mbp) promoter in both, mammals and zebrafish (Li et al., 2007; Stolt et al., 2002), suggesting their importance for oligodendrocyte maturation. Furthermore, oligodendrocytes lacking Sox10 in zebrafish mutants have been shown to undergo apoptosis after axon-oligodendrocyte contact, indicating a role of sox10 or its downstream targets in axon-oligodendrocyte interactions that regulate cell maintenance and survival (Takada et al., 2010). In mammals, Olig2 also binds to Sox10 to activate the mbp promoter, however, this is not the case in zebrafish (Li et al., 2007). The evolutionary bases for this difference is not yet clear, however, many of the known factors regulating oligodendrocyte lineage progression are conserved between zebrafish and mammals (Czopka and Lyons, 2011). The transcription factor most specific to oligodendrocytes that has been described so far is Myelin Regulatory Factor (Myrf), which is only expressed in oligodendrocytes and absent in other cells of the CNS (Cahoy et al., 2008; Emery et al., 2009). Myrf is a membrane-associated transcription factor that undergoes autoproteolytic cleavage that frees the transcription factor from the endoplasmatic reticulum membrane to directly bind to myelin protein genes, such as MAG, PLP and MBP, in the cell nucleus and stimulate their expression (Bujalka et al., 2013). Unlike other transcription factors that are required for oligodendrocyte development, Myrf is only expressed at the post-mitotic stage, indicating that it is required for the final stage of oligodendrocyte differentiation and myelination (Bujalka et al., 2013).

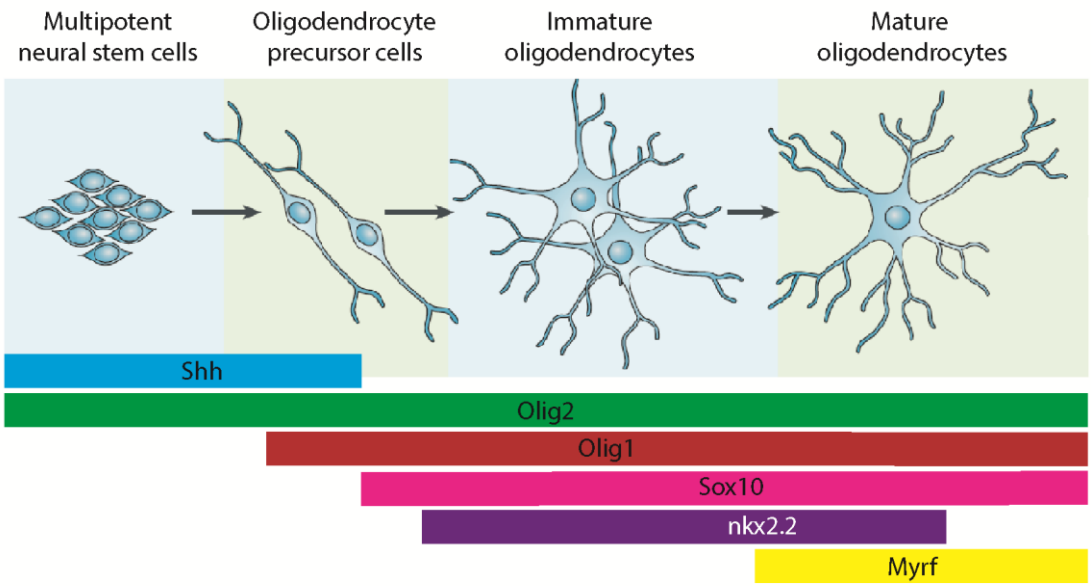

Figure 1.2: Schematic overview of the morphogens and different transcription factors required during oligodendrocyte lineage development. Multipotent neural stem cells give rise to oligodendrocyte precursor cells, which differentiate first into immature, non-myelinating oligodendrocytes and finally into myelinating oligodendrocytes. The Shh morphogen as well as the transcription factors Olig2, Olig2, Sox10, nkx2.2 and Myrf are required for oligodendrocyte lineage development. Image adapted from Rowitch, 2004.

After their cell fate is specified, OPCs proliferate and migrate to form an evenly dispersed population throughout the gray and white matter in the CNS (as reviewed in Miller, 2002; Rowitch, 2004). During their maturation process, OPCs cease to proliferate and differentiate to pre-myelinating oligodendrocytes near the end of embryogenesis and during early postnatal life in mammals (Zhu et al., 2008) and from approximately 48hpf in zebrafish (Kirby et al., 2006; Kucenas et al., 2008). However, a large number of OPCs remain in an undifferentiated state (Dawson et al., 2003a) and continue to proliferate throughout life (Wolswijk and Noble, 1989; Nishiyama et al., 2002), although their proliferation rate declines with age (Levine et al., 1993; Woodruff et al., 2004; Young et al., 2013). OPCs are evenly distributed throughout the CNS and extend their motile filopodia processes that explore their surrounding environment. Upon contact with neighbouring OPC processes, they retract through repulsive cell-cell interactions and, in case of OPC death, proliferate and migrate to repopulate the vacant area during embryonic development (Kirby et

al., 2006) and adulthood (Hughes et al., 2013). Myelinating oligodendrocytes continue to emerge from this OPC population during development and throughout adulthood (Richardson et al., 1988; Rivers et al., 2008; Zhu et al., 2008; Trotter et al., 2010; Young et al., 2013).

1.1.2 Myelin function

The correct formation of a myelinated axon is essential for normal nervous system function and fast signal conduction in the CNS and PNS. The evolution of a complex vertebrate nervous system occurred in time with, and is probably based on, the acquisition of the myelinated axon (Zalc and Colman, 2000; Sherman and Brophy, 2005). In unmyelinated axons, the axon membrane contains diffusely distributed voltage-gated Na^+ as well as K^+ channels, causing an electrical impulse, the action potential, to propagate in a slow, continuous manner along the axon (as reviewed in Catterall, 1984; Ritchie, 1984; Koester, 1985 a and b). The axolemma of myelinated axons, however, is dramatically different with voltage-gated Na^+ channels concentrated in the nodes of Ranvier and the distribution of K^+ channels in the juxta-paranode, the axon area adjacent to the node (Kocsis and Waxman, 1980; as reviewed in Poliak and Peles, 2003; Salzer, 2003). Nodes of Ranvier are short non-myelinated areas of approximately 1µm and are positioned between myelin sheaths along one axon (Ranvier, 1878; Hildebrand et al., 1993; Davis et al., 1996; Kaplan et al., 1997; as reviewed in Salzer, 1997). With the Na^+ channels clustered at the node of Ranvier between two myelin sheaths, the area of depolarization is restricted to the nodes and action potentials can jump from node to node, while the myelin sheaths function as electrical insulator. This form of neuronal signal conduction is called saltatory conduction (Latin. saltare – to jump) and allows much faster impulse propagation compared to an unmyelinated axon of the same calibre (Tasaki, 1982). Thus, myelination and node formation are important developmental steps enabling the axon to conduct impulses at high speed (Rushton, 1951; Waxman and Bennet, 1972; Waxman, 1997). The signal conduction velocity of an axon increases with the diameter of the fibre. The doubling of the diameter of a myelinated axon gives a doubling of the conduction velocity, while the diameter of an unmyelinated axon would have to be four times larger for a doubling of conduction velocity (Hursh,

1939; Rushton, 1951; Waxman and Bennett, 1972). In case of demyelination, distinctive clustering of the voltage-gated ion channels at the node of Ranvier is lost, which leads to a decrease in nerve conduction and neurological impairment (Lassmann et al. 1997; Griffiths et al., 1998; Lappe-Siefke et al., 2003).

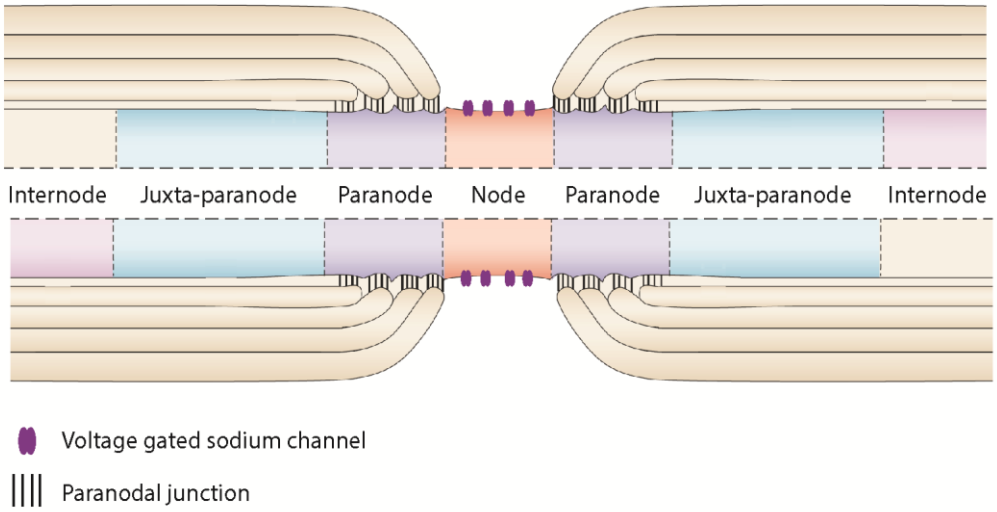

Figure 1.3: Structure of a myelinated axon. Schematic longitudinal view of a myelinated axon, showing the node of Ranvier flanked by the paranode, the juxta-paranode, and the beginning of the internodes. The internode lies under the compact myelin, whereas the myelin sheath is connected to the axon by the paranodal junctions. The node of Ranvier is the myelin-free area between internodes, where the voltage gated sodium channels are clustered and the action potential is generated. Image adapted from Poliak and Peles, 2003.

Besides playing an important role in rapid conduction and providing structural support, myelin sheaths generated by oligodendrocytes are also important for metabolic and trophic support for the axon. Myelinating glia have been shown to produce trophic factors that promote neuronal survival, such as the brain-derived neurotrophic factor (BDNF), the glial cell-derived neurotrophic factor (GDNF) as well as the insulin-like growth factor (IGF), and neuronal cultures showed increased survival if treated with these trophic factors or co-cultured with oligodendrocytes (Dougherty et al., 2000; Wilkins et al., 2001; Wilkins et al., 2003). Furthermore, oligodendrocytes have recently been shown to not only offer trophic support, but also metabolic support (Lee et al., 2012; Fuenfschilling et al., 2012). This metabolic support is proposed to be secreted through cytoplasmic channels within the myelin sheath that are established in close proximity to the axon. One of the main sources

that have been proposed to provide metabolic support for axons is the lactate transporter. The monocarboxylate transporter 1 (MCT1) is highly expressed in oligodendrocytes and can supply the myelinated axon with nutritional support in form of lactate (Lee et al., 2012; Fuenfschilling et al., 2012). A disruption of this mechanism in mutant mice, in which MCT1 is down-regulated in oligodendrocytes, is associated with neurodegeneration (Lee et al., 2012). And, as recently has been shown, metabolic support can also be provided by myelinating oligodendrocytes through the exo-and endocytosis of cargo-containing vesicles (Frühbeis et al., 2013).

However, not all axons in the CNS are myelinated and the percentage of myelinated axons varies in the different CNS areas. For example, more than 70% of the axons in the corpus callosum are unmyelinated (Sturrock, 1980; Young et al., 2013), while almost all axons in the optic nerve are myelinated (Bartsch et al., 1997; Dangata and Kaufman, 1997; Young et al., 2013). Signal propagation requires energy as active transporter, such as Na^+/K^+ ATPases and Na^+/Ca^{2+} exchangers restore the resting potential after action potential generation at the neuron's energy expenditure (Hildebrand et al., 1993; Waxmann, 1997; Howarth et al., 2012). The action potential propagation through saltatory conduction is a much more energy efficient process since axon depolarization and the active transporter restoring the resting potential are restricted to the axon site adjacent to the node (Ritchie, 1982; Hildebrand et al., 1993; Waxmann, 1997). It is therefore possible that axons that are more active than others, e.g. axons that fire action potentials at a higher frequency, require more energy and are therefore myelinated to receive the metabolic support from the oligodendrocyte as well as the more energy efficient mode of signal conduction. The selection process by which an axon is selected for myelination, however, is unknown and it is unclear whether axons that are more active than others are preferentially myelinated.

Another function for myelin has also been proposed recently. Studies reporting an increase in the extent of myelinated axons after social experience in rodents during development (Makinodan et al., 2012) and in adult life (Liu et al., 2012), suggest that myelination is dynamically regulated throughout life and has been proposed to represemt a form of nervous system plasticity, adapting brain functions to environmental stimuli (Fields, 2005). The functional activity of a neuron has long

since been implicated in regulating myelinated axon formation (as reviewed in Zalc and Fields, 2000), and I will investigate the role that axonal function plays during myelin ensheathment in vivo in chapter 4.

1.1.3 Myelin sheath formation

Both, de novo myelination as well as myelin remodelling is generated by newly differentiated oligodendrocytes that continuously emerge from the OPC population (Richardson et al., 1988; Rivers et al., 2008; Zhu et al., 2008; Trotter et al., 2010) as oligodendrocytes initiate the formation of their myelin sheaths within a short time period of only a few hours after they mature into myelinating oligodendrocytes (Czopka et al., 2013).

Pre-myelinating oligodendrocytes extend and retract exploratory processes into their environment in search for axons to myelinate (Hughes et al., 2013).It is unclear, however, whether this mechanism is based on axon-oligodendrocyte interactions or whether the oligodendrocyte processes search their surroundings stochastically. It has been shown that oligodendrocytes continue to emit their processes in the absence of axons in vitro (Kacher et al., 1986) and oligodendrocyte processes sometimes associate with dendrites and neuronal cell bodies (Remahl and Hildebrand, 1985), suggesting a stochastic process behind the oligodendrocyte process extensions. However, oligodendrocyte processes recognize and ensheath only a subset of all the axons in the CNS, while dendrites and neuronal cell bodies as well as other axons remain unmyelinated, indicating that axonal properties are important for the axon-oligodendrocyte interactions underlying myelin sheath formation (Lander, 1989). Furthermore, a study observing live oligodendrocyte behaviour during early zebrafish development indicated that approximately 75% of all nascent myelin ensheathment formed by a single oligodendrocyte are stable, while only 25% are retracted within 2days after sheath formation at a developmental stage, when almost all axons are still unmyelinated (Czopka et al., 2013). This data suggests that oligodendrocytes are relatively accurate during myelin ensheathment rather than selecting the axons stochastically.

In the PNS, myelin ensheathment is generally accepted to occur through the so called "jelly roll" or "carpet crawler" model, whereby during the first ensheathment, the glial membrane extends along the length of the axon to the full longitudinal length of the myelin sheath before it wraps around the axon. Multiple layers of myelin membrane are then created by the continuous movement of the inner myelin layer underneath the previously generated membrane layers (Bunge et al., 1961). In the CNS, however, the number of myelin layers can vary along the length of one myelin sheath, indicating that the myelin ensheathment itself is generated differently in the PNS and CNS, and different models of myelin biogenesis by oligodendrocytes have been proposed (as reviewed in Snaidero and Simons, 2014). In the CNS, helical coiling structures along the myelin sheaths have been observed by light microscopy (Pedraza et al., 2009; Sobottka et al., 2011). These observations lead to two different models, the "liquid croissant" model, in which new layers of myelin membrane are added on top of the inner ones, creating a croissant like structure (Sobottka et al., 2011), and the "serpent" model, in which the multiple myelin layers begin as a single spiral encircling the axon, which then grow laterally, gliding on top of each other, thereby creating the multilayer myelin sheath (Pedraza et al., 2009). A recent study, however, was able to follow the myelin sheath ensheathment by oligodendrocytes at high resolution, which revealed that the sheaths grow by wrapping of the inner myelin layer around the axon underneath the previously deposited membrane layers, similar to the PNS. However, unlike the PNS, the initial first myelin layer does not reach its full longitudinal length before it wraps around the axon. Once oligodendrocytes have determined and established contact with the target axon, the myelin process flattens, and begins to ensheath the axon by wrapping around it, whereby the inner layer has the shortest longitudinal width and continues to wrap around the axon underneath the outer layers, which grow in longitudinal length (Snaidero et al., 2014). Each layer of myelin retains cytoplasmic-rich membrane pockets at its lateral edges, which stay in contact with the axon even during longitudinal growth, and account for the helical coiling pattern observed by light microscopy (Pedraza et al., 2009; Sobottka et al., 2011).

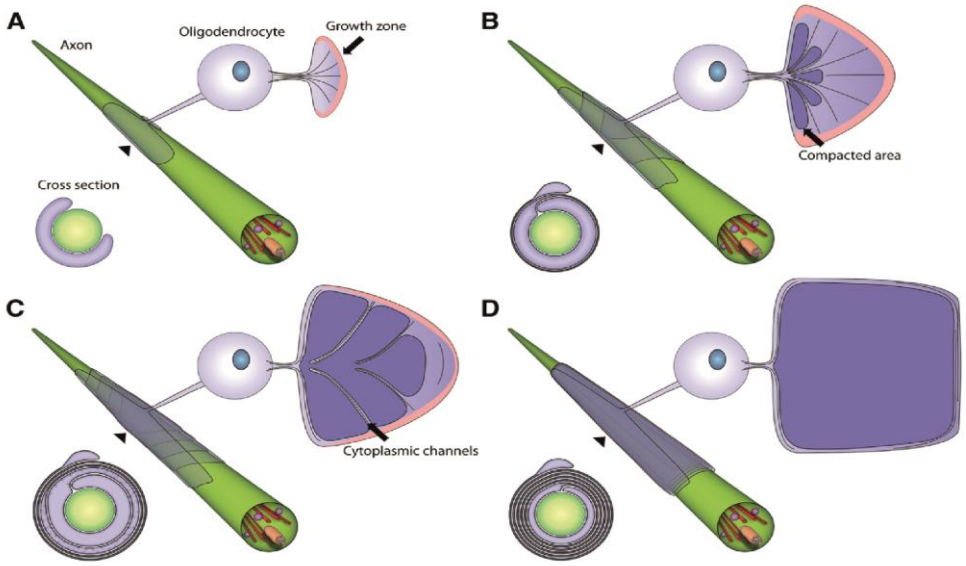

Figure 1.4: Model of myelin ensheathment in the CNS as illustrated by high-resolution imaging by Snaidero et al. (2013). A-D) Schematic model of myelin ensheathment in wrapped (left), unwrapped (right) and cross-sectional view (bottom, left). The unwrapped view shows the localization of cytoplasmic channels, which connect the cell body and the growth zone at the inner tongue. The growth zone is colour coded in pink, while compact myelin is coded in dark purple. The wrapped view shows the position of the membrane layers around the axon, while the cross-sections represent the state of compaction during myelin sheath growth. Image taken from Snaidero et al., 2013.

Myelinated axons are structured into functionally different domains, the node of Ranvier, the paranodal junction, the juxta-paranodes and the internodal region (Arroyo and Scherer, 2000; Peles and Salzer, 2000). During longitudinal growth of the membrane layers, the cytoplasm filled membrane pockets at the lateral edges of the myelin layers move towards the outer edges of the myelin sheath, where they align and form the paranodal loops (Sakurai et al., 1997; Snaidero et al., 2014). The paranodal loops remain uncompacted even after myelin sheath formation and establish axon-oligodendrocyte contact through septate-like axon-glial junctions. This junction is comprised of a cell adhesion complex between the 155kDa isoform of neurofascin (NF155) on the glial paranodal membrane loops and contactin-1 (CNTN1) as well as the contactin-associated protein (CNTNAP1) on the axon (Pedraza et al., 2009; Zonta et al., 2008; Snaidero and Simons, 2014). Voltage-gated Na^+ channels are clustered next to the paranodal loops at the lateral edges of the

membrane layer that ensheathes the axon. During longitudinal growth of the membrane layers, the Na^+ channel cluster is moved along the axon until the Na^+ clusters between two myelin sheaths fuse and form the node of Ranvier in both, the CNS (Boiko et al., 2001; Rasband et al., 1999) and the PNS (Vabnick et al., 1996; Ching et al., 1999; Zhang et al., 2012). These observations suggest that the node of Ranvier are formed by axon-glial contact through the paranodal cell adhesion complex, the subcellular mechanisms regulating node formation are, however, still unclear (Sherman and Brophy, 2005). Interestingly, mice that lack NF155, CNTN1 or CNTNAP1, the axon-glial cell adhesion complex proteins, not only show defects in node of Ranvier formation, but also in the longitudinal growth of the myelin sheaths, indicating that the axon-glial adhesion complex might also play a role in the longitudinal growth of the myelin sheath (Zonta et al., 2008; Susuki et al., 2013; Snaidero and Simons, 2014). Apart from mediating the axon-glial interaction that attaches the myelin sheath to the axon and might be involved in the longitudinal myelin sheath growth, the paranode is also thought to separate the electrical activity of the node of Ranvier from the internodal region under the compact myelin sheath and to prevent axolemma proteins from lateral diffusion (Dupree et al., 1999). The juxtaparanode is positioned in a short zone just beyond the innermost membrane loop of the paranodal junction and contains a high proportion of K^+ channels, which are highly concentrated towards the paranode and more diffusely distributed towards the internode (Dupree et al., 1999). These K^+ channels are thought to prevent re-entrant excitation during saltatory conduction and to maintain the resting potential in the internode. The internode extends from the juxtaparanode and lies underneath the compact myelin, which comprises the main body of the myelin sheath. The molecular components of the node of Ranvier, the paranode, the juxtaparanode and the internode and their assembly are extensively reviewed in Poliak and Peles, 2003 and Salzer, 2003.

As an extension of the glial cell membrane, myelin contains a high proportion of lipids, which constitutes approximately 70-75% of the myelin membrane composition, depending on region and species investigated (Jahn et al., 2009). The other 30-45% of the myelin membrane is comprised of different proteins that are either embedded in the lipid bilayer or attached to its surface (Jahn et al., 2009), such

as myelin basic protein (MBP) and proteolipid protein (PLP), myelin associated glycoprotein (MAG), myelin/oligodendrocyte protein (MOG), myelin protein zero (P0), and the peripheral nerve myelin protein 22 (PMP22) (Kirschner and Blaurock, 1992; as reviewed in Quarles et al., 2007). There are, however, some differences in the protein composition in mammals and zebrafish. P0 is expressed in myelinating oligodendrocytes and Schwann cells in zebrafish (Brosamle and Halpern, 2002) but is only expressed in myelinating Schwann cells in mammals (Sakamoto et al., 1987).
In order to generate the myelin sheath, oligodendrocytes are required to produce vast amounts of myelin proteins. In the case of myelin basic protein (mbp), the mRNA is translated distant from the cell body in the cell processes and close to the growing myelin sheath (Colman et al., 1982). As multiple overlying layers of myelin membrane are formed, myelin proteins between adjacent layers interact, which results in the compaction of the myelin layers in the myelin sheaths. Myelin compaction is mediated by the coordinated expression of myelin specific proteins. Myelin proteins that are essential for myelin compaction in the CNS and PNS include MBP, the proteolipid (PLP) and MPZ or P0 (as reviewed in Baumann and Pham-Dinh, 2001; Hartline and Colman, 2007). MBP is a small protein localized at the cytoplasmic side of the myelin membrane and is proposed to bring the membrane layers into tight apposition through cationic interaction with negatively charged membrane lipids and polyanionic membrane proteins (Boggs, 2006). Shiverer mutant mice, almost completely lack compact myelin in the CNS due to an autosomal recessive mutation in the mbp gene (Popko et al.,1987; Readhead et al., 1987) and conversely, disrupted mbp mRNA localisation can lead to ectopic appearance of myelin-like membranes along parts of the oligodendrocyte that is not ensheathing axons (Lyons et al., 2009). These observations illustrate the importance of the myelin protein and their precise localization during myelin sheath formation.

1.2 Axonal selection during myelination

Myelination is extremely complex and occurs in different parts of the CNS at different times during development. Even in one area of the CNS, oligodendrocytes are presented with a large range of axons of different calibre sizes (the cross-sectional size of the axon), neurotransmitter subtypes and functional as well as

developmental states. The selection process by which an axon is selected for myelination and the axonal properties that determine whether an axon will be myelinated or not, are unknown. Axonal properties that could determine whether axons are selected for myelination might be the expression of inductive signalling molecules, their neurotransmitter type, functional activity (e.g. action potential firing rate), axon calibre size or a combination of all. I will briefly introduce the relevance of these axonal properties in axon selection during myelination below.

1.2.1 Axonal size as a mechanism behind axonal selection

In the PNS, axons above a threshold diameter of 1µm are myelinated, while axons below this threshold are not (Duncan, 1934). Experimental increase of axon diameter in the PNS can even induce myelination of axons that were previously unmyelinated (Voyvodic, 1989), indicating that the physical size of the axon might indeed determine whether an axon is myelinated. In the CNS, however, there is no strict threshold above which an axon is always myelinated. Although there appears to be a minimum axon diameter, below which axons are not myelinated, as the smallest reported myelinated axon in the CNS has a diameter of approximately 0.2-0.3µm (Remahl and Hildebrand, 1982). The largest axons are almost always myelinated (Hildebrand et al., 1993) but there is a middle range of axon diameter between 0.2 and 0.8µm, in which myelinated as well as unmyelinated axons can be found (Matthews and Duncan, 1971; Waxman and Bennett, 1972; Remahl and Hildebrand, 1982). Based on these observations, the physical size of an axon alone may be a factor in the axonal selection process during myelination but may not the only criterion by which CNS axons are selected for myelination.

Oligodendrocytes have been shown to myelinate in the absence of axonal signals and form compact myelin sheaths around paraformaldehyde treated axons (Rosenberg et al., 2008) and even form myelin like structures around inert polystyrene fibres (Lee et al., 2012). Interestingly, the inert polystyrene fibres were only myelinated when their diameter was above 0.4µm, while smaller fibres remained unmyelinated. Thus, axonal properties such as physical axon size appear to be inductive for myelination. However, as there is no clear cut-off in axon calibre size above which an axon is myelinated and there are myelinated as well as unmyelinated axons in the diameter

range of 0.2 to 0.8µm, inductive and / or repulsive axonal signals must influence the axonal selection process during myelination, perhaps in addition to axonal calibre. It has been observed that the largest axons in the nervous system are also the first to be myelinated, e.g. in the mouse spinal cord, the thickest fibres are myelinated at P1, while the smallest axons are myelinated after P20 (Hildebrand et al., 1993) and in the zebrafish spinal cord, the Mauthner axon, which is a multi-fold larger in calibre than the other spinal cord axons, is also the first to be myelinated (Almeida et al., 2011). These observations suggest that axon calibre might be one of the axon properties influencing myelination. Furthermore, the addition of supernumery large calibre axon in the zebrafish spinal cord resulted in an increase in the generation of myelin sheaths per oligodendrocyte in the zebrafish spinal cord (Almeida et al., 2011). This finding suggests that axon calibre is capable of regulating the myelinating capacity of individual oligodendrocytes. However, it is unclear, whether the physical property of large calibre axons increased the myelinating behaviour of the oligodendrocytes or whether this was due to an increase in axonal signal expression by the additional axons that are fated for myelination.

Another indication that axon calibre may be a factor influencing myelination stems from a loss of function study in which mice without functional non-receptor tyrosine Fyn kinase in oligodendrocytes show hypomyelination in small calibre axons, while the larger calibre axons remain myelinated (Umemori et al., 1994). This would suggest that the myelination of small and large calibre axons might be regulated by different, perhaps to some extent overlapping, mechanisms. The physical size of larger calibre axons may facilitate myelin ensheathment better as the ensheathment of small calibre axons may require more cytoskeletal flexibility to wrap around the axon. Myelination of smaller calibre axons might therefore require more inductive axonal signals, activating downstream signalling pathways, than the myelination of larger calibre axons.

Overall, it seems that there are fundamental differences in the myelination of CNS and PNS axons and that different criteria underlie axonal selection. Axon calibre might be one of the axonal properties determining which axons are myelinated and which axons are not.

On the other hand, it is possible that the appearance of the largest calibre axons as the myelinated axons (Matthews and Duncan, 1971; Waxman and Bennett, 1972; Remahl and Hildebrand, 1982) is because myelin ensheathment itself acutally promoted axon calibre growth. In this case, axon calibre would be regulated by myelin ensheathment or extrinsic signals from oligodendrocytes. In the PNS, hypomyelination caused by disrupted expression of important myelin proteins such as peripheral myelin protein-22 (PMP-22), an important myelin protein expressed in Schwann cells and found in PNS myelin in so called *Trembler* mice (Suter et al., 1992), or myelin-associated glycoprotein (MAG) (Yin et al., 1998), have been shown to lead to a decrease in axonal neurofilament phosphorylation (de Waegh et al., 1992) associated with a decrease in axon diameter (Pollard and McLeod, 1980; Perkins et al., 1981; Yin et al., 1998). Furthermore, mutant mice lacking mTor, a core kinase important for cell growth and differentiation in mammalian cells, in Schwann cells show normal axonal growth in quadriceps nerves prior to myelination but showed a retarded axonal calibre growth post myelination (Sherman et al., 2012). The lack of axonal calibre growth, again, was caused by a decrease in axonal neurofilament phosphorylation (Sherman et al., 2012). These findings suggest that axon calibre of PNS axons can be modulated by axon-glial interactions after myelin ensheathment. In the CNS, unilateral x-irradiation to ablate OPCs and their progeny in the optic nerve of mice has led to a decrease in optic nerve axon calibre compared to non-irradiated control side (Colello et al., 1994). This finding suggests that axon calibre in the CNS might also be regulated by extrinsic oligodendrocyte signals, however, from this study it is unclear whether extrinsic signals from oligodendrocytes or myelin ensheathment itself can regulate axon calibre growth of the myelinated axon. Hypomyelination caused by the disruption of important myelin protein expression, such myelin basic protein (MBP) in *Shiverer* mice (Readhead and Hood, 1990), resulted in reduced phosphorylation of axonal neurofilaments and neurofilament accumulation, indicating that myelin ensheathment itself might be able to regulate axon calibre growth of myelinated axons in the CNS (Sanchez et al., 2000).

It remains unclear, whether the axon calibre of myelinated axons is the cause or the result of myelin ensheathment in the CNS. In chapter 3 of this thesis, I will

characterize axonal properties, such as axon calibre before and after the onset of myelination, and under normal condition as well as in the absence of myelin ensheathment at cellular resolution in order to elucidate whether axon calibre can induce myelin ensheathment or whether the axon calibre of myelinated axons is a result of myelin ensheathment.

1.2.2 Axonal signalling as a mechanism behind axonal selection

Although no local axonal signals have yet been shown to be crucial for CNS myelination in vivo, some molecules have been demonstrated to have an inductive effect on myelin ensheathment.

Axonal signalling molecules that are essential for myelination in the PNS are relatively well known. Axonal expression of a single growth factor, neuregulin-1 type III (NRG1-III), is essential in the PNS for every stage of the Schwann cell lineage progression, from Schwann survival and proliferation to inducing myelination and regulating myelin thickness, by binding to the transmembrane receptor complex ErbB3- ErbB2 and activating downstream signalling pathways in Schwann cells (Jessen and Mirsky, 2005; Lyons et al., 2005; Salzer and Nave, 2006). The growth factor NRG1-III is expressed at a higher level on large calibre PNS axons than on small calibre axons (Taveggia et al., 2005) and experimental overexpression of NRG1-III on smaller calibre axons has been shown to induce myelination of previously unmyelinated axons (Michailov et al., 2004; Taveggia et al., 2005). NRG1-III is also expressed at a high level on large calibre PNS axons and expressed at a lower level on small calibre axons (Taveggia et al., 2005). The myelination of large calibre axons, which have been shown to myelinated if their axon diameter is above 1µm (Duncan, 1934), might be due to the higher NRG1-III expression levels in this larger calibre axons. The 1µm threshold in axon diameter might therefore represent a certain level of NRG1-III expression level that is sufficient to induce PNS myelination.

In the CNS, however, genetic ablation of NRG1-III expression in axons and the NRG1-III receptor ErbB expression in oligodendrocytes causes little or no myelin defects depending on the CNS region and developmental stage investigated (Brinkmann et al., 2008; Taveggia et al., 2008; Makinodan et al., 2012). However,

there is evidence for a modulatory role of NRG1-III during myelination as conditional loss of function of the ErbB receptor in oligodendrocytes leads to hypomyelination in the prefrontal cortex (PFC), whereby oligodendrocytes formed fewer and thinner myelin sheaths, but only if the disruption of ErbB receptor expression occurred during a critical developmental period between P3 and P5 (Makinodan et al., 2012). Interestingly, this pattern of hypomyelination was also seen in animals raised in social isolation during this critical developmental time period, which also showed reduced NRG1-III expression in their PFC, indicating that neuronal activity might promote myelination through the NRG1-III ErbB pathway. While genetic disruption of NRG1-III expression did not result in general hypomyelination of CNS axons, overexpression of NRG1-III can cause hypermyelination in form of an increase of myelin sheath thickness and the myelination of small calibre axons in the neocortex that normally would not be myelinated (Brinkmann et al., 2008). As the physical size of large axons might be one of the axon properties inducing myelination (see above, Remahl and Hildebrand, 1982; Lee at al., 2012) and the myelination of smaller calibre axons can be experimentally induced by overexpression of NRG1-III (Brinkmann et al., 2008), the myelination of smaller calibre axons might depend on the expression of axonal signalling molecules such as NRG1-III. Interestingly, the levels of NRG1-III expression in different axons have been shown to correlate with the levels of neuronal activity, e.g. the rate of action potential firing (Ziskin et al., 2007; Liu et al., 2011). Together, these data suggest that neuronal activity might regulate the expression level of key axonal signalling molecules such as NRG1-III and that the myelination of smaller calibre axons in particular might depend on the activity mediated expression of these signalling molecules, which I will discuss in further detail in chapter 4.

Other axon-oligodendorcyte signals that have been shown to influence myelination in the CNS are neuronal laminins, which interact with integrins expressed by oligodendrocytes. The integrin receptor has 8 subunits, which are expressed at different developmental stages throughout the oligodendrocyte development (as reviewed in O'Meara et al., 2011). Particularly beta-1-integrin is thought to influence myelin sheath formation in oligodendrocyte through activation of the MAPK and

AKT signalling pathways, as genetic ablation of beta-1-integrin results in an increase in unmyelinated axons correlated with a decrease in MAPK activity (Lee et al., 2006) and AKT activity (Barros et al., 2009) in the optic nerve and spinal cord of mice, respectively. Interestingly, particularly small calibre axons were affected, indicating that beta1 integrin can regulate the extent of myelination by regulating the myelination of small rather than large calibre axons (Camara et al., 2009) and therefore appears to have a modulatory effect on CNS myelination.

Other axon-oligodendrocyte interactions that have been described negatively regulate myelination. The polysialytated form (PSA) of the neuronal cell adhesion molecule NCAM (PSA-CAM) on the surface of axons inhibits the myelination of these axons and only PSA-CAM negative axons have been shown to be myelinated in the optic nerve of mice (Charles et al., 2002). Furthermore, the down-regulation of PSA-CAM isoforms immediately precedes the onset of myelination (Charles et al., 2002), and while the precise axon-oligodendrocyte interactions behind this mechanism are still unknown, these observations indicate that this axonal signal can regulate the onset of myelination in CNS axons. Other axon-oligodendrocyte interactions have been identified between the Notch1 receptor on oligodendrocytes and its neuronal ligand Jagged1. Jagged1 expression has been shown to decrease with the onset of myelination, after which Jagged 1 was only expressed in unmyelinated axons in the mouse optic nerve (Wang et al., 1998) and myelinated axon number was shown to increase in the optic nerve and cerebellum of Notch-1 mutant mice (Givogri et al., 2002). This indicates that Jagged1-Notch signalling can regulate CNS myelination during, also, by negatively regulating the onset of myelination (as reviewed in Taveggia et al., 2010). However, the mechanism through which the Notch-receptor interacts with other ligands, such as Delta, is not clear as the Delta-Notch signalling pathway has previsouly been shown to regulate oligodendrocyte specification and differentiation during zebrafish development (Park and Appel, 2003).

Other non-neuronal signalling molecules have been found to have a positive effect on the extent of myelination such as tyrosine Fyn kinase (Wake et al., 2011; Czopka et al., 2013) or onset of myelination, such as Wnt-β-catenin (Fancy et al., 2009) or a negative effect, such as GPR17 (Chen et al., 2009), and LINGO-1 (Mi et al., 2005). Interestingly, activity of the tyrosine Fyn kinase has been indicated to be regulated

by the synaptic release of glutamate from stimulated axons in vitro (Wake et al., 2011). After stimulation, glutamate was released through axonal synaptic vesicle exocytosis, which bound to one of the main glutamate receptors in the oligodendrocyte, the NMDA receptor, and thereby activated a downstream signalling pathway that increased tyrosine Fyn kinase activity. Tyrosine Fyn kinase activity in myelinating oligodendrocyte processes coincided with increased local synthesis of MBP, indicating that NDMA receptor activation in oligodendrocyte through glutamate can regulate myelin sheath formation (Wake et al., 2011). This data suggests that neuronal activity might regulate the extent of myelin sheath formation in vitro in the CNS. However, a thorough in vivo study using mice lacking the functional subunit of the NMDA receptor did not show any defect in myelination (De Biase et al., 2011), questioning the functional relevance of the proposed NMDA receptor mediated pathway in controlling myelination in vivo. The NMDA receptor mediated activation of tyrosine Fyn kinase suggested by Wake et al. might not be necessary for myelination in vivo per se, but might have a modulatory role regulating the extent of myelination instead. Indeed, tyrosine Fyn kinase, has been shown to regulate the extent of myelination in vivo. Constitutive activation and reduction of Fyn kinase in oligodendrocytes resulted in a respective increase and decrease of myelin sheaths per oligodendrocyte in the zebrafish spinal cord (Czopka et al., 2013). Importantly, the increase in the number myelinated axons did not result from ectopic myelination of small axons below the minimum axon diameter that is normally myelinated, but from an increase in the number of myelinated axons with a diameter between 0.3 and 0.9µm. As described in the section above, axons with a diameter in this range can be myelinated in the CNS but not all of them are, indicating that these axons may require additional axonal signalling to induce the tyrosine Fyn kinase pathway in order to be myelinated. Furthermore, the loss of functional non-receptor tyrosine kinase Fyn in oligodendrocytes has been shown to decrease the number of myelinated axons with a small calibre, while the number of myelinated axons with a large calibre remained intact (Umemori et al., 1994). This data also suggest that the smaller calibre axons require inductive signalling molecules in order to be selected for myelination. I will introduce and discuss the above described concepts in more detail in chapter 4.

Overall, these findings suggest that neuronal activity might lead to axon-oligodendrocyte signalling that could induce myelination. This axon-oligodendrocyte signalling, however, might not be required for myelination per se but have a modulatory function by regulating the myelination of smaller calibre axons. Extensive further studies are required in order to determine whether axon-oligodendrocyte signalling is required for myelination or simply modulating the extent of myelination on small calibre axons. Further characterization is also needed to elucidate whether neuronal activity can induce myelination through the expression of axonal molecules such as NRG1-III or through synaptic vesicle release of neurotransmitters, such as glutamate. High resolution imaging during myelination in the absence of axonal synaptic vesicle release would reveal whether axonal neurotransmitter release could initiate the axon-oligodendrocyte signalling that might induce myelination. In order to elucidate whether axon-oligodendrocyte signalling could be required for regulating the myelin extent per oligodendrocyte and the myelination of axons of a specific calibre, I performed single cell resolution of individual oligodendrocytes in the absence of synaptic vesicle release and will present this data in chapter 4.

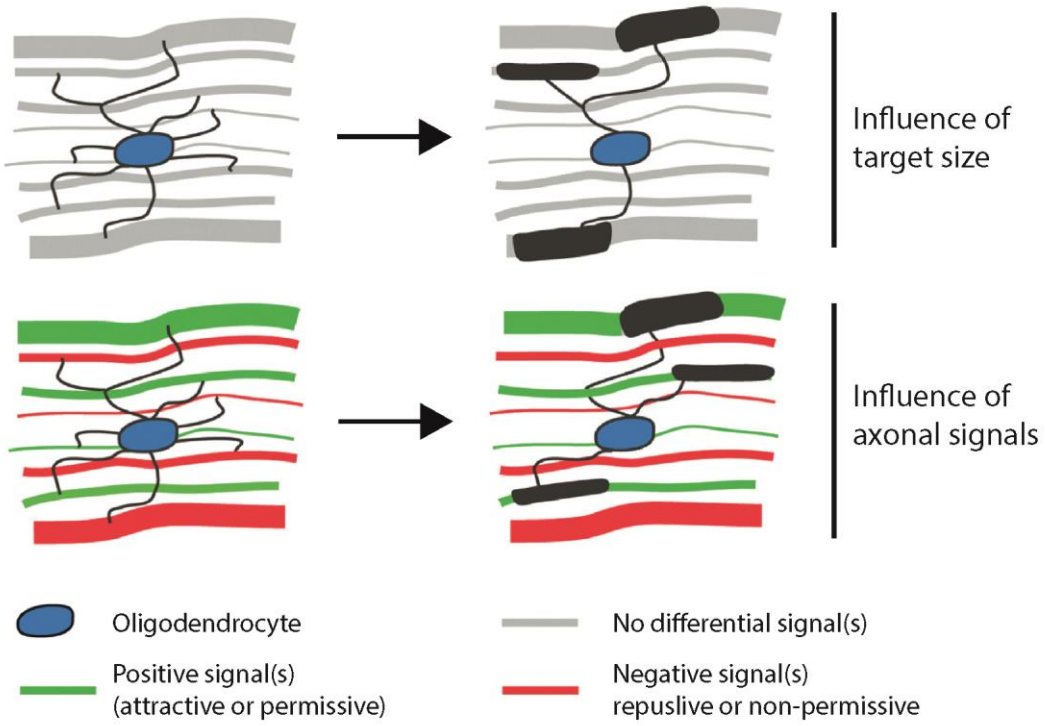

Figure 1.5: Schematic model of different signals that might regulate axon selection during myelination. Pre-myelinating oligodendrocytes extend exploratory processes that interact with the axonal environment (left) before ensheathing specific axons (right). (Top) In the absence of differential signals emitted by axons, oligodendrocytes preferentially ensheath axons of large calibre, while axons of intermediate calibre are sometimes myelinated and the smallest calibre axons remain unmyelinated. (Bottom) The expression of positive axonal signals might influence the axon selection during myelination. Axons of large and intermediate calibre might only be ensheathed when they express the positive or permissive signal, while the smallest calibre axons and axons that do not express the positive signal or negative signals remain unmyelinated. So far, the axonal signals essential for myelination remain unknown. Image adapted from Simons and Lyons, 2003.

1.3 Zebrafish as a model organism

Zebrafish have become increasingly significant for biological research in recent years and are now regarded as one of the most important vertebrate model organisms. Two of the main advances in using zebrafish as an investigative model are live imaging (Kirby et al., 2006; Buckley et al., 2010; Jung et al., 2010; Czopka et al., 2013) as well as genetic and chemical screening (Nuesslein-Volhard and Dahm, 2002; Hong et al., 2009, Hao et al., 2010, Jung et al., 2012; as reviewed in

Taylor et al., 2010), which are complementary to many standard laboratory models, where accessibility for live imaging or drug applications can become a problem, particularly in the CNS (Czopka and Lyons, 2011).

Due to their small size and transparency at larval stages, zebrafish are ideal for live imaging at high resolution at a cellular and even sub-cellular level (Czopka and Lyons, 2011). Transgenic zebrafish larvae expressing fluorescent reporter proteins in specific cells therefore allow the visualization of these cells during their development and their interactions with other cells. Zebrafish also have a relatively rapid development and progress from fertilized egg to larvae within 3-5 days (Kimmel et al., 1990). Zebrafish larvae have a relatively simple but rapidly developing nervous system, and many transgenic reporter lines have been created to study neuronal development and circuitry formation (Eaton et al., 2001; Lewis and Eisen, 2003; Korn and Faber, 2005) as well as oligodendrocyte development and myelination (Pogoda et al., 2006; Kucenas et al., 2008; Buckley et al., 2010; Jung et al., 2010; Kirby et al., 2006; Almeida et al., 2011; Czopka et al., 2013). Transgenic reporter lines expressing fluorescent protein expression in neurons, such as the Tg(cntn1b:mCherry) (Czopka et al., 2013), in OPCs and mature, myelinating oligodendrocytes, such as the Tg(nkx2.2a:GFP) (Kucenas et al., 2008; Czopka et al., 2013) and Tg(sox10(7.2):mRFP) (Kirby et al., 2006) and in myelinating oligodenrdrocytes only, such as the Tg(mbp:GFP) as well as Tg(mbp:mCherry) (Almeida et al., 2011; Czopka et al., 2013), are particularly useful in live imaging the dynamic axon-oligodendrocyte interactions in vivo.

In order to investigate myelination in zebrafish, it is important to consider the similarities and differences between mammalian myelination and zebrafish myelination. During evolution, after the divergence of tetrapods from the phylogenetic tree, duplications of the genome resulted in the presence of multiple genes in zebrafish for the mammalian genes. This, for example, occurred for the proteolipid protein (PLP) and its splice variant DM20, which can be found in multiple paralogues in fish (Schweitzer et al., 2006). The main known difference in zebrafish and mammalian myelin is the expression of myelin protein zero (P0) by oligodendrocytes in the zebrafish CNS, whereas the structural function of P0 during myelin formation is replaced by PLP/DM20 in the mammalian CNS and P0 is only

expressed by Schwann cells in the mammalian PNS (Waehneldt et al., 1986; Kirschner et al., 1989). The longer and more stable isoform of PLP, DM20, first appeared approximately 400 million years ago, after the divergence of bony fish (Nave et al., 1987), and it has been proposed that the evolution of this more stable isoform allowed the functional replacement of P0 and stable integration of PLP in the mammalian CNS myelin (Waehneldt, 1990; Yoshida and Colman, 1996). It is important to consider these structural differences and similarities in myelin protein composition when interpreting data obtained from zebrafish research. However, a large number of myelin genes and proteins known to play an important role during myelination are conserved between zebrafish and mammals and their homologs can be found in zebrafish (for review, see Broesamle and Halper, 2002; Buckley et al., 2008). Novel genetic regulators of PNS myelination, such as the adhesion G-protein-couple receptor Gpr126, were discovered in genetic screens in zebrafish (Monk et al., 2009), which is also essential in mammalian PNS myelination (Monk et al., 2011; Mogha et al., 2013). The analyses in this PhD thesis are based on the cellular behaviour of myelinating oligodendrocytes and their interactions with axon during the selection process that determines which axons will be myelinated. These cellular interactions in the CNS are still only incompletely understood in mammalian research models, direct comparisons cannot be drawn. However, the myelinating behaviour of oligodendrocytes described in rodents, such as OPC proliferation, migration and differentiation to myelinating oligodendrocytes, the dynamic extension and retractions of exploratory oligodendrocyte processes before myelination (Hughes et al., 2013; for review see Emery, 2010; He and Lu, 2013; Boulanger and Messier, 2014), are also found in zebrafish oligodendrocytes (Kirby et al., 2006; Kucenas et al., 2008; Almeida et al., 2011h; Czopka et al., 2013). Zebrafish are therefore an ideal model system to study axon-oligodendrocyte interactions and insights into axon selection during myelination obtained in this PhD thesis are therefore likely to be conserved in higher vertebrates and valuable for future research in mammalian systems.

1.3.1 Zebrafish spinal cord neurons

As previously noted, the cellular basis of myelination in the CNS remains unknown and I have used zebrafish to address open questions due to their suitability for live imaging of cellular interactions the CNS. In order to investigate the axonal properties, such as axon calibre before and after myelination, the different neurons that are fated for myelination must be identified. The neurons of the zebrafish spinal cord have previously been classified and extensively described in their morphology (Bernhardt et al., 1990; Clarke et al., 1984; Hale et al., 2001; Kuwada et al., 1990; Mendelson, 1986) and neurotransmitter type (Higashijima et al., 2004). However, it is unknown which of these neurons are fated for myelination and whether their axonal properties are different from those neurons not fated for myelination. In this PhD thesis, reticulo spinal (RS) neurons (Mendelson, 1986), Rohon Beard (RB) sensory neurons (Clarke et al., 1984), commissural primary ascending (CoPA) interneurons, circumferential descending (CiD) interneurons, circumferential ascending (CiA) interneurons, commissural bifurcating longitudinal (CoBL) interneurons are identified and their myelination status characterized. I will describe below, the axonal morphologies and their positions in the spinal cord that are unique to the different neurons and that were used for identification.

RS cell bodies are located in the hindbrain, while their axon projects longitudinally and caudally along the ventral spinal cord.

The cell body of CoPA interneurons is located dorsally in the spinal cord and has a characteristic dendritic branches extending rostrally and caudally from the cell body. CoPA axons cross the spinal cord dorsal to the Mauthner axon and, after crossing the mid-line, they project rostrally to ascend in the dorsal tract up to the hindbrain. Even the axons of CoPA interneurons in the posterior spinal cord areas near the tail terminate in the hindbrain, indicating that even the most caudally located CoPA can ascend the full length of the spinal cord.

CiD interneurons have cell bodies of varying shapes located in the middle and dorsal regions of the spinal cord with a caudally projecting ipsilateral axon. They also have a smaller second axon, which projects rostrally, however, the axon calibre is often smaller than that of the main, caudally projecting axon.

CoBL interneurons have relatively small cell bodies located dorsally in the spinal cord. CoBL interneurons are unipolar with an axon that projects ventrally before turning medially to cross the spinal cord and to bifurcate on the contralateral side to their cell body, of which one projects rostrally and the other projects caudally. Both terminate approximately 4 segments from the cell body.

CiA interneurons also have a dorsal cell body but have a circumferential axons that projects ipsilateral to its cell body and ascends dorsally and rostrally but has a smaller axon bifurcating shortly behind the axon initial segment, which project caudally.

The cell bodies of RB sensory neurons and their axons are located in the dorsal spinal cord and have two ipsilateral longitudinal axons, one ascending and one descending. The ascending axon terminates in the hindbrain. Input from the periphery is provided by a peripheral axon that arises as a side-branch of the longitudinal descending axon and projects caudally until the point when it leaves the spinal cord and branches profusely in the periphery. RB neurons undergo apoptosis and the majority of them are gone by 3-4dpf, however, a minority of RB cells still remain after 5dpf (Williams et al., 2000).

In order to compare the myelination status of individual neurons, it is important to choose neurons in similar developmental state at the time of analysis. Amongst the first neurons that develops in the zebrafish spinal cord, amongst other such as the primary motor neurons, are the RB sensory neurons, which are first detected at 18-10hpf. Commisural neurons, such as the CoPA interneuron, appear at 17-18hpf but continue to increase in number until approximately 28hpf. The first CiD, CiA and CoBL interneurons appear at 22-23hpf (Hale et al., 2001). The first RS neurons are detected between 22-24hpf and continue to appear up to 48hpf. RS extend their axons to the spinal cord in two waves of development, the first wave appears in the rostral spinal cord between 20 and 24hpf, while the second arrives at approximately 30-34hpf (Mendelson, 1986). Overall, RB, RS, CiD, CoPA, CoBL and CiA neurons appear within the first 24 hours of zebrafish development and should therefore have reached similar developmental stages at the time of analysis.

Neuron cell type	Picture of neuron	Soma postition / # per hemi-segment	Cell body & dendrite morphology	Maximum axon length
Reticulospinal		Ventral / axon projects through length of spinal cord	Number and location of dentrites vary.	Extends length of cord.
Rohon Beard (RB)	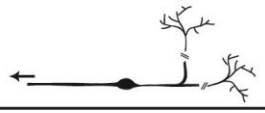	Dorsal of all other cells / 1-4 cells per hemi-segment	Bipolar, large somata.	Caudally projecting axon extends > 20segments. Rostrally projecting axon extends 10 segments.
Commisural Primary Ascending (CoPA)		Dorsal, lateral to CoLA cell bodies / cell # varies in alternate segments	Bipolar, T shape, dorsal dendrites.	Extends length of cord / axon corsses cord dorsal to Mauthner axon. Ascend in dorsal cord.
Commisural Longitudinal Ascending (CoLA)		Dorsal, medial to CoPA cell bodies / 1 cell per hemi-segments	Dorsal dendrite extends caudally. Midlateral processes extend rostrally and caudally.	5 segments/ axon crosses cord dorsal to Mauthner axon. Ascends extending dorsally. Minor descending branch.
Circumferental Ascending (CiA)		Midcord lateral / mutlitple cells per hemi-segment	Unipolar, simple cell body.	Varies, the caudally projecting axon extends ipsilaterally over several segments. Minor descending branch.
Circumferental Descending (CiD)		Midcord lateral / mutlitple cells per hemi-segment	Unipolar, simple cell body	13 segments/ axon ipsilateral, extends ventral to Mauthner axon then turns dorsal and caudally. Minor ascending branch.
Commisural Bifurcating Longitudinal (CoBL)		Dorsal / mutlitple cells per hemi-segment	Unipolar, simple cell body	4 segments/ axon projects ventrally, crossing cord dorsal to Mauthner axon before bifurcating and extending dorsally.

Table 1.1: Overview of the key morphological features of the neurons investigated. Arrows indicate direction of axon growth; dashed line indicates contralateral growth; double stroke indicates long distances between the depicted axon features. For additional information and standard deviations, see text. Table adapted from Hale et al., 2001 and Bernard et al., 1990.

Previous studies investigating the relationship between axon calibre and myelination (see above), primarily studied axon calibre growth in context of myelination using electron micrographs of transversal section of the optic nerve or spinal cord (Colello et al., 1994; Sanchez, 1996, 2000). While this is a great technique to accurately measure axon calibre size, it does not give any information on axonal morphology before and after myelination or on what types of axons are fated for myelination or remain unmyelinated. In this PhD thesis, I will analyze the individual neurons and their axonal properties, such as axon calibre and axon branching before and after the onset of myelination, which will provide insight into the axonal selection process during myelination. Furthermore, I will investigating the axon calibre of specific large calibre axon, such as the RS, in absence of myelinating oligodendrocytes in order to reveal whether the myelin ensheathment itself can regulate axon calibre size.

1.4 Statement of aims

1. To identify a subset of spinal cord neurons that is fated for myelination and a subset of spinal cord neurons that remain unmyelinated and characterize their axonal properties, such as axon calibre and axon branching, in relation to their myelination status.
2. To investigate whether axon calibre growth can be regulated by myelin ensheathment under normal condition and in absence of myelin ensheathment.
3. To investigate the influence of synaptic vesicle release on the extent of myelin formed per oligodendrocyte by quantifying the number and length of myelin sheaths formed per oligodendrocyte.
4. To characterized the influence of synaptic vesicle release on the behaviour of myelinating oligodendrocytes and the dynamic growth of myelin sheaths using time-lapse analysis.

2. Materials and Methods

2.1 Fish husbandry and transgenic tools

The zebrafish used in this thesis were kept and raised in the Queen's Medical Research Institute animal facility under standard conditions (Westerfield, 2007). The fish lines were kept at 26.5°C at a 14 hours light and 10 hours dark cycle. The embryos were obtained by natural spawning through pair matings and kept at 28.5°C in 0.00001% methylene blue conditioned aquarium water or embryo medium (zebrafish book, zfin.org). The embryo staging occurred according to standard procedures as described elsewhere (Kimmel et al., 1995). All experiments were performed under the British Home Office regulations.

Fish lines used:

Tg(sox10(7.2):mRFP)	(Kirby et al., 2006)
Tg(nkx2.2a:GFP)	(Kucenas et al., 2008)
Tg(mbp:EGFP)	(Almeida et al., 2011)
Tg(mbp:EGFP-caax)	(Almeida et al., 2011)
Tg(mbp:mCherry-caax)	unpublished
Tg(cntn1b:mCherry)	(Czopka et al., 2013)
Tg(s1011:Gal4, UAS:Kaede)	(Scott et al., 2007)
Tg(HuC:Gal4)	generated for this thesis, unpublished
Tg(Cntn1b:KalTA4)	unpublished

Constructs generated:

UAS:EGFP	unpublished

Constructs used:

mbp:mCherry-caax	unpublished
UAS:GFP-cntn1a	unpublished

For UAS:EGFP construct generation, p5E_UAS, pME_EGFP, p3E_pA and pDestTol2CG2 from Tol2Kit were recombined through multisite Gateway technology (Kwan et al., 2007). For the generation of the stable transgenic line Tg(HuC:Gal4), 10ng/µl of plasmid DNA encoding HuC:Gal4, generated by Dr. Tim Czopka, and 25ng/µl *transposase* mRNA was injected in fertilized AB eggs

(Zebrafish National Resource Center (ZIRC)) between the 1-4 cell stages using a Pneumatic Picopump PV830 (World Precision Instruments Ltd, Hertfordshire, UK) and a Micromanipulator M3301R (World Precision Instruments Ltd, Hertfordshire, UK). The pDestTol2CG2 used for the generation of the HuC:Gal4 construct includes a cmcl2:EGFP-pA expression cassette and successful integration of HuC:Gal4 into the genome was therefore detected by cmcl2:EGFP expression in the cytoplasm of myocytes (Kwan et al., 2007; Huang et al., 2003; Auman et al., 2007). GFP positive F1 fish were outcrossed to AB wildtype in order to identify fish with germ-line transmission of the HuC:Gal4 plasmid. The F2 generation was raised and screened for stable HuC:Gal4 genome integration.

To indicate that a stable transgenic line was used in the figure images, the "Tg" designation was added, e.g. Tg(mbp:mCherry-caax), while figure images of individual cells were obtained through mosaic expression and were labelled by the construct name, e.g. mbp:mCherry-caax.

2.2 Transmission electron microscopy

Tissue preparation for transmission electron microscopy

Zebrafish were terminally anaesthetised in MS222 and fixed in by immersion primary fixative containing 4% paraformaldehyde and 2% Glutaraldehyde in 0.1M sodium cacodylate buffer for 2hours at room temperature (RT). To facilitate immersion of the fixative, the embryos were irradiated by microwaves (irradiation cycle: 100 Watt for 1 minute with 1minute pause, which was repeated once, followed by 450 Watt for 20 sec and 20 sec pause, which was repeated 5 times) in eppendorf tubes, whereby no more than 5 embryos were fixed per tube to allow optimal immersion. The fish were then fixed in a secondary fixative containing 2% osmium tetroxide in 0.1M sodium cacodylate and 0.1M imidazole buffer, microwave irradiated (microwave stimulation cycles as described above) and left at RT for 1-3hours. The fish were then en bloc stained with a saturated uranyl acetate solution in water ON and subsequently dehydrated in ethanol and microwave irradiated (microwave stimulation cycle: 250 Watt for 1 minute with 1 minute pause, which was repeated once and followed by 10 minutes at RT for each ethanol concentration)

at ethanol concentrations 50%, 75%, 95% and 100%. The 100% ethanol dehydration was repeated twice and the fish were subsequently transferred into a 100% acetone and microwave irradiated (microwave stimulation cycles as described for the ethanol dehydration). The fish were then pre-infiltrated ON at RT by an EMBED/acetone 1:1 solution, which was replaced the next day by 100% EMBED, whereby the acetone was allowed to evaporate for at least 6 hours. The EMBED infiltrated tissue samples were then embedded and aligned in 100% EMBED in silicon moulds and the EMBED blocks were solidified at 65°C for 24hours.

Microtome sectioning

The EMBED embedded tissue blocks were trimmed in the shape of a trapezoid around the embedded fish. The region of interest in the spinal cord at somite 15 was subsequently cut into 80nm thick section on a microtome (Reichert Jung Ultracut Microtome, Leica, Wetzlar, Germany), caught in the knife boat filled with water and picked up with a perfect loop (Perfect Loop, Leica EM accessory EM UC7, Leica, Wetzlar, Germany). The sections were then allowed to dry on electron microscopy grids with hexagonal grid pattern (PELCO 300 Mesh Grids, Ted Pellar Inc., Redding, CA, USA) on a hot plate at approx. 180°C.

Section staining

Prior to imaging, the sections on the grids were prepared for the lead staining by placing the grids in a 1:1 solution of saturated uranyl acetate (~8%) and absolute ethanol for 5minutes. After briefly washing the grids in a stream of 50% ethanol, the grids were allowed to dry on Whatman paper and subsequently placed in Sato lead stain for 5minutes. To avoid precipitation of the lead, the samples in the lead stain are kept in a container, i.e. a petri dish, with 2 to 3 NaOH pellets in the periphery of the container. The grids are then washed in a stream of DI water, allowed to dry on Whatman paper and stored at RT until the imaging.

Transmission electron imaging and image processing

The TEM images were taken on a Phillips CM120 Biotwin transmission electron microscope at the Science Faculty, Electron Microscope Facility, Daniel Rutherford Building, King's Buildings, Mayfield Road, Edinburgh EH9 3JH, United Kingdom.

Images in dm3 format obtained at the Phillips CM120 Biotwin transmission electron microscope were converted to tiff format using the batch-convert tool in Image J (National institute of health, Bethesda, MD, USA). Tiles were subsequently fused using the automated photo-merge tool in Photoshop CS3 (Adobe, San Jose, CA, USA).Figure panels were compiled using Adobe Photoshop CS3 (Adobe, San Jose, CA, USA) and Adobe Illustrator CS6 (Adobe, San Jose, CA, USA).

2.3 Confocal image acquisition

Prior to confocal image acquisition the embryos were screened for fluorescence on a Leica stereo fluorescence microscope (Leica, Wetzlar, Germany).

Live embryos were anaesthetised in MS222 (tricaine methane-sulfonate, Sigma-Aldrich Company Ltd, Gillingham, UK) and embedded in 1.3-1.5% low melting point agarose (Ultrapure ^{TM} LMP Agarose, Invitrogen, Carlbad, USA) on a cover glass (Menzel-Glaeser, 22x22mm or 22x50mm, no. 1 thickness (0.13 – 0.16 mm), Braunschweig, Germany). After the agarose had polymerized, a silicon grease (Dow Corning® high-vacuum silicone grease,Sigma-Aldrich Company Ltd, Gillingham, UK) outline was made around the cover glass, which was then filled with embryo medium containing anaesthetic and placed on a microscope slide (Super Premium Microscope Slides, VWR International bvba, Leuven, Belgium).

Confocal images and time-lapse movies were acquired with the Zen2009 software on a Zeiss LSM 710 confocal microscope (both from Carl Zeiss Microscopy, Oberkochen, Germany) using 20x and 63x lenses (Zeiss Plan-Apochromat 20x dry, NA=0.8 and Zeiss C-Apochromat 63x, water immersion, NA=1.2, Carl Zeiss Microscopy, Oberkochen, Germany). During time-lapses the agarose embedded fish were staged on a temperature controlled microscope stage at 28°C (Tempcontrol 37, Zeiss, Oberkochen, Germany) to keep the fish under optimal conditions. Brightfield images were acquired with the Axiovision software on an Axio Scope.A1 microscope (both from Carl Zeiss Microscopy, Oberkochen, Germany). All

fluorescent and brightfield live images and timelapse movies represent a lateral view of the zebrafish spinal cord, anterior to the left and posterior to the right as well as dorsal on top and ventral on bottom.

After image acquisition, the fish were carefully cut free from the agarose using microsurgical blades (Performance Microsurgical Blades, Katena, Stockport, UK) and transferred into anaesthetic free embryo medium or dispatched using a Home Office approved Schedule 1 method.

Confocal image processing

Images for each experiment were taken at similar laser intensity and optical gain setting on the Zen2009 software and after acquisition, opened in Image J (National institute of health, Bethesda, MD, USA), aligned if appropriate using the stack-reg plugin and staged using the Z-project function for figure images. Figure panels were compiled using Adobe Photoshop CS3 (Adobe, San Jose, CA, USA) and Adobe Illustrator CS6 (Adobe, San Jose, CA, USA).

2.4 Statistical analysis

All statistical analysis was performed using the Graphpad Prism 5 software (GraphPad Software Inc., San Diego, CA, USA). Statistical tests were chosen according to experimental design as specified in the figure legends. Direct experimental comparisons of treatment and control group were analysed by student's t-tests (under the assumption of normality distribution), whereas experiments with more than two variables were analysed by ANOVA. P-values of >0.05 were considered statistically insignificant. P-values <0.05 were represented by * symbol, <0.01 by ** and <0.001 by ***. Throughout the thesis, error bars illustrated mean ± standard deviation (SD) or standard error of the mean (SEM) as specific in the results text and figure legends.

2.5 Material and methods specific to chapter 3: Characterizing the relationship between axon calibre and myelination of individual neurons in vivo.

Individual neuron analysis

Individual neurons were labelled using the Gal4-UAS system (Asakawa and Kawakami, 2008; Halpern et al., 2008). The stable transgenic Gal4 driver lines Tg(HuC:Gal4) and Tg(Cntn1b:KalTA4) express the transcription activator protein Gal4 in all neurons and a subset of mature neurons, respectively. In order to label individual neurons in the transgenic Gal4 lines, plasmid DNA encoding UAS:EGFP and UAS:GFP-cntn1a (courtesy of Dr. Matt Voas) was injected. Through the subsequent binding of Gal4 to the UAS, the fluorescent reporter proteins were expressed in individual neurons. In order to ascertain the myelin ensheathment along the axons, myelin was labelled by crossing the transgenic Gal4 lines with Tg(sox10:mRFP), which labels myelinating oligodendrocytes, to create double transgenic fish Tg(HuC:Gal4) x Tg(sox10:mRFP) and Tg(Cntn1b:KalTA4) x Tg(sox10:mRFP).

10ng/µl of DNA plasmid encoding UAS:EGFP or UAS:GFP-cntn1a and 25ng/µl *transposase* mRNA were injected in fertilized Tg(HuC:Gal4) x Tg(sox10:mRFP) and Tg(Cntn1b:KalTA4) x Tg(sox10:mRFP) eggs between the 1-4 cell stages using a Pneumatic Picopump PV830 (World Precision Instruments Ltd, Hertfordshire, UK) and a Micromanipulator M3301R (World Precision Instruments Ltd, Hertfordshire, UK).

The GFP or GFP-cntn1a labelled neurons were identified based on their morphology as described in Bernhardt et al., 1990; Clarke et al., 1984; Hale et al., 2001; Kuwada et al., 1990; Mendelson, 1986 and imaged at Zeiss LSM 710 confocal microscope (Carl Zeiss Microscopy, Oberkochen, Germany) at 20x and 63x magnification. Images were opened in Image J (National institute of health, Bethesda, MD, USA) and the GFP and mRFP channels merged using the colour tools.

For every neuron type, axonal regions of approximately 30-50µm were selected for axon calibre measurements and axonal regions of approximately 135-250µm were selected for myelin ensheathment and axon branching measurements. As RS axons project through the length of the spinal cord, axon regions for measurements were selected between somites 10-16 and somites 20-26. Axon regions in CiD, CoBL and

CiA neurons were selected proximal to the cell body, just behind the axon bifurcation. Axon regions in RB neurons were selected close to the cell body and axon regions in CoPA neurons were selected after the axon crosses the midline and projects dorsally.

Axon calibre was obtained in the fluorescent images by measuring the length and area of the selected axon region using the freehand drawing and measuring tool in Image J (National institute of health, Bethesda, MD, USA) and the lasso and measuring tool in Adobe Photoshop CS3 (Adobe, San Jose, CA, USA), respectively. The measured axon area was subsequently divided by the measured axon length, thus amounting to the axon calibre of the selected region.

The myelin profiles were obtained using the freehand drawing tool in Image J (National institute of health, Bethesda, MD, USA) to measure the length of the myelin sheaths along the selected axon region. The sum of the all myelin sheaths along the selected axon region was then divided by the total length of the selected axon region.

The axon branch number was counted using the counter tool in Image J (National institute of health, Bethesda, MD, USA) along the length of the selected axon region, which was then divided by the total length of the selected axon region.

Olig2 MO microinjections

In order to inhibit oligodendrocyte development in the zebrafish embryo, 3ng of Olig2 morpholino (Olig2 MO, Gene Tools, LLC, Philomath, USA) in diethylpyrocarbonate (DEPC) treated water, was injected into fertilized eggs between the 1-4 cell stages using a Pneumatic Picopump PV830 (World Precision Instruments Ltd, Hertfordshire, UK) and a Micromanipulator M3301R (World Precision Instruments Ltd, Hertfordshire, UK). Olig2-ATG-MO sequence: 5'-ACACTCGGCTCGTGTCAGAGTCCAT 3'(Zannino and Appel, 2009).

Analysis of the myelination status of the 20 axons with largest calibre per hemi spinal cord in the transmission electron micrographs

Transmission electron micrographs (TEM) of the spinal cord sections of 4dpf old embryos at somite area 8-10 were acquired at 3800x magnification and processed as described above. The perimeter of the 20 axons with the largest axon calibre in the hemi spinal cord were traced and measured using the lasso and measuring tool in Adobe Photoshop CS3 (Adobe, San Jose, CA, USA). Axon perimeter was subsequently converted to axon diameter, assuming circularity.

2.6 Material and methods specific to chapter 4: Synaptic transmission regulates dynamic oligodendrocyte behaviour and myelination

tettx mRNA microinjections

For the TetTx treatment, fertilized eggs were injected with 1nl of 100ng/µl (100pg) *tettx* mRNA between the 1-4 cell stages using a Pneumatic Picopump PV830 (World Precision Instruments Ltd, Hertfordshire, UK) and a Micromanipulator M3301R (World Precision Instruments Ltd, Hertfordshire, UK). Controls were injected at the same developmental stage with 1nl of nuclease free water. All embryos were dechorionated at 1dpf.

Tissue preparation and patch-clamp recording

All tissue preparations and patch-clamp recordings described below were performed by Dr. Jessica Ausborn, Karolinska Institute, Sweden.

Zebrafish were anesthetized in MS222 (0.03%) in extracellular solution and pinned to their lateral side through the notochord using tungsten needles (Fine Science Tools GmbH, Heidelberg, Germany) in a Sylgard-lined recording chamber. The spinal cord neurons were exposed for patch-clamp recording by removing the muscles over one segment. In order to prevent muscle contraction through the extracellular stimulation, the fish were paralyzed with 6.25µM α-bungarotoxin (Sigma-Aldrich Company Ltd, Gillingham, UK) for 10 minutes prior to the recording. Patch-clamp electrodes were pulled from borosilicate glass (1.5mm outer diameter, 0.87mm inner diameter, Hilgenberg, Malsfeld, Germany) using a PC-10 dual-stage glass micropipette puller (Tritech Research, Inc., Los Angeles, USA). The intracellular solution contained

120mM K^+ gluconate, 5mM KCL, 10mM HEPES, 4mM ATP-Mg^{2+}, 0.3mM GTP-Na^+, 10mM Na^+-phoshpocreatine, pH7.4 with KOH 275mOsm. Yielding residences lay between 8-12MΩ.

Synaptic activity in the spinal cord neurons was induced by extracellular electrical stimulation using a glass electrode placed above the otic vesicle. The synaptic activity of spinal cord neurons was examined in current-clamp as well as voltage clamp. Inward excitatory currents were recorded in neurons held at the reversal potential of chloride-mediated inhibition, at -65mV. Outward inhibitory currents were recorded in neurons held at the reversal potential of Na^+ mediated excitation, at 0mV.

Quantification of myelinated and unmyelinated axons above 0.3µm diameter in the transmission electron micrographs

Tile images of hemi-spinal cords at 4dpf were acquired at the TEM at 3800x magnification and processed as described above. All axons in the hemi spinal cord with a perimeter of approximately 1µm or above were traced and measured in the transmission electron micrographs (TEM) using the lasso and measuring tool in Adobe photoshop CS3 (Adobe, San Jose, CA, USA) and subsequently converted to diameter. Of the axons with a diameter above 0.3µm, the number of myelinated and unmyelinated was quantified. Colour code was added to the TEM images using the lasso and pain bucket tools in Adobe photoshop CS3 (Adobe, San Jose, CA, USA).

Single oligodendrocyte analysis

To generate a transgenic zebrafish with sparse mosaic labelling of individual oligodendrocytes, fertilized eggs were injected between the 1-4hpf with 10ng/µl plasmid DNA encoding mbp:mCherry-caax and 25ng/µl *transposase* mRNA using a Pneumatic Picopump PV830 (World Precision Instruments Ltd, Hertfordshire, UK) and a Micromanipulator M3301R (World Precision Instruments Ltd, Hertfordshire, UK). The expression of the mbp:mCherry-caax has the advantage that the mCherry protein is located in the oligodendrocyte membrane, which is ideal for visualizing the myelin sheaths. Zebrafish embryos with mosaic expression of mbp:mCherry-caax were screened for single oligodendrocytes and imaged at 3dpf and 4dpf. Confocal z-

stacks of single oligodendrocytes were opened in Image J (National institute of health, Bethesda, MD, USA) and the length and number of individual internodes were measured throughout the z-stack using the freehand drawing tool.

Oligodendrocyte counts

In order to quantify the number of oligodendrocytes in the zebrafish spinal cord, z-stacks of a lateral view of spinal cord of Tg(mbp:EGFP) fish were taken at somites 8-11 at 20x magnification. In this line, GFP is expressed in the cytoplasm of oligodendrocytes, which facilitates the quantification of all oligodendrocyte cell bodies. All oligodendrocyte cell bodies were counted throughout the z-stack using the Image J software (National institute of health, Bethesda, MD, USA) count tool.

Timelapse analysis of individual oligodendrocytes

Oligodendrocytes of similar morphology and dorsal spinal cord position were selected in Tg(nkx2.2a:GFP) fish to minimize variability. The timelapse movies were acquired at time intervals of 10 minutes between each frame and at a 2µm interval between the z-stacks, over night between 2-3dpf and 3-4dpf at 20x resolution. The time-lapse movies were processed by maximum intensity projections in the Zen2009 software (Carl Zeiss Microscopy, Oberkochen, Germany). Myelin sheaths were defined as longitudinal sheath like structures >5µm in length that were visible for more than 1 time frame, as these structures >5µm are not just transient axon oligodendrocyte contacts but myelin ensheathments. All structures between 2µm and 5µm in length were counted as small axon-oligodendrocyte contacts <5µm.

For the quantification of the number of myelin sheaths >5µm and small axon-oligodendrocyte contacts <5µm, the number of all myelin sheaths and small axon-oligodendrocyte contacts was measured at each time frame during the movie in Image J (National institute of health, Bethesda, MD, USA). The endpoint of the analysis was 6 hours after first sheath formation for each oligodendrocyte analysed.

The growth rate of individual myelin sheaths was obtained by measuring the myelin sheath length at each time frame during the movie using the free-hand line and measuring tools in Image J (National institute of health, Bethesda, MD, USA). As

each sheath was taken as a unit, each sheath was analysed for 6 hours after its formation.

Oligodendrocyte transplantation

The oligodendrocyte transplantation and imaging described below was performed by Dr. Marion Baraban, at the Centre for Neuroregeneration, Edinburgh.

To generate genetic chimeras, cells were transplanted at blastula stages. Cells were transplanted between controls, from TetTx treated animals to controls and from controls to TetTx treated animals. Cells from the donor embryo were labelled with Oregon Green Dextran (0.2% w/v, Invitrogen, Paisley, UK). In order to quantify myelin sheath number and length per oligodendrocyte, donor embryos used were Tg(mbp:EGFP-caax) and Tg(sox10:mRFP). Transplanted oligodendrocytes that were not associated with axons of transplanted neurons were images using the Zeiss LSM 710 confocal microscope (both from Carl Zeiss Microscopy, Oberkochen, Germany).

2.7 Buffers and stocks

10mM HEPES buffered E3 Embryo medium (2L)

ddH_2O (15MW)	1920ml
50x HEPES	40ml
50x E2 medium	40ml
Adjust to pH 7.2 with NaOH (5M)	

50x HEPES buffer stock (500mM)

HEPES crystals	95.58g
ddH_2O (18MW)	500ml

50x E3 stock solution (1L)

NaCl (250mM)	14.61g
KCl (8.5mM)	0.63g
$CaCl_2$ (16.5 mM)	1.83g
$MgSO_4$ (16.5mM)	4.07g
Make up to 1L with ddH_2O (18MW)	

25x Tricaine stock (100ml solution)

MS222	0.4g
ddH_2O	98ml
Tris buffer (1M, pH 9)	2ml

Tissue preparation for transmission electron microscopy:

Primary fixative (10ml)

Paraformaldehyde (EM grade, 16%)	2.5ml
Glutaraldehyde (EM grade, 25%)	0.8ml
Sodium cacodylate buffer (0.1M)	6.7ml

Secondary fixative for EM (10ml)

Osmium Tetroxide (4%)	5ml
Sodium cocadylate (0.1M)	2.5ml
Imidazole buffer (0.1M)	2.5ml

Imidazole 0.1 M (50ml)	350mg imidazole
	50 ml dH_2O
Sodium Cacodylate Buffer (1M) (40ml)	8.56 g
sodium cacodylate	40 ml dH_2O
Uranyl acetate Saturated solution (~8%) (100ml)	8 g
uranyl acetate	100 ml dH_2O

EMBED with benzyldimethylamine (BDMA)

EMBED	100 ml
Dodecenyl succinic anhydride (DDSA)	45 ml
Methyl-5-norbornene-2,3-dicarboxylic anhydride (NMA)	60 ml
Benzyldimethylamine (BDMA)	6.15ml

Sato's lead stain (50ml)

Lead citrate	0.2g
Lead nitrate	0.15g
Lead acetate	0.15g
Sodium citrate	1g
NaOH (5M)	1.8ml
ddH_2O	48.2ml

2.8 Chemical materials

Embryo medium:

HEPES crystals (N-(2-Hyroxyethyl)piperazine-N'-2-ethanesulfonic Acid, Thermo Fisher Scientific, Waltham, MA, USA)

Sodium chloride, NaCl (Sigma-Aldrich Company Ltd, Gillingham, UK)

Potassium chloride, KCl (Sigma-Aldrich Company Ltd, Gillingham, UK)

Calcium chloride, $CaCl_2$ (Sigma-Aldrich Company Ltd, Gillingham, UK)

Magnesium sulfate, $MgSO_4$ (Sigma-Aldrich Company Ltd, Gillingham, UK)

Tricaine solution

MS222 (Ethyl 3-aminobenzoate methanesulfonate, Sigma-Aldrich Company Ltd, Gillingham, UK)

Tris base (Hydroxymethyl-aminomethane, Sigma-Aldrich Company Ltd, Gillingham, UK)

Embedding during confocal imaging

UltraPure™ Low Melting Point Agarose (Invitrogen, Carlbad, USA)

Construct generation:

One Shot TOP10 Chemically Competent E. coli (Invitrogen, Carlbad, USA)

LB-AGAR Medium (capsules) (MP Biomedicals, LLC, UK)

LB Nutrient Agar powder (Bio-Rad, Hercules, USA)

Multisite Gateway Cloning kit (Invitrogen, Carlbad, USA)

S.O.C. medium (Invitrogen, Carlbad, USA)

Tissue preparation for TEM:

Paraformaldehyde (EM grade, 16%, Ted Pella Inc., Redding, USA)

Glutaraldehyde (EM grade, 25%, Ted Pella Inc., Redding, USA)

Sodium cacodylate (Agar Scientific, Stansted, UK)

Ethanol absolute (EM grade, Sigma-Aldrich Company Ltd, Gillingham, UK)

Acetone absolute (EM grade, Sigma-Aldrich Company Ltd, Gillingham, UK)

Osmium-Tetroxide (Electron Microscopy Sciences, Hatfield, UK)

Uranyl acetate (Taab, Aldermaston, UK)

Embed-812 kit with benzyldimethylamine (BDMA) (Electron Microscopy Sciences, Hatfield, UK)

Lead citrate (Sigma-Aldrich Company Ltd, Gillingham, UK)

Lead nitrate (Sigma-Aldrich Company Ltd, Gillingham, UK)

Lead acetate (Sigma-Aldrich Company Ltd, Gillingham, UK)

Sodium citrate (Sigma-Aldrich Company Ltd, Gillingham, UK)

Sodium hydroxide, NaOH (Sigma-Aldrich Company Ltd, Gillingham, UK)

Microinjections

ddH_2O (Nuclease free water, Qiagen,Manchester,UK)

Phenol-Red (Phenolsulfonphthalein, Sigma-Aldrich Company Ltd, Gillingham, UK)

Olig2 MO microinjections

Olig2 MO, Gene Tools, LLC, Philomath, USA

DEPC-treated H_2O, ultra-pure (Invitrogen, Carlbad, USA)

Phenol-Red (Phenolsulfonphthalein, Sigma-Aldrich Company Ltd, Gillingham, UK)

2.9 Non-chemical materials

Corning® 10 cm petri dishes (Sigma-Aldrich Company Ltd, Gillingham, UK)

Cover glass (Menzel-Glaeser, 22x22mm or 22x50mm, no. 1 thickness (0,13 - 0,16 mm), Braunschweig, Germany)

Super Premium Microscope Slides (VWR International bvba, Leuven, Belgium)

Dow Corning® high-vacuum silicone grease (Sigma-Aldrich Company Ltd, Gillingham, UK)

Performance Microsurgical Blades (Katena, Stockport, UK)

Whatman chromatography paper (Thermo Fisher Scientific, Waltham, USA)

3. Characterizing the myelination fate of individual neurons and the relationship between axon calibre and myelination

3.1 Introduction

Myelination occurs in different areas of the CNS at different times during development and is extremely complex. The onset of myelination varies in different CNS areas and follows a caudorostral gradient in the brain (Yakovlev and Lecours, 1966; Baumann and Pham-Dinh, 2001) and in a rostrocaudal gradient in the spinal cord (Yakovlev and Lecours, 1966; Schwab and Schnell, 1989; Baumann and Pham-Dinh, 2001; Almeida et al., 2011). In humans, the onset of myelination begins in the spinal cord during the second half of fetal life, but peaks postnatally, whereas in other CNS areas, such as the neocortex, myelination (Sakai et al., 2011; Groeschel et al., 2010; Miller et al., 2012), continues into the third decade of life (Miller et al., 2012). The onset of myelination in the rat spinal cord begins at postnatal day 1 and 2 in the ventral funiculus, fasciculus cuneatus and ventro-lateral funiculus (Schwab and Schnell, 1989), and at postnatal days 10 to 12 in areas such as the corticospinal tract, Lissauer tract and the commissures, and continues into adulthood (Schreyer and Jones, 1982; Schwab and Schnell, 1989). In zebrafish, the onset of myelination starts in the end of 2 days post fertilisation (dpf) in the ventral medial hindbrain (Broesamle and Halpern, 2002), in the spinal cord between 2dpf and 3dpf (Almeida et al., 2011), where myelination has also been shown to continue into adulthood (Jung et al., 2010). Together these findings show that different axonal tracts, even in the same CNS area, are myelinated at distinct times during development. However, it is unclear why or how some axonal tracts are myelinated before others. In all CNS areas, oligodendrocytes are presented with a large variety of axons, of different calibre (the cross- sectional size of an axon), neurotransmitter type and state of activity (Hildebrand and Hahn, 1978; Hildebrand, 1993; Murray and Blakemore, 1980; Baumann and Pham-Dinh, 2001). Axons with these different properties are situated in direct proximity to one another (Peters et al., 1991) and the cellular mechanism by which oligodendrocytes choose the axons that they will myelinate from those that remain unmyelinated at each time-point during development is incompletely understood. One of the axonal properties that could influence axon selection during myelination is axon calibre. Axon calibre is one of the main axon properties that determine signal conduction velocity and is therefore a key component of normal nervous system function (Rushton, 1951; Waxman, 1980).

Axon calibre is also very diverse in the vertebrate spinal cord (Matthews and Duncan, 1971; Waxman and Bennett, 1972; Remahl and Hildebrand, 1982; Hildebrand et al., 1993; Perge et al., 2012), ranging from 0.1 to almost 100µm in the Goldfish Mauthner axon (Funch et al., 1981), the largest calibre axon in teleost fish (as reviewed in Bierman et al., 2009). This represents an almost 100,000 fold difference in area. It is generally recognized that large calibre axons tend to be myelinated whereas small calibre axons remain unmyelinated (Friede, 1972) and it was observed that myelinated axon areas have a larger axon calibre than unmyelinated axon areas of the same axon in the cat ventral funiculus of the spinal cord and corpus callosum (Remahl and Hildebrand, 1990). However, from these observations it is unclear whether the axons are myelinated because of their large calibre or whether the axon calibre is increased due to axon-oligodendrocyte signalling during myelination. In the first case, the biophysical property of the axon's calibre itself would be a property that facilitated or even drove ensheathment and myelination. In the latter case, all axons would be of similar calibre prior to myelination and only after myelin ensheathment would they expand their axon calibre, thereby creating the diverse range of axon calibres in the CNS. There is experimental evidence for both of these potential cellular mechanisms and I will introduce them briefly below.

Axon calibre as a mechanism to induce myelination

Axon calibre is linearly correlated with signal conduction velocity so that a doubling of the axon diameter results in the doubling of the conduction speed (Hursh, 1939; Rushton, 1951; Waxman and Bennett, 1972, Hildebrand, 1993; Waxman, 1997). The action potential firing rate has also been shown to increase with the axon calibre, ranging from ~1hz in unmyelinated olfactory fibre axons of 0.35µm diameter to 40hz in myelinated foliar tract axons of 1.3µm in the cerebellum and even 60->100hz in myelinated vestibular axons of 3-9µm (Perge et al., 2012). To accommodate high conduction velocity and action potential firing rates without myelin, a vertebrate organism would have to economise on the number of large calibre axons that the nervous system could contain within its endoskeleton (Hildebrand, 1993; as reviewed in Hartline and Colman, 2007). The evolution of myelin and salutatory conduction in

vertebrates increased nerve impulse conduction velocity over 20-fold for axons of the same cross sectional size (Werner et al., 2013), thereby allowing smaller calibre axons to transmit nerve impulses without decline in conduction velocity. It is possible that saltatory conduction in very small calibre axons might not confer significantly enhanced impulse transmission and very small calibre axons are therefore not myelinated (Waxman, 1997; Perge et al., 2012). Furthermore, signal propagation requires a high amount of energy from the neuron's expenditure as ion transporters, such as Na^+/K^+ ATPases and Na^+/Ca^{2+} exchangers are required to restore the resting potential after action potential generation (Hildebrand et al., 1993; Waxmann, 1997; Howarth et al., 2012). By propogation of action potentials by saltatory conduction, fewer active ion transporters are required as membrane depolarization is restricted to nodes of Ranvier and the transporters are localized to the axon sites adjacent to the node of Ranvier (Ritchie, 1982; Hildebrand et al., 1993; Waxmann, 1997). Thus, action potential generation is much more energy efficient in myelinated axons. It is therefore conceivable that large calibre axon with a high action potential firing rate (Perge et al., 2012) and the requirement of rapid signal conduction are more likely to be myelinated in order to preserve cellular energy and to optimize signal conduction.

In the PNS, the calibre of an axon correlates strictly with its myelination status. Axons above a threshold of ~1µm in diameter are myelinated, whereas axons smaller than that are not myelinated (Sherman and Brophy, 2005). Furthermore, myelination in the PNS can be induced when axon calibre of normally unmyelinated axons is experimentally enlarged in the rat superior cervical ganglion (Voyvodic, 1989). Myelination in the CNS, however, does not occur according to such a threshold. Myelinated as well as unmyelinated axons in the axon calibre range between 0.3µm and 0.9µm are found in the same spinal cord areas. However, almost all large calibre axons with a calibre above 0.9µm are myelinated (see Chapter 4; Matthews and Duncan, 1971; Waxman and Bennett, 1972; Remahl and Hildebrand, 1982; Hildebrand et al., 1993), indicating that while axon calibre might not be the only factor influencing myelination, it might be an axon property that influences axon selection during myelination. Oligodendrocytes in vitro are even able to differentiate in complete absence of axonal signals (Raff, et al., 1985), and even produce myelin

basic protein (MBP) and form myelin like membrane sheets at the tips of their oligodendrocyte processes (Knapp et al., 1987). Oligodendrocytes have even been shown to form compact myelin around paraformaldehyde treated DRG axons (Rosenberg et al., 2008) and in mono-culture form myelin like structures around inert polystyrene fibres (Lee et al., 2012). Interestingly, in the absence of axonal signals, the polystyrene fibres were only ensheathed by myelin like structures if the fibre calibre was above 0.4µm (Lee et al., 2012). This indicates that, in the complete absence of axonal signals, the physical size of axon calibre alone can indeed facilitate myelination by oligodendrocytes.

In vivo, it has been observed that the largest calibre axons in the mouse spinal cord are myelinated at P1, whereas smaller calibre axons are not myelinated before P20 (Hildebrand et al., 1993), indicating that the largest calibre axons in the CNS are also the first to be myelinated. In the rat optic nerve, axon calibre increases in a strict gradient, where the area close to the eye is a multi-fold larger than the area close to the chiasm, and it has been shown that myelination occurs in the same gradient, even though oligodendrocyte differentiation occurs in the reverse gradient, from chiasm to the eye, suggesting that oligodendrocyte differentiation is not the only criterion for the onset of myelination, but that axon calibre plays an important role during myelination in vivo (Colello et al., 1995). However, these data were obtained from imaging sections at different time-point during the development by transmission electron microscopy (TEM) or immuno fluorescent imaging. While TEM is a very reliable technique to obtain accurate axon calibre and myelin thickness at high resolution, it has only limited temporal resolution. The difficulty in elucidating the causal relationship between axon calibre and myelination at high, single cell resolution by using tissue sections is that the calibre of an individual myelinated axon can only be measured at a single time-point either before or after the axon has been myelinated, rather than before and after myelination. It is therefore unclear, whether individual myelinated axons of large calibre are myelinated because of their axon size or whether the axon calibre has increased due to the myelin ensheathment.

A recent in vivo experiment using time-course analysis of the fluorescent zebrafish reporter line Tg(mbp:GFP-caax) showed that the very large caliber Mauthner axon is also the first axon to be myelinated (Almeida et al., 2011). Importantly, the Mauthner

axon has been shown to have a relatively large axon caliber between 0.6µm and 1.2µm at 18-20hpf, even before the axon has reached its full length (Jontes et al., 2000; Kimmel et al., 1982), indicating that the axon calibre is already relatively large prior to the onset of myelination. Furthermore, when supernumery Mauthner neurons and their large caliber axons are experimentally added to the zebrafish spinal cord by temporary reduction of Notch1a function during development or by injection of *hox1b* mRNA, all Mauthner axons were robustly myelinated without an increase in oligodendrocyte number in the spinal cord (Almeida et al., 2011). The addition of these supernumery large caliber Mauthner axons led to an increase of myelin sheaths formed per oligodendrocyte. This finding suggests that axons of large calibre can influence the myelinating capacity of oligodendrocytes and that large axon calibre can induce myelin ensheathment. However, axon calibre in this study was not measured during the time-course and it is possible that the axon calibre of the Mauthner axons expanded in size after the onset of myelination.

Overall, these findings suggest that axon calibre might be determined to some extent prior to the onset of myelination and that the axon calibre might regulate whether an axon is myelinated. However, more single cell analysis of different individual axons before the onset of myelination and after myelination is required in order to elucidate the precise mechanism behind axon calibre growth before and after myelination and the role that myelin ensheathment can play during axon calibre growth.

Oligodendrocyte signaling as a mechanism to induce axon calibre growth

There is a wide range of small calibre and large calibre axons in the CNS between 0.3µm and 0.9µm that can be both myelinated and unmyelinated (see Chapter 4; Matthews and Duncan, 1971; Waxman and Bennett, 1972; Remahl and Hildebrand, 1982; Hildebrand et al., 1993) and it is generally unknown whether axon calibre of myelinated and unmyelinated axons is differentially regulated in the CNS (Hildebrand, 1993). It has been shown that after axons make synaptic contacts, the synthesis of neurofilament subunits is increased and the rates of neurofilament axonal transport increases several-fold leading to an increase in axon calibre (Hoffman et al., 1983; Willard and Simon, 1983). This indicates that axon calibre is regulated to some extent by the amount of synaptic connections that an axon forms.

Even along the same axon, however, the axon calibre is not uniform and axon areas of larger calibre have been observed to coincide with myelinated areas that are ensheathed by oligodendrocyte or Schwann cell processes (Remahl and Hildebrand, 1990; Sanchez et al., 1996), leading to the hypothesis that axon-glial interactions during myelin ensheathment could increase axon calibre locally in addition to neuron intrinsic mechanisms. However, it is unclear whether the axon calibre is expanded due to axon-glial interactions in myelinated axon areas or whether axon areas of large calibre are myelinated because of their physical size or the expression of signalling molecules that correlate with calibre.

Early studies using a series of cross-sections of optic nerve axons from juvenile and adult mice and rats imaged by TEM revealed that axonal cytoskeleton composition is primarily comprised of neurofilament and microtubules (Friede and Samorajski, 1970). Furthermore, the ratio of microtubules to neurofilament number was shown to correlate with the axon calibre, whereby small calibre axons had a higher number of microtubules and a lower number of neurofilaments while larger caliber axons had a lower number of microtubules and a higher number of neurofilaments, indicating that axon calibre size may primarily depend on the number of neurofilament in the axon (Friede and Samorajski, 1970; Hoffman et al., 1985; Lasek et al., 1985; Yamasaki et al., 1992). Interestingly, the microtubule to neurofilament ratio was found to be higher in unmyelinated axons than in myelinated axons, suggesting that the axonal cytoskeleton might undergo changes after myelin ensheathment. However, the TEM images were only taken at 2 different time-points during the development and evidence for a causative role for myelin ensheathment in changing the axonal cytoskeleton and thereby increasing axon calibre is still missing. In neurons, 3 neurofilament subunits, the neurofilament light (NF-L), neurofilament medium (NF-M) and neurofilament heavy (NF-H), named after their molecular mass, assemble to generate neurofilaments (Hoffman and Lasek, 1975; Nixon et al., 1998; Zhu et al., 1997; Elder et al., 1998; Barry et al., 2012) and the composition of the neurofilament hetero-polymers generally varies with the developmental stage of the neuron (Shaw and Weber, 1982; Shen et al., 2010). Mice with a null mutation in all neurofilament subunits (Zhu et al., 1997) or only in NF-M (Elder et al., 1998a) or NF-H (Elder et al., 1998,b), show a decrease in axon calibre of myelinated L5 lumbar root axons in

adult mice (Zhu et al., 1997; Elder et al 1998, a and b; Elder et al., 2001), suggesting that these subunits are required for radial growth. NF-M and NF-H have distinctively long carboxyl-terminal domains that have been shown to become highly phosphorylated after the newly synthesized neurofilaments are integrated into the axon of retinal ganglion cells by immuno-labeling of phosphorylation-dependent neurofilament epitopes (Nixon et al., 1998). Furthermore, axon calibre has been shown to increase according to the phosphorylation state of NF-M and NF-H along the axon through an increase in lateral spacing between the neurofilaments within the axon (Nixon et al., 1998). Interestingly, myelination of the retinal ganglion axons coincided with the same axonal region in which the axon calibre started expanding, approximately 150µm from the eye, and importantly, unmyelinated optic nerve axons showed no neurofilament accumulation and calibre expansion (Nixon et al., 1998), indicating the myelin ensheathment might promote neurofilament phosphorylation and axon calibre expansion. But here again, the cryostat sections only showed the axon calibre at one time-point after myelination and it is unclear whether the neurofilament phosphorylation and axon calibre expansion occurred before the myelin ensheathment or because of it. More recent studies, in which either the NF-M or NF-H were replaced with subunits missing the COOH tails that extend from the neurofilament surface and contain the phosphorylation sites, resulted in a decreased axon calibre of L5 lumbar root motor axons but only in mice with deficient NF-M COOH terminus, whereas axon calibre in NF-H deficient mice was not impaired in 6 month old adults (Garcia et al., 2003; Garcia et al., 2009; Rao et al., 2003). These findings suggest that the NF-M COOH terminus is the critical domain regulating axon calibre.

In the PNS, hypomyelination in Trembler mice, caused by a disruption of peripheral myelin protein 22 (PMP-22) expression (Suter et al., 1992), an important myelin protein in PNS myelin, has been shown to reduce axonal neurofilament phosphorylation and increase neurofilament densities (de Waegh and Brady, 1990; de Waegh et al., 1992), leading to a decrease in axon diameter (Pollard and McLeod, 1980; Perkins et al., 1980). This was even the case in nerve grafts, in which a 7mm long segment of the Trembler sciatic nerve, including Trembler Schwann cells, was inserted between the stumps of a control sciatic nerve, leading to a reduction in

neurofilament transport and phosphorylation specifically in the grafted nerve area, while the control segments adjacent to the grafted Trembler segment remained unperturbed (de Waegh et al., 1992). This study indicates that axon calibre in the PNS can be directly increased through local axon-glial interactions. Similarly, hypomyelination either induced by diphtheria toxin A expression or SV40 large T antigen under the peripheral myelin protein zero gene (P0) promoter has also been shown to lead to neurofilament dephosphorylation and reduction of axonal diameter in the sciatic nerve (Cole et al., 1994). Diphtheria toxin A expression under the P0 promoter led to the ablation of myelinating Schwann cells (Messing et al., 1992; Cole et al., 1994) and severe hypomyelination, while expression of SV40 large T antigen under the P0 promoter inhibited Schwann cell differentiation to some extent and resulted in a mild hypomyelination. Interestingly, the degree of neurofilament dephosphorylation and axon calibre reduction correlated with the severity of hypomyelination in the two mutant lines (Cole et al., 1994). Together, these studies indicate that local axon-glial interactions mediated by myelin ensheathment can regulate neurofilament phosphorylation and axon calibre growth in the PNS. Furthermore, mice lacking mTor, a kinase important for normal cell growth and differentiation, in murine Schwann cells showed normal Schwann cell differentiation and axon sorting, but showed a deficit in myelin ensheathment resulting from a decrease in P0 expression (Sherman et al., 2012). Quadriceps nerves in these mutants had normal axon diameters before the initiation of myelination, but showed retarded axonal growth in diameter after the onset myelination as a result of a decrease in neurofilament phosphorylation (Sherman et al., 2012). This finding also suggest that axon calibre growth in the PNS is regulated independently of myelin ensheathment before the onset of myelination but is increased after the onset of myelination by axon-glial interactions mediated by myelin ensheathment. Mice with a null mutation in the myelin-associated glycoprotein (MAG), which does not result in hypomyelination, also have a reduced axon calibre as well as decreased neurofilament spacing and phosphorylation, indicating that specific myelin proteins can induce the neurofilament changes associated with axon calibre growth (Yin et al., 1998). Overall, these findings suggest that the axon calibre growth in PNS axons

after myelination can be increased by axon-glial signals, which are likely transmitted by specific myelin proteins in the Schwann cell myelin sheath.

The role of myelin ensheathment by oligodendrocytes in regulating axon calibre in the CNS is less well understood. A study in rodent optic nerve applying unilateral x-irradiation to ablate OPCs and their progeny led to smaller axon calibre in optic nerve axons compared to the non-irradiated side (Colello et al., 1994). The reduction in axon calibre, however, was small and might reflect a side effect of the x-irradiation rather than a direct effect of the absence of myelinating oligodendrocyte signaling as the non-irradiated optic nerve was the only control in this study. Furthermore, from this study, it is unclear whether the extrinsic signal that might underlie axon calibre growth in the CNS is emitted from the oligodendrocyte themselves or triggered by myelin proteins in the myelin sheath after ensheathment. Another study investigating the relationship between axon calibre and myelination in the optic nerve under normal conditions, reported that the axon calibre of myelinated axons is increased in comparison to unmyelinated axons, while axon that are ensheathed by oligodendrocyte membrane but not yet fully myelinated with compact myelin are of intermediate calibre (Sanchez et al, 1996). The fact that axons that are wrapped by oligodendrocyte membrane but not yet myelinated are of intermediate calibre was interpreted in a way that oligodendrocyte contact with axons alone can trigger axon calibre growth even before myelin sheath compaction. However, this data was based on TEM images from 3 time-points, at P9, P16 and P21 after the onset of myelination and it is unclear whether the large calibre axons were myelinated because of their calibre size or whether their calibre expanded due to the myelin ensheathment. It is possible that the axons of intermediate calibre are simply myelinated at a later time-point than large calibre axons and were therefore in the process of being ensheathed by oligodendrocytes at the time-point of analysis. Hypomyelination caused by a naturally occurring mutation in myelin basic protein (MBP), an important myelin protein essential for myelin sheath compaction, in *Shiverer* mice (Readhead and Hood, 1990, as reviewed in Nave, 1994) resulted in decreased phosphorylation of neurofilaments as well as neurofilament accumulation and thereby a reduced axon calibre in the retinal ganglion axons that were completely unmyelinated (Sanchez, 1996). This finding indicates that axon calibre growth in the

CNS could indeed be regulated by axon-oligodendrocyte interaction during myelination. Oligodendrocytes in Shiverer mice fail to assemble compact myelin, which leads to hypomyelination (Rosenbluth, 1980), they can, however, form uncompacted, sheath like structures around axons, in which non-compact myelin proteins like CNPase are found (Aggarwal et al., 2011), and axons that were ensheathed by oligodendrocyte membrane but not fully myelinated with compact myelin in *Shiverer* mice showed normal axon calibre size in the optic nerve at P21 (Sanchez et al., 1996; Sanchez, 2000). Again, this data is based on TEM images of a single time-point and it therefore is unclear whether oligodendrocyte contact alone can induce the axon calibre expansion or whether these axons were able to reach a normal axon calibre independently of and prior to oligodendrocyte contact. In the latter case, the relatively large axon calibre could in turn have been the axonal property that attracted the oligodendrocyte process to ensheath the axon, even in absence of myelin basic protein expression.

Together, the studies described above suggest that axon-oligodendrocyte contact might regulate CNS axon calibre in vivo. However, direct evidence is still missing and it is difficult to draw conclusions about whether axon calibre is the result or the causation of myelin ensheathment based on studies with limited temporal resolution of data points after the onset of myelination. There is a wide range of small calibre and large calibre axons in the CNS that can be both myelinated and unmyelinated (see Chapter 4; Matthews and Duncan, 1971; Waxman and Bennett, 1972; Remahl and Hildebrand, 1982; Hildebrand et al., 1993) and it is unknown whether the calibre of myelinated axons with small calibre is smaller simply because they have been myelinated at a later time-point than larger calibre axons and they will grow in calibre over time or whether the calibre of small myelinated axon remains small because the axon calibre is not regulated by extrinsic signals emitted by oligodendrocytes and myelin ensheathment. Quantification of axon calibre of individual myelinated and unmyelinated neurons before the onset of myelination and after the onset of myelination will reveal whether myelin ensheathment can indeed influence axon calibre growth. Investigating individual myelinated axons of different neuron subtypes will also reveal whether this is the case for all myelinated neurons. Furthermore, investigating axon calibre growth in the complete absence of

oligodendrocyte lineage cells will reveal whether axon-oligodendrocyte contact itself can induce axon calibre growth. These analyses will help to elucidate whether axon calibre growth is generally regulated by extrinsic signals emitted from oligodendrocytes or determined by neuron intrinsic or circuitry specific properties.

The neurons investigated in this chapter

Previous studies primarily investigated axon calibre growth in context of myelination using electron micrographs of transversal section of the brain or spinal cord. While this is a great technique to accurately measure axon calibre size at one time-point, it does not give any information on axon calibre and general axonal morphology before and after myelination or on what types of axons are fated for myelination or remain unmyelinated. Although a lot is known about axonal outgrowth and axonal path-finding mechanism (for reviews see Raper and Mason 2010) in neurons as well as the development of OPCs and myelinating oligodendrocyte (for reviews see Emery 2010; He and Lu 2013), relatively little is known about the differential development of axons fated for myelination and those axons which remain unmyelinated in the CNS. To this date, the morphological differences between CNS axons that will be myelinated and those that remain unmyelinated are unknown. Defining the individual axons that will be myelinated during the onset of myelination and those that will not has been difficult in previous studies due to the inaccessibility and complexity of the mammalian CNS. In order to investigate whether axons of neurons fated for myelination have a different axon morphology and calibre compared to axons of neurons not fated for myelination, single neurons should be investigate before and after the onset of myelination. Zebrafish are an ideal model organism for this, as they are transparent during embryonic development, which allows the labeling and live imaging of individual neurons and their axon morphology before and after the onset of myelination. Previous studies employing the advantages of the zebrafish as a model organism (see chapter 1, Introduction), have independently investigated neuronal development (Bernhardt et al., 1990; Hale et al., 2001; Higashijima et al., 2004), oligodendrocyte development (Kirby et al., 2006) and myelination (Almeida et al., 2011; Czopka et al., 2013) at single cell resolution. But how these three components interact during myelinated axon formation in the CNS remains

unknown. Here, I investigate the development of single axons in the context of myelination in vivo, for the first time. The neurons in the zebrafish spinal cord have previously been classified and described with respect to their morphology (Bernhardt et al., 1990; Clarke et al., 1984; Hale et al., 2001; Kuwada et al., 1990; Mendelson, 1986) and neurotransmitter type (Higashijima et al., 2004). In this study, reticulo spinal (RS) neurons (Mendelson, 1986), Rohon Beard (RB) sensory neurons (Clarke et al., 1984), commissural primary ascending (CoPA) interneurons, circumferential descending (CiD) interneurons, circumferential ascending (CiA) interneurons, commissural bifurcating longitudinal (CoBL) interneurons (for a detailed description of the individual neurons) see chapter1 Introduction) were selected based on their unique morphologies and positions within the spinal cord. Some of these neurons are myelinated during the early zebrafish development, while some are not. I investigate the axon calibre of these neurons before and after the onset of myelination and quantify their myelin ensheathment, or lack of, over time. Furthermore, I characterize the differences in axon morphology of these neurons over time. Finally, I investigate axon calibre growth in the absence of oligodendrocyte contact and myelination by blocking OPC differentiation to myelinating oligodendrocytes using a translation-blocking antisense morpholino oligonucleotide (MO) against Olig2 that has previously been described (Zannino and Appel, 2009).

3.2 Results

3.2.1 Labelling of individual neurons by mosaic GFP or Kaede expression.

CNS myelination is an ongoing process that starts during early development and continues into adult life (Miller et al., 2012). Although distinct axonal tracts have been shown to be myelinated at different times during development (Schreyer and Jones, 1982; Schwab and Schnell, 1989), the differential development of myelinated and unmyelinated axons is still unclear.

In order to identify the neuronal subtypes that are fated to be myelinated during early zebrafish development and to characterize their axonal phenotype, I either used the Tg(s1011:Gal4,UAS:Kaede) (Scott et al., 2007), which expresses the fluorescent reporter protein Kaede in the cytoplasm of a subset of spinal cord neurons or I labelled individual neurons by mosaic GFP expression using the Gal4-UAS system (Asakawa and Kawakami, 2008; Halpern et al., 2008). The transgenic lines Tg(HuC:Gal4) and Tg(Cntn1b:KalTA4) drive Gal4 in neurons and a subset of neurons, respectively. By injecting plasmid DNA containing UAS driving fluorescent reporter proteins, such as GFP, in the HuC:Gal4 and Cntn1b:KalTA4 lines, the fluorescent protein is mosaically expressed in individual neurons (Figure 3.1, A). One of the plasmids containing a UAS driving the fluorescent reporter protein was UAS:GFP, which expresses GFP in the cytoplasm of Gal4 positive cells. The other plasmid used in this chapter was UAS:GFP-cntn1a, a protein in which GFP was fused to contactin1a (cntn1a). Cntn1a is one of the two zebrafish homologs (cntn1a and cntn1b) of mammalian Cntn1 (Haenisch et al., 2005). It is a member of the immunoglobulin superfamily of recognition molecules expressed in neurons and glia cells (Schweitzer et al., 2006) and is linked to the cell membrane through a glycosylphosphatidylinositol (GPI) anchor (Haenisch et al., 2005; Schweitzer et al., 2006). Axonal cntn1 has been described to fulfil multiple functions including roles in axon growth (as reviewed in Falk et al., 2002) and promoting oligodendrocyte differentiation through binding to the notch receptor (Hu et al., 2006). Importantly, axonal cntn1 is a membrane protein in the paranodal junction that forms a cell-recognition complex with another axonal membrane protein Caspr and binds to their glial partner neurofascin 155, a mechanism essential for the formation of the axon-glial junction at the paranodes during myelination (as reviewed in Poliak and Peles,

2003; Sherman and Brophy, 2005). Neurons expressing GFP-cntn1a are labelled by GFP anchored to the cell membrane by the GPI-anchor of cntn1a. Importantly, the GFP expression anchored to the cell membrane of neurons specifically disappeared after the myelin ensheathment of that part of the axon (Figure 3.2). This could even be seen to be the case when the oligodendrocyte cell membrane made first contact with the axon, even before full myelin ensheathment and compaction of the myelin sheath (Figure 3.2, bottom, middle). While the precise mechanism by which the paranodes and nodes of Ranvier are formed during myelination is not completely known (Sherman and Brophy, 2005), the expression pattern of GFP-cntn1a during myelination indicates that the zebrafish cntn1a protein is actively excluded from the axonal membrane in the internode and localised to the nodes of Ranvier after myelin ensheathment.

The cytoplasmic expression either of the Kaede protein in the Tg(s1011:Gal4,UAS:Kaede) line or of UAS:GFP in individual neurons had the advantage of a very bright fluorescent protein expression, which allowed me to visualize and describe the individual morphologies of the different neuronal subtypes. Furthermore, it allowed me to measure axon calibre of myelinated and unmyelinated axon areas (Figure 3.1, B). The UAS:GFP-cntn1a expression anchored to the unmyelinated neuronal membrane had the advantage that upon myelin ensheathment, GFP expression was excluded from the internode and only unmyelinated areas of the axons were visible (Figure 3.2, A and B). UAS:GFP-cntn1a is therefore an excellent tool to quantify myelin ensheathment along the axon and to measure axon calibre before myelin ensheathment. The localization of the GFP-cntn1a protein anchored to the cell membrane resulted in a clear outline of the cell, ideal for measuring axon calibre. There are, however, two disadvantages in using GFP-cntn1a to measure axon calibre. First, the myelinated axon area is not visible and therefore only unmyelinated axon areas can be measured. Second, the GFP expression anchored to the membrane of GFP-cntn1a expressing neurons is relatively dim in comparison to the cytoplasmic GFP expression and measuring axon calibre of small calibre axons requires good fluorescent protein expression. As the different localization of fluorescent proteins might affect the axon calibre measurements, axon calibre (measured in axons of CiD neurons as a test example)

with cytoplasmic fluorescent protein expression and with fluorescent protein expression anchored to the membrane was compared (Figure 3.3, A). The average axon calibre was not significantly different in CiD neurons at 3-5dpf and 6-12dpf when labelled by cytoplasmic fluorescent protein expression or by fluorescent protein expression anchored to the membrane (Two-way ANOVA, p = 0.93) (Figure 3.3, B). Thus, in subsequent analyses, axon calibre measurements using Tg(s1011:Gal4,UAS:Kaede) and UAS:GFP or UAS:GFP-cntn1a to label individual neurons were combined in the analysis of axon calibre of individual neurons over time.

Furthermore, the different localization of fluorescent proteins either in the cytoplasm or anchored to the cell membrane might affect the number of axon branches visible along the axons. The number of axon branches per 100µm were therefore quantified using either Tg(s1011:Gal4,UAS:Kaede) and UAS:GFP to express GFP in the neuron cytoplasm or UAS:GFP-cntn1a to express GFP anchored to the cell membrane. The average branch number per 100µm in axons of CiD neurons labelled by cytoplasmic fluorescent protein expression was 1.7 +/- 1.4 at 3-5dpf and 1.76 +/- 0.6 at 6-12dpf and the average axon branch number per 100µm labelled by GFP anchored to the cell membrane was 1.72 +/- 1.3 at 3-5dpf and 1.3 +/- 0.78 at 6-12dpf (Tg(s1011, UAS:Kaede) or UAS:GFP 3-5dpf n = 24, 6-8dpf n = 3; UAS:GFP-cntn1a 3-5dpf n = 5, 6-8dpf n = 6; Two-way ANOVA, p = 0.67) (Figure 3.3, C). The average axon branch number per 100µm in CiD axons was therefore not significantly different. Thus, in subsequent analyses, Tg(s1011:Gal4,UAS:Kaede) and UAS:GFP or UAS:GFP-cntn1a was used to label individual neurons in the quantification of the axon branch number per 100µm in individual neurons over time.

In order to identify which of the neurons analysed are fated for myelination and which neurons remain unmyelinated, I used Tg(s1011:Gal4,UAS:Kaede) or the Gal4 driver lines Tg(HuC:Gal4) and Tg(cntn1b:KalTA4)) together with the transgenic Tg(sox10:mRPF) line, which labels oligodendrocytes and myelin sheaths (Figure 3.1 and 3.2). Thus, in the subsequent analyses, myelin ensheathment of the axons of the different neuronal subtypes over time was measured using Tg(s1011Gal4,UAS:Kaede)xTg(sox10:mRFP) or Tg(HuC:Gal4)xTg(sox10:mRFP)

and Tg(cntn1b:KalTA4)xTg(sox10:mRFP) injected either by the UAS:GFP or UAS:GFP-cntn1a plasmid.

Based on observations in the optic nerve that myelinated areas are larger in calibre than unmyelinated areas along the same axon, it has been proposed that myelin ensheathment can locally increase the axon calibre of the myelinated area (Remahl and Hildebrand, 1990; Sanchez et al., 1996). Myelinated and unmyelinated areas along the same axon in CiD neurons were therefore compared using either the transgenic Gal4 driver lines Tg(HuC:Gal4)xTg(sox10:mRFP) or Tg(cntn1b:KalTA4)xTg(sox10:mRFP) injected with the UAS:GFP plasmid or the transgenic line Tg(s1011Gal4,UAS:Kaede)xTg(sox10:mRFP) to label neurons with cytoplasmic GFP expression in a background with labelled myelin (Figure 3.3, D). The average axon calibre of the myelinated axon areas was 0.52 +/- 0.12µm at 3-5dpf and 0.47 +/- 0.12 at 6-12dpf and the average axon calibre of unmyelinated areas along the same axons was 0.55 +/- 0.12µm at 3-5dpf and 0.50 +/- 0.18 at 6-12dpf (Tg(s1011, UAS:Kaede) or UAS:GFP labelled axons on which myelinated areas were measured 3-5dpf n = 22, 6-8dpf n = 16; axons on which unmyelinated areas were measured 3-5dpf n = 17, 6-8dpf n = 7) (Figure 3.3,E). Thus, in contrast to in the optic nerve, myelinated areas and unmyelinated areas along the same axon in CiD neurons did not vary in axon calibre (Two-way ANOVA, p = 0.47) (Figure 3.3,E). Axon calibre was therefore measured independently of whether the axon area was myelinated or not in the subsequent analyses.

The onset of myelination occurs between 2dpf and 3dpf in the zebrafish spinal cord, when the largest calibre axon, the Mauthner axon is myelinated (Almeida et al., 2011). Other, smaller calibre axons are myelinated from 3dpf onwards and by 6dpf, there is robust myelination in the zebrafish spinal cord (Almeida et al., 2011). In order to characterize axon calibre and myelin ensheathment of the different neurons over time, the time-points for measurements of the individual neurons were binned to before the onset of myelination at 2dpf, during the onset of myelination at 3-5dpf and after the onset of myelination at 6-12dpf.

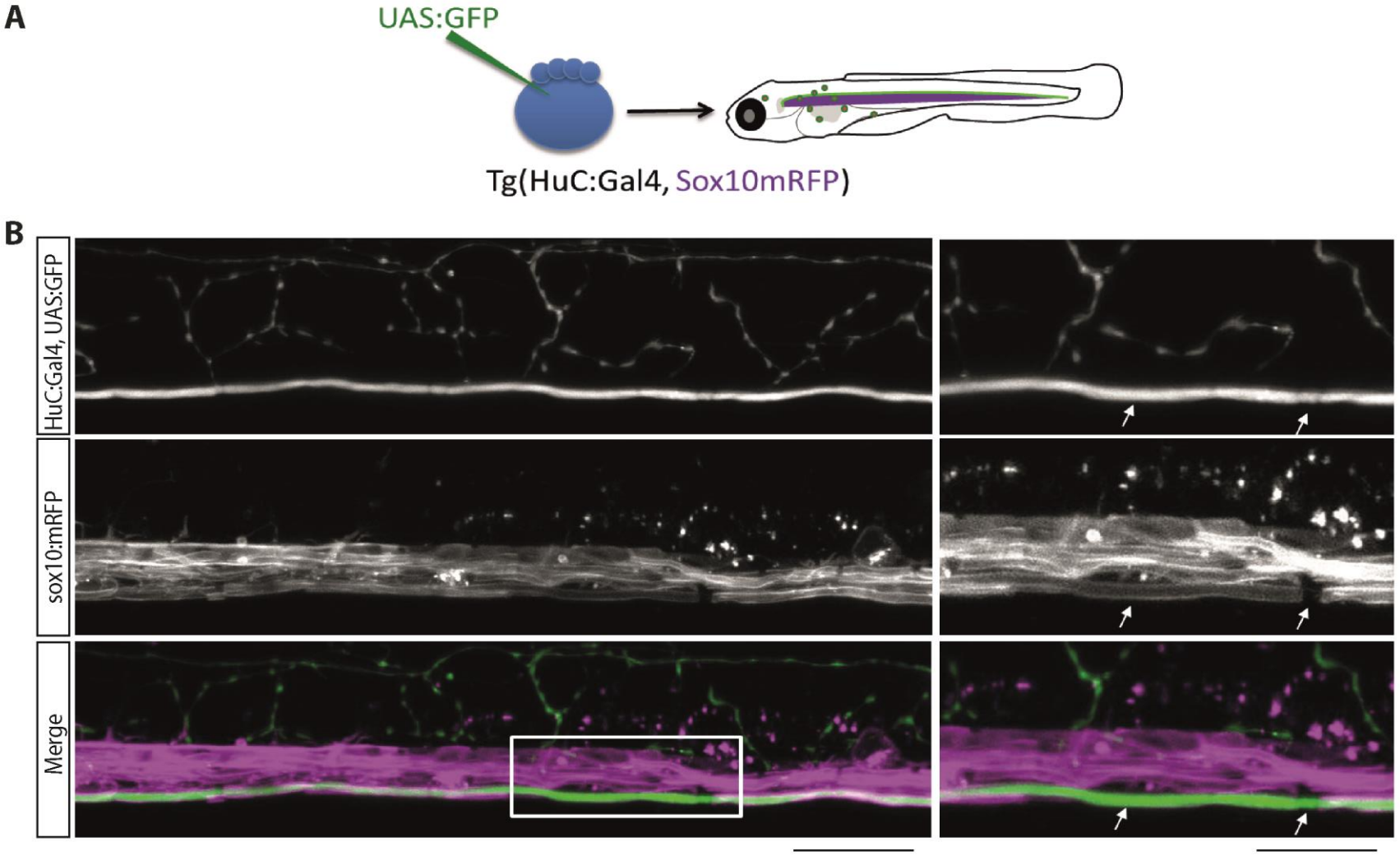
A
UAS:GFP
Tg(HuC:Gal4, Sox10mRFP)
B
HuC:Gal4, UAS:GFP
sox10:mRFP
Merge

Figure 3.1: Cytoplasmic labelling of individual neurons. (A) Injection scheme. 10pg of UAS:GFP was injected into Tg(HuC:Gal4)xTg(sox10:mRFP). (B) Reticulospinal neuron labelled with cytoplasmic GFP in a background of labelled myelin sheaths shows the myelinated areas along axon (left, scale bar = 30um). Zoom in shows the axon area marked with a rectangle on the left (right, scale bar = 20um). Arrows indicate myelinated areas along the axon, while the star indicates an area between two myelin sheaths, which is likely a node of Ranvier.

A
GFP-cntn1a
sox10:mRFP
Merge
B
GFP-cntn1a
sox10:mRFP
Merge

Figure 3.2: Labelling of individual neurons using the GPI anchored fusion protein UAS:GFP-cntn1a. (A) Example reticulospinal neuron labelled by UAS:GFP-cntn1a driven by huC:Gal4 in a Tg(sox10:mRFP) background. GFP is anchored to the cell membrane through the GPI anchor of cntn1a (top, scale bar = 20um) and is extruded in myelinated areas (see white rectangles). Images such as this were used to measure the myelinated areas along axons and axon calibre of unmyelinated areas. (B) Zoom in shows the axon area marked with a rectangle in A (bottom, scale bar = 10um). Arrows indicate myelin sheaths and the concordant extrusion of GFP from the cell membrane in the myelinated area (bottom left, middle and right). GFP is also extruded in areas of axon-oligodendrocyte contact where the axon is not yet fully wrapped (bottom, middle).

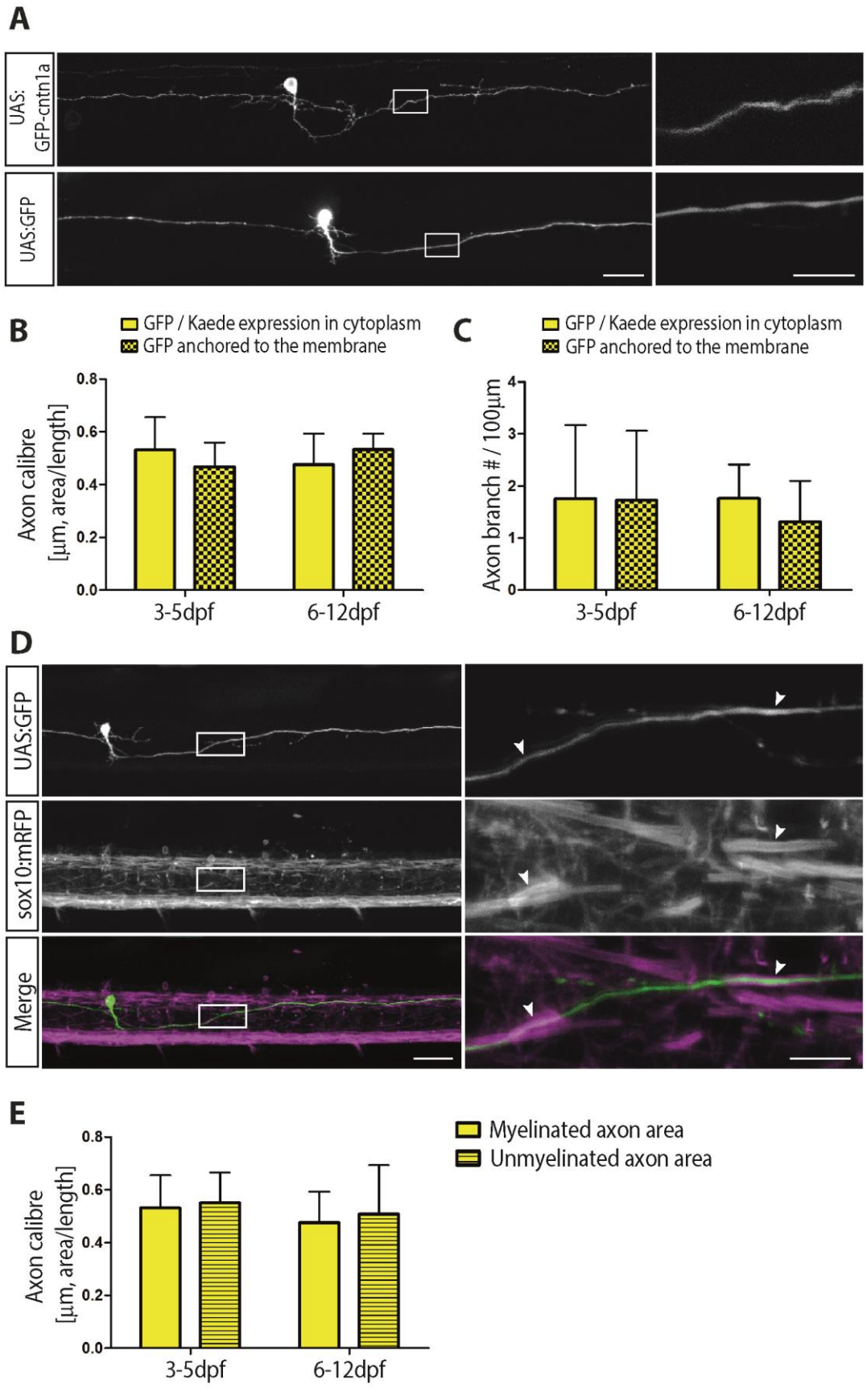
A
UAS: GFP-cntn1a
UAS:GFP
B
GFP / Kaede expression in cytoplasm
GFP anchored to the membrane
Axon calibre [µm, area/length]
0.8
0.6
0.4
0.2
0.0
3-5dpf
6-12dpf
C
GFP / Kaede expression in cytoplasm
GFP anchored to the membrane
Axon branch # / 100µm
4
3
2
1
0
3-5dpf
6-12dpf
D
UAS:GFP
sox10:mRFP
Merge
E
Axon calibre [µm, area/length]
0.8
0.6
0.4
0.2
0.0
3-5dpf
6-12dpf
Myelinated axon area
Unmyelinated axon area

Figure 3.3: The axon calibre of CiD neurons is the same using cytoplasmic and membrane anchored GFP labelling and in cytoplasmic GFP labelled myelinated and unmyelinated areas along the axon. (A) CiD neuron labelled by UAS:cntn1a with GFP expression in the cell membrane and a CiD neuron labelled by UAS:GFP with GFP expression in the cytoplasm, both at 3dpf . Zoom in on the right side shows the axon area marked with the white rectangle on the left side (left scale bar = 10µm, right scale bar = 5µm). Images like this were used to measure axon calibre over time. (B) Quantification of axon calibre between 3-5dpf and 6-12dpf, measured in axons labelled with cytoplasmic fluorescent protein expression using either Tg(s1011, UAS:Kaede) or UAS:GFP compared to membrane anchored GFP expression using UAS:GFP-cntn1a. The average axon calibre of CiD neurons labelled with either Tg(s1011, UAS:Kaede) or UAS:GFP was 0.53 +/- 0.12µm at 3-5dpf and 0.47 +/- 0.11 at 6-12dpf , and of CiD neurons labelled with UAS:GFP-cntn1a 0.46 +/- 0.09µm at 3-5dpf and 0.53 +/- 0.06 at 6-12dpf (Tg(s1011, UAS:Kaede) or UAS:GFP 3-5dpf n = 22, 6-8dpf n = 16; UAS:GFP-cntn1a 3-5dpf n = 8, 6-8dpf n = 5; Two-way ANOVA, p = 0.93).
(C) Quantification of axon branch number per 100µm in axons of CiD neurons labelled by cytoplasmic fluorescent protein expression using either Tg(s1011, UAS:Kaede) or UAS:GFP compared to membrane anchored GFP expression using UAS:GFP-cntn1a. The average axon branch number per 100µm of CiD neurons labelled with either Tg(s1011, UAS:Kaede) or UAS:GFP was 1.7 +/- 1.4 at 3-5dpf and 1.76 +/- 0.6 at 6-12dpf , and of CiD neurons labelled with UAS:GFP-cntn1a 1.72 +/- 1.3 at 3-5dpf and 1.3 +/- 0.78 at 6-12dpf (Tg(s1011, UAS:Kaede) or UAS:GFP 3-5dpf n = 24, 6-8dpf n = 3; UAS:GFP-cntn1a 3-5dpf n = 5, 6-8dpf n = 6; Two-way ANOVA, p = 0.67).
(D) CiD interneuron labelled by cytoplasmic UAS:GFP expression (top) in a background with Tg(sox10:mRFP) labelled myelin sheaths (middle) at 5dpf. Zoom in on the right side shows the axon area marked with the white rectangle on the left side (left, scale bar = 15µm, right scale bar = 5µm). Images like this were used to measure axon calibre and myelin ensheathment over time.
(E) The average axon calibre of myelinated axon areas labelled either by Tg(s1011, UAS:Kaede) or UAS:GFP was 0.52 +/- 0.12µm at 3-5dpf and 0.47 +/- 0.12 at 6-12dpf, while the average axon calibre of unmyelinated areas of the same axons was 0.55 +/- 0.12µm at 3-5dpf and 0.50 +/- 0.18 at 6-12dpf (Tg(s1011, UAS:Kaede) or UAS:GFP labelled axons on which myelinated areas were measured 3-5dpf n = 22, 6-8dpf n = 16; axons on which unmyelinated areas were measured 3-5dpf n = 17, 6-8dpf n = 7; Two-way ANOVA, p = 0.47).

3.2.2 The axon calibre growth and myelin ensheathment of reticulo spinal neurons (RS)

The cell fate of oligodendrocyte lineage cells is established first in the anterior areas of the pMN domain before the posterior areas (as reviewed in Jessel, 2000 and Rowitch, 2004). Oligodendrocytes therefore mature to myelinating oligodendrocytes according to this anterior-posterior gradient and so does the onset of myelination (Schwab and Schnell, 1989 as reviewed in Jessel, 2000; Baumann and Pham-Dinh, 2001 and Rowitch, 2004). RS cell bodies are located in the hindbrain, but their axons project caudally throughout the length of the spinal cord. I was interested in whether the axon calibre of RS neurons would grow according to the anterior-posterior gradient of oligodendrocyte differentiation and onset of myelination in the spinal cord, e.g. larger axon calibre in anterior regions where myelination has started and a smaller calibre in posterior regions where myelination has not yet begun, or whether the whole length of the axon is of uniform calibre independently of myelination.

Two axon areas were therefore investigated, a proximal area in the anterior spinal cord at approximately somite area 10-16 (Figure 3.5, A, left shows somites 10-11) and an area much more distal to the cell body, in the posterior spinal cord at approximately somite area 20-26 (Figure 3.5, A, right shows somites 19-20). These axon areas were selected for axon measurements.

The average myelin ensheathment at somite area 10-16 was 0% +/- 0 at 2dpf, 39% +/- 31 at 3-5dpf and 83% +/- 19 at 6-12dpf (2dpf n = 10, 3-5dpf n = 14, 6-8dpf n = 19; One-way ANOVA p = <0.0001) (Figure 3.4, B, dark blue), while the average myelin ensheathment at somite area 20-26 was 0% +/- 0 at 2dpf, 0.4% +/-0.7 at 3-5dpf and 4.6% +/- 8.7 at 6-12dpf (2dpf n = 19, 3-5dpf n = 6, 6-8dpf n = 6; One-way ANOVA p = 0.34) (Figure 3.4, B, light blue). Thus, RS neurons are fated for myelination and the myelin ensheathment of RS axons increased over time. Myelin ensheathment in the distal axon area was only found at later time-points between 6-12dpf. The myelin ensheathment of RS axons therefore followed the anterior-posterior gradient of oligodendrocyte differentiation and myelination (Schwab and Schnell, 1989 as reviewed in Jessel, 2000; Baumann and Pham-Dinh, 2001 and Rowitch, 2004).

The average axon calibre of RS neurons increased from 0.4 +/-0.2µm at 2dpf to 1.1 +/-0.3µm at 3-5dpf and to 1.2 +/-0.4µm at 6-12dpf at somite area 10-16 (2dpf n = 10, 3-5dpf n = 14, 6-8dpf n = 19; One-way ANOVA p = <0.0001) (Figure 3.4, C, dark blue). The average axon calibre in the more posterior somite area 20-26 showed a smaller increase from 0.4 +/- 0.2µm at 2dpf to 0.5 +/-0.1µm at 3-5dpf and 0.6 +/-0.1µm at 6-12dpf , which, however, was not significant (2dpf n = 19, 3-5dpf n = 6, 6-8dpf n = 6; One-way ANOVA p = 0.07) (Figure 3.4, C, light blue). Interestingly, the axon calibre of RS axon was not uniform. The proximal axon area in the anterior spinal cord, on average, had a larger axon calibre compared to the distal axon area in the posterior spinal cord and also showed a higher percentage of myelin ensheathment according to the anterior-posterior gradient of oligodendrocyte differentiation and myelination. This could indicate that axon calibre of RS axons increases with the amount of myelin ensheathment around the axon. On the other hand, RS extend their axons to the spinal cord in two waves of development, the first wave appears in the rostral spinal cord between 20 and 24hpf, while the second arrives at approximately 30-34hpf (Mendelson, 1986). It is therefore possible, that RS neurons are not fully matured by 2dpf and that their axon calibre grows as the axon matures during the time of my analysis between 2-12dpf, independently of myelin ensheathment. It has been shown that axon calibre is increased to some extent after synaptic contacts are formed (Hoffman et al., 1983; Willard and Simon, 1983). It is unclear whether this is a local effect and axon calibre is increased in the immediate proximity of the synaptic contact or a general axon calibre increase along the length of the axon. In the first case, it is possible, that axon areas proximal to the cell body in the anterior spinal cord region might have formed more synaptic contacts in the neuronal network than the distal axon areas in the posterior spinal cord region. The proximal axon calibre might, therefore, be larger in comparison with the distal region, due to an increase of synaptic connections. Thus, in order to draw firm conclusions whether axon calibre can be regulated by oligodendrocyte contact or myelin ensheathment, a manipulation that allows axonal development in complete absence of oligodendrocytes is required.

Overall, RS axons have the potential to be myelinated and their myelin ensheathment occurs to the anterior-posterior gradient of oligodendrocyte differentiation and

myelination in the spinal cord. Furthermore, the axon calibre in RS neurons increased over time in a proximal-distal gradient.

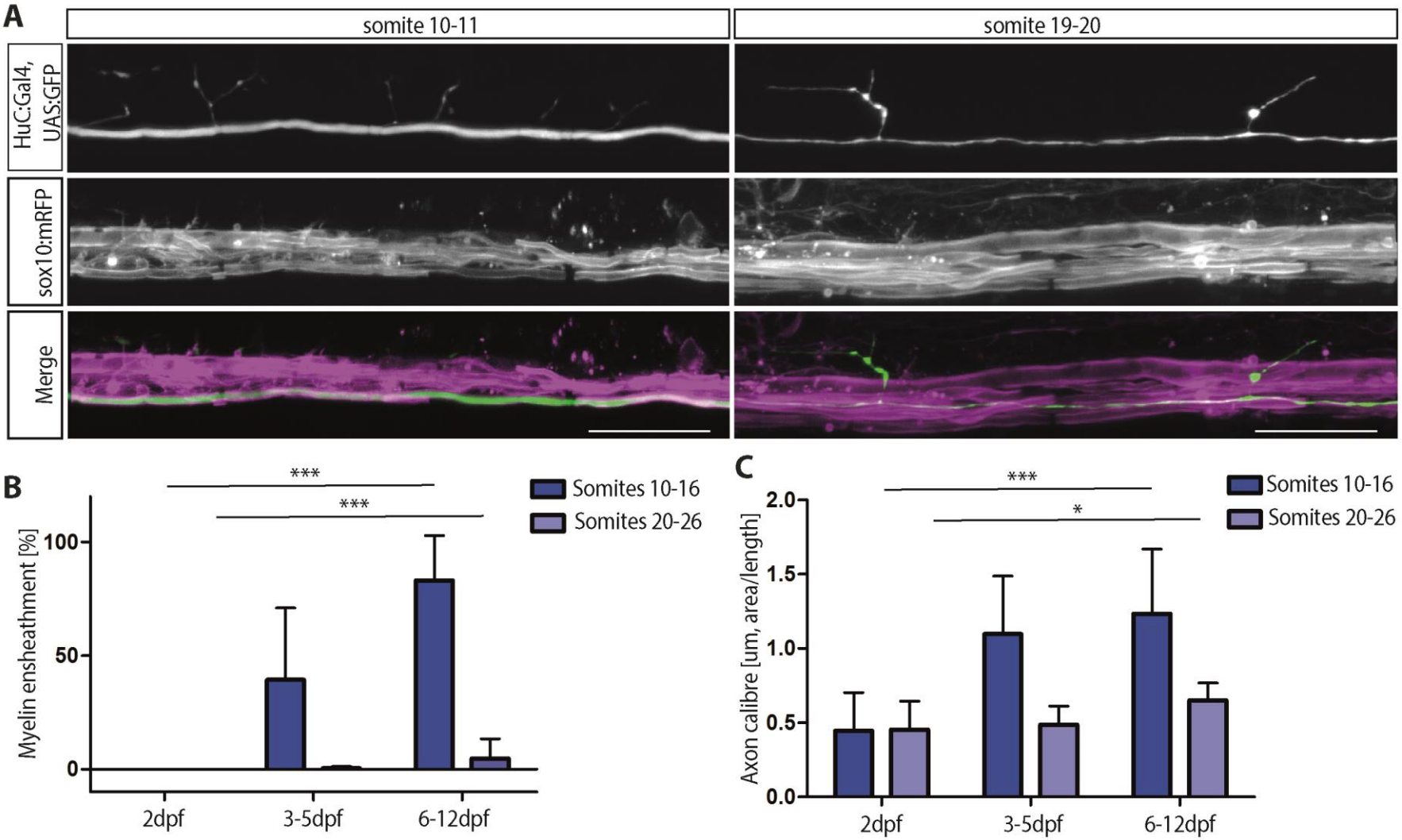
A
somite 10-11
somite 19-20
HuC:Gal4, UAS:GFP
sox10:mRFP
Merge
B
***
***
Somites 10-16
Somites 20-26
Myelin ensheathment [%]
100
50
0
2dpf
3-5dpf
6-12dpf
C
***
*
Somites 10-16
Somites 20-26
Axon calibre [um, area/length]
2.0
1.5
1.0
0.5
0.0
2dpf
3-5dpf
6-12dpf

Figure 3.4: Axon calibre growth and myelin ensheathment in RS axons. (A) GFP labelled RS axon and the surrounding myelin sheaths at somite area 10-11 and somite area 19-20. B) The average myelin ensheathment increases over time at somite area 10-16 from average 0% +/- 0 at 2dpf to 39% +/- 31 at 3-5dpf and to 83% +/- 19 at 6-12dpf (One-way ANOVA p = <0.0001). The average myelin ensheathment at somite area 20-26 increased more slowly from 0% +/- 0 at 2dpf to 0.4% +/-0.7 at 3-5dpf and to 4.6% +/- 8.7 at 6-12dpf (One-way ANOVA p = 0.34). (C) The axon calibre in RS neurons shows an anterior-posterior gradient and increases over time. The average axon calibre increases from 0.4 +/-0.2µm at 2dpf to 1.1 +/-0.3µm at 3-5dpf and to 1.2 +/-0.4µm at 6-12dpf at somite area 10-16 (One-way ANOVA p = <0.0001). The average axon calibre in somite area 20-26 also shows a slow increase from 0.4 +/- 0.2µm at 2dpf to 0.5 +/-0.1µm at 3-5dpf and 0.6 +/- 0.1µm at 6-12dpf (One-way ANOVA p = 0.07).
For these measurements, neurons were labelled either by injection of plasmids containing UAS:GFP or UAS:GFP-cntn1a into Tg(HuC:Gal4) or Tg(cntn1b:KaLT4) or by Tg(s1011, UAS:Kaede). Myelin sheaths were labelled by using the transgenic line Tg(sox10:mRFP) crossed to the transgenic lines above. Number of RS axons measured at somite 10-16: 2dpf n = 10, 3-5dpf n = 14, 6-8dpf n = 19 and at somite 20-26: 2dpf n = 19, 3-5dpf n = 6, 6-8dpf n = 6).

3.2.3 The axon calibre growth and myelin ensheathment of commissural primary ascending interneurons (CoPA)

In order to identify other neurons fated for myelination in the zebrafish spinal cord and to further investigate the relationship between axon calibre and myelinaiton, I selected the CoPA neuron for additional axon calibre and myelin ensheathment measurements. Unlike the RS neurons, CoPA axons project rostrally through the spinal cord. Their cell body is located in the spinal cord and their axon always terminates in the hindbrain. Axon areas proximal to the cell body, after the axon had crossed the midline and was projecting dorsally, were selected for measurements.

The average myelin ensheathment of CoPA axons was from 0% +/- 0 at 2dpf, 33.3% +/- 31.0 at 3-5dpf and 61.3% +/- 39.7 at 6-12dpf (2dpf n = 6, 3-5dpf n = 20, 6-8dpf n = 13; One-way ANOVA p = 0.02) (Figure 3.5, D). CoPA neurons, therefore, have the potential to be myelinated (Figure 3.5, A, B, C and D), and the myelin ensheathment increases over time (Figure 3.5, C and D).

The average axon calibre of CoPA interneurons did not increase significantly between 2dpf, 3-5dpf and 6-12dpf, with an average axon calibre of 0.6 +/-0.2µm at 2dpf, 0.6 +/-0.2µm at 3-5dpf and 0.6 +/-0.2µm at 6-12dpf (Figure 3.5, B and E) (2dpf n = 6, 3-5dpf n = 20, 6-8dpf n = 13; One-way ANOVA p = 0.94). Indicating that unlike RS axons, the axon calibre of CoPA axon does not increase concomitant with the onset of myelination and is therefore not positively regulated by myelin ensheathment. This finding suggests that axon calibre of CoPA neurons might be regulated either by a neuron intrinsic mechanism or by the interactions in the neuronal circuit. The axon calibre of CoPA neurons is smaller at very early stages such as 1dpf compared to later stages, such as 4dpf, when it is visibly increased (Figure 3.5, A). CoPA neurons appear between 17-18hpf but continue to increase in number until approximately 28hpf (Hale et al., 2001). It is therefore possible that the axon calibre of immature CoPA axons is small and that the axon calibre increases as the axon matures. This increase in axon calibre during axon maturation might either be due to a mechanism intrinsic to CoPA that regulates axon calibre growth or to the amount of synaptic input the CoPA axon receives during maturation. CoPA axons might therefore be fully mature by 2dpf and their axon calibre does not increase further. Alternatively, the axon calibre of CoPA neurons might have been regulated by extrinsic signals emitted from OPCs as OPCs are already present in the spinal cord before 2dpf (as reviewed in Miller, 2002; Rowitch, 2004). A manipulation that allows CoPA axons to develop in the complete absence of oligodendrocyte lineage cells is required in order to conclude that CoPA axons are regulated by a neuron intrinsic mechanism or by the interactions with the neuronal circuit.

Furthermore, the proximal-distal gradient of the CoPA axon follows the reverse direction of the anterior-posterior gradient of myelination. In the cases, when I was able to reliably follow one CoPA axon through the spinal cord to a distal position in the hindbrain, no difference was seen between the proximal and distal axon area in the CoPA axon (Figure 3.5, F), indicating that there is no general proximal-distal gradient of axon calibre in CoPA neurons. Given, that the axon calibre of CoPA neurons did not change with myelination, this finding suggests that axon calibre of the CoPA axon is regulated independently of a proximal-distal axon gradient and of myelin ensheathment.

Overall, CoPA neurons are fated to be myelinated and their myelin ensheathment increases over time, while their average axon calibre does not increase between 2dpf and 12dpf.

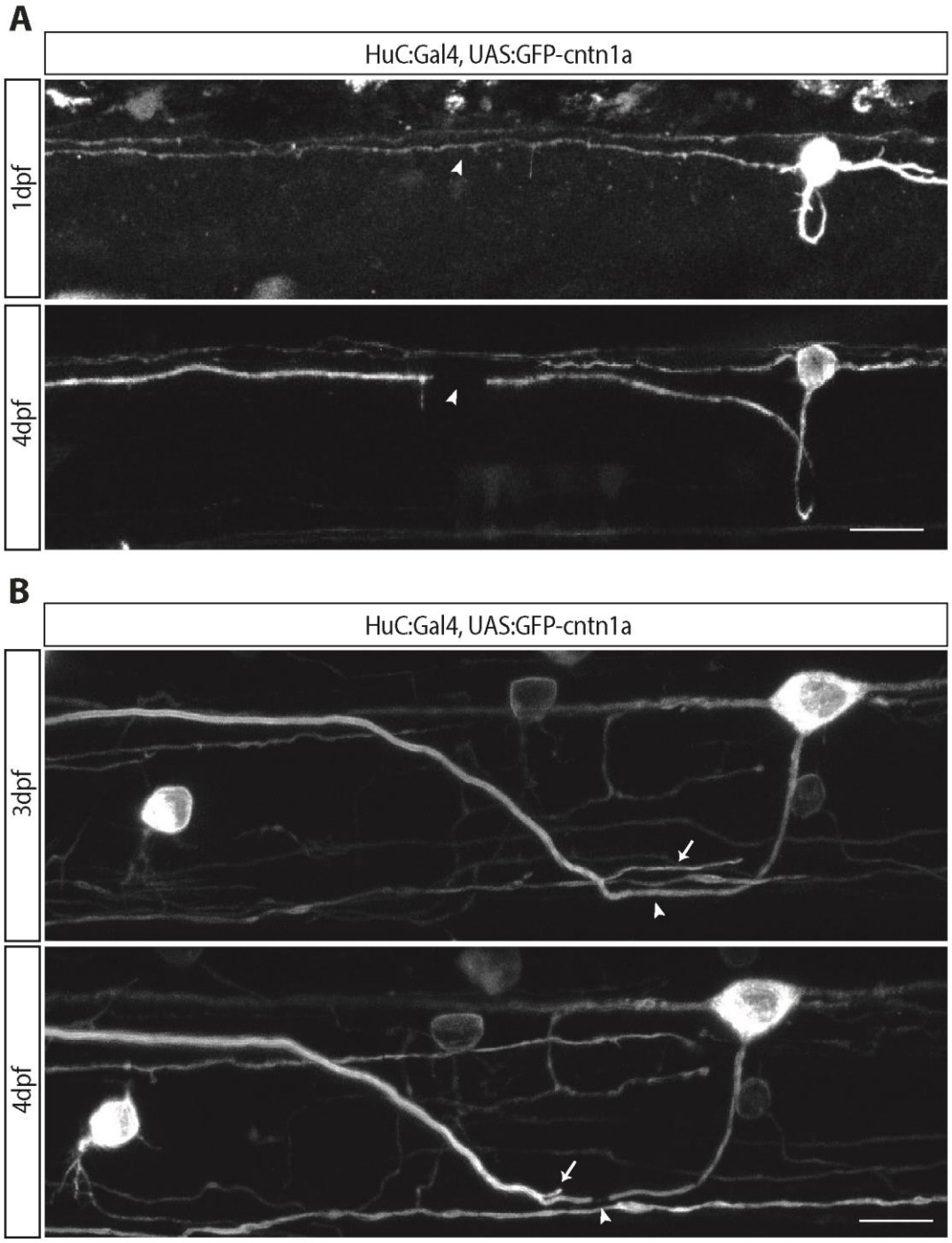
A
HuC:Gal4, UAS:GFP-cntn1a
1dpf
4dpf
B
HuC:Gal4, UAS:GFP-cntn1a
3dpf
4dpf

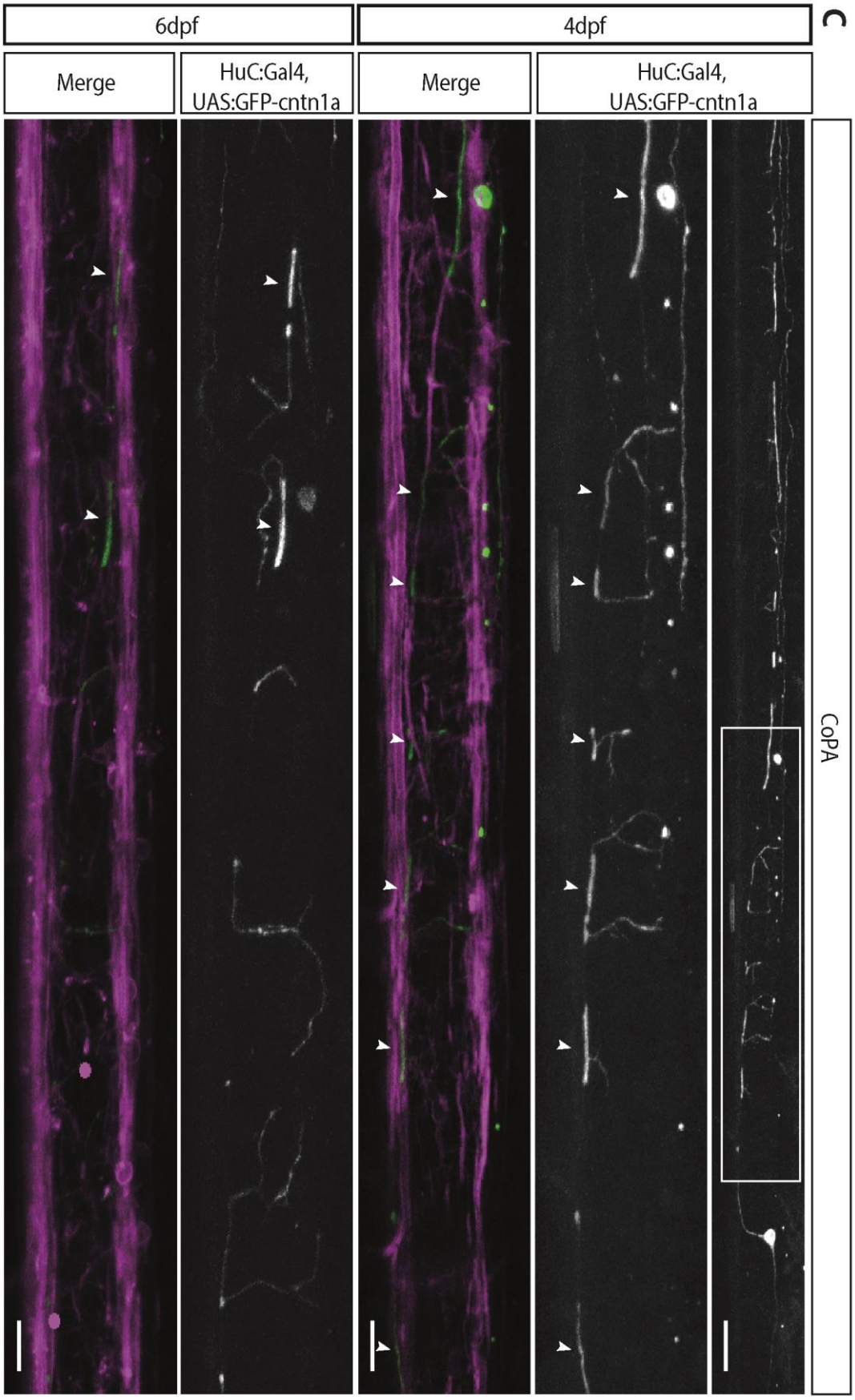
6dpf
4dpf
C
Merge
HuC:Gal4,
UAS:GFP-cntn1a
Merge
HuC:Gal4,
UAS:GFP-cntn1a
CoPA

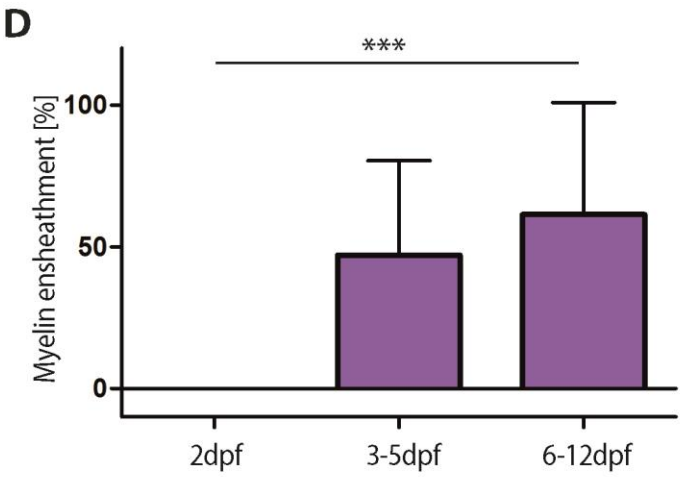
D
***
Myelin ensheathment [%]
100
50
0
2dpf
3-5dpf
6-12dpf

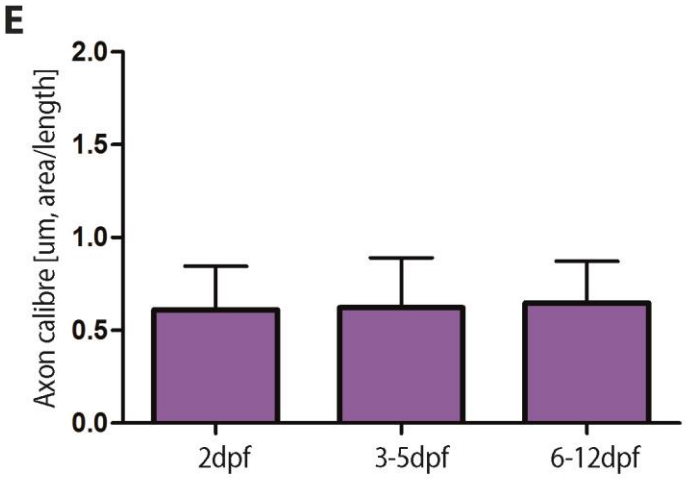
E
Axon calibre [um, area/length]
2.0
1.5
1.0
0.5
0.0
2dpf
3-5dpf
6-12dpf

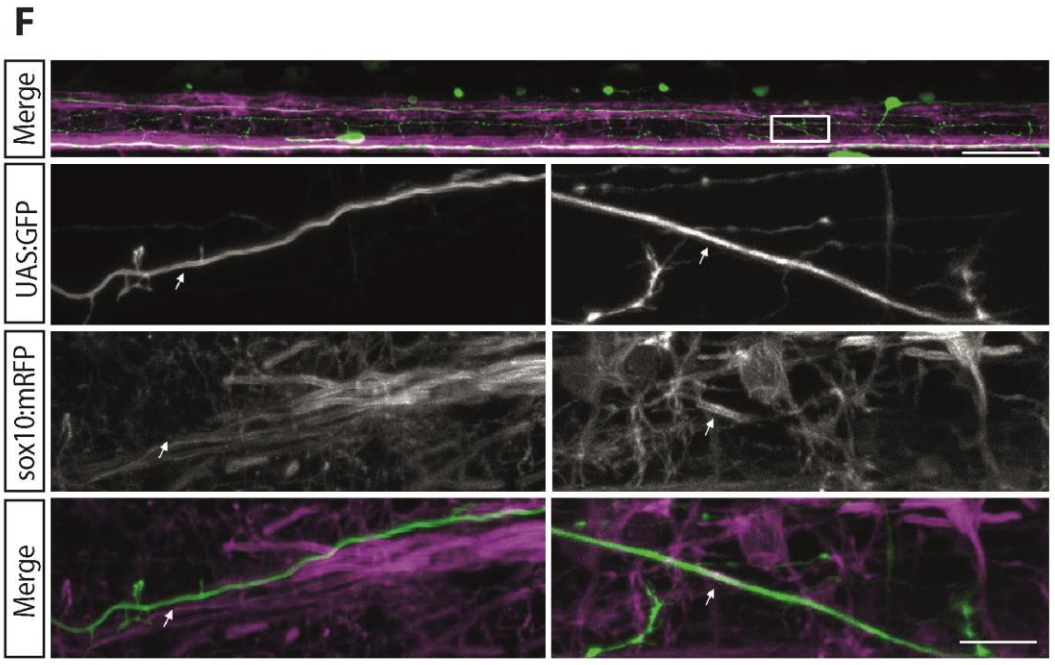
F
Merge
UAS:GFP
sox10:mRFP
Merge

Figure 3.5: Axon calibre growth and myelin ensheathment in CoPA interneurons. (A) GFP-cntn1a labelled CoPA interneuron at 1dpf (top) and at 4dpf (bottom, scale bar = 20um) before and after the formation of the first myelin sheaths. The GFP was extruded from the membrane in myelinated axon areas indicated by the arrow tip. (B) GFP-cntn1a labelled CoPA interneuron at 2dpf (top) and at 4dpf (bottom, scale bar = 10um) before and after the formation of the first myelin sheaths. The GFP was extruded from the membrane in myelinated axon areas indicated by the arrow tip. Note the axon branch that is decreased in size after onset of myelination indicated by the arrow.
(C) Overview of a GFP-cntn1a labelled CoPA interneuron at 4dpf (top, scale bar = 25µm) and a zoom in of the area shown in the rectangle at 4dpf as well as 6dpf (scale bar = 10um). The GFP was extruded from the membrane in myelinated axon areas so that only few areas of the axon were visible as indicated by the arrow tips. (D) The average myelin ensheathment increased steadily from 0% +/- 0 at 2dpf to 33.3% +/- 31.0 at 3-5dpf and to 61.3% +/- 39.7 at 6-12dpf (One-way ANOVA p = 0.02).
(E) The average axon calibre in CoPA interneurons did not increase significantly between 2dpf, 3-5dpf and 6-12dpf, with an average axon calibre of 0.6 +/-0.2µm at 2dpf, 0.6 +/-0.2µm at 3-5dpf and 0.6 +/-0.2µm at 6-12dpf (One-way ANOVA p = 0.94).
(F) Lateral overview of a CoPA neuron in a Tg(sox10:mRFP) background (top). Zoom in shows an axon area proximal to the cell body as indicated in the white box in the overview (right) and an axon area distal to the cell body in the hindbrain area (left), located outside of the area shown in the overview (top, scale bar = 50µm; bottom, scale bar = 15µm).
For these measurements, neurons were labelled either by injection of plasmids containing UAS:GFP or UAS:GFP-cntn1a into Tg(HuC:Gal4) or Tg(cntn1b:KaLT4) or by Tg(s1011, UAS:Kaede). Myelin sheaths were labelled by using the transgenic line Tg(sox10:mRFP) crossed to the transgenic lines above.
Number of CoPA axons measured in C and D: 2dpf n = 6, 3-5dpf n = 20, 6-8dpf n = 13.

3.2.4 The axon calibre growth and myelin ensheathment of circumferential descending interneurons (CiD)

CiD interneurons have axons that bifurcate in proximal regions, close to the cell body. One axon branch projects rostrally, the other caudally (Figure 3.6, A), whereby the caudally projecting axon grows first during axonal development. The rostrally projecting axon was rarely seen at 2dpf, indicating that the axon bifurcates at a later time-point during development and the rostrally projecting axon was therefore analysed from 3dpf onwards.

The average myelin ensheathment of CiD axons in the caudally projecting axons was 0% +/- 0 at 2dpf, 30% +/- 34 at 3-5dpf and 67% +/- 36 at 6-12dpf (2dpf n = 6, 3-5dpf n = 35, 6-8dpf n = 20; One-way ANOVA p = <0.0001) (Figure 3.6, B), while the average myelin ensheathment of the rostrally projecting axon was only 9.0% +/- 17.3 at 3-5dpf and 48.3% +/- 29.1 at 6-12dpf (3-5dpf n = 30, 6-8dpf n = 18; Two-tailed student's t-test p = <0.0001) (Figure 3.6, B). Thus, CiD neurons are myelinated during the onset of myelination in the zebrafish spinal cord.

The average axon calibre of the caudally projecting axon in CiD interneurons was 0.5 +/-0.1µm at 2dpf, 0.6 +/-0.2µm at 3-5dpf and 0.5 +/-0.1µm at 6-12dpf (2dpf n = 6, 3-5dpf n = 35, 6-8dpf n = 20; One-way ANOVA p = 0.33) (Figure 3.6, C), while the average axon calibre of the rostrally projecting axon was 0.43 +/-0.2µm at 3-5dpf and 0.34 +/-0.1µm at 6-12dpf (Two-tailed student's t-test p = 0.28) (Figure 3.6, C). The average axon calibre of the caudally projecting axon did therefore not increase significantly between 2dpf and 12dpf and neither did the rostrally projecting axon from 3dpf to 12dpf. The average axon calibre between the caudally projecting axon and the rostrally projecting axon was significantly different (Two-way ANOVA between the average axon calibre of the caudally and rostrally projecting axon at 3-5dpf and at 6-12dpf p = 0.003).

This indicates that similar to CoPA neurons, the axon calibre of CiD neurons does not change after the onset of myelination and is therefore regulated independently of myelin ensheathment by a neuron intrinsic mechanism or by the in- or output of synaptic connections in their circuitry. It is possible, however, that extrinsic signals emitted from OPCs might have influenced their axon calibre prior to the onset of my analysis. Again, a manipulation in which CoPA and CiD axons are investigated in the complete absence of oligodendrocyte lineage cells is required to conclude whether the axons of CoPA and CiD neurons truly are regulated through neuron intrinsic or circuit intrinsic mechanisms.

Interestingly, at the time-points measured, the axon calibre of the caudally projecting axon is larger than the caudally projecting axon, while the caudally projecting axon is also myelinated at a higher percentage compared to the rostrally projecting axon.

This might either be due to the fact that the rostrally projecting axon is growing out at later points during the development and might mature after the caudally projecting

axon or due to the smaller axon calibre in rostrally projecting axons. In either case, the rostrally projecting axon might develop the axonal properties required for myelination at a later time-point than the caudally projecting axon.

Overall, CiD neurons are fated for myelination and their myelin ensheathment increases over time, while their average axon calibre does not increase between 2dpf and 12dpf.

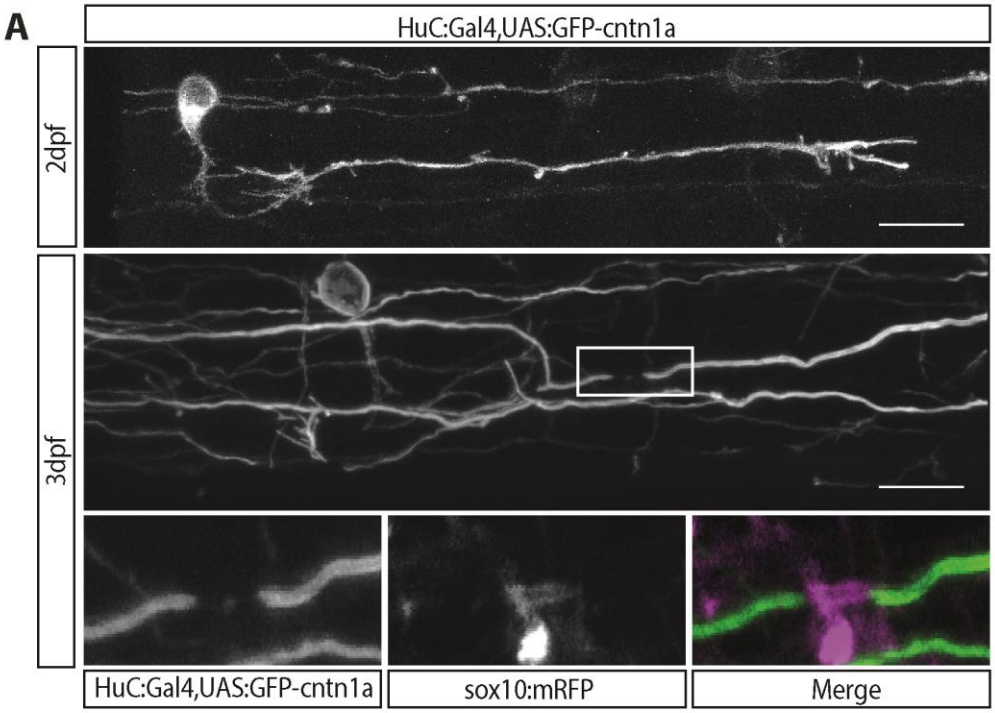
A
HuC:Gal4,UAS:GFP-cntn1a
2dpf
3dpf
HuC:Gal4,UAS:GFP-cntn1a
sox10:mRFP
Merge

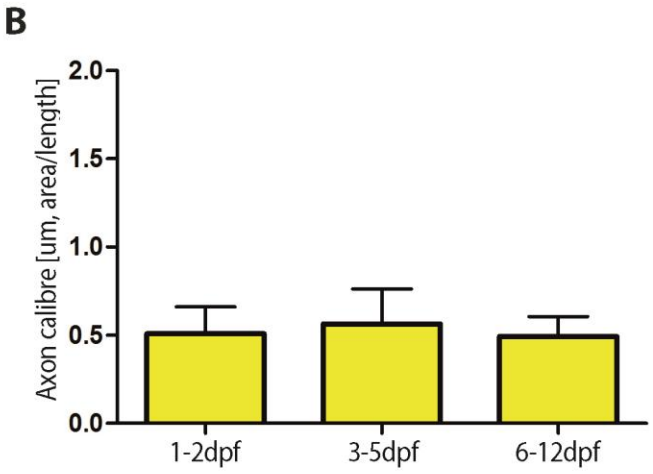
B
Axon calibre [um, area/length]
2.0
1.5
1.0
0.5
0.0
1-2dpf
3-5dpf
6-12dpf

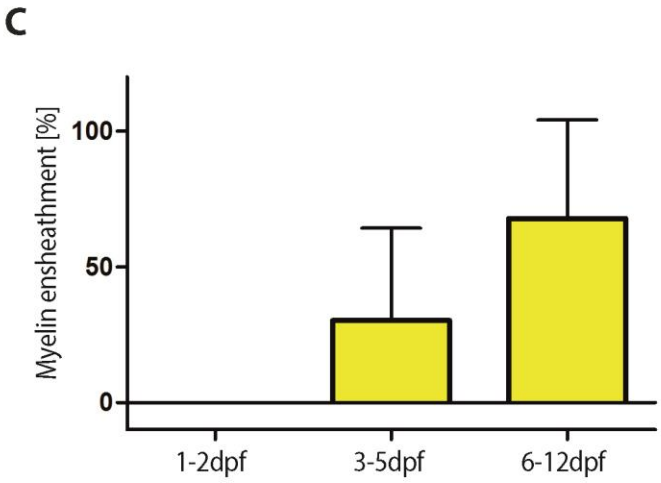
C
Myelin ensheathment [%]
100
50
0
1-2dpf
3-5dpf
6-12dpf

Figure 3.6: Axon calibre growth and myelin ensheathment in CiD interneurons. (A) GFP-cntn1a labelled CiD interneuron at 2dpf (top, scale bar = 10um) and at 3dpf (middle, scale bar = 10um) before and after the formation of the first myelin sheath. The GFP was extruded from the membrane in myelinated axon areas. The zoom in (bottom) shows the axon area in the white rectangle with the mRFP labelled myelin sheath and a merge. (B) The average myelin ensheathment increased steadily in the caudally projecting axon from 0% +/- 0 at 2dpf to 30% +/- 34 at 3-5dpf and to 67% +/- 36 at 6-12dpf (One-way ANOVA p = <0.0001) as well as in the rostrally projecting axon from 9.0% +/- 17.3 at 3-5dpf and to 48.3% +/- 29.1 at 6-12dpf (Two-tailed student's t-test p = <0.0001). (C) The average axon calibre in CiD interneurons did not increase significantly between 2dpf, 3-5dpf and 6-12dpf, with an average axon calibre of the caudally projecting axon of 0.5 +/-0.1µm at 2dpf, 0.6 +/-0.2µm at 3-5dpf and 0.5 +/-0.1µm at 6-12dpf (One-way ANOVA p = 0.33). The average axon calibre of the rostrally projecting axon did not change significantly between 3-5dpf and 6-12 dpf with an average axon calibre of 0.43 +/-0.2µm at 3-5dpf and 0.34 +/-0.1µm at 6-12dpf (Two-tailed student's t-test p = 0.28).

For these measurements, neurons were labelled either by injection of plasmids containing UAS:GFP or UAS:GFP-cntn1a into Tg(HuC:Gal4) or Tg(cntn1b:KaLT4) or by Tg(s1011, UAS:Kaede). Myelin sheaths were labelled by using the transgenic line Tg(sox10:mRFP) crossed to the transgenic lines above. Number of caudally projecting CiD axons measured in B and C: 2dpf n = 6, 3-5dpf n = 35, 6-8dpf n = 20 and number of rostrally projecting CiD axons measured in B and C: 3-5dpf n = 30, 6-8dpf n = 18.

3.2.5 Rohon Beard (RB) sensory neurons are not myelinated during early zebrafish development

RB sensory neurons are amongst the first neurons to develop in the zebrafish and start to undergo apoptosis at approximately 3-4dpf, although a minority of RB cells can still be found past 5dpf (Williams et al., 2000). The latest time-point at which RB neurons were imaged here was 8dpf. The average myelin ensheathment of RB axons was 0% +/- 0 at 2dpf to 0.7% +/- 3.9 at 3-5dpf and to 0.2% +/- 0.9 at 6-12dpf (2dpf n = 6, 3-5dpf n = 23, 6-8dpf n = 11; One-way ANOVA p = 0.77) (Figure 3.7, B). Most RB neurons imaged did not show any myelin sheaths with the exception of two RB neurons with very small myelin sheaths at 6dpf (Figure 3.7, C). This is interesting, as it indicates that ensheahtments can be made around axons that are usually not myelinated, but that these cases are rare. This observation suggests that neurons that normally remain unmyelinated lack an axonal property or signal required the

ensheathment and maintenance of myelin sheaths. Since the function of the RB neuron is replaced by DRG neurons from approximately 3-4dpf onwards and the RB neurons undergo apoptosis thereafter, it is possible that the RB axons are not fully functional anymore by the time-point of myelination and might therefore not be myelinated. It will be very interesting to monitor the activity of RB axons and correlate it with the onset of myelination and, in case there might be more events of myelin ensheathment around RB axons, follow these small ensheathments over time and observe whether they will be removed after the oligodendrocyte does not receive the right axonal signals to fully myelinate the axon.

The average axon calibre in RB neurons was 2dpf, 3-5dpf and 6-12dpf, with an average axon calibre of 0.59 +/-0.2µm at 2dpf, 0.47 +/-0.2µm at 3-5dpf and 0.39 +/-0.09µm at 6-12dpf (2dpf n = 6, 3-5dpf n = 23, 6-8dpf n = 11; One-way ANOVA p = 0.33) (Figure 3.7, D). There is a trend towards a decrease of axon calibre over time, which, however, it is not statistically significant. RB neurons are amongst the first neurons to develop in the zebrafish spinal cord and are first detected between 10-18hpf (Hale et al., 2001). It is therefore possible that the axon calibre of RB neurons might have been increased before the start of the analysis at 2dpf, similar to the axon calibre of CoPA interneurons that was very small in images taken at 1dpf. It will be interesting to investigate the axon calibre growth of these axons that regulate their axon calibre growth before the onset of myelination in order to elucidate the neuron intrinsic or circuitry specific mechanisms of axon calibre growth.

Overall, myelin sheaths on RB axons were extremely rare and most axons remained unmyelinated after the onset of myelination. The axon calibre of RB sensory neurons did not increase between 2dpf and 12dpf.

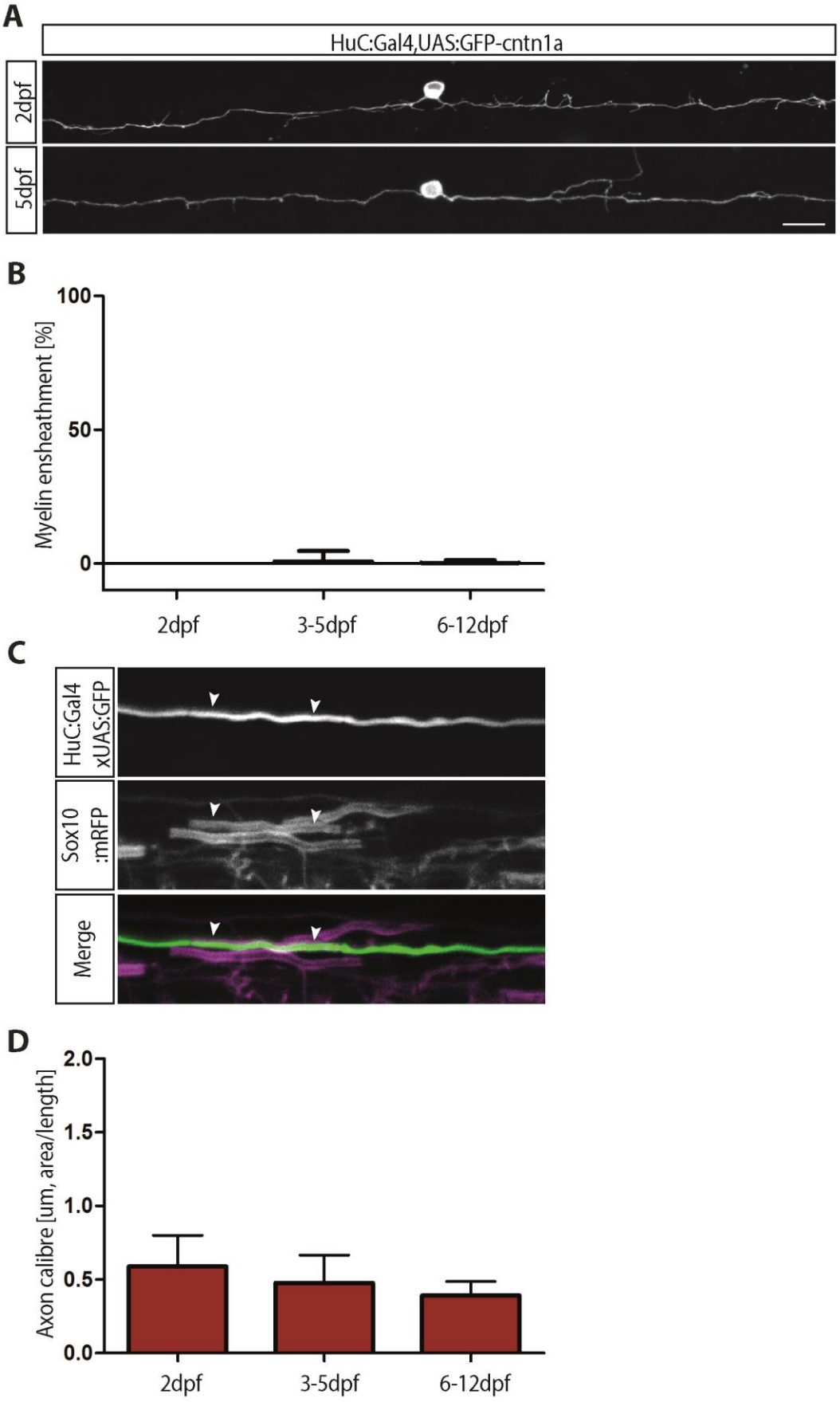
A
HuC:Gal4,UAS:GFP-cntn1a
2dpf
5dpf
B
Myelin ensheathment [%]
100
50
0
2dpf
3-5dpf
6-12dpf
C
HuC:Gal4 xUAS:GFP
Sox10 :mRFP
Merge
D
Axon calibre [um, area/length]
2.0
1.5
1.0
0.5
0.0
2dpf
3-5dpf
6-12dpf

Figure 3.7: Axon calibre growth and myelin ensheathment in RB neurons. (A) GFP-cntn1a labelled RB neuron at 2dpf (top, scale bar = 10um) and at 5dpf (bottom, scale bar = 10um). This RB axon was not myelinated between 2dpf and 5dpf. (B) Most of the RB neurons imaged did not show any myelin sheaths with the exception of very rare small myelin sheaths at 3-5dpf and 6-12dpf. The average myelin ensheathment is 0% +/- 0 at 2dpf to 0.7% +/- 3.9 at 3-5dpf and to 0.2% +/- 0.9 at 6-12dpf (One-way ANOVA p = 0.77). (C) One of the rare myelin sheaths seen on RB axons at 6dpf. (D) The average axon calibre in RB neurons does not increase significantly between 2dpf, 3-5dpf and 6-12dpf, with an average axon calibre of 0.59 +/-0.2µm at 2dpf, 0.47 +/-0.2µm at 3-5dpf and 0.39 +/-0.09µm at 6-12dpf (One-way ANOVA p = 0.33).
For these measurements, neurons were labelled either by injection of plasmids containing UAS:GFP or UAS:GFP-cntn1a into Tg(HuC:Gal4) or Tg(cntn1b:KaLT4) or by Tg(s1011, UAS:Kaede). Myelin sheaths were labelled by using the transgenic line Tg(sox10:mRFP) crossed to the transgenic lines above. Number of RB axons measured in B and D: 2dpf n = 6, 3-5dpf n = 23, 6-8dpf n = 11.

3.2.5 Commisural bifurcating longitudinal (CoBL) interneurons are not myelinated during early zebrafish development

CoBL interneurons have a bifurcating axon, with one part projecting rostrally and one part projecting caudally (Figure 3.8, A). The average myelin ensheathment of both CoBL axons was 0% +/- 0 at each time-point (One-way ANOVA p = NA) (Figure 3.8, C). Therefore, none of the imaged CoBL interneurons were myelinated between 2dpf and 12dpf. This could be due to the axon not being fully matured at these time-points. However, the first CoBL interneurons appear between 22-23hpf at the same time-point as CiD neurons that are fated for myelination (Hale et al., 2001). Considering there is no myelin ensheathment on axons even at 12dpf, it seems unlikely that the lack of myelination of CoBL neurons is due to the immaturity of CoBL neurons.

The average axon calibre of the rostrally projecting CoBL axon was 0.43 +/- 0.2µm at 2dpf, 0.53 +/- 0.3 at 3-5dpf and 0.6 +/- 0.3 at 6-12dpf (2dpf n = 4, 3-5dpf n = 17, 6-8dpf n = 29; One-way ANOVA p = 0.54) (Figure 3.8, B), while the average axon calibre of the caudally projecting CoBL axon was 0.41 +/- 0.2µm at 2dpf, 0.48 +/- 0.4 at 3-5dpf and 0.6 +/- 0.3 at 6-12dpf (2dpf n = 4, 3-5dpf n = 17, 6-8dpf n = 29; One-way ANOVA p = 0.65) (Figure 3.8, B). The average axon calibre in CoBL interneurons shows a small increase over time, which, however, was not significantly

different. As axons of CoBL neurons remain unmyelinated during the early zebrafish development, they must obviously regulate their axon calibre independently of myelination either through a neuron intrinsic mechanism or through interactions with their neuronal circuit. It is very intriguing, that the average axon calibre of CoBL axons at 3-5dpf and 6-12dpf lies between approximately 0.5µm - 0.6µm, even though there are myelinated axons with a calibre of only 0.3µm in the spinal of rodents and zebrafish (see Chapter 4; Matthews and Duncan, 1971; Waxman and Bennett, 1972; Remahl and Hildebrand, 1982; Hildebrand et al., 1993) and CiD as well as CoPA axons are of the same average calibre, yet axons of CoBL neurons remain completely unmyelinated. The fact that there are axons of smaller calibre than CoBL axons that are myelinated indicates that the axon calibre of CoBL axons is not too small to be ensheathed by oligodendrocytes. This demonstrates that axon calibre cannot be the only axon property determining whether an axon will be myelinated or not in the axon selection during myelination. Thus, there must be another axon property influencing myelination.

Overall, CoBL interneurons were not myelinated during the early zebrafish development and their axon calibre did not change significantly between 2dpf and 12dpf.

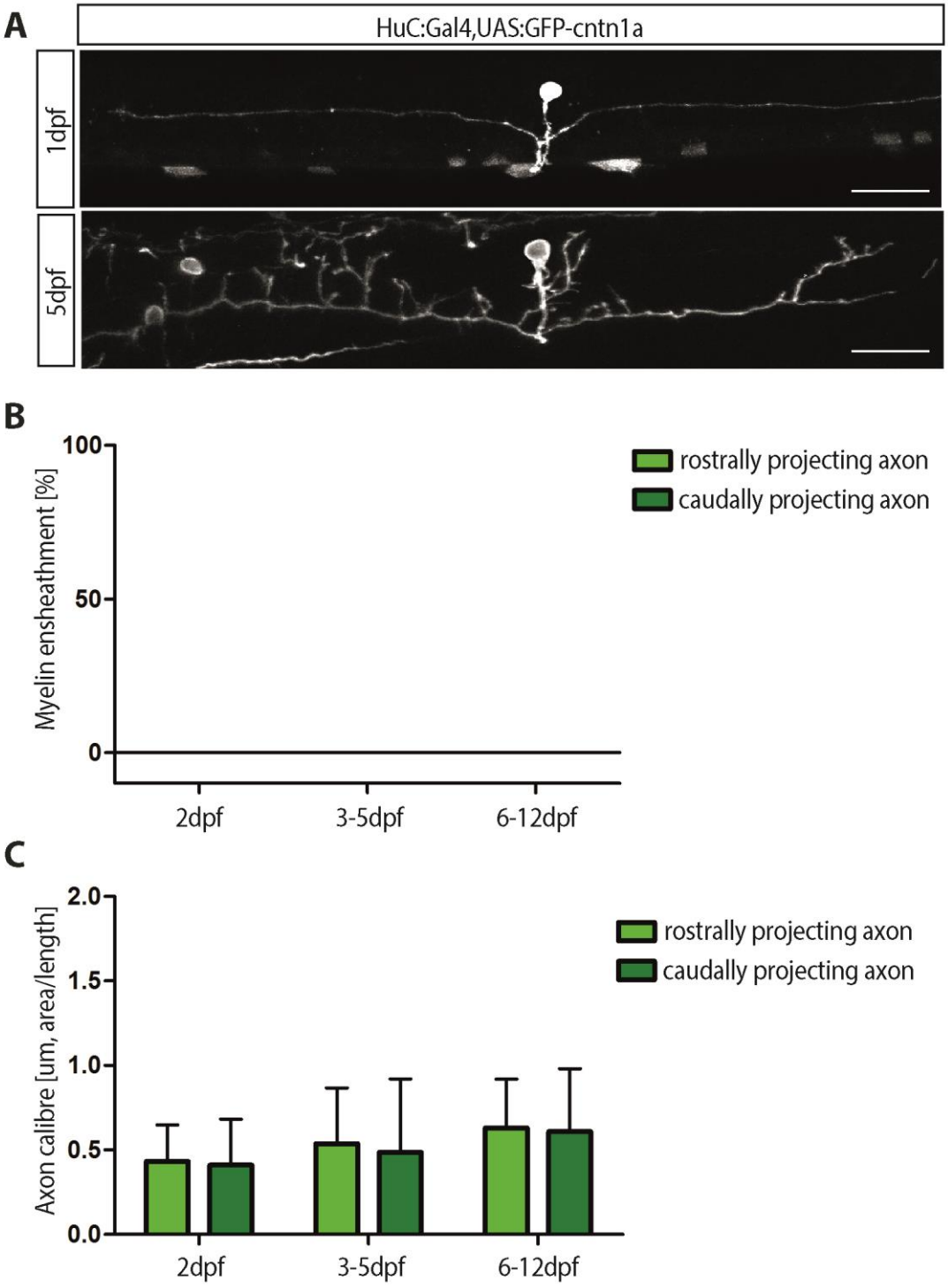

Figure 3.8: Axon calibre growth and myelin ensheathment in CoBL interneurons. (A) GFP-cntn1a labelled CoBL interneuron at 1dpf (top, scale bar = 15µm) and at 5dpf (bottom, scale bar = 15µm). The rostrally and caudally projecting CoBL axons remained unmyelinated between 1dpf and 5dpf. (B) None of the imaged CoBL interneurons were myelinated between 1dpf and 12dpf. The average myelin ensheathment was 0% +/- 0 at each time-point (One-way ANOVA p = NA).

(C) The average axon calibre in CoBL interneurons showed a small increase over time, with an average axon calibre of the rostrally and caudally projecting axon of 0.43 +/- 0.2µm at 2dpf, 0.53 +/- 0.3 at 3-5dpf and 0.6 +/- 0.3 at 6-12dpf (One-way ANOVA p = 0.53) and 0.41 +/- 0.2µm at2dpf, 0.48 +/- 0.4 at 3-5dpf and 0.6 +/- 0.3 at 6-12dpf (One-way ANOVA p = 0.65), respectively.
For these measurements, neurons were labelled either by injection of plasmids containing UAS:GFP or UAS:GFP-cntn1a into Tg(HuC:Gal4) or Tg(cntn1b:KaLT4) or by Tg(s1011, UAS:Kaede). Myelin sheaths were labelled by using the transgenic line Tg(sox10:mRFP) crossed to the transgenic lines above. Number of rostrally projecting CoBL axons measured in B and C: 2dpf n = 4, 3-5dpf n = 17, 6-8dpf n = 29 and number of caudally projecting CoBL axons 2dpf n = 4, 3-5dpf n = 17, 6-8dpf n = 29).

3.2.6 Circumferential ascending (CiA) interneurons are not myelinated during early zebrafish development

CiA interneurons have bifurcating axons with one axon projecting rostrally and one axon projecting caudally (Figure 3.9, A). As the caudally projecting axon is formed at a time-point after the first rostrally projecting axon, the rostrally projecting was chosen for analysis. The average myelin ensheathment of CiA axons was 0% +/- 0 at each time-point (2dpf n = 2, 3-5dpf n = 6, 6-8dpf n = 8; One-way ANOVA p = NA) (Figure 3.9, B). Therefore, like CoBL interneurons, none of the imaged CiA interneurons were myelinated between 2dpf and 12dpf. Again, it is unlikely that axon immaturity could be a factor as CiA neurons appear at 22-23hpf (Hale et al., 2001), the same time-point as the myelinated CiD neurons and the unmyelinated CoBL appear in the spinal cord. CiA neurons should therefore be mature by 12dpf, however, even at this time-point no myelin sheath was found on CiA axons.

The average axon calibre in CiA interneurons was 0.37 +/- 0.1µm at 2dpf, 0.32 +/- 0.1 at 3-5dpf and 0.34 +/- 0.2 at 6-12dpf (2dpf n = 5, 3-5dpf n = 6, 6-8dpf n = 4; One-way ANOVA p = 0.94) (Figure 3.9, C). The CiA axon is therefore the smallest calibre axon analysed. However, even with a relatively small axon calibre of approximately 0.3µm, the axon calibre of CiA neurons is not physically too small to be myelinated as myelinated axons of a similar size have been found in the CNS (see Chapter 4; Matthews and Duncan, 1971; Waxman and Bennett, 1972; Remahl and Hildebrand, 1982; Hildebrand et al., 1993). This again, suggests that axon calibre is not the only factor influencing the axon selection during myelination. Overall, like CoBL interneuron, CiA interneurons remained unmyelinated between 2dpf and

12dpf and the average axon calibre in CiA interneurons also did not change during this time.

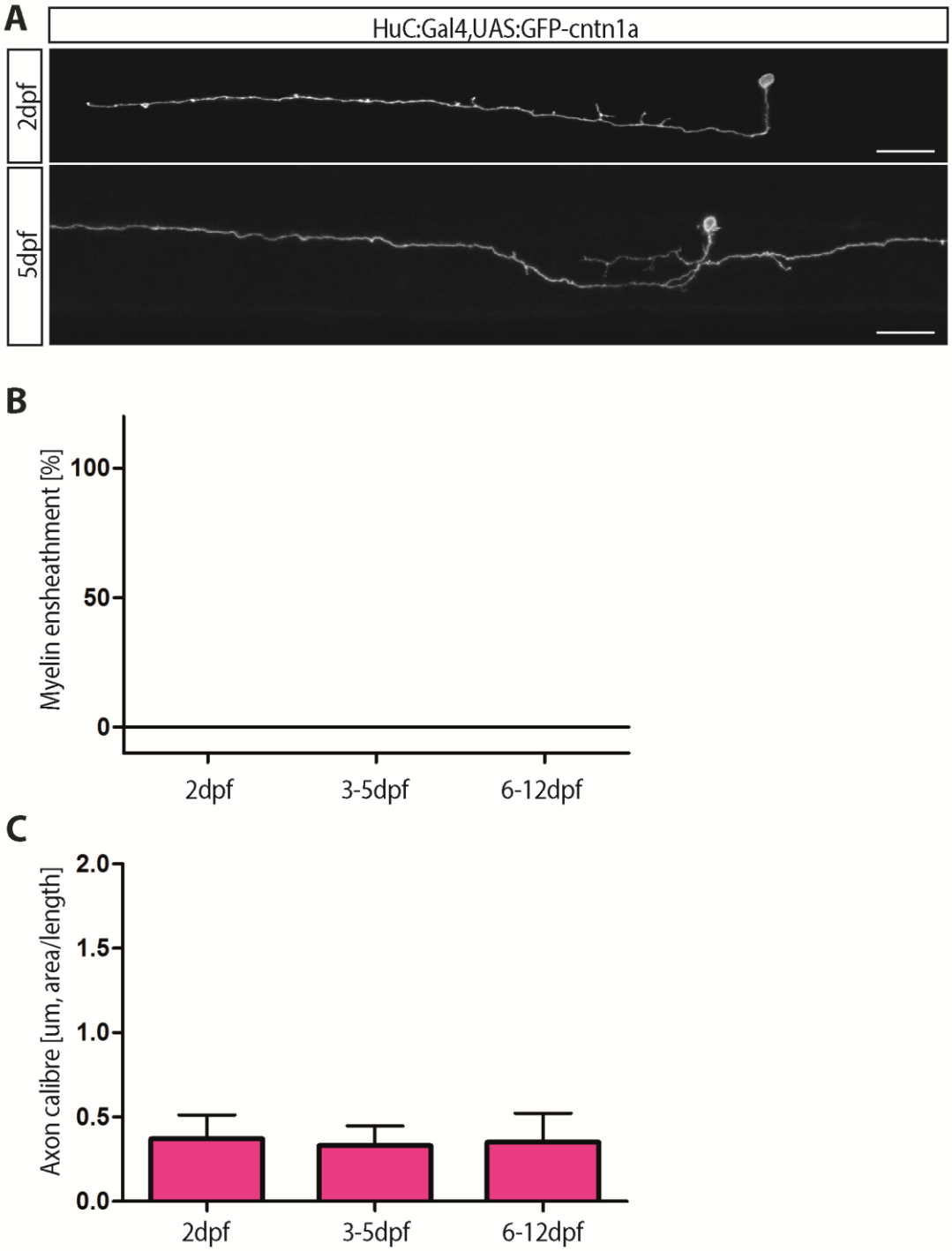

Figure 3.9: Axon calibre growth and myelin ensheathment in CiA interneurons. (A) GFP-cntn1a labelled CiA interneuron at 2dpf (top, scale bar = 20um) and at 5dpf (bottom, scale bar = 20um). No myelin sheath was formed around the CiA axon between 2dpf and 5dpf. (B) None of the imaged CiA interneurons were myelinated between 1dpf and 12dpf. The average myelin ensheathment is 0% +/- 0 at each time-point (One-way ANOVA p = NA). (C) The average axon calibre in CiA interneurons did

not increase over time, with an average axon calibre of 0.37 +/- 0.1µm at2dpf, 0.32 +/- 0.1 at 3-5dpf and 0.34 +/- 0.2 at 6-12dpf (One-way ANOVA p = 0.94).

For these measurements, neurons were labelled either by injection of plasmids containing UAS:GFP or UAS:GFP-cntn1a into Tg(HuC:Gal4) or Tg(cntn1b:KaLT4) or by Tg(s1011, UAS:Kaede). Myelin sheaths were labelled by using the transgenic line Tg(sox10:mRFP) crossed to the transgenic lines above. Number of caudally projecting CoBL axons measured in B and C: 2dpf n = 5, 3-5dpf n = 6, 6-8dpf n = 4.

3.2.7 Axon calibre growth and myelin ensheathment in individual neurons occurs according to their neuronal type

Amongst others axons reticulo spinal (RS) neurons, commissural primary ascending (CoPA) interneurons, circumferential descending (CiD) interneurons, commissural bifurcating longitudinal (CoBL) interneurons, circumferential ascending (CiA) interneurons, Rohon Beard (RB) sensory neurons were frequently labelled by plasmid DNA containing either UAS:GFP or UAS:GFP-cntn1a injected in the transgenic Gal4 driver lines Tg(Huc:Gal4) or labelled by Tg(s1011, UAS:Kaede) and were therefore selected for the analysis. These neurons were described previously (see 3.2 Introduction; Bernhardt et al., 1990; Hale et al., 2001; Kuwada et al., 1990; Higashijima et al., 2004). This subset of neurons the zebrafish spinal cord was recognized based on their different axonal and dendritic morphologies and axonal positions in the zebrafish spinal cord, unique to the individual neuronal subtype they belong to (Figure 3.10, A), and their myelin ensheathment as well as their axon calibre was measured over time (Figure 3.10, B and C, respectively; Table 3.1).

The myelin ensheathment and axon calibre was measured in CoPA, CiA, RB, CoBL, CiD and RS axons between 2dpf and 12dpf and binned according to groups, before myelination, during the onset of myelination and multiple days after the onset of myelination, 2dpf, 3-5dpf and 6-12dpf, respectively (Figure 3.10, B and C). As the myelin ensheathment and axon calibre varied in the individual neuron types, I wanted to compare them side by side in order to draw general conclusions about the similarities that neurons fated for myelination share in comparison to neurons that are not myelinated during early zebrafish development.

RS axons were myelinated during the onset of myelination and the average myelin ensheathment as well as the average axon calibre increased over time. The axons of CoPA neurons were also myelinated. The average myelin ensheathment of CoPA interneurons also increased steadily, they axon calibre, however, did not increase between 2-12dpf. The average myelin ensheathment of caudally projecting CiD axons also increased steadily, whereas the axon calibre of CiD axons did not. None of the imaged CoBL interneurons were myelinated between 2dpf and 12dpf. CoBL axon calibre showed a trend towards increase over time, which however, was not significant. Also, none of the imaged CiA interneurons were myelinated between

2dpf and 12dpf and the CiA axon calibre did increase significantly. Most of the RB neurons imaged did not show any myelin sheaths with the exception of very rare small myelin sheaths at 3-5dpf and 6-12dpf. RB axons showed a trend towards decrease over time, which was not significant.

Overall, axons of RS, CoPA and CiD neurons were myelinated during early zebrafish development, while axons of RB only rarely showed small myelin sheaths and axons of CoBL and CiA neurons never showed any myelin sheaths. Only the RS axons increased significantly in average axon calibre between 2dpf to 12dpf, while the axon calibre of the other neurons investigated did not changed significantly during this time frame. Axon calibre growth in width in RB, CoPA, CiD, CoBL and CiA neurons might have occurred before 2dpf and did not change significantly until 12 dpf. Importantly, this data suggests that axons of some neurons, such as RS, increase in calibre which coincides with the onset of myelination. However, axons of other neurons, such as CoPA and CiD neurons, do not increase with the onset of myelination and remain constant between 2dpf and 12dpf during the zebrafish development.

In order to elucidate whether there is a significant difference between the axon calibre of neurons fated for myelination and axons that are not fated for myelination during early development, RS, CoPA and CiD neurons were grouped as neurons fated for myelination and RB, CoBL and CiA neurons grouped as neurons that are not myelinated. When comparing the axon calibre of neurons fated for myelination and neuron that remained unmyelinated during analysis, there was no significant difference in axon calibre between the groups at 2dpf (Two-tailed student's t-test $p = 0.25$), however at 3-5dpf as well as at 6-12dpf, the axon calibre of neurons fated for myelination (RS, CiD and CoPA) was significantly larger compared to the axon calibre of neurons that remained unmyelinated (CoBL, RB, CiA) (Two-tailed student's t-test $p = 0.01$at 3-5dpf and $p = 0.03$ at 6-12dpf, respectively). This data indicates that axons fated for myelination are generally larger in calibre than axons that remain unmyelinated during the early zebrafish development. This suggests that axon calibre can be an axon property influencing axon selection during myelination. However, the fact that there are myelinated axons with an axon calibre smaller than

the axon calibre of the unmyelinated RB, CoBL, CiA indicates that axon calibre cannot be the only axon property determining axon selection during myelination.

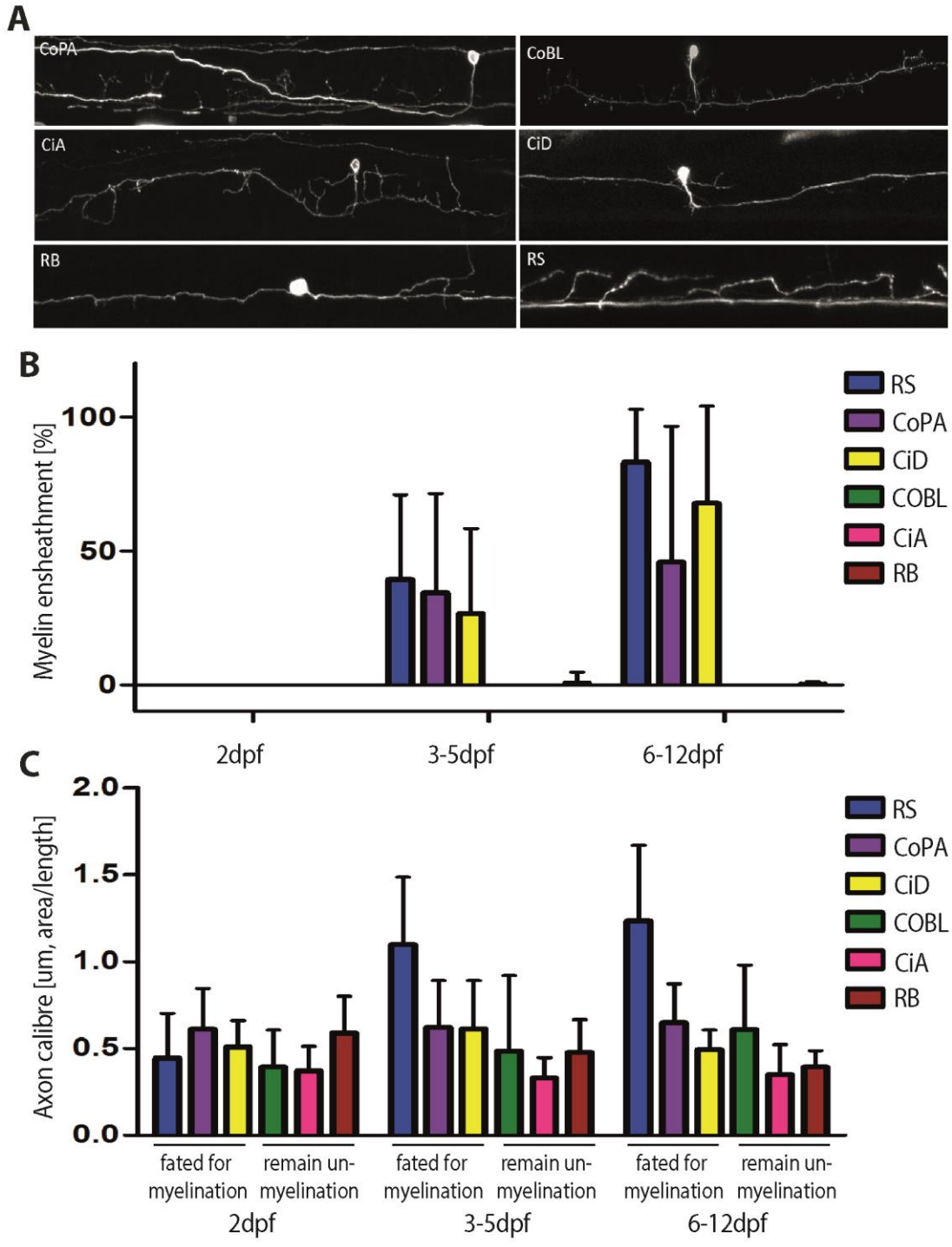

Figure 3.10: Overview of axon calibre growth and myelin ensheathment in individual neurons. (A) Overview of the characteristic morphologies found in Commisural Primary Ascending interneuron (CoPA), Commisural Bifurcating Longitutinal interneurons (CoBL), Circumferential Ascending interneuron (CiA), Circumferential Descending interneuron (CiD), Rohon Beard neuron (RB) and Reticulospinal axon (RS).(B) Myelin ensheathment was measured between 2dpf and 12dpf and binned according to developmental stages to 2dpf, 3-5dpf and 6-12dpf.

The average myelin ensheathment of RS increased over time at somite area 10-16 from an average of 0% +/- 0 at 2dpf to 39% +/- 31 at 3-5dpf and to 83% +/- 19 at 6-12dpf (2dpf n = 10, 3-5dpf n = 14, 6-8dpf n = 19; One-way ANOVA p = <0.0001). The average myelin ensheathment of CoPA interneurons increased from 0% +/- 0 at 2dpf to 33.3% +/- 31.0 at 3-5dpf and to 61.3% +/- 39.7 at 6-12dpf (2dpf n = 6, 3-5dpf n = 20, 6-8dpf n = 13; One-way ANOVA p = 0.02).

The average myelin ensheathment of CiD interneurons increased from 0% +/- 0 at 2dpf to 30% +/- 34 at 3-5dpf and to 67% +/- 36 at 6-12dpf (2dpf n = 6, 3-5dpf n = 35, 6-8dpf n = 25; One-way ANOVA p = <0.0001). CoBL axons did show myelin ensheathment, the average ensheathment is therefore 0% +/- 0 at each timepoint (2dpf n = 4, 3-5dpf n = 17, 6-8dpf n = 29; One-way ANOVA p = NA). The average myelin ensheathment of CiA axons is 0% +/- 0 at each time-point (2dpf n = 2, 3-5dpf n = 6, 6-8dpf n = 8; One-way ANOVA p = NA). The average myelin ensheathment of RB was 0% +/- 0 at 2dpf to 0.7% +/- 3.9 at 3-5dpf and to 0.2% +/- 0.9 at 6-12dpf (2dpf n = 7, 3-5dpf n = 23, 6-8dpf n = 11; One-way ANOVA p = 0.77). (C) Axon calibre was measured between 2dpf and 12dpf and binned according to developmental stages to 2dpf, 3-5dpf and 6-12dpf. The average axon calibre of RS axons at somites 10-16 increased from 0.4 +/-0.2µm at 2dpf to 1.1 +/-0.3µm at 3-5dpf and to 1.2 +/-0.4µm at 6-12dpf at somite area 10-11 (2dpf n = 10, 3-5dpf n = 14, 6-8dpf n = 19; One-way ANOVA p = <0.0001). The average axon calibre of CoPA axons did not increase from 0.6 +/-0.2µm at 2dpf, 0.6 +/-0.2µm at 3-5dpf and 0.6 +/-0.2µm at 6-12dpf (2dpf n = 6, 3-5dpf n = 20, 6-8dpf n = 13; One-way ANOVA p = 0.94). The average axon calibre of the caudally projecting CiD axons also did not increase from 0.5 +/-0.1µm at 2dpf, 0.6 +/-0.2µm at 3-5dpf and 0.5 +/-0.1µm at 6-12dpf (2dpf n = 6, 3-5dpf n = 35, 6-8dpf n = 20; One-way ANOVA p = 0.33). Neither, did the average axon calibre of the rostrally projecting CoBL axons increase from 0.41 +/- 0.2µm at 2dpf, 0.48 +/- 0.4 at 3-5dpf and 0.6 +/- 0.3 at 6-12dpf (2dpf n = 4, 3-5dpf n = 17, 6-8dpf n = 10; One-way ANOVA p = 0.65), nor did the average axon calibre of the rostrally projecting CiA axons change with an average axon calibre of 0.37 +/- 0.1µm at 2dpf, 0.32 +/- 0.1 at 3-5dpf and 0.34 +/- 0.2 at 6-12dpf (2dpf n = 5, 3-5dpf n = 6, 6-8dpf n = 4; One-way ANOVA p = 0.94). The average axon calibre of RB axons also did not change significantly from 0.59 +/-0.2µm at 2dpf, 0.47 +/-0.2µm at 3-5dpf and 0.39 +/-0.09µm at 6-12dpf (2dpf n = 7, 3-5dpf n = 23, 6-8dpf n = 11; One-way ANOVA p = 0.33).

For these measurements, neurons were labelled either by injection of plasmids containing UAS:GFP or UAS:GFP-cntn1a into Tg(HuC:Gal4) or Tg(cntn1b:KaLT4) or by Tg(s1011, UAS:Kaede). Myelin sheaths were labelled by using the transgenic line Tg(sox10:mRFP) crossed to the transgenic lines above.

3.2.8 Axons fated for myelination have fewer branches than axons not fated for myelination

In order to investigate whether there might be differences in the axon morphology of neurons fated for myelination or neurons that remain unmyelinated apart from axon calibre, I measured the number of axon branches per 100µm along the axons of the individual neurons (Figure 3.11, B; Table 3.1). RS showed relatively low axon branching throughout, 1.4 +/- 1.5 at 2dpf , 2.1 +/- 1.2 at 3-5dpf and 1.9 +/- 0.9 at 6-12dpf (2dpf n = 10, 3-5dpf n = 14, 6-8dpf n = 19; One-way ANOVA p = 0.37) (Figure 3.5, A; Figure 3.11, B). CoPA interneurons also showed low branching with 0.9 +/- 0.8 at 2dpf, 1.1 +/- 0.7 at 3-5dpf and 1.7 +/- 1.0 at 6-12dpf (2dpf n = 6, 3-5dpf n = 20, 6-8dpf n = 13; One-way ANOVA p = 0.09) (Figure 3.6, A, B and C; Figure 3.11, B). CiD interneurons showed a small, but insignificant increase in branch number over time from 0.38 +/- 0.05 at 2dpf, to 1.74 +/- 1.3 at 3-5dpf and to 1.4 +/- 0.7 at 6-12dpf (2dpf n = 6, 3-5dpf n = 35, 6-8dpf n = 20; One-way ANOVA p = 0.31) (Figure 3.7, A; Figure 3.11, B). CoBL interneurons also showed a small trend towards increased branch number over time, which was, however, not significant. The average branch number in CoBL neurons was 1.4 +/- 1.0 at 2dpf, 4.0 +/- 3.6 at 3-5dpf and 4.3 +/- 3.8 at 6-12dpf (2dpf n = 4, 3-5dpf n = 17, 6-8dpf n = 29; One-way ANOVA p = 0.33) (Figure 3.8, A; Figure 3.11, B). A significant increase in average axon branch number was seen in CiA interneurons with a steady increase from 1.5 +/-0.3 at 2dpf, 3.7 +/- 1.6 to 3-5dpf and 5.5 +/-1.2 to 6-12dpf (2dpf n = 5, 3-5dpf n = 6, 6-8dpf n = 4; One-way ANOVA p = 0.001) (Figure 3.10, A; Figure 3.11, B). RB neurons were highly branched during very early development with an average of 4.1+/- 1.8 branches per 100um at 2dpf, but the average branch number decreased to 1.0 +/- 0.9 at 3-5dpf and to 1.1 +/- 0.7 at 6-12dpf (2dpf n = 7, 3-5dpf n = 23, 6-8dpf n = 11; One-way ANOVA p = <0.0001) (Figure 3.8, A; Figure 3.11, B).

Overall, RB sensory neurons had a high number of branches at very early development, which decreased over time. As the function of RB neurons in the nervous system is replaced by DRG neurons from approximately 3-4dpf onwards, while RB neurons undergo apoptosis (Williams et al., 2000), the decrease in axon branch number at later time-points of analysis might reflect the functional reduction of RB neurons.

On average, RS, CoPA and CiD neurons had a low number of branches throughout the time of analysis (1.2 +/- 1.2 at 2dpf, 1.6 +/- 1.1 at 3-5dpf, 1.8 +/- 1.0 at 6-12dpf), while CoBL and CiA interneurons showed a large number of axon branches (1.5 +/- 0.7 at 2dpf, 4.0 +/- 3.2 at 3-5dpf and 4.6 +/- 3.5 at 6-12dpf). This represents an over two-fold increase in axon branching in neurons that are not myelinated compared to neurons fated for myelination. In direct comparison of neurons fated to be myelinated and neurons that are not myelinated, the axons of CoBL and CiA neurons had significantly more branches per axon than the axons of RS, CoPA and CiD neurons (Two-way ANOVA $p = <0.0001$). This suggests that axons that are fated for myelination have a lower number of axon branches compared to axons that are not fated for myelination. This is the first demonstration that axons that are myelinated have a different axon morphology than axons that remain unmyelinated. This could have multiple implications. A smoother axon surface, less interrupted by axon branches in axons fated for myelination could facilitate myelin ensheathment more easily, compared to the axons with a more branched morphology. Furthermore, these different axon morphologies might reflect the function or position that each neuron has in the spinal cord nervous system. Axons of RS, CiD and CoPA neurons project over long distances in the spinal cord. Their function is therefore likely the transmission of action potential over a long distance, facilitated by saltatory conduction. Saltatory conduction in axons of CoBL and CiA interneurons, on the other hand, with their highly branched morphology and relatively short axons (CoBL axons terminate approximately 4 segments from the cell body (Bernard et al., 1990)), might simply not be advantageous and non-saltatory signal conduction might be sufficient in these axons.

Alternatively, axon branching has been shown to be inhibited by so called myelin inhibitors, which are also thought to be the reason for the limited ability for neuro-regeneration in the adult CNS (as reviewed in Filbin, 2003; Yiu and He, 2006) and increased axon branching in RS, CoPA and CiD axons after 3dpf onwards might be suppressed by the expression of myelin inhibitors. I will discuss these possibilities further in the discussion of this chapter.

Overall, the different neurons did not only show different axon calibre sizes, growth over time as well as myelin ensheathment, the individual neurons also differed in

their axon branching (Figure 3.11, A), whereby neurons fated to be myelinated had less axon branches than axons that remained unmyelinated.

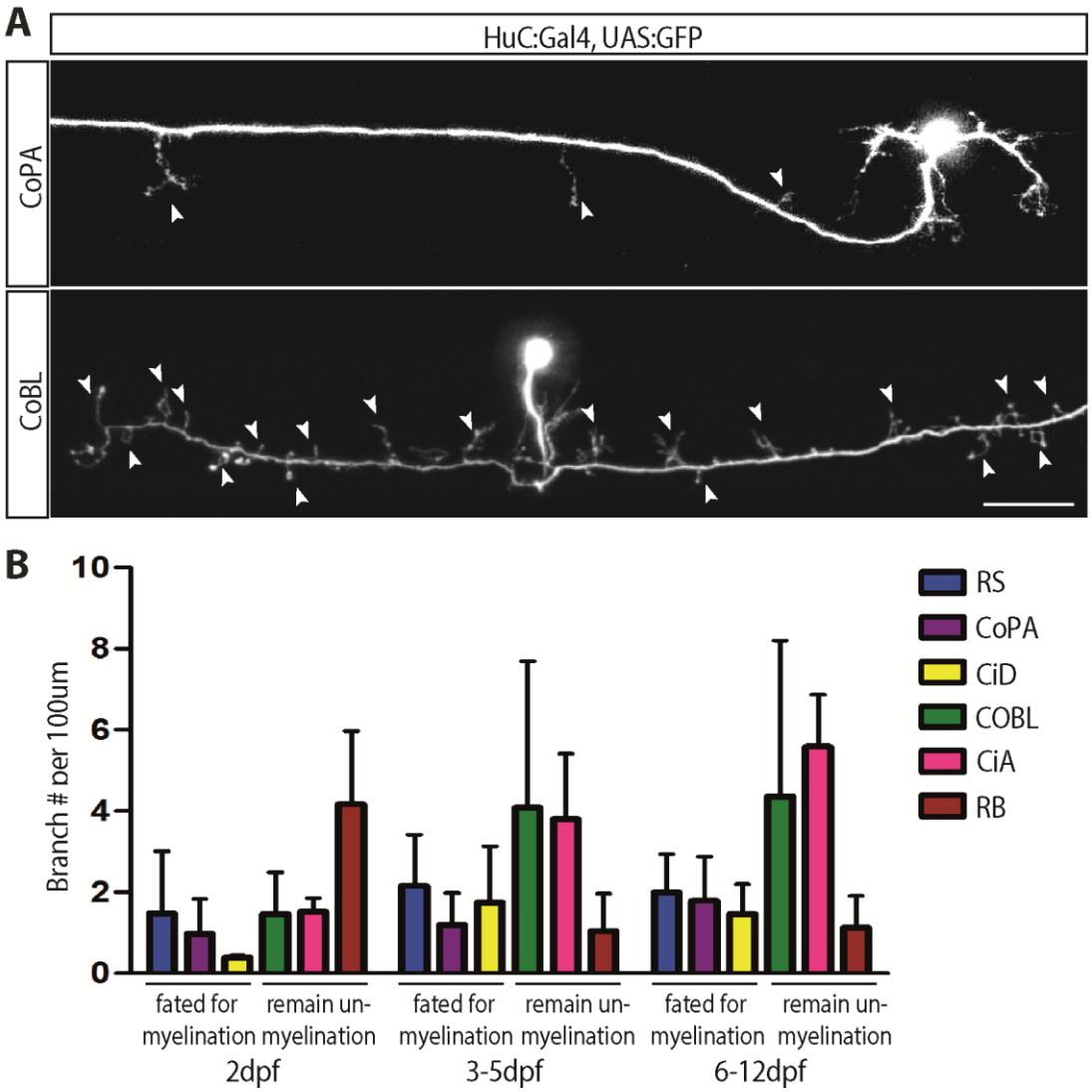

Figure 3.11: Axons fated for myelination have fewer branches than axons not fated for myelination after the onset of myelination. (A) GFP labelled CoPA interneuron (top) and CoBL interneuron at 4dpf (bottom) (scale bar = 10um). (B) The average axon branch number per 100um varies in the individual neurons. RS show low branching with an average of 1.4 +/- 1.5 branch per 100um at 2dpf, 2.1 +/- 1.2 at 3-5dpf and 1.9 +/- 0.9 at 6-12dpf (2dpf n = 10, 3-5dpf n = 14, 6-8dpf n = 19; One-way ANOVA p = 0.37). CoPA neurons show low branching with an average of 0.9 +/- 0.8 branch per 100um at 2dpf, 1.2 +/- 0.8 at 3-5dpf and 1.7 +/- 1.0 at 6-12dpf (2dpf n = 6, 3-5dpf n = 20, 6-8dpf n = 13; One-way ANOVA p = 0.09). CiD neurons show a small increase in branch number from 0.38 +/- 0.05 at 2dpf, to 1.74 +/- 1.3 at 3-5dpf and 1.4 +/- 0.7 at 6-12dpf (2dpf n = 6, 3-5dpf n = 35, 6-8dpf n = 20; One-way ANOVA p = 0.31). Axon branching increases in CoBL interneurons from 1.4 +/- 1.0 at 2dpf to 4.0 +/- 3.6 at 3-5dpf and 4.3 +/- 3.8 at 6-12dpf (2dpf n = 4, 3-5dpf n = 17, 6-8dpf n = 29; One-way ANOVA p = 0.33). A similar increase in average axon branching is seen in CiA interneurons, steadily increasing from 1.5 +/-0.3 at 2dpf, to 3.7 +/- 1.6 at 3-5dpf and 5.5 +/-1.2 at 6-12dpf (2dpf n = 5, 3-5dpf n = 6, 6-8dpf n = 4; One-way ANOVA p = 0.001). RB neurons are highly

branched with on average of 4.1+/- 1.8 branch per 100um at 2dpf, but show low branching with an average of 1.0 +/- 0.9 at 3-5dpf and 1.1 +/- 0.7 at 6-12dpf (2dpf n = 7, 3-5dpf n = 23, 6-8dpf n = 11; One-way ANOVA p = <0.0001). Overall, RS, CoPA and CiD neurons have a significantly lower number of axon branches per 100µm than CoBL and CiA neurons (Two-way ANOVA p = 0.01).

For these measurements, neurons were labelled either by injection of plasmids containing UAS:GFP or UAS:GFP-cntn1a into Tg(HuC:Gal4) or Tg(cntn1b:KaLT4) or by Tg(s1011, UAS:Kaede). Myelin sheaths were labelled by using the transgenic line Tg(sox10:mRFP) crossed to the transgenic lines above.

Neuron cell type	Picture of neuron	Soma postition / # per hemi-segment	Cell body & dendrite morphology	Maximum axon length	Myelination status	Average axon calibre [area / length] at 2dpf, 3-5dpf, 6-12dpf	Average axon branch #/100μm at 2dpf, 3-5dpf, 6-12dpf
Reticulospinal		Ventral / axon projects through length of spinal cord	Number and location of dentrites vary.	Extends length of cord.	Myelinated.	At somites 10-16: 0.4μm, 1.1μm, 1.2μm.	At somites 10-16: 1.4, 2.1, 1.9
Rohon Beard (RB)	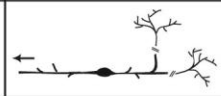	Dorsal of all other cells / 1-4 cells per hemi-segment	Bipolar, large somata.	Caudally projecting axon extends > 20segments. Rostrally projecting axon extends 10 segments.	Normally not myelinated. Rarly shows small ensheathment.	0.6μm, 0.5μm, 0.4μm.	4.1, 1.0, 1.1
Commisural Primary Ascending (CoPA)		Dorsal, lateral to CoLA cell bodies / cell # varies in alternate segments	Bipolar, T shape, dorsal dendrites.	Extends length of cord / axon corsses cord dorsal to Mauthner axon. Ascend in dorsal cord.	Myelinated.	0.6μm, 0.6μm, 0.6μm.	0.9, 1.2, 1.7
Commisural Longitudinal Ascending (CoLA)		Dorsal, medial to CoPA cell bodies / 1 cell per hemi-segments	Dorsal dendrite extends caudally. Midlateral processes extend rostrally and caudally.	5 segments/ axon crosses cord dorsal to Mauthner axon. Ascends extending dorsally. Minor descending branch.	Myelinated.	Data too prelimiary.	Data too prelimiary.
Circumferental Ascending (CiA)		Midcord lateral / mutlitple cells per hemi-segment	Unipolar, simple cell body.	Varies, the caudally projecting axon extends ipsilaterally over several segments. Minor descending branch.	Not myelinated.	0.4μm, 0.3μm, 0.3μm.	1.5, 3.7, 5.5
Circumferental Descending (CiD)		Midcord lateral / mutlitple cells per hemi-segment	Unipolar, simple cell body	13 segments/ axon ipsilateral, extends ventral to Mauthner axon then turns dorsal and caudally. Minor ascending branch.	Myelinated.	0.5μm, 0.6μm, 0.5μm.	1.4, 1.7, 1.4
Commisural Bifurcating Longitudinal (CoBL)	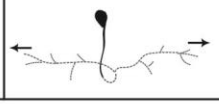	Dorsal / mutlitple cells per hemi-segment	Unipolar, simple cell body	4 segments/ axon projects ventrally, crossing cord dorsal to Mauthner axon before bifurcating and extending dorsally.	Not myelinated.	0.4μm, 0.5μm, 0.6μm.	1.4, 4.0, 4.3

Table 3.1: Overview of the key morphological features of the neurons investigated. Arrows indicate direction of axon growth; dashed line indicates contralateral growth; double stroke indicates long distances between the depicted axon features. For additional information and standard deviations see text. Table adapted from Hale et al., 2001 and Bernard et al., 1990, with additional data obtained during my PhD.

3.2.9 Axon calibre is not regulated by oligodendrocyte contact or myelin ensheathment.

The axon calibre of RS neurons increased over time and coincided with the onset of myelination. However, the axon calibre of CoPA and CiD neurons did not increase with the onset of myelination and remained the same throughout the time of analysis. These findings suggest that while the axon calibre of some neurons, such as CoPA and CiD neurons, is regulated independently of myelin ensheathment, the axon calibre of RS neurons might be increased by axon-oligodendrocyte interactions. Furthermore, previous studies have implicated that the axon-oligodendrocyte interactions regulating axon calibre growth in the optic nerve might be induced by extrinsic signals emitted from oligodendrocytes and could occur even in the absence of myelin ensheathment (Colello et al., 1994; Sanchez et al., 1996, 2000). While the axon calibre of CoPA and CiD neurons is not increased after myelin ensheathment, their axon calibre might still have been regulated by extrinsic signals emitted by OPCs before the onset of myelination.

Thus, in order to test whether axon calibre can be regulated by any axon-oligodendrocyte interactions, including extrinsic signals emitted by oligodendrocyte and myelin ensheathment, I used the olig2 morpholino (olig2 MO) (Zannino and Appel, 2009) to inhibit oligodendrocyte development in the zebrafish embryo (see chapter 2 Materials and Methods). Myelinating oligodendrocytes were almost completely vacant from the spinal cord up to 4dpf, and almost no myelin was formed in olig2 MO treated animals (Figure 3.12, A and B). As expected, the PNS was not affected by the olig2 MO treatment and the pLL was robustly myelinated both in controls and olig2 MO treated animals (Figure 3.12).

To quantify the axon calibre in the absence of myelination, the axon calibre and myelination status of the 20 largest calibre axons per hemi spinal cord was assessed in electron micrographs of transversal section of controls (Figure 3.13, A, B and C, left) and olig2 MO treated animals (Figure 3.13, A, B and C, right) (control animal n = 5, olig2 MO animal n = 5). Measuring axon calibre from images taken at a lateral view by fluorescent microscopy has the great advantage that the axon calibre of individual axons can be followed over time and specific neuron types can be easily identified and imaged before and after the onset of myelination. However, since the

axon calibre is in fact the cross sectional size of an axon, this method of axon calibre measurement is not the most accurate. In order to achieve the most accurate measurements of axon calibre in the absence of oligodendrocytes, electron microscopy was chosen for the olig2 MO experiment.

The Mauthner axon was excluded from analysis as a few myelin sheaths were formed around the Mauthner axons even in the olig2 MO treated animals. The olig2 MO treatment is not a genetic knock-out and likely is not a complete loss of function. When assessing the efficiency of the olig2MO knock-down using Tg(mbp:GFP-caax), myelination was found in the spinal cord at 5dpf (data not shown), indicating that the olig2 MO is only efficient in inhibiting oligodendrocyte lineage cell formation until approximately 4dpf. It is therefore likely that the few myelin sheaths found around the Mauthner axons in some animals were generated by oligodendrocytes that formed as the effect of the olig2 MO wore off over time.

In controls, on average, 83% +/- 9.7 of the 20 axons with largest calibre are myelinated, while 17% +/- 9.7 are unmyelinated. In Olig2 MO injected animals, 7 +/- 15.6% of the 20 axons with largest calibre per hemi spinal cord are myelinated, while 93 +/- 15.6% are unmyelinated, indicating that the olig2 MO treatment was successful in reducing myelination (control animal n = 5, olig2MO animal n = 5) (Figure 3.13, D). The average axon diameter of the 20 axons with the largest calibre in control animals was 1.11 +/- 0.06 µm and the average diameter of the 20 largest calibre axons in Olig2 MO injected animals was 1.17 +/- 0.1 µm (control n = 5, olig2MO n = 5) (Two-tailed student's t-test, p = 0.9) (Figure 3.13, E). Of the 20 axons with largest calibre in control animals 43% were locate in the dorsal spinal cord, whereas 57% were located in the ventral spinal cord. Of the 20 axons with largest calibre in olig2 MO treated animals 48% were locate in the dorsal spinal cord, whereas 52% were located in the ventral spinal cord. Axons of RS neurons are located in the ventral spinal cord, whereas axons of CoPA and CiD neurons first project ventrally but then turn in an upwards curve to project dorsally and the majority of the axon is located in the dorsal spinal cord. If only the axon calibre of RS neuron would have been impaired by the absence of oligodendrocytes and myelin ensheathment, while the axon calibre of CoPA and CiD axons would have been unimpaired, there would have been a shift in the percentage of largest calibre axons

towards the dorsal spinal cord. The distribution of large calibre axons in the spinal cord, however, was unaffected by the olig2 MO treatment, indicating that the axon calibre of RS as well as CoPA and CiD neurons is regulated independently of extrinsic signals emitted by oligodendrocyte lineage cells and myelin ensheathment.

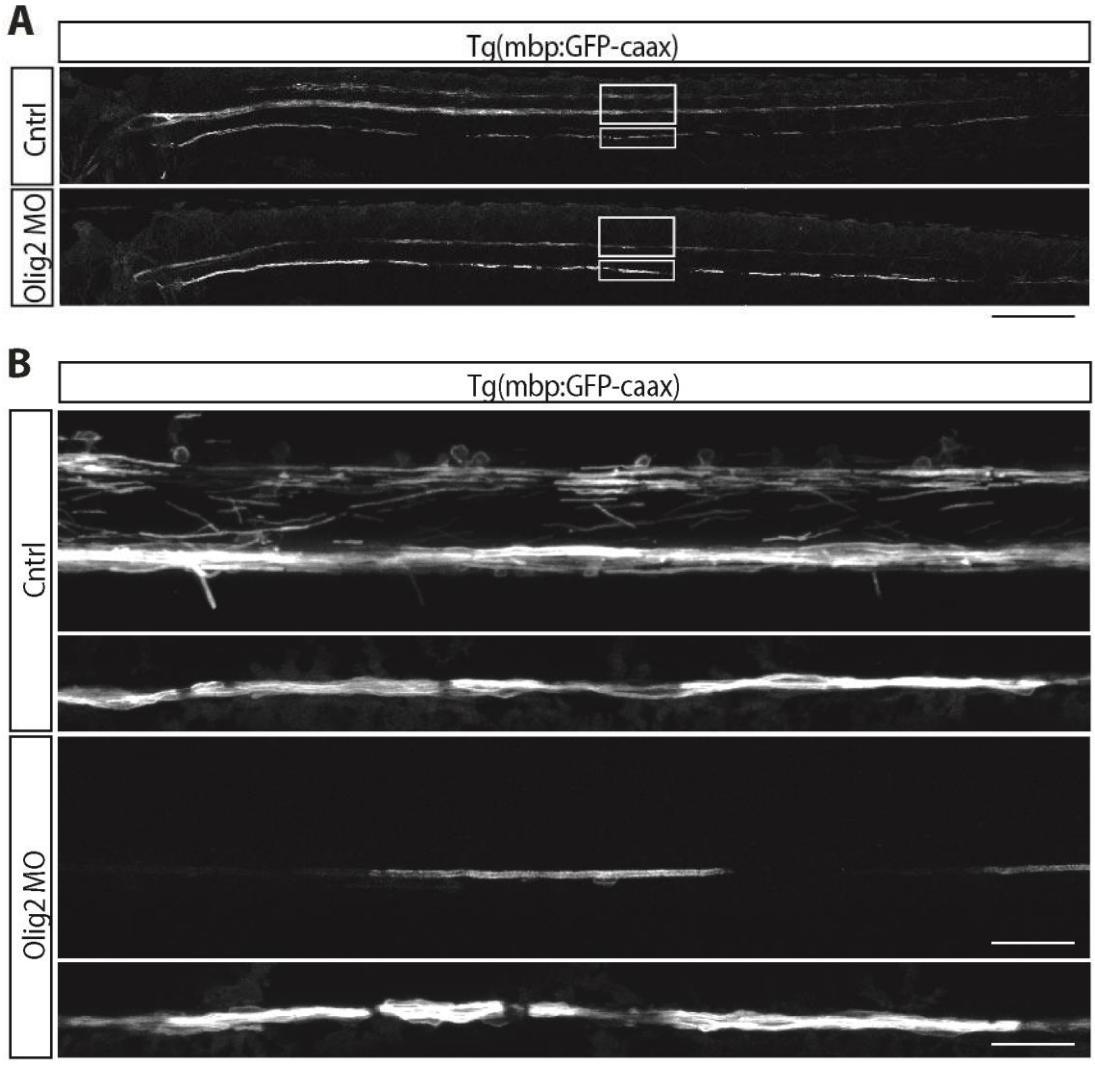

Figure 3.12: The olig2 MO treatment is effectively reducing the myelination in the CNS but not the PNS. (A) At 4dpf, the spinal cord of control animals showed robust myelination in the ventral and dorsal spinal cord as well as in the pLL. Olig2 MO treated animals did not show myelin signal in the dorsal spinal cord and only little myelin signal in the ventral spinal cord, while the pLL showed robust myelination (scale bar = 230um). (B) Zoom in on the areas indicated with white rectangles in A (spinal cord scale bar = 50um, pLL scale bar = 15µm).

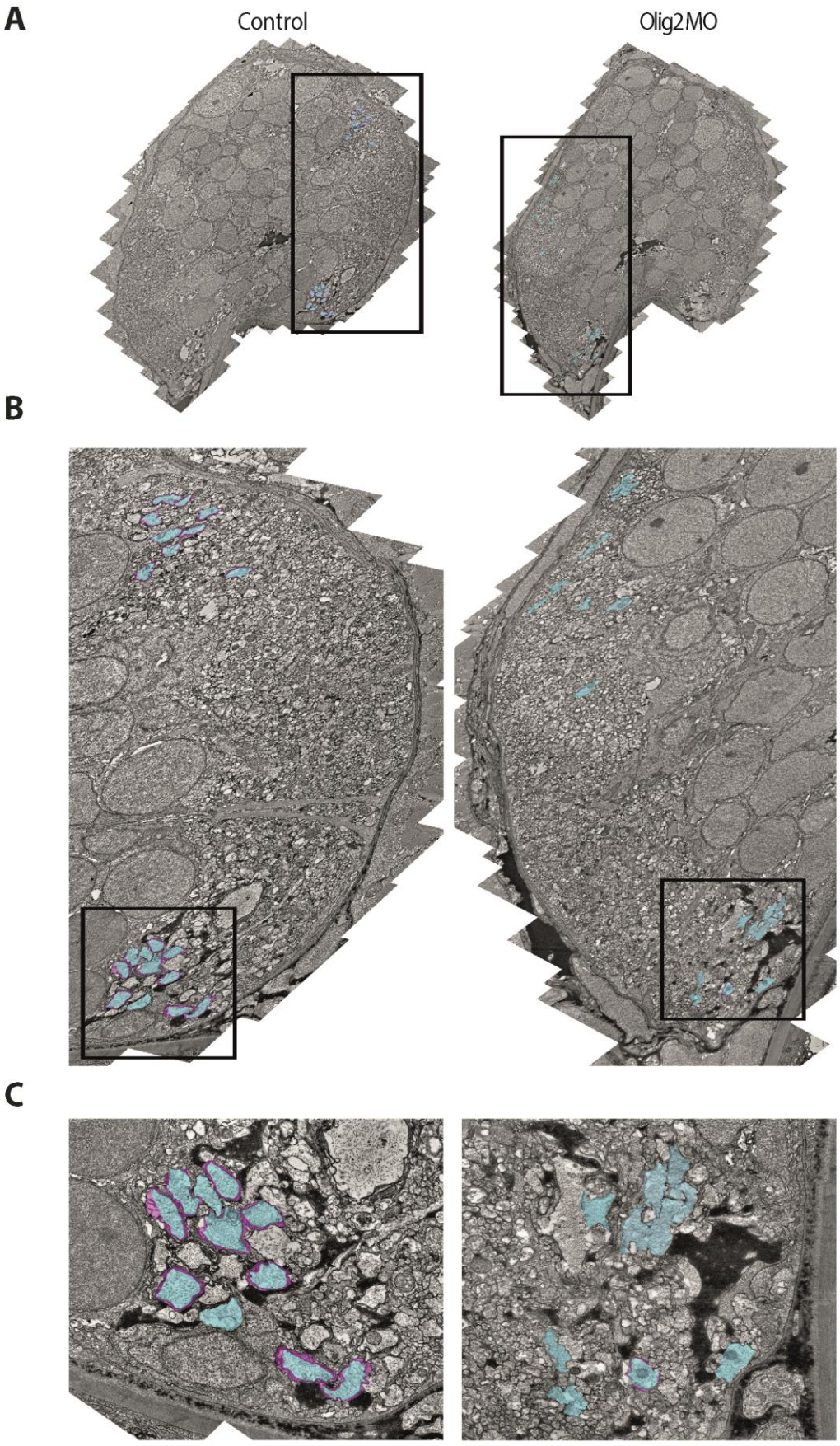
A
Control
Olig2MO
B
C

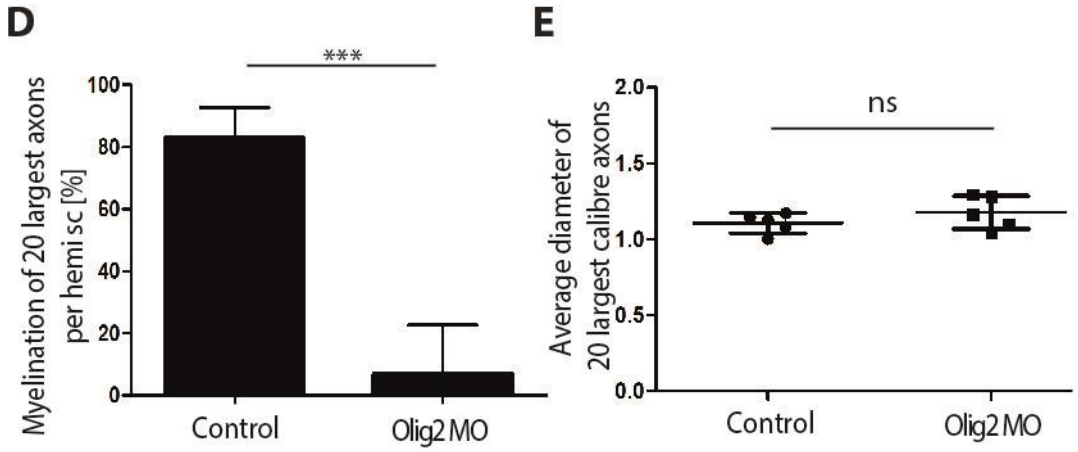

Figure 3.13: Myelin ensheathment does not regulate axon calibre. The 20 largest calibre axons per hemi spinal cord (excluding the Mauthner axon) and the myelin wrapped around them are colour coded in blue and purple, respectively. (A) Electron micrographs of a tranversal spinal cord section of control injected animals (left) and Olig2 MO injected animals (right). Areas marked with a black rectangle are shown in B. (B) Electron micrographs of hemi spinal cord sections of control injected animals (left) and Olig2 MO injected animals (right). Areas marked with a black rectangle are shown in C. (C) Electron micrographs of the ventral spinal cord area showing the Mauthner axon and the surrounding large calibre axons. (D) Of the 20 axons with the largest calibre per hemi spinal cord, on average 83% +/- 9 are myelinated while 17% +/- 9 are unmyelinated in control animals. On average, in Olig2 MO injected animals, 7% +/- 15.6 of the 20 axons with largest calibre per hemi spinal cord are myelinated, while 93%+/- 15.6 are unmyelinated (control n = 5, olig2MO n = 5). (E) The average axon diameter of the 20 largest calibre axons in control injected animals is 1.11 +/- 0.06 µm, while the average diameter of the 20 largest calibre axons in Olig2 MO injected animals is 1.17 +/- 0.1 µm (control n = 5, olig2MO n = 5) (Two-tailed student's t-test, p = 0.9).

3.3 Discussion

Only specific subsets of spinal cord neurons are myelinated during early zebrafish development

The nervous system of the early zebrafish embryo is relatively simple with only a limited number of neurons, which makes it a good model system to study individual neurons (Kuwada et al., 1990). The spinal cord neurons that I selected for the analysis in this chapter have been described in detail according to their morphology (Kuwada et al., 1990; Bernhard et al., 1990; Hale et al., 2001) and neurotransmitter type (Higashijima et al., 2004). However, which of these neurons are myelinated and which remain unmyelinated during the early zebrafish development has not been investigated so far.

The neurons fated to be myelinated during early development were RS neurons, CoPA and CiD interneurons, while the axons of CoBL, CiA and RB neurons were not myelinated during the early development up to 12dpf.

Of course, there are many other neuron subtypes in the zebrafish spinal cord that have not been investigated in this study, such as ventral longitudinal descending (VeLD), dorsal longitudinal ascending (DoLA), commissural secondary ascending (CoSA), unipolar commissural descending (UCoD), ventral medial (VeMe), multipolar commissural descending (MCoD) (Bernard et al., 1990) and the commissural longitudinal ascending (CoLA) (Hale et al., 2001). These neurons might be fated for myelination as well and might have myelinated axons in the early embryonic development, but were unfortunately not investigated in this study as they were only rarely labelled by the Tg(s1011,Kaede) or by the injection of either UAS:GFP or UAS:GFP-cntn1a into the Tg(HuC:gal4) or Tg(cntn1b:kalTA4) lines. It will be interesting to label these neurons with other transgenic lines that will label them more efficiently in order to investigate their myelination status in future studies.

It is possible that RS, CoPA and CiD neurons simply are more mature and advanced in their neuronal development during the time of analysis, while CoBL, CiA and RB may be not fully developed at these time-points and may be myelinated in time. The myelination status of these neurons was not followed post 12dpf in my analysis as, due to limitations of fluorescent microscopy, it is difficult to live image the spinal cord of adult zebrafish as the tissue around the spinal cord becomes too thick.

However, RB are amongst the first neurons to develop in the zebrafish nervous system and undergo apoptosis from approximately 3.5dpf onwards (Williams et al., 2000) and therefore it is unlikely that they are not mature at the time of analysis. CoBL and CiA interneuron are also described to appear at approximately the same time-point at which RS, CoPA and CiD neurons are generated (Bernard et al., 1990) and it seems unlikely that they mature at a much slower rate than the myelinated neurons. The time of neuronal birth does therefore not correlate with the myelination fate of the individual neurons.

When comparing the different morphologies of the axons, it became obvious that, although they all have their individual shape, axon of neurons fated for myelination have different axon morphologies than the axons of neurons that remained unmyelinated. Axons of neurons that fated for myelination generally have a slightly larger axon calibre and show less axon branching than axons that remain unmyelinated, which I will discuss below. The relative position of the axons of the individual neurons in the spinal cord, however, was also distinctly different.

Axons of RS, CiD and CoPA neurons project over long distances in the spinal cord and the main length of their axons lies in the myelinated axon tracts in the ventral and dorsal spinal cord, respectively. Their axons might therefore be myelinated to secure the transmission of action potentials over a long distance, facilitated by saltatory conduction. RB axons are also located in the dorsal spinal cord, however, RB neurons undergo apoptosis approximately between 3-4dpf (Williams et al., 2000) and their axons might not have been selected for myelination due to the changes in the cellular structure and cell membrane composition concomitant with apoptosis (as reviewed in Elmore, 2007). CoBL and CiA interneurons, on the other hand, project in the lateral area of the spinal cord, a region that remains unmyelinated even in the adult zebrafish spinal cord (Jung et al., 2010), indicating that CoBL and CiA axons might not be myelinated even in the adult animal. Considering their axon position in the lateral spinal cord and their relatively short axons, CoBL axons terminate approximately 4 segments from their cell body (Bernard et al., 1990), their function might be more important for local signal transmission and simply not require myelination. The myelination status of an axon might therefore reflect their function and position in the spinal cord.

Not all glutamatergic neurons are myelinated

Of the neurons selected for this study, only the axons of RS, CoPA and CiD neurons were fated to be myelinated. It is tempting to speculate that there might be a correlation between myelination and a certain neurotransmitter, whereby only neurons of a certain neurotransmitter subtype might be myelinated. OPCs have been shown to receive transient glutamatergic synapses (Bergles et al. 2010, De Biase et al. 2010, Kukley et al. 2010) as well as GABAergic synapses (Lin and Bergles, 2004) from axons, which have been shown to elicit post-synaptic excitatory currents through NaV channels in the OPCs and might therefore influence OPC behaviour. Furthermore, synaptic glutamate release has recently been implicated in promoting myelination in vitro (Wake et al., 2011) (see chapter 4 for more information). Axonal glutamate release might therefore induce the myelin ensheathment by oligodendrocytes. If that is the case, glutamatergic neurons and other neurotransmitters that might bind to oligodendrocyte receptors through the axon-oligodendrocyte synapse would be myelinated, while neurons of other neurotransmitter types might not be.

The neurotransmitter properties of the neurons identified in the zebrafish spinal cord have been described previously in great detail (Bernhardt et al., 1990; Clarke et al., 1984; Hale et al., 2001; Kuwada et al., 1990; Mendelson, 1986). The different neurotransmitter subtypes have been examined by expression of different markers, such as the vesicular glutamate transporter (VGLUT) to label glutamatergic neurons, the glycine transporter (GLYT2) to label glycinergic neurons and glutamic acid decarboxylase (GAD65/67) to label GABAergic neurons (Higashijima et al., 2004).

RS, CoPA and CiD neurons have been identified as glutamatergic. Interestingly, these neurons are also the ones fated for myelination in the early zebrafish development. The interneurons in this study that are not myelinated during the time-points of analysis, CoBL and CiA, were both identified as glycinergic. However, there is also a glutamatergic subset of CoBL interneurons, and RB sensory neurons are also glutamatergic. None of the imaged CoBL interneurons were myelinated and RB axon only very rarely showed a small myelin sheath, suggesting that not all glutamatergic neurons are fated to be myelinated. Furthermore, CoLA interneurons, a neuron type, which was rarely labelled and therefore not included in the analysis, are

also glycinergic and have been found to be myelinated in my preliminary analysis (data not shown). This indicates that glycinergic neurons can be myelinated as well and that glutamate release is not the only neurotransmitter correlating with myelination. It will be interesting to see whether GABAergic neurons will be myelinated or whether the only neurons with myelinated axons are either glutamatergic or glycinergic.

Neurons fated for myelination show less axon branching than neurons that remain unmyelinated

The formation of axon collaterals, or axon branches, is generally regarded as one of the main mechanisms in the CNS to establish neuronal networks through synaptic connections (O'Leary et al., 1990; Snider et al., 2010). Axon branching can occur through three different cellular mechanisms: fillopodial branching (Bastmeyer and O'Leary, 1996), lamellopodial branching (Flynn et al., 2009), whereby filopodial or lamellopodial sprouting matures into a stable branch, as well as branching through growth cone pausing, whereby the leading axon growth cone undergoes phases of extension and retraction and filopodial or lamellopodial branches are generated at these locations of growth cone pause (Halloran and Kalil, 1994) (for review see Filbin, 2003). Although a lot is known about the molecular and cellular mechanism behind axonal branching, the fate of axon branches in relation to myelination is unclear. So far, it is unknown, whether axon branches disappear once the axon is myelinated or whether the myelin sheath is formed between axon branches or even whether there is a morphological difference in the axon branch number between myelinated axons and unmyelinated axons.

There were clear differences in the axon branch pattern seen in the individual neuron types analysed. Axons of all neurons analysed, except for RB, had a small number of branches at 2dpf but a small increase in axon branch number (in case of RS, CiD and CoPA) or more extensive increase in axon branch number (in case of CoBL and CiA) was seen at later time-points. The increased axon branching likely reflects increased functional maturity of the axons and the increased establishment of synaptic connections in the neuronal network as neurons connect with their synaptic targets through axon branching (Gallo et al., 2011; Gibson and Ma, 2011; Bilimoria

and Bonni, 2013). RB on the other hand, had extensive axon branching at 2dpf, the branching decreased at 3-5dpf and 6-12dpf. The decrease in axon branching in RB axons very likely reflects their functional redundancy by post 3-4dpf, given that RB undergo apoptosis during early development and their function is replaced by DRG neurons in Xenopus (Lamborghini et al., 1987) and zebrafish (Williams et al., 2000).

One of the main differences between axons of neurons fated for myelination and axons of neurons that remained unmyelinated was the difference in their axon branch patterns. Axons of RS, CoPA and CiD neurons had significantly fewer axon branches than axons of CoBL and CiA axons. While axons of CoBL and CiA neurons show a great increase in the number of axon branching between 2dpf and 3-5dpf and between 3-5dpf and 6-12dpf, the axons of RS, CoPA and CiD neurons remain relatively stable and do not increase between 3-5dpf and 6-12dpf. Interestingly, the onset of myelination occurs from 3dpf and it is either possible that a smooth, less branched surface facilitates myelin ensheathment and those axons are therefore more likely to be myelinated or that myelin ensheathment inhibits axon branching of RS, CoPA and CiD axons, while the unmyelinated axons of CoBL and CiA neurons are not hindered to extend multiple axon branches.

Axon branch outgrowth has been shown to be inhibited in myelinated axons by so called myelin inhibitors, which are believed to be one of the main factors inhibiting axonal regeneration in the CNS after nerve injury (Berry et al., 1982, as reviewed in Filbin, 2003). There are three identified myelin inhibitors, Nogo-A acting through the Nogo receptor Ngr (Caroni and Schwab, 1988; Schnell and Schwab, 1990; Chen et al., 2000), the Nogo receptor ligand oligodendrocyte-myelin glycoprotein (Omgp) (Wang et al., 2002) and the myelin-associated glycoprotein (Mag) (McKerracher et al., 1994; Mukhopadhyay et al., 1994). Young neurons, however, have been shown not to be inhibited in their neurite outgrowth by Mag, in fact, it was shown that Mag even increased neurite growth in mouse embryonic spinal cord neurons (Turnley et al., 1998; Johnson et al., 1986), indicating a dual function for this protein in regulating neurite outgrowth. As all the neurons investigated in this study are embryonic it is questionable whether Mag inhibits neurite growth here. It is possible that these myelin inhibitors expressed during myelination inhibited a possible increase in axon branching in RS, CoPA and CiD axons, while the unmyelinated

CoBL and CiA axons were not inhibited in their axon branching. Alternatively, these morphological differences might be important in axon selection during myelination. Axons with less extensive branching might be preferentially myelinated by oligodendrocytes, perhaps due to the physical properties of an unbranched axon. Apart from axon calibre, the physical properties that facilitate axon ensheathment are unknown, however, as only axons are ensheathed rather than dendrites or cell bodies (Lander, 1989; Hildebrand et al., 1993), it is conceivable that the physical properties of axons can be important in the axon selection during myelination.

It is also possible that the formation of relatively short myelin sheaths between multiple axon branches and around axons of smaller calibre might simply not be advantageous for conduction velocity or energy efficiency compared to non-myelinated signal conduction. I will further investigate the role that functional activity has in axon selection during myelination in chapter 4.

From the findings in this study, it is impossible to conclude whether axon branching occurs due to the absence of myelin inhibitors or whether myelination occurs due to the absence of extensive axon branching. It will be very interesting to investigate whether the axons of RS, CoPA and CiD neurons would exhibit a more branched axon morphology in the absence of oligodendrocyte contact and myelin ensheathment in the olig2MO treated animals. The establishment of a more branched axon morphology in RS, CoPA and CiD neurons in absence of myelin ensheathment would indicate that the myelin inhibitors described above indeed underlie the different axon branching pattern seen in myelinated and unmyelinated axons. If the axon branching of RS, CoPA and CiD axons remains unchanged in the absence of myelin ensheathment might indicate that the smooth less branched axon surface of RS, CoPA and CiD neurons might facilitate myelin ensheathment.

Axon calibre as a mechanism regulating myelination

Oligodendrocytes, in vitro, have been shown to differentiate in neuron-free cultures (Knapp et al., 1987; as reviewed in Lubetzki, Demerens and Zalc, 1997) and can form compact myelin sheaths around paraformaldehyde fixed axons (Rosenberg et al., 2008) or even ensheath inert polystyrene fibres in the absence of axonal signals (Lee et al.,2012). Importantly, these nanofibres were only ensheathed if the calibre of

the fibres was above 0.4µm (Lee et al., 2012), demonstrating an important role of axon calibre during myelination. In vivo, large calibre axons have been demonstrated to influence the myelinating behaviour of oligodendrocytes in zebrafish (Almeida et al., 2011) and the onset of myelination in the rodent optic nerve has been shown to follow the axon calibre gradient from the eye to the chiasm, whereas oligodendrocytes differentiation follows the reverse direction, from the chiasm to the eye (Colello et al., 1995). Together these findings suggest that axon selection during myelination can be influenced by axon calibre in vivo. If this was the case, large calibre axons would be more likely to be myelinated. In this chapter, I investigated whether axon calibre might correlate with myelin ensheathment of the individual neurons.

When I grouped the average axon calibre of the neurons fated for myelination (RS, CiD and CoPA) and the neurons that remain unmyelinated (CoBL, RB, CiA) over time, the average axon calibre of neurons fated for myelination was subtly, but significantly, larger than the average axon calibre of the neuron that remain unmyelinated. Furthermore, RS axons had the largest axon calibre of all neurons analysed and also had the highest percentage of myelin ensheathment along the axon, while CoPa and CiD with a smaller axon calibre showed a lower percentage of myelin ensheathment along the axon. This suggests that axons calibre might be an axon property that influences axon selection during myelination. However, the axon calibre of CoBL neurons increases with time and is at 6-12dpf as large as axons of CiD and CoPA neurons, but CoBL axons remain unmyelinated, even at a time-point when their axon calibre was equal to myelinated axons from CoPA and CiD neurons. Furthermore, all the axons analysed in this chapter had an average axon calibre of at least 0.3µm or above by 3dpf and it has been shown that there are myelinated axons with a calibre of only 0.3µm in the vertebrate spinal cord (see Chapter 4; Matthews and Duncan, 1971; Waxman and Bennett, 1972; Remahl and Hildebrand, 1982; Hildebrand et al., 1993), demonstrating that none of the axons analysed were too small to be myelinated. Together, these findings show that axon calibre alone cannot be the only axon property that regulates axon selection during myelination. Other axon properties such as neuronal activity or the expression of signalling molecules on the axon membrane (see introduction) must be involved in the axon-

oligodendrocyte interactions during myelination. Overall, my findings suggest that axon calibre can influence the axon selection during myelination, but that other factors in addition to axon calibre regulate myelination.

Olig2 MO treatment to reduce myelinating oligodendrocytes in the zebrafish spinal cord

The motor neuron progenitor domain (pMN) gives rise to OPCs (see introduction) in the zebrafish spinal cord. OPC differentiation is regulated by several key transcription factors (for review see Boulanger and Messier, 2014). One of them is the basic helix-loop-helix oligodendrocyte lineage transcription factor 2 (olig2) downstream of sonic hedgehog signalling, which is essential for motor neuron formation and oligodendrocyte specification (Novitch et al., 2001; Pogoda et al., 2006; Zhou et al., 2001; Zhou & Anderson, 2002). Olig2 is expressed throughout the oligodendrocyte lineage, from progenitor cells to myelinating oligodendrocytes (Li and Richardson, 2008; see chapter 1), and a knock-out of olig2 ablates oligodendrocytes in the mouse CNS (Lu et al., 2002). Inhibition of olig2 translation through the olig2 MO in zebrafish therefore prevents OPC formation and differentiation to myelinating oligodendrocytes. Oligodendrocyte development and myelination was successfully reduced by the olig2 MO treatment, up to 4dpf as shown in the fluorescent imaging of Tg(mbp:GFP-caax), with the exception of very few myelin sheaths formed around the Mauthner axon. One of the disadvantages of MOs to knock-down gene expression is that MO efficiency is reduced over time and the inhibition of olig2 translation over time is limited. An undergraduate student that I supervised during my PhD tested the efficiency of the olig2MO treatment using Tg(mbp:GFP-caax) animals treated with olig2MO found robust mbp expression in the spinal cord of 5dpf (data not shown), indicating that the olig2 MO is only efficient in inhibiting oligodendrocyte lineage cell formation until approximately 4dpf. The few myelin sheaths found around the Mauthner axons in the olig2MO treated animals were therefore likely formed by oligodendrocytes that formed as the effect of the olig2 MO wore off over time. The myelin sheaths observed around the Mauthner axon therefore indicate that oligodendrocytes have developed in the olig2 MO treated animals by 4dpf. As oligodendrocyte contact has been shown to

influence axon calibre growth even in absence of compact myelination (Sanchez et al., 1996), potential pre-myelinating oligodendrocytes in the spinal cord might have had an effect on axon growth of the reticulo spinal axons measured in the analysis. However, as axon ensheathment was still necessary for the increase in axon calibre in the study (Sanchez et al., 2000) and as nearly all axons were not ensheashethed in the olig2MO treated animals, it seems unlikely that the axon calibre of all reticulospinal neurons measured is influenced by oligodendrocyte contact. A precise assessment of the number and differentiation state of the OPCs that developed in the olig2MO treated animals by 4dpf is required when interpreting the results from the olig2MO treatment. OPCs can be labelled by crossing the transgenic lines Tg(sox10:mRFP) and Tg(olig2:GFP), whereby double labelling is required as both transgenic lines express their fluorescent proteins in oligodendrocyte lineage cells but also in different subsets of neurons. Only double labelled cells are truly oligodendrocyte lineage cells. A more endurable tool to inhibit olig2 expression for a longer period of time would be a genetic knock-out using the CRISPR-Cas genome editing technique (Hwang et al., 2013). However, as shown in the fluorescent imaging of Tg(mbp:GFP-caax) and electron micrographs by 4dpf, only few mbp positive cells were found and the myelin ensheathment was reduced by 91% in the Olig2 MO treatment. The treatment was therefore successful in inhibiting the majority of OPC lineage formation.

The axon calibre in axons with the potential to be myelinated grows independently of myelin ensheathment

Not all of the neurons fated for myelination, RS neurons, CoPA and CiD interneurons, showed a significant increase in their axon calibre size after the onset of myelination. RS neurons have the largest calibre axons investigated in this thesis and their calibre increases over time. However, because increase in axon calibre coincides with the onset of myelination, it was impossible to discern whether the RS were ensheathed because of their calibre size or whether axon calibre was increased due to myelin ensheathment. In order to test whether the axon calibre of neurons fated to be myelinated, such as RS neurons, might be regulated by oligodendrocyte contact or myelin ensheathment, oligodendroglial cell fate determination was

inhibited by olig2 MO knockdown, thereby inhibiting the formation of all oligodendrocyte lineage cells. The axon calibre of the 20 axons with largest calibre per hemi spinal cord was not affected in the absence of the majority of oligodendrocytes. Approximately 10 out of the 20 axon with largest calibre per hemi spinal cord were RS axons, suggesting that even the axon calibre growth of RS is also independent of oligodendrocyte contact and myelin ensheathment.

These findings contradict previous studies, which implied oligodendrocyte contact (Sanchez et al., 2000; Colello et al., 1994, Colello et al., 1995) and myelination (Sanchez et al., 1996) to regulate axon calibre of the rodent optic nerve. These studies suggested that oligodendrocyte contact alone is sufficient to regulate axon calibre growth (Sanchez et al., 1996) and only x-irradiation of the oligodendrocytes (Colello et al., 1994; Colello et al., 1995) lead to an inhibition of the oligodendrocyte effect on axon calibre and a subsequent decrease in axon calibre. However, the phenotypes in these studies were comparatively small, given the small variance of axon calibre sizes in the optic nerve, and the x-irradiation of oligodendrocytes in the optic nerve could have had a negative influence on axon calibre growth. Inhibition of the formation of oligodendrocyte lineage cells by olig2 MO knock-down did not have any adverse effect on the spinal cord neurons as the axon calibre measured was not affected. It is possible that the neurons in olig2 MO treated animals might have been affected by axonal swelling due to a MO side-effect, which could have led to a false positive result. If this had been the case, the electron micrographs of olig2 MO treated animals would have shown a defect in the neurofilament distribution of the spinal cord axons. The neurofilament distribution in the spinal cord axons of olig2 MO treated animals, however, was normal in comparison to the control animals, suggesting that no axonal swelling took place.

Axon calibre growth might be locally regulated by oligodendrocyte contact or myelin ensheathment depending on the region in the CNS. The previous studies linking axonal growth with oligodendrocyte contact were performed in the optic nerve and even studies in mutant mice lacking compact myelin, such as the *Shiverer* line, focused on the optic nerve (Sanchez et al., 2000), while the axon calibre in absence of oligodendrocytes and myelination in this study were measured in spinal cord axons. Characterizing the calibre growth of optic nerve axons in olig2 MO treated

animals would clarify whether axon calibre growth is regionally dependent on oligodendrocyte contact and myeliantion.

Furthermore, the previous studies employed rodent models, while this study uses zebrafish as a model organism. The physiological differences between mammals and teleosts might account for the discrepancies between these results and the previous studies. Myelin in the teleost CNS contains myelin protein zero (MPZ/P_0), which is only found in the mammalian PNS (Jarjour et al., 2012). Differences in myelin composition might indicate a difference in the regulatory mechanism behind myelin formation and hints at the potential role that myelin might have during axon growth. It would be interesting to test whether a complete oligodendrocyte knock-down in mammalian models would also not have an effect on axon calibre growth of spinal cord neurons.

Another possible explanation for the discrepancies between this study and previous studies is that there might have been a small delay in axon calibre growth in the absence of oligodendrocytes, which was compensated for at 4dpf when the fish were fixed for electron microscopy. This seems unlikely, however, as the axon calibre of CoPA and CiD axons was relatively constant between 2dpf and 12dpf and did not increase with the onset of myelination at 3dpf. Time course imaging of RS, CoPA and CiD axons between 2dpf and 12dpf in olig2 MO treated animals would help to exclude the possibility that subtle or transient effects might have been missed in the analysis of this study.

Overall, these findings demonstrate that the axon calibre of zebrafish spinal cord neurons can be regulated independently of oligodendrocyte contact or myelin ensheathment.

Potential neuronal signals that might regulate axon calibre

This analysis demonstrates that extrinsic properties supplied by myelin ensheathment and oligodendrocyte contact do not regulate axon calibre growth in neurons fated for myelination in the CNS. Neuronal specific properties might therefore regulate axon calibre growth. The neuron specific regulation of axon calibre growth could either be intrinsic to each neuron according to its neuronal subtype or regulated by a neuronal circuit through synaptic input.

Mouse models lacking myelin such as the *Trembler* (de Weagh et al., 1992) or *Shiverer* line (Sanchez et al., 2000) show a decrease in neurofilament phosphorylation, which is concomitant with a reduction in axon calibre, indicating that changes in axonal neurofilament phosphorylation might influence axon calibre. Phosphorylation of the carboxyl group at the terminus of the heavy and medium neurofilament subunits has been shown to regulate neurofilament density as they cause repulsion amongst the neurofilament subunits, which leads to the radial increase of axon calibre (Nixon et al., 1994). Most previous studies investigating axon calibre in context with myelination in mammalian models have indicated that loss of oligodendrocyte contact or myelin ensheathment can regulate neurofilament number and phosphorylation and thereby decrease axon calibre (Colello et al., 1994; Colello et al., 1995; Sanchez et al., 1996; Sanchez et al., 2000). However, in the light of this study, it is also conceivable that neurofilament number or phosphorylation can be regulated either by a neuron intrinsic mechanism or by synaptic input from other neurons in a circuit. A recently published study investigated axon calibre of cortical axons and found a correlation between the axon calibre of individual axons and the axon calibre of axons in the area of origin as well as the target area of those individual axons (Tomasi et al., 2012; Innocenti et al., 2013), indicating that the neuronal circuit of an axon can influence axon calibre. Similar finding was made in an important study demonstrating that when the submandibular duct, the target of servical ganglion neurons, is dissected in 4 week old rats, the axon calibre of the ganglion axons was decreased at 30 weeks of age. The dissection at birth of one of the sympathetic nerves innervating the gland led to an increase in axon calibre of the remaining sympathetic neurons at 30 weeks of age (Voyvodic, 1989). This indicates that axon calibre in the PNS might be regulated by target size in the neuronal circuit. Furthermore, it has been shown that, once axons make synaptic contacts with other axons, the synthesis of neurofilament subunits and other cytoskeletal axon components increases and axonal transport of these proteins decreases (Hoffman et al., 1983; Willard and Simon, 1983). Together, these findings indicate that axon calibre might be regulated by synaptic interactions in a neuronal circuit. Another neuron specific factor that might influence axon calibre growth is neuronal activity, which might influence neurofilament number and phosphorylation. So far, there is

little direct evidence that more active axons also have a larger axon calibre than less active axons. However, neuronal electrical activity could induce the synthesis of axonal cytoskeleton proteins such as neurofilament or activate potential internal signalling pathways to increase neurofilament phosphorylation. Likewise, axonal synaptic activity could induce a feedback loop, activating potential pathways that increase neurofilament number or phosphorylation. Of course, neuronal activity of an axon is also influenced by the input that axon receives in its circuitry. In a circuitry context, it is possible that synaptic input from neighbouring neurons determines axonal neurofilament number and density, and thereby axon calibre, in order to optimize the signal conduction within the neuronal network. Adapting axon calibre size through excitatory or inhibitory inputs would be an efficient mechanism to optimally synchronize the arrival time of signals from different origins or increase signal conduction in the absence of myelination. It would be very interesting to experimentally decrease synaptic input in a described circuit, perhaps by laser ablation of the trigeminal nerves to reduce synaptic input on the Mauthner axons (Kohashi and Oda, 2008; Issa et al., 2011) and subsequently measure Mauthner axon calibre. If axon calibre could indeed be regulated by excitatory or inhibitory inputs from neighbouring axons, it is possible that neurons in the absence of myelin in olig2 MO treated animals developed an increased number of synaptic boutons or stronger synaptic connections to increase axon calibre in order to compensate the loss of myelin ensheathment and the axon calibre of their axons therefore remained unchanged compared to controls. It might be interesting to characterize the level of synaptic input in olig2 MO treated animals by quantifying the synaptic boutons expressed along the axons and monitoring synaptic activity. Quantification of synaptic bouton number could be achieved either by immuno-labelling of one of the major synaptic vesicle protein, synaptophysin or expression of a synaptophysin-fluorescent reporter fusionprotein (Meyer and Smith, 2006), while synaptic activity could be monitored by expression of a calcium indicator, such as GCaMP (Chen et al., 2013) fused to synaptophysin.

In chapter 4, I will further investigate the relationship between axon calibre and axon function in an experimental set up where axonal function is reduced globally and

through that, will describe and discuss the role that axon calibre and neuronal activity play in axon selection during myelination.

4. Synaptic transmission regulates dynamic oligodendrocyte behaviour and myelination

4.1 Introduction

Axonal signals have long been implicated to play an important role in regulating myelination in the peripheral nervous system (PNS) as well as in the central nervous sytem (CNS). Myelin sheath thickness has been shown to correlate with axon calibre in the PNS (Friede and Samorajski, 1968a, Berthold et al., 1983) and in the CNS (Friede and Samorajski, 1968b; Friede et al., 1971; Hildebrand and Hahn, 1978; Hildebrand et al. 1993). Furthermore, myelin thickness and internodal length are adjusted to the conduction properties of axons in order to maximize conduction velocities and the precise timing of signal transmission in the PNS (Rushton, 1951; Waxman, 1997) and the CNS (Sugihara et al., 1993).

Together, these findings indicate that axon-glial signaling might underlie the formation of an optimally functioning myelinated axon.

Somewhat surprisingly, in the PNS, axonal expression of a single growth factor, neuregulin-1 (NRG1), is the pivotal signal that controls Schwann cells at essentially every stage of the lineage progression by activating the transmembrane receptors ErbB2 and ErbB3 in Schwann cells. NRG-1 type III-ErbB signalling is required for Schwann cell survival, proliferation and differentiation (Jessen and Mirsky, 2005; Lyons et al., 2005; Salzer and Nave, 2006). NRG-1 type III is also, at a certain threshold level, essential to induce PNS myelination in vitro as well as in vivo (Lyons et al., 2005; Taveggia et al., 2005). NRG-1 type III expression levels on myelinated axons have even been shown to regulate Schwann cell membrane growth in order to adjust the myelin sheath thickness to precisely match the axon caliber (Michailov et al., 2004).

As Nrg1-ErbB signaling only has a minor role in CNS myelination (see chapter 1 Introduction), the molecular and cellular mechanisms behind CNS myelination are unknown. For example, it is unclear how the specific axon fated for myelination is chosen by oligodendrocytes, what initiates the onset of myelination of these axons at the appropriate moment during development and more specifically, what determines the length of a myelin sheath and the myelin sheath thickness for optimal signal conduction per axon or what are the mechanism maintaining the myelin sheath thickness according to axon calibre once the axon calibre changes throughout the development of the organism. Given the complexity of these cellular behaviours, it is

likely that there is more than one mechanism regulating myelination and that there are intrinsic and extrinsic factors controlling myelination. Since the conduction properties of active neurons are an important variable in myelinated axons it is possible that neuronal activity might mediate some of the axon-oligodendrocyte interactions regulating axon ensheathment and myelin sheath number, length and thickness. The role that neuronal activity might play during myelination has been investigated in different systems, with controversial results (as reviewed in Fields, 2005; Zalc & Fields, 2000) as I will discuss below.

MRI studies indicate that neuronal activity can increase white matter volume

Neuronal activity has been suggested to be a major regulatory mechanism promoting myelination based on MRI studies using magnetic resonance diffusion tensor imaging (DTI) to investigate the influence of neuronal activity on white matter. White matter, which is essentially myelinated fibre tracts in the CNS, has been shown to be increased in the corpus callosum of children with higher cognitive abilities in bimanual co-ordination tasks (Johansen-Berg et al. 2007) as well as in different brain regions associated with motor function in jugglers (Schmithorst et al., 2005) as well as in piano players (Bengtsson et al. 2005). Interestingly, the white matter increase in piano players was regionally specific for each age period in which the piano practice occurred (Bengtsson et al. 2005). This indicates that training induced neuronal activity can regulate the amount of white matter in certain brain areas but only during a period when the involved fiber tracts are under maturation. This suggests that neuronal activity might only regulate myelination / white matter in regionally specific time periods during development.

Together, these findings indicate that an increase in neuronal activity by training of certain tasks may induce regionally specific plasticity in myelinated fibre tracts, essential for optimal cognitive performance. The observed increase in white matter by DTI has been interpreted as increased myelination caused by neuronal activity during training (Bengtsson et al., 2005). However, while DTI is a non-invasive technique suited for in vivo analysis, white matter changes are measured indirectly through voxel-wise estimates of the directional diffusion of water, which is more

restricted along myelinated axons than unmyelinated axons or other tissue, called fractional anisotropy (FA) (Basser et al., 1994). FA is a complex measure, representing various properties of white matter, such as axonal density, axon diameter and myelination (Beaulieu, 2002) and cannot clarify the cellular mechanisms behind the increase of white matter correlated with neuronal activity.

The observed increase in white matter volume could therefore be due to an increase in axon number, axon calibre and axon branching or indeed, an increase in myelin sheath number or myelin thickness. The cellular mechanisms by which neuronal activity might regulate myelination remain unknown. In order to characterize the role of neuronal activity during myelination, studies with higher cellular resolution are needed.

Studies investigating the effect of neuronal activity on the myelination of the optic nerve in animals reared in the dark give conflicting results

Neuronal activity has long since been thought to induce myelination but early studies investigating the myelination of optic nerve fibres in absence of neuronal activity provided conflicting results. The optic nerve, which is almost completely myelinated in most organisms, shows comparatively few myelin sheaths in the naturally blind cape mole rat (Omlin, 1997), indicating that the relatively low level of neuronal activity is correlated with a low level of myelination in the optic nerve of the blind animal. Several studies applied dark-rearing of the animal model in order to decrease neuronal activity, with contrasting results. Dark rearing of mice after birth resulted in a reduced number of myelinated axons in the optic nerve at approximately 3 and 4 weeks after birth (Gyllensten and Malmfors, 1963). Interestingly, the percentage of myelinated axons was decreased more in thicker axons >1µm in diameter than thinner axons <1µm in comparison with controls, even though both groups were significantly smaller, suggesting that the thicker axons in the optic nerve might require activity more than thinner ones (Gyllensten and Malmfors., 1963). However, it has been shown that post-natal dark rearing in mice causes a delay in cell nuclei - and neuropil growth in the visual cortex (Gyllensten, 1959c), suggesting that optic nerve neurons might have developmental delays, which might have caused a delay in

the onset of myelination in dark reared mice, which might account for the reduction of myelinated axons.

Another study using dark rearing to decrease neuronal activity in cats showed only a temporary effect as the number of myelinated axons in the optic nerve was only reduced in 3 week old cats but was nearly identical to controls at 4 weeks (Moore et al., 1976). The n number in this study was very low as only two kittens were reared in the dark and the authors themselves concede that myelination is taking place very rapidly at this stage of development and variation in age of only a few days could account for the difference seen at 3 weeks. Other studies even reported an increase in the number of myelinated axons in the optic nerve of dark reared rats at approximately 4weeks of dark rearing, and even after introduction to normal light conditions after 4 weeks of dark rearing (Fukui et al., 1991). However, this increase in myelinated axon number is not statistically significant, while only the decrease in unmyelinated axon number is statistically significant. The increase in myelinated axon number also coincides with an increase in average axon calibre. This increase was due to an increase in axon calibre rather than an increase in myelin sheath thickness. Since axon calibre might in fact induce myelination (see chapter 3), the increase in axon calibre might mask a small myelination phenotype in relation to neuronal activity. Furthermore, the myelin thickness of a myelinated axon usually correlates with the axon calibre and is accordingly increased with the axon calibre under normal conditions (Friede and Samorajski, 1968b; Friede et al., 1971; Hildebrand and Hahn, 1978; Hildebrand et al. 1993), suggesting that the absence of neuronal activity lead to an abnormal development of myelinated axons in dark reared rats.

Premature, artificial eye opening of young rabbits at the 5^{th} postnatal day to increase neuronal activity, on the other hand, resulted in an increased level of myelin basic protein (mbp) in rabbits with premature eye opening between the 7^{th} and 10^{th} postnatal day compared to controls (Tauber et al., 1980), suggesting that an increase in neuronal activity might promote myelination. However, the number of myelinated axons was not assessed in this study and it is unclear, whether the increase of mbp results from an increase in myelin sheath thickness or an increase in myelin sheath number concomitant with an increase in myelinated axon number, or both.

While the study increasing neuronal activity did not assess myelinated axon number at all, the number of myelinated axons in the optic nerve of dark reared animals in the studies described above was assessed by electron microscopy. While this is a very good tool to quantify the number of myelinated and unmyelinated axons at a certain time-point of development, it does not reveal the cellular mechanism behind a potential role of neuronal activity during the different stage of myelinated axon formation. It remains unclear, whether the absence of neuronal activity can influence the number of myelinating oligodendrocyte or whether oligodendrocytes form a reduced number of myelin sheaths resulting in a reduced number of myelinated axons in the CNS.

Overall, these conflicting data could not clarify the role that neuronal activity might have on myelination and elucidate the cellular axon-oligodendrocyte mechanisms behind it.

Effects of neuronal activity on early stage of OL lineage progression

Neuronal electrical activity has also been suggested to influence earlier stages in the oligodendrocyte lineage prior to myelination.

Neuronal activity has been shown to promote oligodendrocyte precursor cells (OPCs) proliferation in an in vivo experiment, in which the number of mitotic oligodendrocytes was decreased by approximately 90% 4 days after axon transection of the developing optic nerve in rats (Barres and Raff, 1993). The same result was seen when the optic nerve was transected in mutant mice whose axons degenerate at a very slow rate after axon transection and whose axolemmal composition was not changed after axon transection (Perry et al., 1991), reducing the possibility that the observed increase in OPC proliferation is due to a potential loss of glial mitogens on the axon surface (Barres and Raff, 1993). Intraocular injection of the sodium channel blocker TTX, which silences axonal electrical activity, led to a similar decrease in OPC proliferation, indicating that the OPC proliferation depends on electrical activity in axons (as described above, Barres and Raff, 1993).

In accordance with that, enhanced neuronal activity has been shown to increase the OPC proliferation rate in a recent in vivo study using optogenetic stimulation in

young and adult mice (Gibson et al., 2014). Optogenetic stimulation is a technique by which a light-sensitive ion channels are expressed in specific neurons and whereby light excitation of the ion channel induces neuronal activity. 3hours after a 30min period of stimulation of cortical layer V projection neurons, a 4-fold increase in mitotic OPCs was found in the premotor cortex and in the subcortical white matter projections of the corpus callosum. A similar increase was seen in neuronal precursor cells after the optogenetic stimulation. Daily stimulation of 2.5min (30s cycles with 2min intervals) for 7 days at P35 and P84 resulted in a continued increase of mitotic OPCs and a concomitant increase in oligodendrocyte number 4 weeks after the stimulation. These findings indicate that the OPC who proliferated in response to neuronal activity also differentiated to oligodendrocytes in young animals as well as in adults (Gibson et al., 2014). These findings suggest that OPC proliferation is directly promoted by neuronal activity, however, the optogenetic stimulation has also shown an increase in neuronal progenitor cells, which presumably led to an increase in mature neurons. It is therefore unclear whether the stimulation of neuronal activity or the increase in neuron number itself might have promoted the increase in OPC proliferation, as oligodendrocyte numbers are usually matched to the number and length of axons requiring myelination, e.g. in the optic nerve (Barres and Raff, 1994).

On the other hand, OPCs have been shown to stop their proliferation as they differentiate (Gao et al., 1997), and neuronal activity has been shown to reduce OPC proliferation and stimulate differentiation. Neuronal activity evoked by stimulation at 10hz for 24h of DRG-OPC co-cultures resulted in a decrease of OPC proliferation immediately after the stimulation (Stevens et al., 2002). The decrease in proliferation was inhibited by adenosine receptor antagonists and replicated by application of 100µM adenosine for 48h in cerebral slice cultures, indicating that adenosine, a derivative of the adenosine-tri-phosphat (ATP) that is released by stimulated axons (Stevens and Fields, 2000), plays a role in the activation of the activity-dependent inhibition of OPC proliferation (Steven et al., 2002). Neuronal activity induced glutamatergic activation of NMDA receptors in OPCs has been also shown to influence OPC behaviour in vitro and in vivo. Glutamatergic activation of specific NMDA receptor subunits increased the differentiation rate of multi-potent stem cell

cultures (MSCs) derived from the rat subventricular zone to oligodendrocytes rather than neurons or astrocytes at 10DIV after 3 days of incubation with NMDA receptor agonists (Cavaliere et al., 2012). However, selective activation of the metabotropic glutamate receptor lead to a small decrease in the oligodendrocyte differentiation rate, indicating that there might be multiple regulatory mechanisms involved. Interestingly, glutamate and NMDA exposure was shown to modulate oligodendrocyte morphology resulting in increased oligodendrocyte branching and an increased area covered by oligodendrocyte processes (Cavaliere et al., 2012). This indicates that OPC and pre-myelinating oligodendrocyte behaviour might be regulated by glutamate mediated NMDA receptor activation.

Furthermore, glutamate mediated NMDA receptor activation has been shown to promote OPC cell migration and inhibit OPC proliferation in purified OPCs in culture (Gallo et al., 1996, Gudz et al., 2006) and cerebral slice cultures (Yuan et al., 1998). In a recent in vivo study, OPCs have been shown to receive glutamatergic synapses from thalamocortical fibres in the mouse barrel cortex and to accumulate in the septa separating the barrels under normal conditions (Mangin et al., 2012). Sensory deprivation of these thalamocortical inputs resulted in increased OPC proliferation and a decrease in cell migration with a more uniform distribution in the input deprived barrel cortex, indicating that glutamatergic synaptic activation can regulate OPC proliferation and migration (Mangin et al., 2012). The sensory deprivation, however, did not directly ablate the axon-OPC synapses and the authors themselves concede that the demonstrated proliferation and migration of the NG2 cells might stem from secondary effects of thalamocortical innervation.

As thalamocortical innervation appears to decrease OPC proliferation on one hand, while increased neuronal activity in the optic nerve and cortex appears to increase OPC proliferation on the other, more work is needed in order to clarify these seeming discrepancies. It is possible that, neuronal activity has regional specific effects on OPC proliferation, different in thalamocortical areas than in the premotor cortex, the corpus callosum and the optic nerve. Or the effects of neuronal activity on OPC proliferation might be inducing at some points during development and inhibiting at others. Given the opposite effects of neuronal activity on OPC proliferation observed

in the different studies, it seems likely that there is more than one mechanism by which neuronal activity might regulate OPC behaviour prior to myelination.

One possible mechanism through which neuronal activity might regulate OPC behaviour are axon-OPC synapses. OPCs have been shown to receive transient glutamatergic synapses (Bergles et al. 2010, De Biase et al. 2010, Ge et al., 2009; Kukley et al. 2008 and 2010) as well as GABAergic synapses (Lin & Bergles, 2003) from axons (Figure 4.1). These axon-OPC synapses are functional and glutamate as well as GABA release in response to neuronal activity has been demonstrated to bind to AMPA, NMDA and GABA receptors and elicit post-synaptic excitatory currents through NaV channels in the OPCs. Excitatory postsynaptic currents have been recorded in OPC in response to spontaneous as well as evoked activity of glutamatergic neurons in the hippocampus (Bergles et al., 2000), optic nerve (Kukley et al., 2007), the corpus callosum (Kukley et al., 2007, Ziskin et al., 2007), cerebellum (Lin et al., 2005; Karatodir et al.,2008), the auditory pathway (Mueller et al., 2009) and the barrel cortex (Manging et al., 2012). Excitatory currents in OPCs were also recorded in response to the activation of GABAergic neurons (Lin and Bergles, 2003, Jabs et al., 2005).

Neural evoked excitation of these axon-oligodendrocyte synapses may be one mechanism by which neuronal activity might regulate oligodendrogenesis and myelination. A direct effect of OPC receptor activation on OPC behaviour, however, has not been demonstrated to date and the function of the axon-oligodendrocyte synapse remains unknown (Gallo et al., 2008; Almeida and Lyons, 2013). Furthermore, the synaptic connections as well as the AMPA, NMDA receptors and NaV channels expression are downregulated during the transition from OPCs to premyelinating oligodendrocytes (De Biase et al. 2010; Kukley et al., 2010), suggesting that these synaptic connections might not be involved during the myelination process itself.

Overall, the studies described above suggest that neuronal activity might regulate OPC behaviour prior to myelination. Cellular behaviours such as migration, proliferation, differentiation and survival of an oligodendrocyte lineage cell, however, are extremely dynamic and difficult to interpret in vitro or in fixed tissue as it has been done in previous studies. To this day it is unclear, whether neuronal

activity can directly induce OPC proliferation or differentiation. Higher resolution analysis following the cellular behaviour by live imaging will elucidate the intrinsic and extrinsic signals that regulate behaviour of oligodendrocyte lineage cells prior to and during myelination.

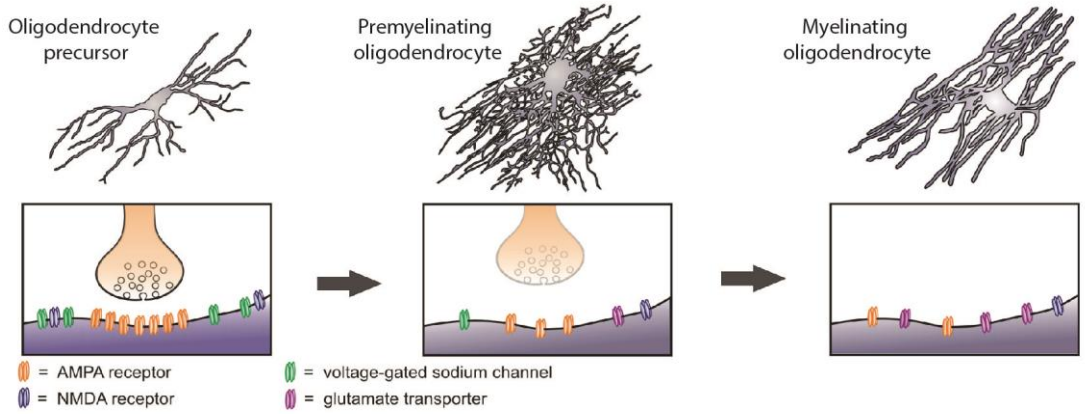

Figure 4.1: Schematic model of the axon-OPC synapse. Oligodendrocyte lineage cells undergo several morphological changes during cell differentiation from oligodendrocyte precursor cell (OPC) to premyelinating oligodendrocyte and to the mature, myelinating oligodendrocyte. OPCs receive glutamatergic and GABAergic (not shown) synapses from axons through which excitatory postsynaptic currents are elicited in the OPC after neurotransmitter binding to AMPA or GABA (not shown) receptors on the OPC surface. Gene expression profiling during these stages shows that mRNAs encoding for surface voltage gated NaV channel subunits and glutamate receptor as well as GABA receptors (not shown) decrease as the OPC differentiates into myelinating oligodendrocytes. The functional role of these axon-OPC synapses in vivo is yet to be determined. Image adapted from De Biase, Nishiyama and Bergles, 2010.

Electrical activity might induce myelinated axon formation

In order to investigate whether neuronal activity can induce myelination and to elucidate the cellular mechanisms underlying a potential neuronal activity dependent increase in myelination, in vitro studies have stimulated and inhibited neuronal electrical activity in neuron-glial co-cultures.

In vitro, neuronal stimulation of DRG co-cultures by electrical impulses of 10hz has been shown to promote OPC differentiation and myelin sheath formation 3-4 days after a 24h period of stimulation (Stevens et al., 2002) and even 21days after a 5h

stimulation at 10hz (Wake et al. 2011). A 10Hz stimulation of mixed cortical co-cultures at 24h after daily stimulation of 1h for 7days also resulted in an increased number of myelinating oligodendrocytes (Gary et al., 2012). Interestingly, stimulation at 1Hz or 100Hz showed no significant difference in the number of myelinating oligodendrocytes compared to non-stimulated controls (Gary et al., 2012). Other in vitro studies, reported that stimulation of DRG neurons using 5 days of electrical impulses at low frequencies (0.1Hz) inhibited myelination by Schwann cells and lead to a decrease in the number of myelinated axon, whereas stimulation at higher frequencies (1Hz) had no effect on myelinated axon number (Itoh et al, 1995; Stevens et al. 1998). Together, these findings indicate that neuronal activity might only influence myelination at a certain frequency of axonal depolarization and action potential firing.

The positive effect of 10Hz stimulation on myelinating oligodendrocyte number and myelin sheath number in the studies described above was inhibited by application of the sodium channel blocker tetrodotoxin (TTX), to the culture (Stevens et al., 2002, Wake et al., 2011, Gary et al., 2012). TTX binds to voltage-gated sodium channels present on the axon and blocks their opening, resulting in an inhibition of axon depolarization and thereby action potential generation (Lee and Ruben, 2008). The positive effect that electrical stimulation had on myelination was therefore interpreted to be exerted through axonal depolarization and action potential firing in neurons (Stevens et al., 2002, Wake et al., 2011, Gary et al., 2012).

In accordance with these findings, inhibition of neuronal electrical activity by pharmacological application of TTX for 2, 4 and 6 days resulted in a decrease in the number of myelinated axons in cultured embryonic brain slices at 18-21days in vitro (DIV) (Demerens et al. 1996). The number of myelinating oligodendrocytes and number of neuronal cell bodies was not different and there was no evidence for axonal injury detected by electron microscopy, indicating that the number of myelin sheaths and thereby the number of myelinated axons decreased (Demerens et al. 1996). Interestingly, the decrease in myelinated axon number after TTX application was most pronounced when the toxin was added just before the onset of myelination and was not detected at all at later time-points. By 28DIV, the number of myelinated axons had normalized in TTX treated cultures, indicating that the decrease in

myelinated axon number by inhibition of axonal electrical firing is only transient. When TTX was applied at 18-21DIV, after the onset of myelination, no effect of the toxin on the number of myelinated axons was found, implying that the activity dependent regulation of myelination is specific to certain time-points during cellular development. Stimulation of neuronal activity by pharmacological application of α-scorpion toxin, a neurotoxin, which slows sodium channel inactivation and thereby induces repetitive action potential firing in neurons, at 8 DIV for 2 days also led to increase in the number of myelinated axons at 18DIV, without a significant effect on myelinating oligodendrocyte and neuron cell body number (Demerens et al. 1996).

However, in direct contrast to this study, a spinal cord explant co-culture in vitro study using TTX to inhibit axonal electrical activity before the onset of myelination showed no effect on the onset of myelin formation and oligodendrocyte development (Shrager and Novakovic, 1995) and failed to recapitulate these findings. The number of myelinated axons as well as myelin thickness, measured by quantification of myelin lamellae surrounding myelinated axons by electron microscopy, was unchanged in cultures at 22DIV in continuous presence of 200nM TTX (Shrager and Novakovic, 1995). It is possible that the transient effect of axonal firing during myelination was missed by the TTX application in the latter study, however, this seems unlikely as both studies applied TTX before the onset of myelination. The discrepancies between the studies might be accounted for by the fact that one used embryonic brain explants while the other focused on spinal cord explants. Activity dependent regulation of CNS myelination might therefore be region specific. Furthermore, the latter study used the continuous presence of TTX to inhibit axonal firing, however, prolonged application of TTX can lead to the up-regulation of excitatory receptors in axonal synapses through synaptic scaling (O'Brien et al., 1998; Gainey et al., 2009). Synaptic scaling is a form of synaptic plasticity that adjusts the strength of excitatory synapses to the firing rate of a neuron (as reviewed in Turrigiano 2008). Synaptic scaling might have compensated for the effect of TTX on neuronal firing and therefore might not have inhibited axonal depolarization and action potential firing during the experimental duration of 22days, which might account for the discrepancies between the two studies.

Together, these in vitro data suggest that neuronal electrical activity might promote myelination; however, this effect might be specific to certain regions in the CNS, the frequency of action potential firing or different stages during the cellular development.

In vivo experiments using TTX to inhibit neuronal electrical activity could not clarify whether neuronal activity plays an important role during myelination. Postnatal intravitrous injection of TTX in rats at P7, P10 and P15, respectively, inhibited oligodendrocyte progenitor cell (OPC) proliferation in the optic nerve, which lead to a decrease in myelinating oligodendrocyte number after 2 days (Barres and Raff, 1993). While other studies applying intravitreous injections of TTX in the optic nerve of rats at the onset of myelination at P4 and examined at P6 showed no effect on the number of OPC proliferation but the number oligodendrocytes that form myelin sheaths was dramatically decreased in the optic nerve. However, intravitreous TTX injection on P5 with examination at P7 showed no effect on the number of myelinating oligodendrocytes (Demerens et al., 1996). These results suggest that, in vitro as well as in situ, the effect of electrical activity during myelination may be limited to a narrow time frame.

In contrast to this study, however, another study applying intraocular TTX injections every second day from P0 to P9 showed a normal number of myelinated axons in the rat optic nerve at P9 (Colello et al. 1995) and intraocular TTX injections every 2.5 days for 30 and 60 days during regeneration of the optic nerve in goldfish had no effect on the number of myelinated axons in regenerating nerve fibres (Hayes and Meyer, 1989). Furthermore, ventricular injection of TTX in the zebrafish brain also showed no effect on mbp expression levels and sodium channel clustering at nodes of Ranvier (Woods et al, 2006).

Pharmacological application of TTX in in vivo systems, however, can be challenging as new sodium channels can be synthesized after TTX application and sodium channel activity has been reported to return only minutes after TTX diffusion in vitro (Hammerström & Gage, 2000). As TTX was injected only once before the onset of myelination in one of the previous in vivo studies (Woods et al. 2006), it is possible that the treatment was insufficient in inhibiting electrical neuronal activity over the experimental time period, which could account for the lack of an in vivo phenotype.

Some of the other studies (Colello et al. 1995; Hayes and Meyer, 1989), however, used repeated TTX injections, which, similar to continuous TTX application, might have led to synaptic scaling and up-regulation of excitatory receptors in the synapses, thereby potentially compensating for any effects of TTX on axonal firing of action potentials (O'Brien et al., 1998; Gainey et al., 2009). None of the above mentioned studies used electrophysiology to test the continued inhibition of axon depolarization and action potential firing in TTX applications to the time-point of analysis. It is therefore difficult to evaluate the data and to infer the role that neuronal activity plays during myelination. Furthermore, previous in vitro and in situ studies (Barres and Raff, 1993; Demerens et al., 1996), showing an effect of TTX application to myelination, have implicated that the effect of electrical activity on myelination might be dependent on the developmental stage. TTX application in in vivo studies, reporting no effects of neuronal activity on myelination, therefore, could have missed the narrow time frame in which oligodendrocytes might be sensitive to neuronal activity.

From the studies using TTX to inhibit neuronal electrical activity, it remains unclear, whether neuronal activity has a role during myelination and if so, whether this role is restricted to a certain, region-specific time-point during development. It is possible that neuronal activity, rather than being required for myelination, has a modulatory role, regulating the extent or timing of myelination. A decrease in neuronal activity might therefore not lead to myelin defects, while an increase in neuronal activity, however, might results in increased myelination. Further studies, in which the inhibition of neuronal activity is strictly measured and controlled for, are needed to elucidate the role that neuronal activity might have during myelination. These studies should also elucidate, which cellular aspects might underlie the potential influence that neuronal activity might have on myelination, e.g. whether the electrical membrane properties of stimulated axons or whether it is axonal synaptic vesicle release, that induces the oligodendrocyte differentiation and / or myelin ensheathment.

Neuronal activity dependent mechanism of myelination

Other studies using stimulation in order to increase neuronal activity have indicated a positive effect on myelination.

Electric stimulation of DRG-OPC co-cultures at10hz for 24h showed a decrease in OPC proliferation (as described above) and an increase in OPC differentiation to mature, myelinating oligodendrocytes with a more branched morphology (Stevens et al., 2002). This effect of neuronal stimulation was inhibited by the addition of adenosine receptor antagonists. Furthermore, when the co-cultures were treated with 500µM adenosine for 14days or electrically stimulated at 10hz for 24h, mbp expressing oligodendrocytes that formed myelin sheaths were significantly increased after 14days and 3-4 days, respectively (Stevens et al., 2002). These findings suggest that purinergic signaling mediated by adenosine, a derivative of adenosine-tri-phosphat (ATP) which is released by the stimulated axons (Stevens and Fields, 2000), might play a role in oligodendrocyte differentiation and myelination. While axonal ATP release inhibits Schwann cell development and thereby reduces myelination in the PNS (Stevens and Fields, 2000; Stevens et al., 2004), adenosine appears to inhibit proliferation of OPCs and thereby stimulate their differentiation into myelinating oligodendrocytes, thus increasing myelination (Steven et al. 2002). Purinergic signalling through ATP and its derivatives might therefore have different effects in the PNS and the CNS.

Interestingly, ATP did not have an effect on OPC proliferation and differentiation. As the increase in myelinating oligodendrocytes in the study described above might have been an effect of electric stimulation on oligodendrocytes and their precursors themselves, another study devised multi-compartment culture dishes, which enabled the specific stimulation of neurons only. This study aimed to investigate the effects of neuronal stimulation on mature oligodendrocytes, rather than OPCs. Neuronal stimulation at 10Hz for 2-3 weeks at a 0.5s every 2s cycle in also resulted in an increase of myelinating oligodendrocytes 3-4 weeks after the stimulation. The addition of ATP resulted in an increase in the number of mbp positive myelinating oligodendrocytes, however, the addition of adenosine to the co-culture had no effect. Adenosine might therefore play a role during the proliferation and differentiation of

OPCs, while ATP might influence the oligodendrocyte lineage after the precursor stage. The positive effect of ATP on the number of myelinating oligodendrocytes might, however, not be a direct axon-oligodendrocyte interaction. ATP from electrically active axons was found to stimulate the release of the cytokine leukemia inhibitory factor (LIF) from astrocytes in the co-culture, which is known to promote myelination in mature oligodendrocytes in cultures (Stankoff et al., 2002). Therefore, it is unclear whether neuronal activity can increase the number of myelinating oligodendrocytes by direct axon-oligodendrocyte interactions whether this effect is primarily due to the LIF released by astrocytes.

A recently published in vivo study, in which optogenetic stimulation increased OPC proliferation (as described above), also demonstrated a positive correlation between elevated neuronal activity and an increase in myelin sheath thickness resulting in improved motor function (Gibson et al., 2014). Relatively short periods of light stimulation daily (a total of 2.5min for 7 days) of the premotor cortex in awake mice were sufficient to increase OPC proliferation, oligodendrocyte differentiation as well as myelin thickness in the premotor cortex and underlying subcortical white matter in juvenile and adult mice. The increase in oligodendrocyte differentiation and myelin thickness was correlated to improved motor function in the corresponding limb, which was prevented by epigenetic blockade of cell differentiation (Gibson et al., 2014). However, the study did not clarify the cellular mechanisms behind the improved motor function: whether the newly differentiated oligodendrocytes add more myelin sheaths to already myelinated axons and therefore increasing myelin thickness or whether they myelinate previously unmyelinated axons, which would result in an increase in myelinated axon number. Also, the increase in myelin sheath thickness might either stem from the production of thicker myelin sheaths by the newly differentiated oligodendrocytes or by additional myelin “wraps” in the sheaths of already existing oligodendrocytes. Furthermore, the optogenetic mediated increase in neuronal activity also increased neural progenitor proliferation in addition to the increased OPC proliferation rate, which could account, perhaps in part, for the improvement in motor function.

Optogenetic stimulation certainly is a very elegant technique to induce neuronal activity. However, the technique does not clarify whether myelinating

oligodendrocytes react to the ionic changes in the membrane potential of active axons or to axonal signals, such as neurotransmitters, mediated by synaptic vesicle release, or to growth factors secreted over longer distances in response to the mitogenic effect of the optogenetic stimulation. More in depth analysis at a higher, cellular resolution and applying more precise tools to increase or inhibit specific components of neuronal activity, such as local axonal synaptic vesicle release, are needed in order to elucidate the precise axon-oligodendrocyte interactions during myelination.

A recent in vitro study using a DRG-OPC co-culture system with a paradigm of 10hz stimulation for 5hours with 9s stimulation and 5min intervals demonstrated a positive correlation between neuronal stimulation and the number of myelinated axons 21 days after the stimulation (Wake et al., 2011). The effect of neuronal stimulation was prevented when the culture was treated with botulinum toxin A (BnTX) or tetanus toxin (TetTx), which cleave the synaptic vesicle proteins SNAP-25 (Welch et al., 2000) and VAMP-2 (Pellizzari, 1999; Chen et al., 2008), respectively, to inhibit synaptic vesicle release before the OPCs were added to the culture, indicating that synaptic vesicle release induces the increase in myelinated axons. Furthermore, the stimulation was shown to induce rapid Ca^{2+} responses in the OPC processes by calcium imaging, which was prevented by BnTX or by a combination of the ionotropic glutamate receptor antagonists comprised of the AMPA/kainate receptor antagonist 6-cyano-7-nitroquinoxaline-2,3- dione (CNQX) and the NMDA receptor antagonist DL-2-amino-5-phosphonopentanoic acid (AP5), and the metabotropic glutamate receptor antagonist a-methyl-4-carboxyphenylglycine (MCPG) (Wake et al., 2011). Importantly, local mbp translation was also shown to be increased by electric stimulation and inhibited by BnTX and by the NMDA receptor antagonist AP5 as well as the metabotropic glutamate receptor antagonist MCPG. Application of the AMPA/kainate receptor antagonist CNQX did not result in a decrease of local *mbp* translation (Wake et al., 2011).

These findings suggest that glutamate, released from axons by synaptic vesicle exocytosis in response to electrical stimulation, activates NMDA receptors and thereby induces the increase in myelinated axons (Figure 4.2). Furthermore, the electric stimulation also increased the phosphorylation of the Fyn kinase, which was

also inhibited by BnTX and by the glutamate receptor antagonists. The phosphorylated, active Fyn kinase has been implicated as a downstream integrator of axon-oligodendrocyte signals in oligodendrocytes that controls myelination (Umemori et al., 1994; Kraemer-Albers and White, 2011). Furthermore, constitutive activation and reduction of Fyn kinase in vivo has been shown to increase and decrease the amount of myelin sheaths made per oligodendrocyte, indicating a role for the Fyn kinase signaling pathway in fine tuning the extent of myelination (Czopka et al., 2013).

Together, these findings indicate that activity induced glutamate released by synaptic vesicle exocytosis in axons might increase the number of myelin sheaths formed per oligodendrocyte through activation of Fyn kinase in oligodendrocytes. However, local mbp translation in Wake et al. was not directly shown to increase through glutamate mediated activation of NMDA receptors and direct evidence that the activation of NMDA receptors in oligodendrocytes can induce myelin sheath formation is still missing. Overall, the NMDA receptor mediated activation of Fyn kinase axon-oligodendrocyte signaling mechanism inducing myelination in vitro or in vivo has not been demonstrated to date.

This is all the more relevant, as the findings of Wake et al., are in immediate contrast to an in vivo study, in which conditional and constitutive genetic ablation of the obligatory subunit NR1 of the glutamate receptor NMDA receptor in OPCs as well as in myelinating oligodendrocytes failed to show a defect on myelination during development and in adulthood (De Biase et al., 2011). In the absence of NMDA receptor signaling, the NMDA receptor-deficient OPCs formed synapses with glutamatergic axons, proliferated normally and differentiated into myelinating oligodendrocytes without delay in the mouse cortex and subcortical white matter tracts (De Biase et al., 2011) as well as in other white matter and grey matter areas (fimbria and hippocampus, respectively) (Guo et al., 2012). Furthermore, a timed conditional ablation of oligodendroglial NR1 also showed no effect on the severity of spinal cord demyelination in the human MS model experimental autoimmune encephalomyelitis (EAE) (Guo et al., 2012), indicating that NMDA receptors do not mediate white matter injury in demyelinating diseases, as has been previously suggested (Karadottir et al., 2005).

The in vivo studies suggest that NMDA receptor activation has no direct effect on oligodendrocyte differentiation and myelination. However, the NMDA receptor-deficient OPCs showed an increase in calcium-permeable AMPA receptor expression (De Biase et al., 2011), which might substitute for the decrease in calcium influx in the absence of functional NMDA receptors. It is unclear, however, whether AMPA receptor activity could indeed compensate for NMDA receptor activity during oligodendrocyte development as the receptors are associated with distinct intracellular signaling pathways (Kim and Sheng, 2004).

Furthermore, the seemingly direct discrepancies between the in vitro and in vivo studies may be explained by the different levels of analysis.

Wake et al. did not assess the effects glutamate mediated NMDA receptor signaling on myelination itself but focused on local mbp mRNA translation. It has been shown that the majority of myelin sheaths can still be formed, even when mbp mRNA transport to distal OPC processes is disrupted in vivo (Lyons et al. 2009), suggesting that local mbp mRNA translation may not be necessarily required for myelin sheath formation per se, which might account for the lack of myelin phenotype in NMDA receptor deficient mice. Rather than being necessary for myelination, neuronal activity mediated local translation might therefore modulate the number of myelinated axons or timing of myelination along axons.

Myelination in NMDA receptor deficient mice was assessed by immuno-staining for myelin basic protein (MBP) in at P7 in the rostral and caudal forebrain, western blot analysis of MBP, 2′,3′-cyclic nucleotide 3′-phosphodiesterase (CNP), and myelin associated glycoprotein (MAG) in the cortex/subcortical white matter as well as by G-ratio measurements in the corpus callosum from P24-26 and P55-57, indicating that neither the amount of important myelin proteins nor myelin sheath thickness are regulated by NMDA receptor activation in oligodendrocytes (De Biase et al., 2011). Although the assessment of myelination in NMDA receptor deficient mice was extensive in this study, a modulatory role of neuronal activity on myelination might not have been detected as the modulatory effects that activity would have on myelination, such as the number of myelin sheaths formed per oligodendrocyte, would be very subtle. As the number of myelinated axons was not assessed in the white matter electron micrographs, a small decrease in the number of myelinated

axons might not have been detected in the immuno-staining of the rostral and caudal forebrain or might have been too subtle for a significant change in protein expression measured in the western blot analysis.

So far, the modulatory effect that NMDA receptor activation through axonal glutamate release might have in regulating the extent or timing of myelination in the CNS in vivo remains unclear.

Other signaling pathways have also been investigated in order to elucidate the role of neuronal activity during myelination in the CNS. The NRG-1/ErbB signalling pathway has been proposed as a potential mechanism by which neuronal activity might influence myelination as different levels and isoforms of NRG1 have been shown to be distinctly regulated by neuronal firing in adult rat brains (Liu et al., 2011; Ziskin et al., 2007).

In the PNS, axonal expression of NRG-1 type III is essential for Schwann cell survival, migration, proliferation and differentiation (Jessen and Mirsky, 2005; Lyons et al., 2005; Salzer and Nave, 2006). NRG-1 type III is also crucial in regulating PNS myelination, as axons, which express NRG-1 type III above a certain threshold are myelinated by Schwann cells (Lyons et al., 2005; Taveggia et al., 2005) and myelin sheath thickness is determined by NRG-1 type II expression levels (Michailov et al., 2004).

In the CNS, however, NRG-1 type III expression does not appear to be the primary mechanism regulating myelination. Although hypomyelination was reported in the corpus callosum of heterozygous NRG-1 type III knock-out mutants (Taveggia et al., 2008), myelination occurred normally in the optic nerve and spinal cord of these heterozygous mutants. NRG-1 dependent regulation of myelination might therefore be region-specific for example, only essential in the corpus callosum. However, conditional Cre-recombination induced *NRG-1 null* mutants did not show any myelin defects in the corpus callosum, cortex and spinal cord when the knock-out was induced during embryonic development at E12 and throughout adult life at (Brinkmann et al. 2008). Myelination in the *NRG-1 null* mice was assessed by MBP immuno-staining, western blots of MPB, CNP and MAG levels as well as calculation of G-ratios in electron micrographs of the corpus callosum at P10 and in 11 week old mice. Although the quantification of myelinated axons showed a trend towards a

reduction in myelinated axon number, this decrease was not significant. Furthermore, the optic nerve and corpus callosum of ErbB3-ErbB4 double knock-out mutants also showed no myelin defects as assessed by G-ratios and MBP immuno-staining at P11, excluding the possibility that other NRG-1 isoforms might have compensated for the loss of NRG-1 type II and activated the ErbB receptors on oligodendrocytes. However, the myelination of the sciantic nerve in the PNS was highly impaired in the ErbB3-ErbB4 double knock-out, indicating a fundamentally different role for NRG-1/ErbB signalling in the PNS and the CNS.

However, in contrast to these findings, Cre- mediated ErbB3 knock-out in oligodendrocytes at P19 resulted in reduced MBP and MAG expression levels as well as a decrease in myelin thickness in the prefrontal cortex in mice at P65 (Makinodan et al., 2013), while no effects were observed when ErbB3 expression was reduced at P36. Interestingly, the myelin defects in the prefrontal cortex seen by ErbB3 knockdown were also found in socially isolated mice (Liu et al., 2012, Makinodan, et al., 2012). Oligodendrocytes in the prefrontal cortex were less branched and had fewer and thinner myelin sheaths than control oligodendrocytes (Makinodan et al., 2013). The effects of social isolation on prefrontal cortex myelination were restricted to a critical time point between P21 and P35. Mice that were isolated after that time-point showed no myelin defect. This might account for the discrepancy to the previous in vivo study, in which conditional NRG-1 knock-outs had no effect in central nervous system myelination when NRG-1 was ablated at E12 and at P5 (Brinkmann et al., 2008). It is possible that the short critical time-point during which NRG-1 signalling might regulate myelination in certain CNS areas was missed in the conditional knock-out experiments. Furthermore, the NRG-1 dependent regulation of myelination might be restricted to CNS areas such as the prefrontal cortex, while the myelination of other cortical areas, the corpus callosum and spinal cord might be independent from NRG-1 signalling.

Another potential explanation for these conflicting data has been put forward in a recent study, which implied two regulatory mechanisms behind oligodendrocyte differentiation: an activity dependent and an activity independent mode (Lundgaard et al., 2014). This study showed that the application of the extracellular domain of NRG-1 in a DRG co-culture system increased the number of myelinated axons in

electrically stimulated culture but not if neuronal activity was blocked by TTX. In the absence of neuronal activity in the TTX treated cultures, myelination was induced by the addition of growth factor protein brain-derived neurotrophic factor (BDNF), which has been shown to promote the onset of CNS myelination (Xiao et al., 2010), implying that BDNF can initiate myelination independently of neuronal activity and compensate for the NRG-1 mediated induction of myelination. Once the NRG-1 pathway is active, however, myelination is regulated by neuronal activity (Lundgaard et al., 2014). This dual mechanism could explain some of the previous contradictory findings where neuronal activity induced myelination in some experimental set ups but not in others and help elucidate the mechanism by which neuronal activity might regulate myelination.

Overall, these in vitro and in vivo studies indicate that neuronal activity might be able to influence myelin extent, at a certain time-point during development. It is possible, that neuronal activity can regulate CNS myelination through a combination of the above described candidate mechanisms. Alternatively, there might be an activity dependent as well as an activity independent mode of CNS myelination, as indicated in Lundgaard et al. An activity independent mode of myelination in addition to an activity dependent mode would explain why experimental inhibition of activity only showed relatively mild phenotypes. The activity dependent mode of myelination would therefore be modulatory, increasing or decreasing the myelin extent during development.

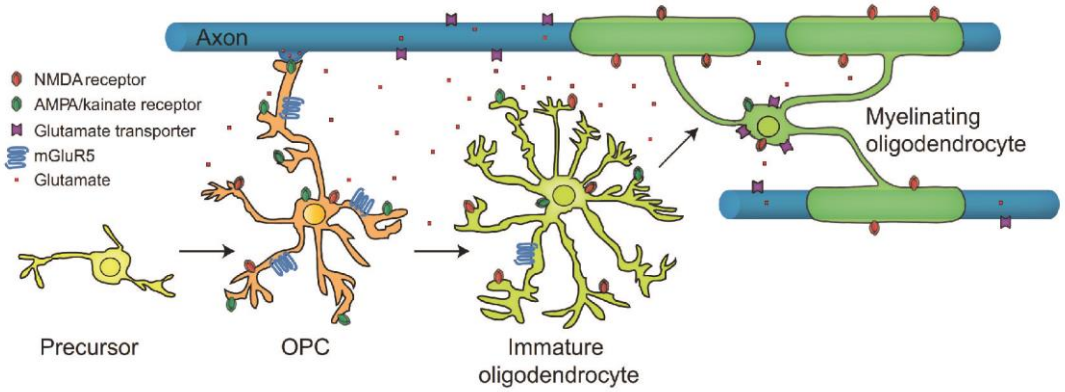

Figure 4.2: Schematic model of the different stages of oligodendrocyte lineage differentiation that might be facilitated through neuronal activity. Oligodendrocytes differentiate from mitotic progenitors to oligodendrocyte precursor cells (OPC) and immature oligodendrocyte into myelinating

oligodendrocytes. OPCs, immature oligodendrocytes and mature oligodendrocytes express glutamate receptors that are activated through axonal glutamate release. Depending on the developmental stage, glutamate activates AMPA receptors in the OPCs, which might promote their differentiation or NMDA receptors in oligodendrocytes and thereby promote myelination. Whether glutamatergic stimulation can indeed induce OPC differentiation and myelination awaits direct in vivo evidence. Image taken from Kolodziejczyk et al., 2010.

Neuronal activity independent myelination

In the PNS, axonal signals, such as NRG-1, are required for all stages of Schwann cell development and myelination (Aguayo et al., 1976; Jessen and Mirsky, 1991; Scherer et al., 1994; Lyons et al., 2005; Taveggia et al., 2005; Salzer and Nave, 2006), but in vitro experiments indicate that oligodendrocytes appear to be less dependent on axon contact. OPCs have been shown to survive, proliferate and differentiate to mature oligodendrocytes in neuron-free cultures (Knapp et al., 1987; as reviewed in Lubetzki, Demerens and Zalc, 1997), co-cultures with inert structures, devoid of axonal signalling such as paraformaldehyde (PFA) fixed DRG neurons (Rosenberg et al., 2008) and polystyrene fibres (Lee et al., 2012). Mature oligodendrocytes in neuron-free cultures extent their processes and can form flat myelin-like forms at the end of these processes (Althaus et al., 1984) and even form multiple layers of myelin membrane around PFA fixed DRG neurons (Rosenberg et al., 2008) as well as inert polystyrene fibres (Lee et al., 2012) as verified by electron microscopy. Interestingly, the myelin sheaths formed in co-cultures with the PFA fixed axons appeared small in longitudinal lengths compared to myelin sheaths in normal DRG-oligodendrocyte co-cultures. Similarly, the compact myelin around PFA fixed axons appeared to have fewer layers of myelin membrane compared to normal myelinated axons (Rosenberg et al., 2008, figure 2). Subtle changes in the number of myelin sheaths formed, longitudinal length of the myelin sheaths or myelin sheath thickness in the absence of axonal signalling could indicate a modulatory role for activity dependent axonal signalling during myelination. Regrettably, however, neither the longitudinal length nor myelin thickness was measured in cultures with fixed neurons.

Another axonal property that might lead to activity independent myelination could be axon calibre. Axon calibre has been observed to be correlated with the initiation of myelination (see chapter 3). In the PNS, axons with a diameter above 1µm are myelinated (Duncan 1934; Voyvodic et al., 1989; Remahl and Hildebrand, 1982), while in the CNS axons with a calibre between approximately 0.3–0.9µm can either be myelinated or unmyelinated and large calibre axons of approximately >0.9µm are always myelinated (see chapter 3; Matthews and Duncan, 1971; Waxmann and Bennett, 1972; Franson and Hildebrand, 1975; Remahl and Hildebrand, 1982; Hildebrand and Waxman, 1984). Interestingly, in the absence of axonal signals, oligodendrocytes were shown to ensheath polystyrene fibres with myelin like sheaths, if they had a diameter of approximately 0.4µm but not if the axon calibre was smaller than that (Lee et al., 2012).

Both, the radial and the longitudinal size of CNS myelin sheaths have been shown to correlate with axon diameter and the longitudinal length of CNS myelin sheaths has been shown to increase according to axon calibre increase (Hess and Young, 1952; McDonald and Ohlrich, 1971; Murray and Blakemore, 1980). If axon calibre itself is a factor inducing myelination, independently of axonal activity, it might not only determine whether an axon will be myelinated or not, but also regulate thickness and longitudinal length of a myelin sheath.

It is unknown, whether axon calibre might be a form of activity independent myelination or whether an activity independent mode of myelination exists at all in vivo. More in depth analysis is needed in order to elucidate the activity dependent and independent mechanisms behind CNS myelination.

Conclusion

While in vitro experiments have the advantage of studying a complex system such as axon-glial signaling during myelination in a confined system without the influence of other cell types, it is hard to interpret the conflicting data with respect to the cellular mechanisms underlying myelination in vivo.

The more recent studies investigating the role of neuronal activity during myelination have indicated that increased neuronal activity can indeed promote myelination,

although this role might be modulatory rather than mandatory. However, while the in vitro studies proposed potential molecular pathways that might be involved in this process, the in vivo studies could not clarify which of these, perhaps in combination, might underlie the neuronal activity mediated myelination. Overall, it is still unclear, which aspect of myelinated axon formation is regulated by neuronal activity, e.g. whether it is oligodendrocyte differentiation, the number and length of myelin sheaths formed per oligodendrocyte or myelin thickness. Furthermore, the cellular mechanisms by which neuronal activity can regulate myelinated axon formation, are also not completely understood, e.g. whether axonal signals released through synaptic vesicle exocytosis or whether ionic changes in the membrane potential of active axons induce the myelinating oligodendrocyte to ensheath the axon. To this date, the axon-glial interactions underlying myelinated axon formation are still mostly unknown. In order to investigate the role of neuronal activity during myelinated axon formation, higher resolution analysis at a molecular and cellular level are needed.

To investigate the role of neuronal activity on the formation of myelinated axons, I manipulated axonal synaptic vesicle release using the neurotoxin Tetanus Toxin (TetTx). TetTx inhibits synaptic transmission by cleaving the pre-synaptic vesicle membrane protein Vamp2 (Pellizzari, 1998; Chen et al., 2008). By injection of 100pg *tettx* mRNA, I analyzed the impact of suppressed synaptic vesicle release on the number of myelinating oligodendrocytes and on the number and length of myelin sheaths formed per oligodendrocyte by transmission electron microscopy and live imaging in transgenic fish lines. For this, transgenic lines were used that express fluorescent marker proteins in OPCs and mature oligodendrocytes (Tg(sox10:mRFP), Tg(nkx2.2aGFP)) and in myelinating oligodentrocytes only (Tg(mbp:EGFP CAAX), Tg(mbp:mCherry-caax), Tg(mbp:EGFP cyto)) as well as in a subset of spinal cord neurons Tg(cntn1a:mCherry) (see chapter 2, Materials and Methods).

4.2 Results

4.2.1 Global expression of TetTx interrupts synaptic transmission

Neuronal activity has long since been thought to regulate myelination, but it is unclear which aspect of neuronal activity might regulate myelination, e.g. electrical potential of the axon membrane, axonal membrane composition or neurotransmitters released through axonal synaptic vesicles. In order to investigate whether synaptic vesicle release can induce oligodendrocytes to form myelin sheaths around axons and to characterize the cellular mechanisms behind these axon-oligodendrocyte interactions, I interrupted synaptic vesicle release by global expression of Tetanus Toxin (TetTx). To ensure a global expression of TetTx in the spinal cord, I injected 100pg of *tettx* mRNA at the one cell stage of fertilized zebrafish eggs so that every cell after mitotic cell divisions contained *tettx* mRNA (see chapter2 Materials and methods).

TetTx treated animals are completely paralysed, but show normal overall development. Their general morphology and blood flow is not impaired up to 3dpf compared to controls (Figure 4.3, A, top and bottom). After 3dpf TetTx treated animals develop heart oedema and their muscle tissue begins to degenerate, presumably due to the complete paralysis (Figure 4.3, B, bottom). Under normal conditions, zebrafish larvae swim to the water surface to inflate their swim bladders between 3dpf and 4dpf. Control injected animals successfully inflated their swim bladders (Figure 4.3, B, top), while TetTx treated animals cannot swim to the water surface due to paralysis and therefore did not inflate their swim bladders (Figure 4.3, B, bottom).

In order to investigate whether the TetTx treatment impairs neuronal development, I imaged the spinal cord of Tg(cntn1b(5kb):mCherry-caax) animals, which label a subset of spinal cord neurons in the zebrafish embryos. In these overview images of the spinal cord at somites 13-15, the overall morphology of the labelled TetTx expressing neurons does not look different to control neurons. Although the animals are completely paralysed, motor neurons and Rohon Beard sensory neurons form axons, which project out of the spinal cord on the ventral and dorsal side, respectively (Figure 4.3, C).

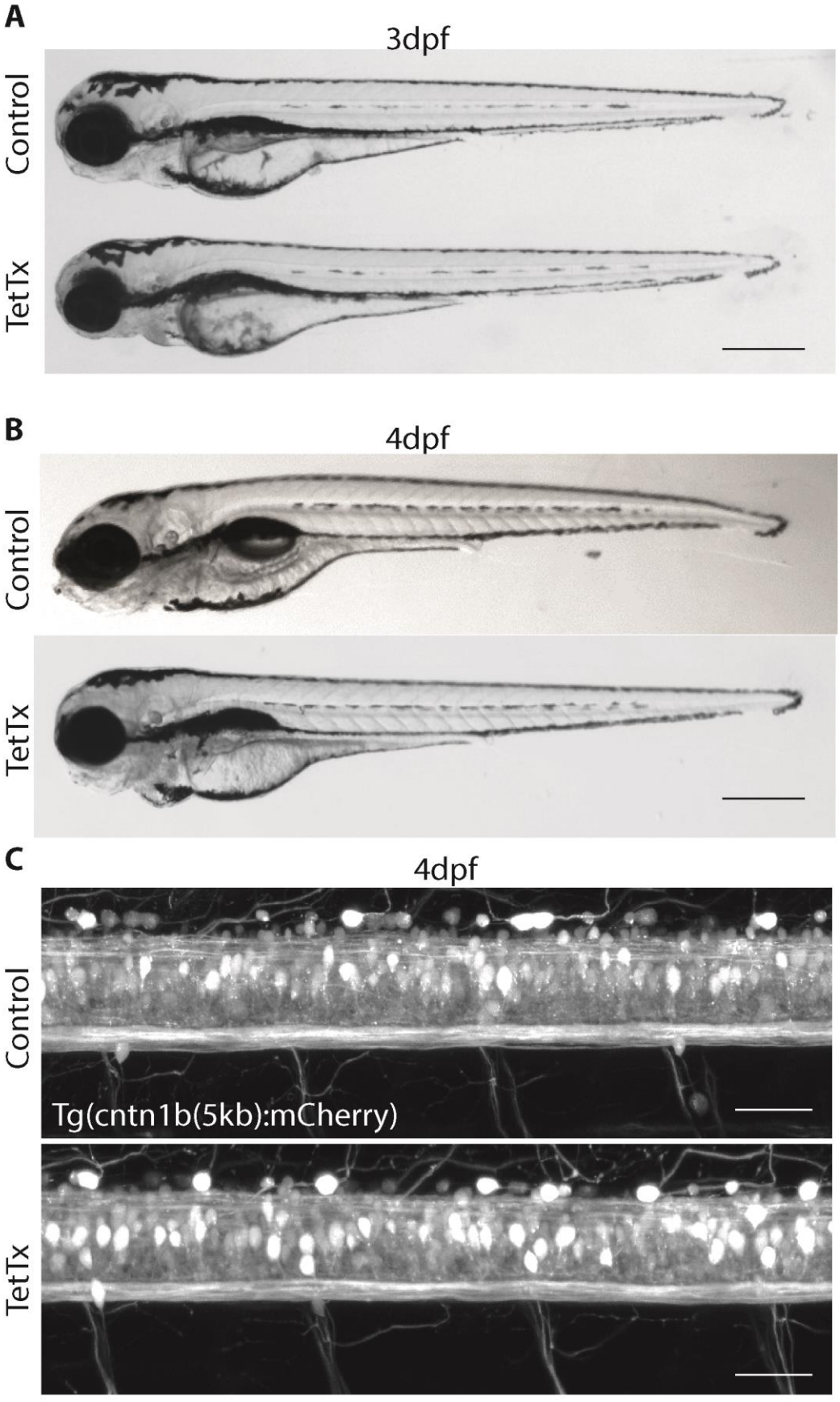
A
3dpf
Control
TetTx
B
4dpf
Control
TetTx
C
4dpf
Control
Tg(cntn1b(5kb):mCherry)
TetTx

Figure 4.3: Global TetTx expression. (A) Lateral view of a control injected animal and a TetTx treated animal at 3dpf (scale bar 300µm). (B) Lateral view of a control injected animal and a TetTx treated animal at 4dpf (scale bar 300µm). (C) A subset of spinal cord neurons labelled in the transgenic line Tg(cntn1b(5kb):mCherry) at somite area 13-15 of a control (top) and a TetTx treated animal at 4dpf (scale bar 40µm).

The global TetTx expression might cause a developmental delay that might not be detected by morphological comparison alone, especially if the delay occurred in the onset of myelination. In the transgenic lines labelling myelinating oligodendrocytes used in this study, the very first myelin sheaths appear in the anterior ventral tract around the Mauthner axon, which is the first axon to be myelinated in the spinal cord (Almeida et al., 2011). Myelination in the spinal cord then gradually follows from anterior to posterior, as well as ventral to dorsal.

In order to detect a possible developmental delay in the onset of myelination, I imaged the onset of spinal cord myelination using Tg(mbp:GFP-caax) at 3dpf as well as 4dpf at an anterior part of the spinal cord (somites 10-14) and a posterior part of the spinal cord (somites 20-24) in order to detect a delay in myelin formation. At 3dpf, controls and TetTx treated animals show myelination in the dorsal and ventral tract at somites 10-14 (Figure 4.4, A, top). According to the anterior-posterior gradient of myelination onset and the ventral to dorsal oligodendrocyte migration gradient, the posterior somites 20-24 showed myelin in the ventral, but not yet in the dorsal tract in both control and TetTx treated animals. At 4dpf, controls as well as TetTx treated animals show myelin in ventral and dorsal tracts at somites 10-14 and 20-24 (Figure 4.4, A, bottom). This indicates that there is no delay in the onset of myelination cause by TetTx expression. The amount of myelin sheaths formed appears reduced in the TetTx expressing animal, which, however, is indicative of a myelin phenotype rather than a developmental phenotype delaying the onset of myelin formation (Figure 4.4, A).

In order to more carefully quantify the onset of myelination, I imaged the most posterior myelin sheath in the spinal cord of TetTx expressing and control animals during early stages of myelin onset at 70hpf, 75hpf and 80hpf (Figure 4.4 B and C). At 70hpf, the most posterior myelin sheath in the spinal cord can be observed on average at somite 5.5 +/- 1.9 in controls and at somite 4.7 +/-2.2 in TetTx treated

animals. At 75hpf, the most posterior myelin sheath in the spinal cord can be observed on average at somite 11.6 +/- 1.9 and at somite 11.5 +/- 2.9 in TetTx treated animals. At 80hpf, the most posterior myelin sheath in the spinal cord can be observed on average at somite 19.2 +/- 1.5 and at somite 19.3 +/- 2.3 in TetTx treated animals (Figure 4.4 C, Two-way ANOVA, $p = 0.68$). Both, controls and TetTx treated animals show a rapid progression of myelination along the anterior-posterior gradient, with the most posterior myelin sheath being formed on average in the same somite area between 70hpf and 80hpf. This demonstrates that TetTx expression does not lead to a delay in the onset of myelination.

A
3dpf
4dpf
Control
TetTx
Control
TetTx
Tg(mbp:GFPcaax), Somite 10-14
Tg(mbp:GFPcaax), Somite 20-24

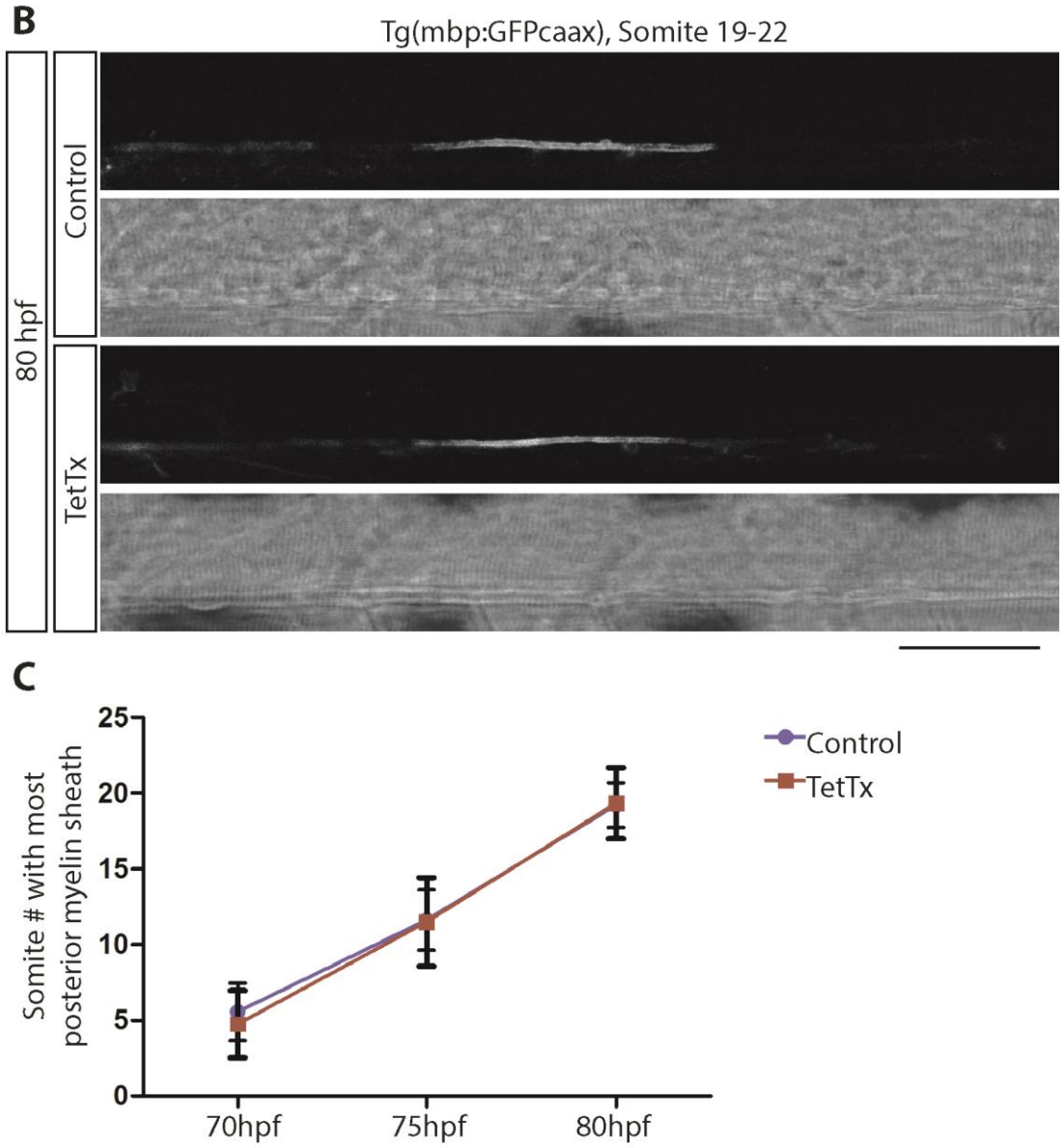

Figure 4.4: Global TetTx expression does not lead to a delay in the onset of myelination. (A) Myelin sheaths labelled in the (Tg(mbp:GFPcaax) can be found at somite 10-14 as well as somite 20-24 at 3dpf and 4dpf in both control and TetTx treated animals (Scale bar 100µm). (B) Myelination occurs according to an anterior-posterior gradient in control and TetTx treated animals. Example of the most posterior myelin sheath in the spinal cord at 80hpf, myelinating the Mauthner axon, situated between somite 19 and 22 in a control animal (top) and TetTx treated animal (bottom) (Scale bar 50µm). (C) At 70hpf, 75hpf, 80hpf, the most posterior myelin sheath in the spinal cord can be observed on average at somite 5.5 +/- 1.9, 11.6 +/- 1.9 and 19.2 +/- 1.5, respectively in controls and at somite 4.7 +/-2.2, 11.5 +/- 2.9 and 19.3 +/- 2.3, respectively in TetTx treated animals (Control 70hpf n=7, 75hpf n=8, 80hpf n=9; TeTx mRNA 70hpf n=4, 75hpf n=8, 80hpf n=9. Two-way ANOVA, p = 0.68).

As an important next step, I tested whether injection of a 100pg *tettx* mRNA in the one cell stage of fertilized zebrafish eggs successfully inhibited synaptic vesicle release up to the last time-point of analysis, at 4dpf. This crucial for a correct interpretation of the results and has been surprisingly lacking in previous in vivo studies using TTX to reduce axonal electrical activity (see introduction to this chapter "Electrical activity").

In collaboration with Abdel El Manira's group at the Karolinska Institute, Sweden, Dr. Jessica Ausborn performed patch-clamp recording in order to confirm that the TetTx treatment is sufficient to inhibit synaptic signal transmission. In the experimental set-up, extra-cellular stimulation was applied to descending spinal cord nerve fibres, which conduct the elicited action potentials to the spinal cord. If synaptic vesicle release was successfully inhibited, the action potentials elicited by the stimulation would not be transmitted through synaptic connections to the spinal cord. The neurons in the zebrafish spinal cord were exposed by dissection of the muscle tissue, a stimulator placed extra-cellularly on top of the hindbrain (Figure 4.5, D) and a recording electrode was attached to the neuronal cell membrane, creating a seal through suction (Figure 4.5, E). The membrane potential was measured in 5 current clamped spinal cord neurons in control and 5 TetTx treated animals; one neuronal cell body was patched and recorded from per animal. While control neurons responded with the so called fictive swimming (Masino and Fetcho, 2005; Ekloef-Ljunggren et al., 2012) a rapid series of depolarization of the membrane potential, which is shown as repetitive spiking in the example trace (Figure 4.5, A, left), neurons in TetTx treated animals only showed very little change in membrane potential after the initial stimulation (Figure 4.5, A, right). In order to investigate potentially remaining cationic currents, such as K^+ currents, after external stimulation in TetTx treated animals, the patched cells were voltage clamped at 0mV, the reversal potential of anionic currents (Figure 4.5, B). Any occurring anionic currents would not lead to a change in membrane potential as the membrane is held at the maximum voltage produced by anionic currents, so that only cationic currents will be recorded. While voltage clamped cells in control animals showed the characteristic repetitive peaks of fictive swimming in the current recording after external stimulus (Figure 4.5, B, left), voltage clamped cells in TetTx expressing

animas showed no cationic currents in response to external stimulus (Figure 4.5, B, right). Similarly, the patched cells were also voltage clamped at -65mV, the reversal potential of cationic currents, in order to measure potential anionic currents, such as Cl^- currents. Again, the voltage clamped cells of control animals responded to external stimulus by repetitive spiking in the current recording (Figure 4.5, C, left), while TetTx treated animals showed no anionic currents in response to external stimulus (Figure 4.5, C, right). In order to quantify the recordings taken from the 5 control animals and 5 TetTx treated animals, the average area between the measured outward currents and the resting potential of the neurons voltage clamped at 0mV was measured. The measured area between the recorded outward currents and the resting potential in TetTx treated animals is significantly decreased compared to the area measured in control animals (Two-tailed student's t-test $p = 0.0076$, Figure 4.5, F). The average area between the recorded inward currents and the resting potential of the neurons voltage clamped at 0mV was also significantly decreased in TetTx treated animals compared to control animals (Two-tailed student's t-test $p = 0.0069$, Figure 4.5, G). The average threshold for the extracellular stimulation to see a response in the patched cell during the set up was not significantly different between TetTx treated animals and the control (Figure 4.5, H). All recordings and data displayed on the graphs were obtained at 2xthreshold of each cell.

Thus, by injection of 100pg *tettx* mRNA in the on cell stage of fertilized zebrafish eggs, synaptic transmission was significantly reduced in TetTx treated animals by 4dpf as verified by patch-clamp recordings after external stimulation. Injection of only 10pg *tettx* mRNA in fertilized eggs at the one cell stage also resulted in complete paralysis up to 4dpf but, importantly, did not reliably reduce synaptic transmission in the spinal cord after extracellular stimulation (data not shown). Therefore, 100pg *tettx* mRNA was injected in all experiments using TetTx treated animals. During these experiments, cell injections were performed by me, while the tissue preparation, patch-clamp recordings and analysis of electrophysiological data were performed by Dr. Jessica Ausborn at the Karolinska Institute.

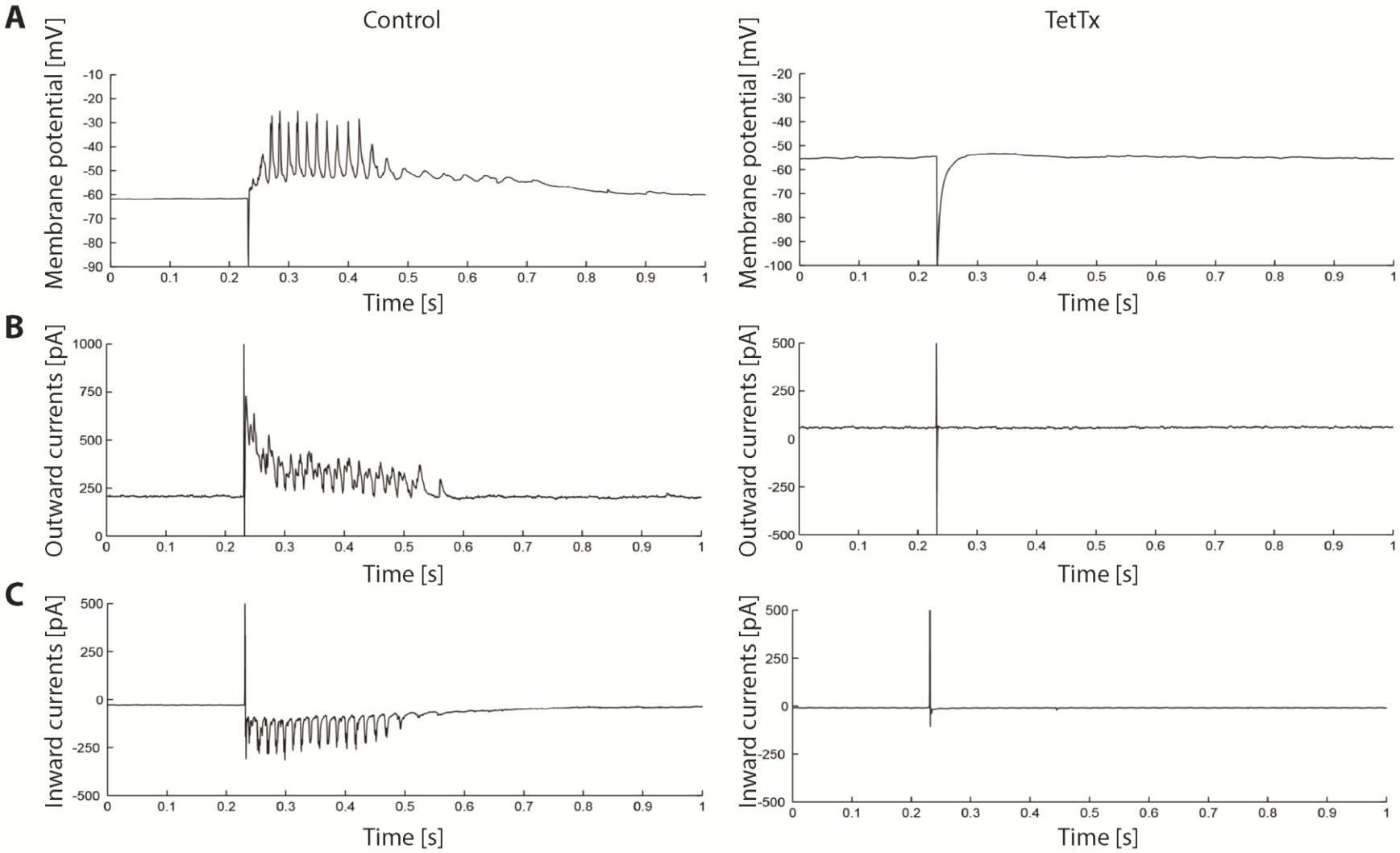
A
Control
TetTx
Membrane potential [mV]
Time [s]
B
Outward currents [pA]
C
Inward currents [pA]

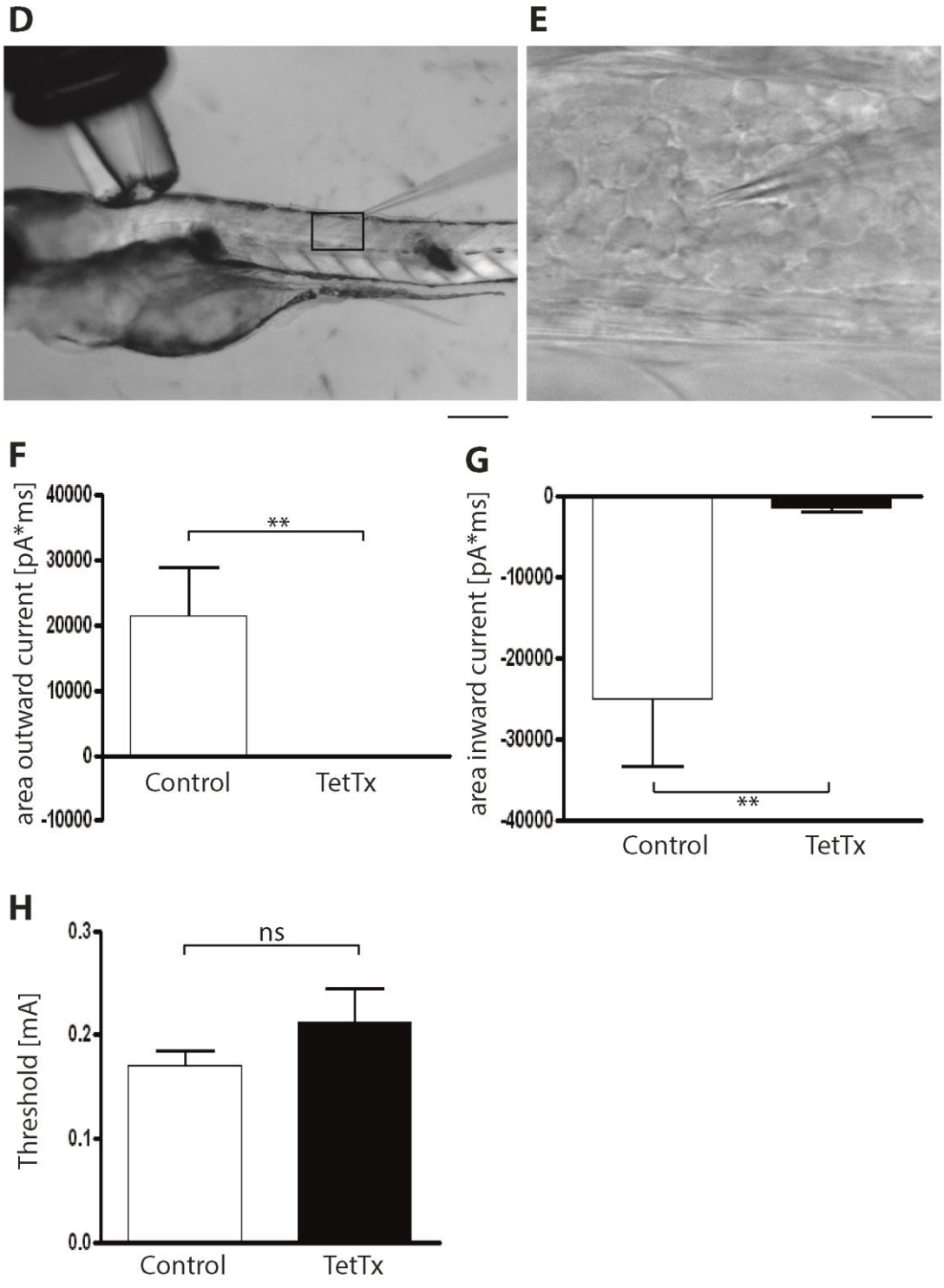

Figure 4.5: Global TetTx expression is sufficient to reduce synaptic transmission. Injection of 100pg *tettx* mRNA leads to a reduction of vesicle mediated synaptic transmission along the spinal cord at 4dpf. (A) Example traces of the membrane potential [mV] change in a current clamped spinal cord neuron after extracellular stimulation in a control (left) and TetTx treated animal (right). (B) Example traces of inhibitory outward current [pA] change in a voltage clamped spinal cord neuron

after extracellular stimulation in a control (left) and TetTx treated animal (right). The cells were clamped at the reversal potential of inward currents (0mV). (C) Example trace of excitatory inward current [pA] change in a voltage clamped spinal cord neuron after extracellular stimulation in a control (left) and TetTx expressing animal (right). The cells were clamped at the reversal potential of outward currents (-65mV). (D) Experimental patch-clamp set up. The spinal cord was exposed by dissection of the muscle tissue. A recording electrode was inserted to patch-clamp spinal cord neurons. Extracellular stimulation was applied above the hindbrain to stimulate descending nerve fibres. The rectangle corresponds to the zoom in pictured in E (Scale bar 200µm). (E) Zoom in of a recording electrode and the patch-clamped spinal cord neuron (Scale bar 10µm). (F) Quantification of the average area between the measured outward currents and the resting potential measured in voltage clamped spinal cord neurons (clamped at 0mV) after extracellular stimulation (control animals n = 5, TetTx treated animals n = 5, one cell measured per animal, two-tailed student's t-test p = 0.0076). (G) Quantification of the average area between the measured inward currents and the resting potential measured in voltage clamped spinal cord neurons (clamped at -65mV) after extracellular stimulation (control animals n = 5, TetTx treated animals n = 5, one cell measured per animal, two-tailed student's t-test p = 0.0069). (H) Quantification of the average extracellular stimulation threshold in control animals (n = 5) and TetTx treated animals (n = 5) in the patch-clamp set up.
All recordings in A and data displayed in F-H were obtained at 2xthreshold of each cell. All TetTx treatments were performed by me, while all tissue preparation for the electrophysiological set-up and all patch clamp recordings were performed by Dr. Jessica Ausborn, a researcher in Abdel El Manira's group at the Karolinska Institute, Sweden.

4.2.2 Reduction of synaptic vesicle release leads to a decrease in the number of myelinated axons in the CNS

After the successful inhibition of synaptic transmission in TetTx treated animals was verified, I investigated the effects of reduced synaptic vesicle release on myelination. Using the transgenic line Tg(mbp:GFP-caax), which visualizes myelin sheaths by GFP expression in the membrane of myelinating oligodendrocytes, I took overview images of the spinal cord of controls and TetTx treated animals at 4dpf. At an overview of somites 8-11, the spinal cord of TetTx treated animals shows a subtle reduction in myelin sheaths formed at 4dpf, which is particularly visible in the dorsal and ventral tract (Figure 4.6, bottom) compared to the spinal cord of control animals (Figure 4.6, top). Interestingly, the myelination of the peripheral lateral line (pLL) in

the PNS does not appear to be visibly affected in TetTx treated animals (Figure 4.6, top and bottom).

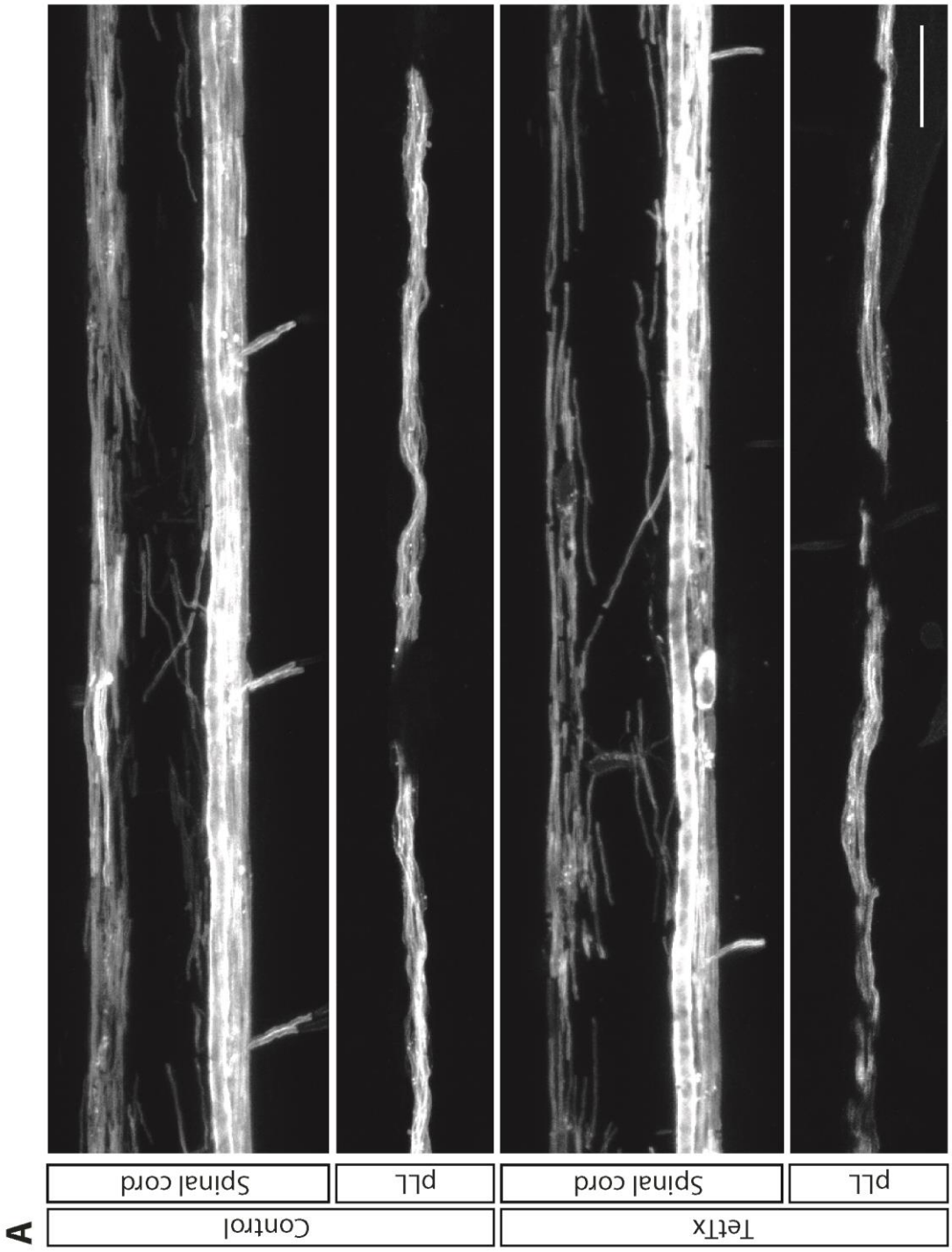

Figure 4.6: Reduction of neuronal vesicle release leads to a reduction in myelin sheaths in the CNS but no visible reduction in the PNS. (A) Somites 8-11 of Tg(mbp:GFPcaax) animals show myelin sheaths labelled by GFP in the spinal cord and peripheral lateral line (pLL) at 4dpf. TetTx treated animals show a visible reduction in myelin sheaths in the spinal cord, however, the myelin sheaths in the pLL show no visible difference to controls (Scale bar 25µm).

To quantify the loss of myelin sheaths in the TetTx treated animals, I cut transversal sections of the spinal cord at somite area 15 and imaged them using transmission electron microscopy (TEM) (Figure 4.7 A and B). Neuronal tissue in the spinal cord was well preserved and no visible morphological differences were found in the spinal cord sections of TetTx treated animals compared to controls. The myelin surrounding the axons was successfully preserved during the tissue preparation and myelinated axons were found mainly in the dorsal and ventral tract of control animals and TetTx treated animals, in accordance with the fluorescent microscopy images of Tg(mbp:GFP-caax) (Figure 4.6). The smallest myelinated axon found in the electron micrographs had a diameter of 0.3µm, while the diameter of the largest myelinated axons, the Mauthner axons, lies between 3-5µm. This has been also shown in previous CNS studies investigating the relationship between axon calibre and myelination. While there is a "critical axon calibre" in the PNS of approximately 1µm above which an axon is myelinated (Duncan 1934; Voyvodic, 1989), no such axon calibre threshold has been found in the CNS and the axon calibre size spectra of myelinated and unmyelinated axons vary considerably in the CNS (Matthews and Duncan, 1971; Franson and Hildebrand, 1975; Remahl and Hildebrand, 1982; Hildebrand and Waxman, 1984). In the CNS, myelinated axons have been found with an axon calibre down to 0.2-0.3µm and unmyelinated axons found with axon calibre up to 0.8µm, even though these are rare and large calibre axons are likely to be myelinated under normal conditions (Remahl and Hildebrand, 1982; Hildebrand and Waxman, 1984).

Axons with the largest calibre were almost all myelinated in control animals (Figure 4.7, A), whereas a number of axons with large calibre remained unmyelinated in the spinal cord of TetTx treated animals (Figure 4.7, B, unmyelinated large calibre axons colour coded in red). In order to quantify the number of myelinated as well as

unmyelinated axons per hemi spinal cord, the diameter of all large calibre axons was traced and all axons with a diameter of 0.3µm or above were counted, while all axons with a diameter below 0.3µm were discarded in the quantification. In controls, the number of myelinated axons per hemi spinal cord was 67.4 +/- 9 .0, while the average number of myelinated axons per hemi spinal cord in TetTx treated animals was 41.0 +/- 8.9. The number of myelinated axons per hemi spinal cord, therefore, was significantly reduced in TetTx treated animals compared to control animals (Student's two-tailed t-test p = 0.0017, control n = 5, TetTx mRNA n = 5, Two-tailed Power analysis: 100% power) (Figure 4.7, C). The average number of unmyelinated axons with a diameter >0.3µm in control animals was 37 +/- 6, compared to 69.8 +/- 11.5 in TetTx treated animals (Figure 4.7, C). This is a significant increase of unmyelinated axons in TetTx treated animals (Student's two-tailed t-test p = 0.0005, control n = 5, TetTx mRNA n = 5, Two-tailed Power analysis: 100% power), in accordance with the reduction of myelinated axons. Overall, the number of axons with a calibre of 0.3µm or above, including myelinated and unmyelinated axons, is 104.4 +/- 12.2 in controls and 110.8 +/- 13.3 in TetTx treated animals, showing no significant decrease, indicating that there is no loss of neurons with calibre >0.3µm due to the TetTx treatment (Two-tailed Student's t-test, p = 0.45). These findings were in accordance with the ratios of myelinated and unmyelinated axons to total number of axons with calibres >0.3µm. On average, control animals exhibited 64.5 +/- 4.1% myelinated to 35.4 +/- 4.1% unmyelinated axons for those with a calibre >0.3µm, while TetTx treated animals showed 37 +/- 7.1 % myelinated to 62.9 +/- 7.1% unmyelinated axons, showing a decrease in myelinated axons by 42% in TetTx treated animals (Figure 4.7, D). This decrease in myelinated axons was not due to a loss of axons with calibres large enough to be myelinated. The percentage of axons with diameter between 0.3-1.9µm of the myelinated axons per hemi spinal cord in control and TetTx treated animals was not different in controls and TetTx treated animals (control n = 5, TetTx mRNA n = 5) (Figure 4.7, E). Similarly, the percentage of axons with diameter between 0.3-1.9µm of the myelinated axons per hemi spinal cord in control and TetTx treated animals was not changed (control n = 5, TetTx mRNA n = 5) (Figure 4.7, F). The Mauthner axon exhibited axon diameters between 3.4-5µm and was excluded from the analysis as it was myelinated in every control

and TetTx treated animal. The total number of axons with axon calibre between 0.3-1.9µm, including myelinating and unmyelinating axons, were not significantly changed in TetTx treated animals, demonstrating again that the TetTx treatment had no adverse effect on axonal calibre growth (control n = 5, TetTx mRNA n = 5; two-way ANOVA p = 0.42) (Figure 4.7, G).

In summary, the inhibition of synaptic vesicle release by the TetTx treatment reduced the number of myelinated axons and increased the number of unmyelinated axons in the zebrafish hemi spinal cord, without causing significant loss in the number neurons with axon calibre >0.3µm.

However, larger calibre axons are more likely to be myelinated (Remahl and Hildebrand, 1982; Hildebrand and Waxman, 1984). Even inert polystyrene fibres in absence of any axonal signals can be ensheathed by myelin-like structures in vitro if their diameter is above 0.4µm and a 5-fold increase in the number of myelin-like sheaths was found on fibres with a diameter larger than 0.5 µm (Lee et al., 2012). Even though there was no overall decrease in the number of axons with a calibre >0.3µm in TetTx treated animals, there might have been a shift in general axon calibre size towards small calibres >0.3µm, which are less likely to be myelinated and which might account for the decrease in the number of myelinated axons and increase in the number of unmyelinated axons found in TetTx treated animals. Axon calibres were therefore binned in two categories, axons with relatively small axon calibre between 0.3µm and 0.9µm and axons with relative large calibre >0.9 to 1.9µm. In controls, 97.3 +/- 2.9% of axons with a calibre of 0.9µm or above were myelinated, while only 52.8 +/- 4.8% of the smaller calibre axons with a calibre between 0.3-0.9µm were myelinated, indicating that axon calibre might influence myelination. In the absence of synaptic vesicle release, 77.1 +/- 13.7% of the larger calibre axons of 0.9µm or above were myelinated compared to the approximately 97% in controls. However, the number of smaller myelinated axons between 0.3-0.9µm calibre was more dramatically decreased in TetTx treated animals, only 26.4 +/- 8.0% of the axons with axon calibre between 0.3-0.9µm were myelinated in the TetTx treated animals compared to the approximately 53% in the controls(two-way ANOVA p= 0.96, control n = 5, TetTx n = 5) (Figure 4.7, H). Interestingly, the Mauthner axon, the axon with the largest calibre in the spinal cord was always

myelinated, regardless of TetTx expression. The myelination of large calibre axons is therefore less severely affected by the inhibition of synaptic vesicle release than the myelination of axons with small to intermediate calibre.

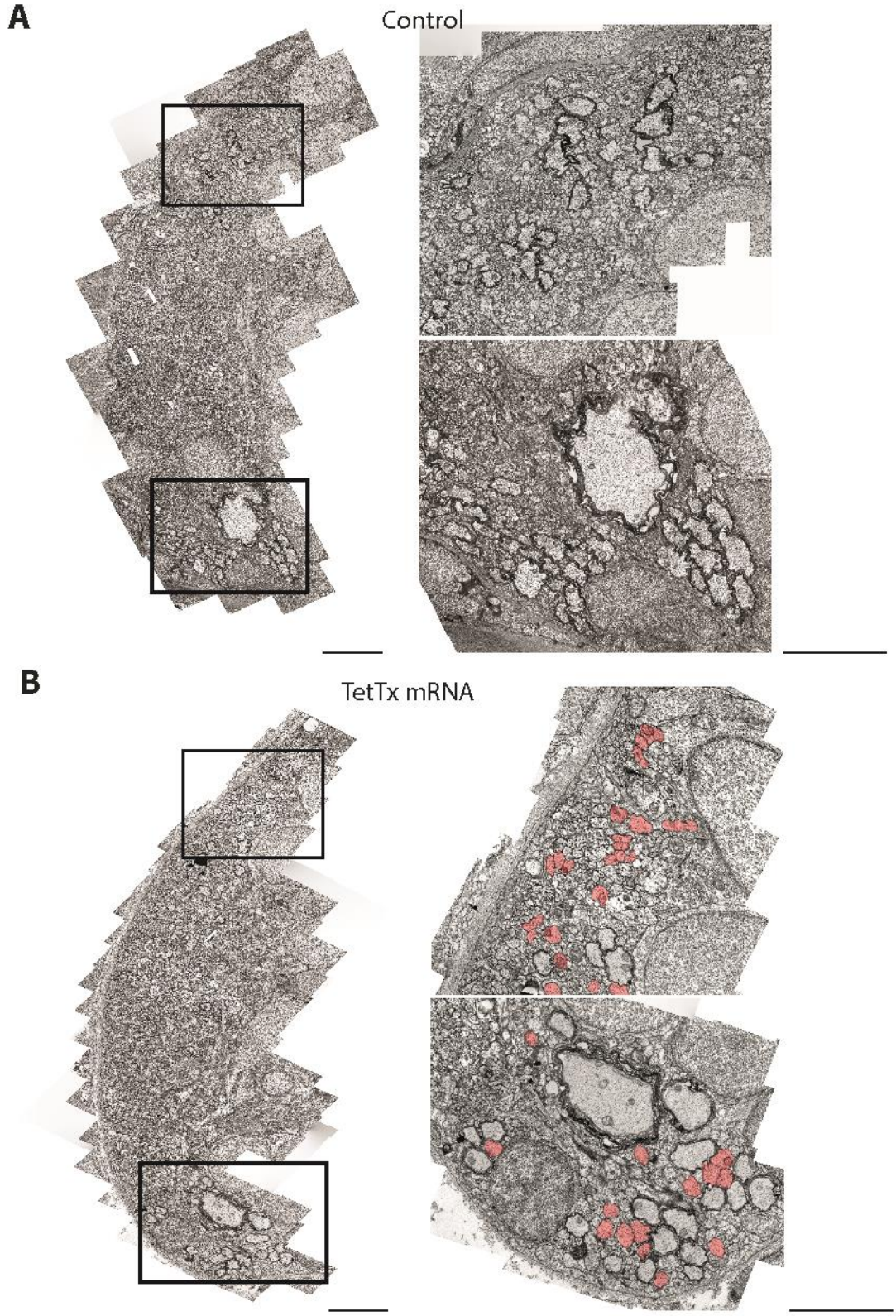
A
Control
B
TetTx mRNA

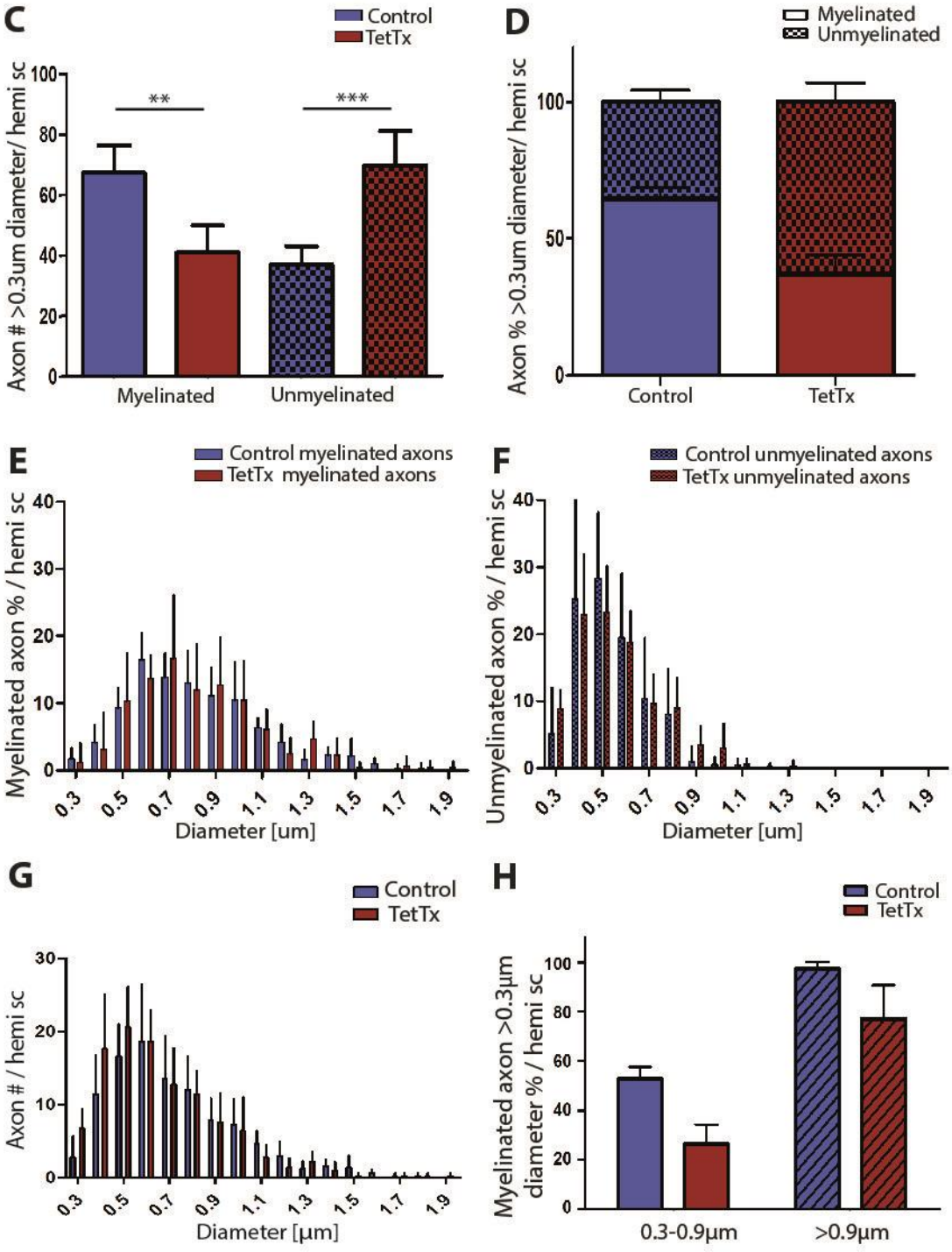

Figure 4.7: Reduction of neuronal vesicle release leads to a reduction in myelinated axons in the zebrafish spinal cord. (A) Electron micrographs of a transversal hemi spinal cord section at somite 15 of a control animal (left) and a TetTx expressing animal (right) at 4dpf (Scale bar 15µm). Rectangles correspond to the areas shown in B. (B) Zoom in of the myelinated fibres in the ventral

and dorsal spinal cord area indicated by rectangles in A. The Mauthner axon and a subset of large calibre axons in the dorsal and ventral spinal cord are myelinated in both the control (left) and TetTx treated animals (right). The TetTx expressing animals show unmyelinated axons with a calibe >0.3µm (colour coded in red), which are mainly myelinated in the controls. (Scale bar 5µm). (C) Quantification of all myelinated and unmyelinated axons per hemi spinal cord in the electron micrographs with an axon calibre >0.3µm diameter. In controls, the average number of myelinated axons per hemi spinal cord was 67.4 +/- 9 compared to TetTx treated animals the average number of myelinated axons per hemi spinal cord was 41 +/- 8.9 (control n = 5, TetTx n = 5; student's two-tailed t-test p = 0.0017). The average number of unmyelinated axons in control animals was 37.0 +/- 6.0 compared to 69.8 +/- 11.5 in TetTx treated animals (control n = 5, TetTx mRNA n = 5; student's two-tailed t-test p = 0.0005; two-tailed power analysis: 100% power). The overall number of axons with a calibre of 0.3µm or above, including myelinated and unmyelinated axons, is 104.4 +/- 12.2 in controls and 110.8 +/- 13.3 in TetTx treated animals, showing no significant decrease in axons with calibre diameter above 0.3µm (two-tailed Student's t-test p = 0.45). (D) Percentage of myelinated and unmyelinated axons with axon diameter >0.3µm per hemi spinal cord. On average, control animals exhibit 64.5 +/- 4.1% myelinated to 35.4 +/- 4.1% unmyelinated axons, while TetTx treated animals show 37 +/- 7.1 % myelinated to 62.9 +/- 7.1% unmyelinated axons (control n = 5, TetTx mRNA n = 5). (E) Percentage of the myelinated axons per hemi spinal cord with a diameter between 0.3-1.9µm in controls and TetTx treated animals (control n = 5, TetTx n = 5). (F) Percentage of the unmyelinated axons per hemi spinal cord with a diameter between 0.3-1.9µm in controls and TetTx treated animals (control n = 5, TetTx n = 5). (G) Quantification of total axon number (including myelinated and unmyelinated axons) per hemi spinal cord with axon calibre between 0.3-1.9µm (two-way ANOVA p= 0.42, control n = 5, TetTx n = 5). (H) The percentage of myelinated axons with intermediate calibre between 0.3-0.9µm and large calibre >0.9 µm per hemi spinal cord in controls and TetTx treated animals. The average percentage of myelinated axons with calibre between 0.3-0.9µm was 52.8 +/- 4.8% in controls and 26.4 +/- 8.0% in TetTx treated animals. The average percentage of myelinated axons with calibre >0.9µm was 97.3 +/- 2.9% in controls and 77.1 +/- 13.7% in TetTx treated animals.

4.2.3 The myelin ensheathment of RS and CiD neurons is reduced in the absence of synaptic vesicle release

Although electron micrographs of transverse spinal cord sections is a reliable technique to quantify the number of myelinated and unmyelinated axons >0.3µm at the cutting plane, it does not allow for longitudinal analysis of the myelination status of the axons. Furthermore, electron micrographs of transverse sections through the

spinal cord do not allow identification of the different neuron subtypes whose myelin ensheathment might be affected in the absence of synaptic vesicle release. The axons with a calibre >0.3µm that are unmyelinated in the cutting plane of TetTx treated animals might be unmyelinated along the whole length of the axon. Alternatively, the axon might have been unmyelinated at the cutting plane but be ensheathed by myelin sheath in other areas along the axon. If the whole axon is unmyelinated, it is possible that all axons of certain neurons may be unmyelinated, which may account for the 40% decrease in the number of myelinated axons in the absence of synaptic vesicle release. In order to test whether the decrease in the number of myelinated axons in the TetTx treated animals is due to the total loss of myelin ensheathment of certain axons or due to a decrease in myelin ensheathment of all axons, I investigated the myelin ensheathment in two neurons that have been identified to be myelinated during the early zebrafish development (see chapter 3). Reticulospinal neurons (RS) and circumferential descending interneurons (CiD) are fated to be myelinated during early development and were imaged before the onset of myelination at 2dpf, during the onset of myelination at 3dpf and after the onset of myelination at 4dpf. The axons of RS (Figure 4.8, A) and CiD (Figure 4.9, A and B) neurons were labelled by the transgenic line Tg(s1011Gal4,UAS:Kaede), while myelin sheaths were labelled by the transgenic line Tg(sox10:mRFP). The percentage of myelin ensheathment along the individual axons was calculated by dividing the total length of all myelin sheaths along the axon by the total axon length measured. The average myelin ensheathment of RS axons was 0 +/- 0% in controls and 0 +/- 0% in TetTx treated animals at 2dpf, 65.9 +/- 24.4% in controls and 46.4 +/- 26.0% in TetTx treated animals at 3dpf and 75.5 +/- 27.9% in controls and 54.9 +/- 31.8% in TetTx treated animals at 4dpf (2dpf control n = 12, TetTx n = 12; 3dpf control n = 20, TetTx n = 19; 4dpf control n = 24, TetTx n = 25; one cell was measured per animal; Two-way ANOVA $p = 0.017$) (Figure 4.8, B). This is a decrease of 30% at 3dpf and 27% at 4dpf. Overall, the myelin ensheathment of RS axons was significantly decreased in TetTx treated animals. The average myelin ensheathment of CiD axons was 0 +/- 0% in controls and 0 +/- 0% in TetTx treated animals at 2dpf, 28.4 +/- 25.3% in controls and 14.8 +/- 16.2% in TetTx treated animals at 3dpf and 69.6 +/- 25.8% in controls and 53.8 +/- 26.3% in TetTx treated animals at 4dpf (2dpf control n = 13, TetTx n = 13; 3dpf

control n = 21, TetTx n = 22; 4dpf control n = 22, TetTx n = 21; one cell was measured per animal; Two-way ANOVA p = 0.017) (Figure 4.9, C). This is a decrease of approximately 47% at 3dpf and 23% at 4dpf. Overall, the myelin ensheathment of CiD axons was significantly reduced in TetTx treated animals.

Axon calibre was also evaluated to again ensure that the TetTx treatment does not have any negative effect on axon calibre growth along the length of certain neurons, which might have gone undetected in the evaluation of axon calibre of all axons >0.3µm per hemi spinal cord by transmission election microscopy. Axon calibre was calculated by dividing the axon area by the axon length measured. The average axon calibre in RS axons was 0.76 +/- 0.2µm in controls and 1.03 +/- 0.2µm in TetTx treated animals at 2dpf, 1.36 +/- 1.0µm in controls and 1.21 +/- 0.5µm in TetTx treated animals at 3dpf and 1.49 +/- 0.8 µm in controls and 1.62 +/- 0.7 µm in TetTx treated animals at 4dpf (2dpf control n = 12, TetTx n = 14; 3dpf control n = 20, TetTx n = 19; 4dpf control n = 18, TetTx n = 19; one cell was measured per animal; Two-way ANOVA p = 0.56) (Figure 4.8, B). The calibre of RS axons increased dramatically between 2dpf and 4dpf, in accordance with the findings in chapter 3. The average axon calibre of RS neurons in TetTx treated animals was not significantly different compared to controls. The average axon calibre of CiD interneurons was 0.35 +/- 0.09µm in controls and 0.33 +/- 0.09µm in TetTx treated animals at 2dpf, 0.48 +/- 0.12µm in controls and 0.48 +/- 0.14µm in TetTx treated animals at 3dpf and 0.57 +/- 0.12 µm in controls and 0.58 +/- 0.16 µm in TetTx treated animals at 4dpf (2dpf control n = 12, TetTx n = 13; 3dpf control n = 21, TetTx n = 24; 4dpf control n = 25, TetTx n = 19; one cell was measured per animal; Two-way ANOVA p = 0.92) (Figure 4.9, D). Also in accordance with the findings in chapter 3, the axon calibre of CiD neurons did not increase as dramatically as it did in RS axons, however unlike the axon calibre of CiD interneurons measured in chapter 3, there is a small increase in the axon calibre of CiD neurons between 2dpf and 4dpf. This is likely due to the different age groups that were binned differently in chapter 3. Whereas in chapter 3, the axons of the neuron subtypes were grouped at 2dpf, between 3-5dpf and 6-12dpf, the axons of RS and Cid neurons were grouped at 2dpf, 3dpf and 4dpf here. This analysis, therefore, reveals greater detail and small changes in axon calibre per day. The increase in average myelin ensheathment of RS

and CiD axons in controls was similar to the myelin ensheathment of uninjected animals in chapter 3.

Interestingly, the decrease in average myelin ensheathment at 4dpf was 28% in RS and 23% in CiD axons, which is a relatively small decrease in comparison to the 40% overall decrease in the number of myelinated axons measured at 4dpf in the electron micrographs. There might be small differences in the effect that the absence of synaptic vesicle release has on the axon ensheathment of different neurons and while the myelination of RS and CiD axon is reduced by 28% and 23%, respectively, the myelination of other neurons fated for myelination might more decreases in the absence of synaptic vesicle release, leading to an average of approximately 40% decrease in overall myelination in the spinal cord. Furthermore, the difference in the decrease in the amount of myelin ensheathment of RS and CiD axons compared to the decrease in the number of myelinated axons in the TEM analysis might stem from the different locations in the spinal cord where the analyses took place. The TEM images were taken from transverse cross sections at somite 15, whereas the areas in which RS and CiD axons were measured were selected according to best visibility of axon and myelin sheaths and therefore varied along the spinal cord. As the onset of myelination in the spinal cord starts from approximately 3dpf (Almeida et al., 2011) and oligodendrocyte maturation and myelination occurs according to a distinct anterior-posterior gradient (Schwab and Schnell, 1989 as reviewed in Jessel, 2000; Baumann and Pham-Dinh, 2001 and Rowitch, 2004), the maturation and myelination state of the RS and CiD axons measured varied according to their anterior- posterior position in the spinal cord as is indicated in the high standard deviations. Future analysis is therefore required in order to see whether the decrease in myelin ensheathment of RS and CiD axons at somite area 15 would match the decrease in myelinated axon number in TetTx treated animals. Future analysis will also include the quantification of myelin ensheathment along different other neurons fated for myelinaiton, such as CoPA and CoLA neurons, at somite area 15. Furthermore, in future experiments, rather than label these neurons with cytoplasmic GFP expression, I would use GFP-cntn1a expression, as the GFP is anchored to the cell membrane of GFP-cntn1a labelled neurons through the GPI anchor of cntn1a and is extruded from the myelin ensheathed axon membrane after cntn1a is restricted

to the node of Ranvier (see chapter 3), which facilitates a more precise measurement of myelinated and unmyelinated areas along one axon.

Overall, both RS and CiD axons were not wholly unmyelinated along their axon length but the myelin ensheathment is reduced along the length of the axons. These findings indicate that the 40% reduction in the number of myelinated axons is not due to the total loss of myelin around certain axons but rather an overall decrease in the myelin ensheathment of all axons fated to be myelinated.

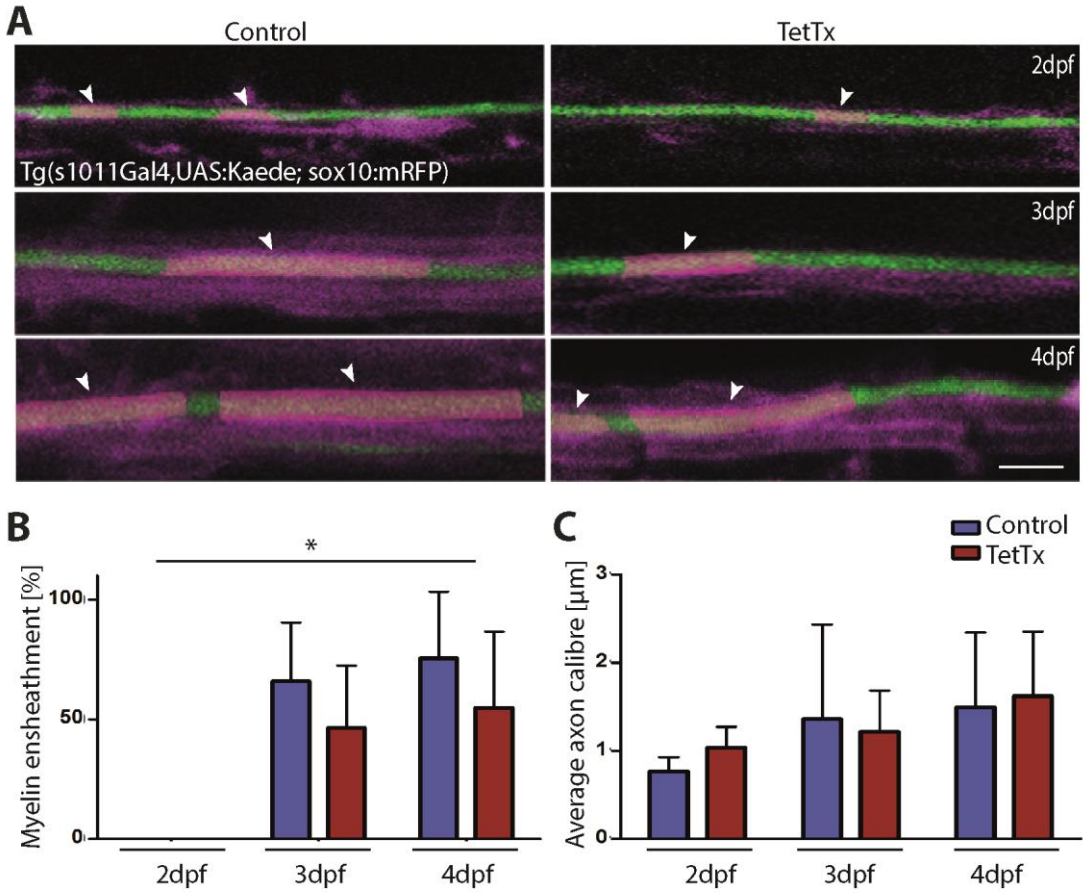

Figure 4.8: Myelin ensheathment and axon calibre of reticulospinal neurons in the absence of synaptic vesicle release. (A) Axons of RS neurons at 2dpf, 3dpf and 4dpf in control (left) and TetTx treated animals (right) and their respective myelin ensheathment labelled by the transgenic line Tg(s1011Gal4,UAS:Kaede; sox10:mRPF). Myelin sheaths around the RS axons are colour coded in pink and indicated by arrows (scale bar = 3µm). (B) Quantification of the average myelin ensheathment percentage of RS axons, calculated from the sum of the length of myelin sheaths divided by the axon length measured, at 2dpf, 3dpf and 4dpf. The average myelin ensheathment is 0+/- 0% in RS of controls and 0 +/- 0% in RS of TetTx treated animals at 2dpf, 65.9 +/- 24.4% in RS of controls and 46.4 +/- 26.0% in RS of TetTx treated animals at 3dpf and 75.5 +/- 27.9% in RS of controls and 54.9 +/- 31.8% in RS of TetTx treated animals at 4dpf (2dpf control n = 12, TetTx n = 12; 3dpf control n = 20, TetTx n = 19; 4dpf control n = 24, TetTx n = 25; one cell was measured per animal; Two-way ANOVA p = 0.0017). (C) Quantification of the average axon calibre of RS axons, calculated from the axon area divided by the axon length measured, at 2dpf, 3dpf and 4dpf. The average axon calibre is 0.76 +/- 0.2µm in RS of controls and 1.03 +/- 0.2µm in RS of TetTx treated animals at 2dpf, 1.36 +/- 1.0µm in RS of controls and 1.21 +/- 0.5µm in RS of TetTx treated animals at 3dpf and 1.49 +/- 0.8 µm in RS of controls and 1.62 +/- 0.7 µm in RS of TetTx treated animals at 4dpf (2dpf control n = 12, TetTx n = 14; 3dpf control n = 20, TetTx n = 19; 4dpf control n = 18, TetTx n = 19; one cell was measured per animal; Two-way ANOVA p = 0.56).

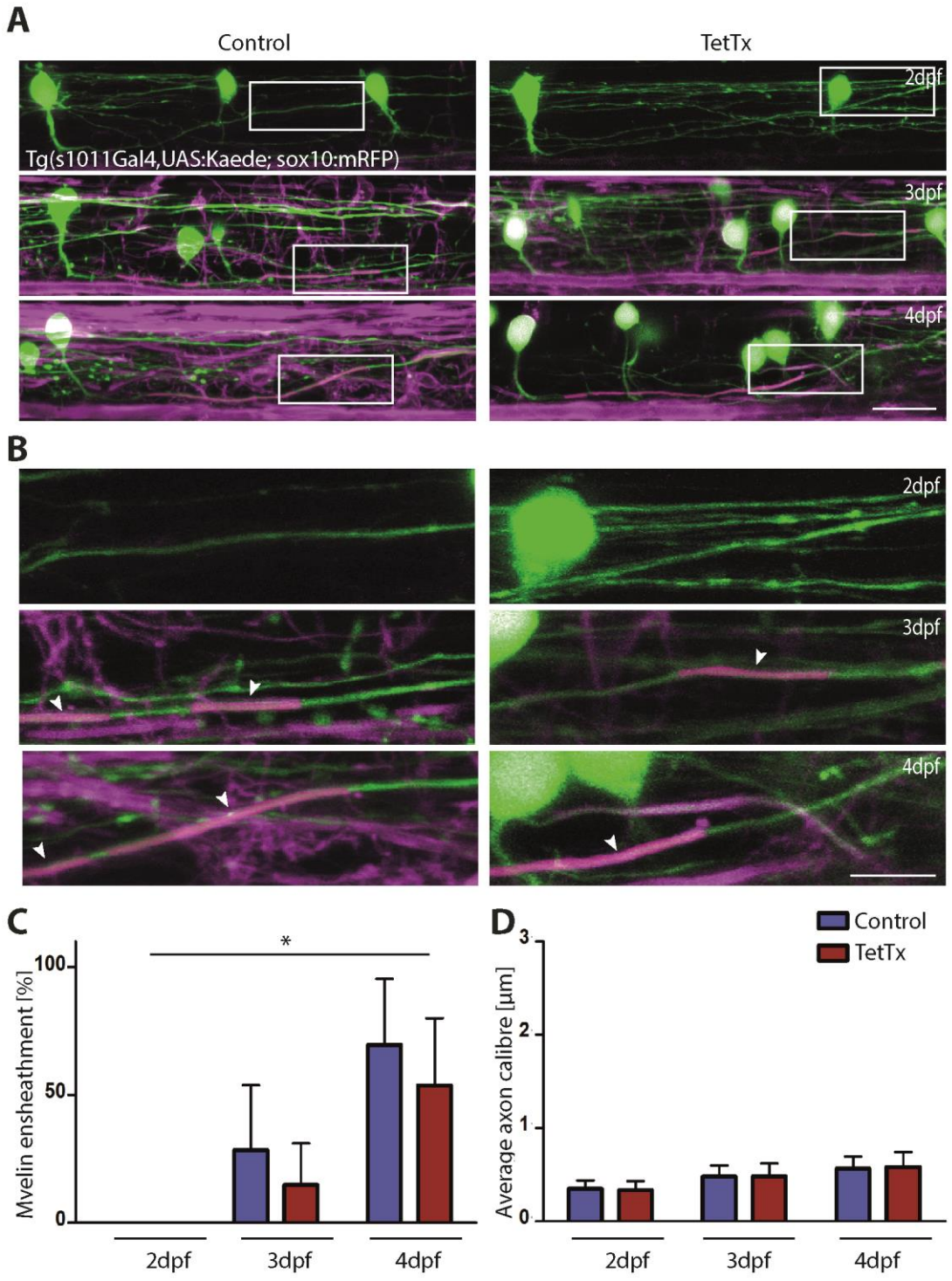

Figure 4.9: Myelin ensheathment and axon calibre of CiD in the absence of synaptic vesicle release. (A) Axons of CiD interneurons at 2dpf, 3dpf and 4dpf in control (left) and TetTx treated animals (right) and their respective myelin ensheathment labelled by the transgenic line Tg(s1011Gal4,UAS:Kaede; sox10:mRPF).. Myelin sheaths around the CiD axons are colour coded in

pink. The white boxes indicate the zoomed in areas in B (scale bar = 10µm). (B) Zoomed in areas indicated in A. Myelin sheaths around the CiD axons are colour coded in pink and indicated by arrows (scale bar = 5µm). (C) Quantification of the average myelin ensheathment percentage of CiD axons, calculated from the sum of the length of myelin sheaths divided by the axon length measured, at 2dpf, 3dpf and 4dpf. The average myelin ensheathment is 0 +/- 0% in CiD of controls and 0 +/- 0% in CiD of TetTx treated animals at 2dpf, 28.4 +/- 25.3% in CiD of controls and 14.8 +/- 16.2% in CiD of TetTx treated animals at 3dpf and 69.6 +/- 25.8% in CiD of controls and 53.8 +/- 26.3% in CiD of TetTx treated animals at 4dpf (2dpf control n = 13, TetTx n = 13; 3dpf control n = 21, TetTx n = 22; 4dpf control n = 22, TetTx n = 21; one cell was measured per animal; Two-way ANOVA p = 0.017). (D) Quantification of the average axon calibre of CiD axons, calculated from the axon area divided by the axon length measured, at 2dpf, 3dpf and 4dpf. The average axon calibre is 0.35 +/- 0.09µm in CiD of controls and 0.33 +/- 0.09µm in CiD of TetTx treated animals at 2dpf, 0.48 +/- 0.12µm in CiD of controls and 0.48 +/- 0.14µm in CiD of TetTx treated animals at 3dpf and 0.57 +/- 0.12 µm in CiD of controls and 0.58 +/- 0.16 µm in CiD of TetTx treated animals at 4dpf (2dpf control n = 12, TetTx n = 13; 3dpf control n = 21, TetTx n = 24; 4dpf control n = 25, TetTx n = 19; one cell was measured per animal; Two-way ANOVA p = 0.92).

4.2.4 Reduction of neuronal vesicle release leads to a small decrease in myelinating oligodendrocytes

As the 40% decrease in the myelinated axons is not due to the loss of neurons with axon calibre >0.3µm, the number of myelinating oligodendrocytes might be reduced. Using the Tg(mbp:GFP), which expresses GFP in the cytoplasm of mbp expressing cells, we counted the number of oligodendrocyte cell bodies in the spinal cord of controls (Figure 4.10, A, top) and TetTx treated animals at 4dpf (Figure 4.10, A, bottom). Between somites 8-11, the average myelinating oligodendrocyte number in control animals was 48.7 +/- 9.4 while the average myelinating oligodendrocyte number in TetTx treated animals was 44.1 +/- 9.1. This is a small but significant decrease in the number of myelinating oligodendrocytes by approximately 10% in TetTx treated animals (Student's two-tailed t-test, p = 0.044, control n = 40, TetTx mRNA n = 36, Two-tailed power analysis: 78% power). However, 90% of myelinating oligodendrocytes are still present in the zebrafish spinal cord, even in the absence of synaptic transmission.

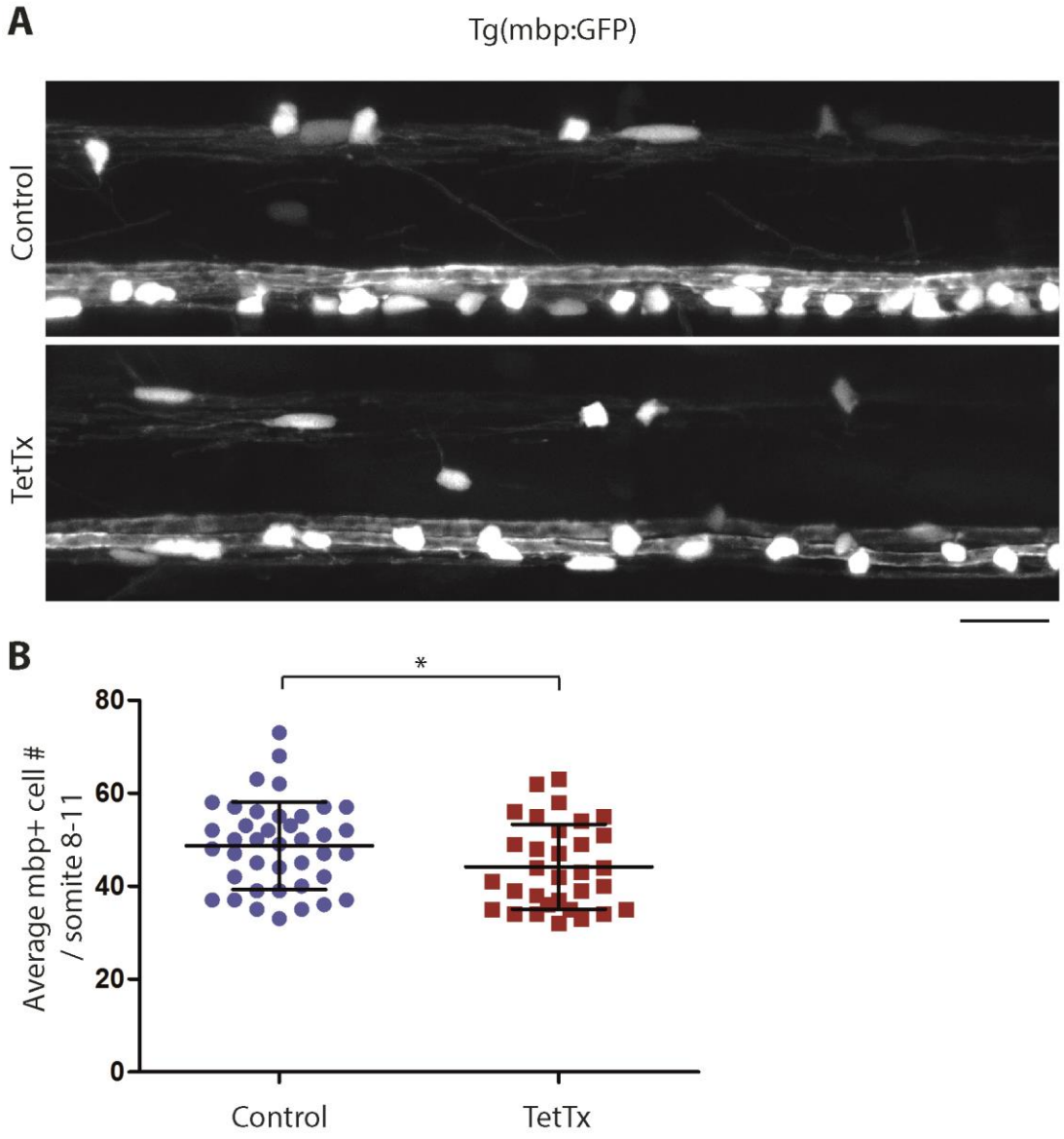

Figure 4.10: Reduction of neuronal vesicle release leads to a small reduction in differentiated oligodendrocyte number. (A) Overview of Tg(mbp:GFP) somites 10-11, which shows mbp expression in the cytoplasm of differentiated oligodendrocytes in the spinal cord of a control (top) and TetTx treated animal (bottom) at 4dpf (Scale bar = 10µm). (B) Quantification of mbp + cells in somite area 8 to 11. The average oligodendrocyte number in control animals was 48.7 +/- 9.4 while the average oligodendrocyte number in TetTx treated animals was 44.1 +/- 9.1 (control n = 40, TetTx mRNA n = 36; student's two-tailed t-test, p = 0.044; two-tailed power analysis: 78% power).

4.2.5 Reduction of synaptic vesicle release leads to a decrease in myelin sheath number per oligodendrocyte

As the 10% reduction in myelinating oligodendrocytes only partially accounts for the 40% loss of myelinated axons in the electron micrographs, we investigated individual oligodendrocyte morphology by mosaic labelling using mbp:mCherry-caax in control and TetTx treated animals (Figure 4.11, A). The oligodendrocytes analysed at 3dpf were not the same cells imaged at 4dpf and thereby represent two independent cohorts.

The average number of myelin sheaths made per oligodendrocyte was 11.7 +/- 3.1 in controls and 9.0 +/- 2.8 in TetTx treated animals at 3dpf (control oligodendrocyte n = 18, animal n = 17, TetTx n = 29, animal n = 25; two-tailed student's t-test p = 0.003), and 11.6+/- 3.1 in controls and 8.1 +/- 2.9 in TetTx treated animals at 4dpf (control oligodendrocyte n = 32, animal n = 17, TetTx oligodendrocyte n = 36, animal n = 24; two-tailed student's t-test p =, p = <0.0001). This is a significant reduction of 23.1% at 3dpf and 30.1% at 4dpf (Figure 4.11, B). The number of myelin sheaths per oligodendrocyte was remarkably similar in controls at 3dpf and 4dpf (Two-tailed Student's t-test, p = 0.91). All oligodendrocytes selected for imaging at 3dpf and 4dpf had formed multiple myelin sheaths at time of imaging. As oligodendrocytes only have a few hours within they form their myelin sheaths, after which they possess a relatively stable number of myelin sheath per oligodendrocyte (Czopka et al., 2013), the majority of oligodendrocytes analysed here were past the initial myelination stage and therefore would be expected to have a stable number of myelin sheaths between 3dpf and 4dpf under normal conditions. Interestingly, the number of myelin sheaths in TetTx was decreased between 3dpf and 4dpf by approximately 1 myelin sheath per oligodendrocyte. This decrease however, was not significant (Two-tailed Student's t-test, p = 0.24).

The average sheath length per oligodendrocyte was not significantly reduced in the absence of synaptic vesicle release as the average sheath length per cell was 25.1 +/- 6.3µm in controls and 23.9 +/- 6.7µm in TetTx treated animals at 3dpf (control oligodendrocyte n = 18, animal n = 17, TetTx n = 29, animal n = 25; two-tailed student's t-test p = 0.57) and 29.9 +/- 7.8µm in controls and 27.7 +/- 7.8µm in TetTx treated animals at 4dpf (control oligodendrocyte n = 32, animal n = 17, TetTx

oligodendrocyte n = 36, animal n = 24; two-tailed student's t-test p = 0.25) (Figure 4.11, C). Even though the myelin sheath length per oligodendrocyte in TetTx treated animals was not significantly different from controls, there was a trend for smaller myelin sheaths in the absence of synaptic vesicle release. The average myelin sheath length per oligodendrocyte between 3dpf and 4dpf was increased by an average of 5.0µm in controls and 3.8µm in TetTx treated animals, indicating that the myelin sheaths continue to grow between 3dpf and 4dpf, both, in control and TetTx treated animals even though myelin sheaths, on average, appear to grow slower in TetTx treated animals. However, it is important to note that the cells at 3dpf and 4dpf represent two different co-horts as the individuals cells were not followed between 3dpf and 4dpf, suggesting that the difference in myelin sheath length might not be a realistic representation of sheath growth within the 2 time-points.

The 40% reduction of myelinated axons in the electron micrographs can therefore be explained by the 10% loss of myelinating oligodendrocytes in addition to the 30% decrease of myelin sheaths formed per oligodendrocyte at 4dpf.

Apart from forming myelin sheaths, oligodendrocytes often showed small axon-OL contacts <5µm (Figure 4.11, A). TetTx treated animals had a significant increase in the number of these axon-OL contacts <5µm. The number of small axon-OL contacts <5µm per cell was 1.3 +/- 0.9 in controls and 2.0 +/- 1.0 in TetTx treated animals at 3dpf (control oligodendrocyte n = 18, animal n = 17, TetTx n = 29, animal n = 25; two-tailed student's t-test p = 0.04) and 0.8 +/- 0.9 in controls and 2.7 +/- 1.3 in TetTx treated animals at 4dpf (control oligodendrocyte n = 32, animal n = 17, TetTx oligodendrocyte n = 36, animal n = 24; two-tailed student's t-test p = <0.0001) (Figure 4.11, D). In controls, the number of small axon-OL contacts <5µm is greater at 3dpf than at 4dpf, whereas in TetTx treated animals, there was a significant increase in the number these axon-OL contacts <5µm at 3dpf and at 4dpf. Although the number myelin sheaths per oligodendrocyte are relatively stable after the initial phase of myelination, approximately 25% of the sheaths will be retracted and myelin sheath retraction can take up to several days (Czopka et al., 2013). The small axon-OL contacts <5µm seen in controls and TetTx treated animals might either be axon-OL contacts that never grew into full myelin sheaths or might have been myelin sheaths that are in the process of retraction. In the both cases, it is likely that a higher

number of axon-OL contacts <5µm would be found at 3dpf as the oligodendrocytes at 4dpf would have had more time to completely retract the axon-OL contact <5µm or unstable myelin sheaths in the process of retraction.

However, the number of small axon-OL contacts <5µm in TetTx treated animals did not decrease between 3dpf and 4dpf. In fact, there is a small increase in the number of axon-OL contacts <5µm between 3dpf and 4dpf. Given that the average number of myelin sheath per oligodendrocyte is decreased by an average of 1 myelin sheath per cell between 3dpf and 4dpf, it is likely that there are unstable sheaths in TetTx treated animals, which are retracted between 3dpf and 4dpf. The number of small axon-OL contacts <5µm 4dpf, however, is larger than the small decrease in sheath number between 3dpf and 4dpf, indicating that these axon-OL contacts <5µm might not be retracted as efficiently as they are under normal conditions.

Overall, the myelin extent, the average length of myelin sheaths multiplied by the number of myelin sheaths, formed per oligodendrocyte was significantly reduced in TetTx treated animals. The average myelin extent was 287.9 +/- 90.4µm in controls and 212.1 +/- 70.3µm in TetTx treated animals at 3dpf (control oligodendrocyte n = 18, animal n = 17, TetTx n = 29, animal n = 25; two-tailed student's t-test p = 0.002) and 341.4 +/- 115.4µm in controls and 218.0 +/- 82.4µm in TetTx treated animals at 4dpf (control oligodendrocyte n = 32, animal n = 17, TetTx oligodendrocyte n = 36, animal n = 24; two-tailed student's t-test p = <0.0001) (Figure 4.11, E). The myelin extent in TetTx treated animals is therefore reduced by 26% at 3dpf and 36% at 4dpf. As the average number of myelin sheaths per oligodendrocytes is not changed significantly between 3dpf and 4dpf, the increase in myelin extent likely reflects the increase in myelin sheath length between 3dpf and 4dpf. The average myelin extent is increased by approximately 50µm between 3dpf and 4dpf in controls, which reflects the increase in average myelin sheath length by 5.0µm between 3dpf and 4dpf. The average myelin extent of TetTx treated animals shows a smaller increase of only 6µm between 3dpf and 4dpf, which reflects the smaller increase in average myelin sheath length of 3.8µm in TetTx treated animals and the small decrease in the average sheath number per oligodendrocyte from 9.0 sheaths per cell to 8.1 sheaths per cell between 3dpf and 4dpf. Although, here again, the amount of myelin extent

was measured in a separate co-hort of cells at 3dpf and 4dpf and might therefore not accurately represent the increase in myelin extent between these time-points.

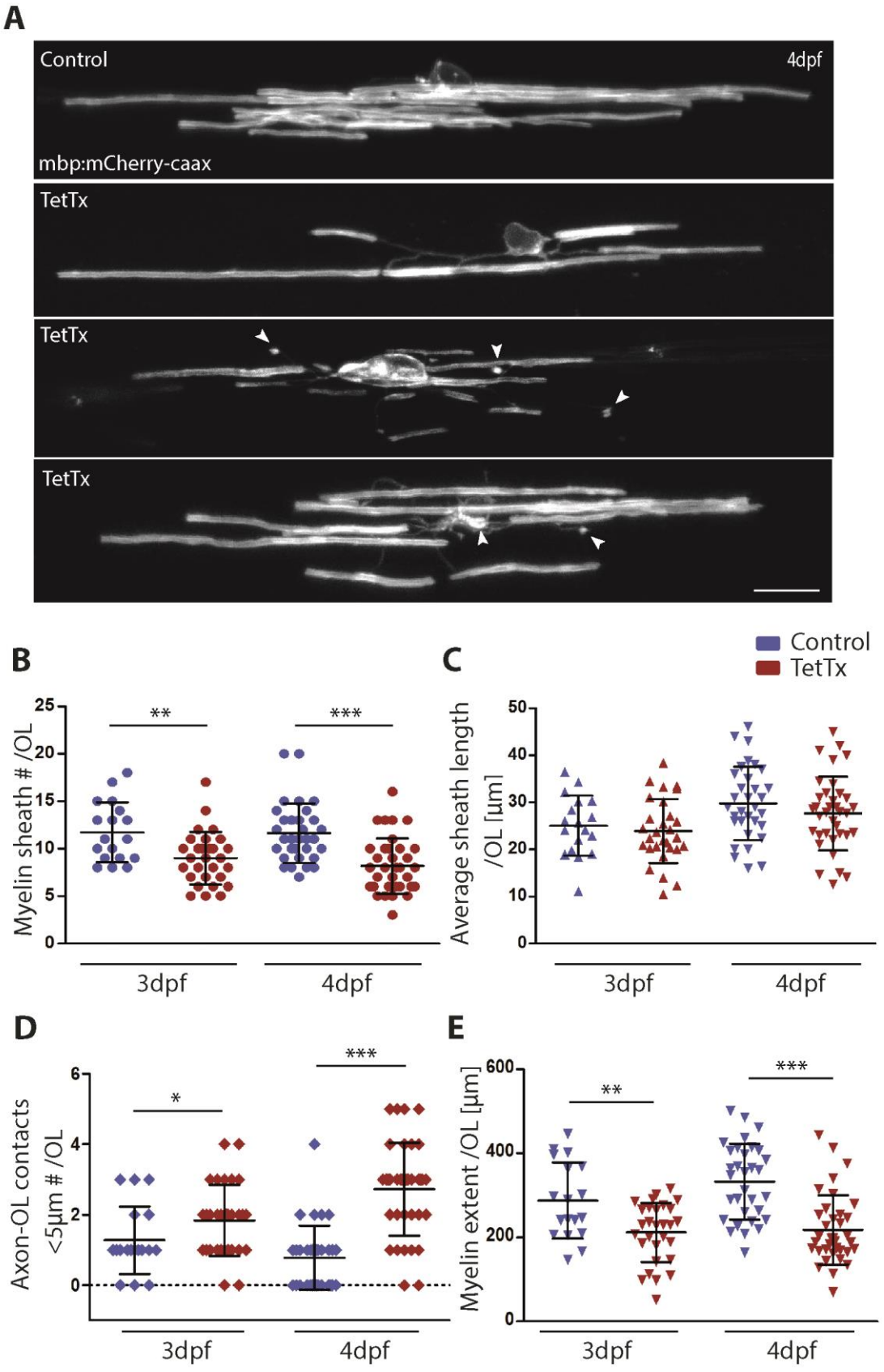
A
Control
4dpf
mbp:mCherry-caax
TetTx
TetTx
TetTx
B
Myelin sheath # /OL
25
20
15
10
5
0
**
***
3dpf
4dpf
C
Control
TetTx
Average sheath length /OL [µm]
50
40
30
20
10
0
3dpf
4dpf
D
Axon-OL contacts <5µm # /OL
6
4
2
0
*
***
3dpf
4dpf
E
Myelin extent /OL [µm]
600
400
200
0
**
***
3dpf
4dpf

Figure 4.11: Oligodendrocytes form a reduced number of myelin sheaths in the absence of neuronal vesicle release. (A) Individual oligodendrocytes labelled by reporter protein mCherry-caax expression under the mbp promoter show an oligodendrocyte in a control animal (top left) and oligodendrocytes in TetTx treated animals (top right, bottom left & right) with varying morphology. Oligodendrocytes in TetTx treated animals often show small axon-OL contacts <5µm (arrows) (Scale bar = 15µm). (B) Quantification of myelin sheath number per oligodendrocyte at 3dpf and 4dpf. The average number of myelin sheaths made per oligodendrocyte was 11.7 +/- 3.1 in controls and 9 +/- 2.8 in TetTx treated animals at 3dpf (control oligodendrocyte n = 18, animal n = 17, TetTx n = 29, animal n = 25; two-tailed student's t-test p = 0.003), and 12.8+/- 3.4 in controls and 8.8 +/- 3.1 in TetTx treated animals at 4dpf (control oligodendrocyte n = 32, animal n = 17, TetTx oligodendrocyte n = 36, animal n = 24 ; two-tailed student's t-test p =, p = <0.0001). (C) Quantification of the average sheath length per oligodendrocyte at 3dpf and 4dpf. The average sheath length per cell of control oligodendrocytes was 25.1 +/- 6.3µm and 23.9 +/- 6.7µm in TetTx treated animals at 3dpf (control oligodendrocyte n = 18, animal n = 17, TetTx n = 29, animal n = 25; two-tailed student's t-test p = 0.57) and 28.6 +/- 6.8µm in controls and 25.3 +/- 7.1µm in TetTx treated animals at 4dpf (control oligodendrocyte n = 32, animal n = 17, TetTx oligodendrocyte n = 36, animal n = 24; two-tailed student's t-test p = 0.25). (D) Quantification of axon-OL contacts <5µm per oligodendrocyte at 3dpf and 4dpf. The number of small axon-OL contacts <5µm per cell was 1.3 +/- 0.9 in controls and 2.0 +/- 1.0 in TetTx treated animals at 3dpf (control oligodendrocyte n = 18, animal n = 17, TetTx n = 29, animal n = 25; two-tailed student's t-test p = 0.04) and 0.8 +/- 0.9 in controls and 2.7 +/- 1.3 in TetTx treated animals at 4dpf (control oligodendrocyte n = 32, animal n = 17, TetTx oligodendrocyte n = 36, animal n = 24; two-tailed student's t-test p = <0.0001). (E) Quantification of the overall myelin extent, measured in the average length of the myelin sheaths per cell multiplied by the number of myelin sheaths per cell. The average myelin extent was 287.9 +/- 90.4 in controls and 212.1 +/- 70.3 in TetTx treated animals at 3dpf (control oligodendrocyte n = 18, animal n = 17, TetTx n = 29, animal n = 25; two-tailed student's t-test p = 0.002) and 341.4 +/- 115.4 in controls and 218.0 +/- 82.4 in TetTx treated animals at 4dpf (control oligodendrocyte n = 32, animal n = 17, TetTx oligodendrocyte n = 36, animal n = 24; two-tailed student's t-test p = <0.0001).

4.2.6 In absence of synaptic vesicle release oligodendrocytes form a reduced number of myelin sheaths during initial myelination

Analysis of single oligodendrocytes at 3dpf and 4dpf showed that the reduction of myelinated axon number in TetTx treated animals is mainly caused by a reduction in myelin sheath number per oligodendrocyte. In order to investigate which cellular mechanism during the dynamic myelin sheath formation in the CNS is impaired by a

reduction of synaptic vesicle release, I used timelapse imaging of oligodendrocytes labelled in Tg(nkx2.2a:GFP) during the initial stages of myelination (see chapter 2 Materials and methods). For the analysis, I therefore selected oligodendrocytes between 2-3dpf or 3-4dpf, when the imaged cell transitioned from the precursor stage to a myelinating oligodendrocyte and formed the first myelin sheath. For the timelapse analysis, oligodendrocytes of similar shape and dorsal spinal cord area were selected to minimize oligodendrocyte variability. Oligodendrocytes have been shown to initiate the formation of all their myelin sheaths within a critical time window of only 5-6 hours after the first myelin sheath was formed (Czopka et al., 2013). Therefore, we analysed each oligodendrocyte for 6 hours after the first myelin sheath formation in controls and TetTx treated animals. During the initial myelination stage, exploratory cell processes are extended from the oligodendrocyte cell body and form putative axon-OL contacts. All structures at the end of an exploratory process between 2µm and 5µm in length were counted as axon-OL contacts that either grew into myelin sheaths or never grew into myelin sheaths, in which case they remained as small contacts or were retracted completely(Figure 4.12, A, top and bottom). I defined myelin sheaths as longitudinal structures >5µm in length that were visible for more than 1time frame as I was confident that structures of this definition are not merely transient axon-OL contacts (Figure 4.12, A, bottom). The reduction in myelin sheath number observed in TetTx treated animals at later stages could be due to different cellular processes: the initial axon-OL contact prior to ensheathment, the initial ensheathment, the formation of a stable myelin sheath, myelin sheath retraction, or a combination of all. If axon-OL contact is reduced during the initial stages of myelination, axon-OL contact would be influenced by synaptic vesicle release when oligodendrocytes extend and retract processes in search for axons prior to ensheathment. If the sheath formation itself is dependent on synaptic vesicle release, the number of axon-OL contacts would be normal but fewer myelin sheaths would be formed in TetTx treated animals. Alternatively, if the maintenance of stable myelin sheaths is dependent on synaptic vesicle release, the same number of nascent myelin sheaths would be formed initially, but a higher proportion of these sheaths would be retracted compared to controls.

During the timelapse movies, controls formed an average of 15.2 +/- 2.7 total axon-OL contacts in TetTx treated animals formed an average of 12.8 +/- 2.1 total axon-OL contacts (control n = 13, TetTx n = 11; student's two-tailed t-test, p= 0.03) (Figure 4.13, D). This suggests that in addition to myelin sheath formation the initial axon-OL contact formation is, to some extent, regulated by synaptic vesicle release and that the reduction in axon-OL contacts is partly caused by the reduction in myelin sheaths formed per oligodendrocyte. The number of myelin sheaths formed per oligodendrocyte was further reduced in TetTx treated animals. Within 6 hours after first sheath formation, control oligodendrocytes formed an average of 12.6 +/- 2.2 sheaths initially, while oligodendrocytes in TetTx treated animals formed only 9.7 +/- 2.7 myelin sheaths per cell (control n = 13, TetTx n = 11, student's two-tailed t-test p = 0.009). Some of these nascent myelin sheaths were retracted within the 6 hours after first sheath formation, so that average number of stable sheaths 6 hours after the first sheath formation was 9.5 +/- 2.0 in controls and 6.9 +/- 2.2 in TetTx treated animals (student's two-tailed t-test p = 0.007) (Figure 4.13, D). My time-lapse analyses, therefore, revealed that oligodendrocytes in TetTx treated animals formed fewer myelin sheaths compared to oligodendrocytes in controls within the first 6 hours after first myelin sheath formation (control n = 13, TetTx n = 11) (Figure 4.13, A, B and C). The formation of all myelin sheaths per oligodendrocyte were initiated within an average of 4.5 +/- 0.8h in controls and within an average of 4.4 +/- 0.8h in TetTx treated animals (Two-tailed student's t-test, p = 0.60, data not shown), suggesting that no more myelin sheaths were produced after the end of the 6 hour analysis. This is in accordance with previous findings (Czopka et al., 2013), showing that the formation of all myelin sheaths per oligodendrocyte is initiated within approximately 5 hours after first sheath formation.

There is a small difference in the number of myelin sheaths number per cell measured at the end of the timelapse movie after initial myelination and the number of sheaths per cell measured in the single oligodendrocyte analysis at 3dpf as well as 4dpf. This is presumably due to a more strict selection of oligodendrocytes during time-lapse movies. Oligodendrocytes exhibit a wide range of different morphologies and the number of myelin sheaths formed per oligodendrocyte varies according to their morphology (Rio Hortega, 1928; Bunge et al., 1961). During the timelapse

movies a particular type oligodendrocyte morphology was chosen, while single oligodendrocytes of varying morphologies were analysed at 3dpf and 4dpf and it is therefore likely that the small increase in myelin sheath number between the two analyses is accounted for by the different oligodendrocyte morphologies analysed rather than the addition of myelin sheaths after the 6 hour period of initial sheath formation during the time-lapse movies.

Furthermore, in the timelapse movies, I noticed that some of the nascent myelin sheaths that are retracted within 6 hours after first sheath formation did not retract completely but remained as small axon-OL contacts <5µm. On the other hand, some of the small axon-OL contacts <5µm never formed myelin sheaths >5µm. At the end of the timelapse analysis, 6 hours after first sheath formation, the average number of axon-OL contacts <5µm was 2.6 +/- 1.9 in controls and 2.4 +/- 1.6 in TetTx treated animals (student's two-tailed t-test $p = 0.74$) and the average number of complete sheath retractions during the 6 hours after first sheath formation was 3.1 +/- 1.2 in controls and 3.5 +/- 1.2 in TetTx treated animals (student's two-tailed t-test $p = 0.36$) (Figure 4.13, D).

In order to compare the different fate of all axon-OL contacts per oligodendrocyte in controls and TetTx treated animals, the number of axon-OL contact to myelin sheath conversion and the number of axon-OL contact that never form a sheath but is retracted or remain as small axon-OL contacts <5µm instead are calculated as percentages.

Of all axon-OL contacts made within 6 hours after first sheath formation, 62.4% convert to myelin sheaths >5µm in controls and 53.9% in TetTx treated animals. The percentage of axon-OL contacts that remain as small axon-OL contacts <5µm at the end of the timelapse was 17.3% in controls and 18.4% in TetTx treated animals. The percentage of axon-OL contacts that retract completely was 20.3% in controls and 27.7% in TetTx treated animals (Figure 4.13, E). In summary, the percentage of axon-OL contacts that form myelin sheaths show a small reduction in TetTx treated animals, while the percentage of axon-OL contacts that are completely retracted and the percentage of axon-OL contacts that remain as small axon-OL contacts <5µm at the end of the time-lapse are subtly increased.

In order to compare the different fate of all nascent myelin sheaths >5µm per oligodendrocyte in controls and TetTx treated animals, the number of nascent sheaths that form stable sheaths and the number of nascent sheaths that are completely retracted or retract to small axon-OL contacts <5µm at the end of the time-lapse are expressed percentages.

Of the nascent myelin sheaths >5µm that were formed within 6 hours after first sheath formation, 83.2% remained stable myelin sheaths >5µm in controls, while 71.0% remained stable myelin sheaths in TetTx treated animals. The percentage of myelin sheaths >5µm that turn to small axon-oligodendrocyte contacts <5µm was 14.6% in controls and 13.1% in TetTx treated animals. The percentage of myelin sheaths >5µm that completely retract was 9.7% in controls and 15.9% in TetTx treated animals. The fate of nascent myelin sheaths >5µm in oligodendrocytes of TetTx treated animals was therefore very similar to control oligodendrocytes once the myelin sheath >5µm was formed (Figure 4.13, F).

The myelin sheaths that were formed per oligodendrocyte 6 hours after first sheath formation were not significantly smaller in length in TetTx treated animals compared to control animals. In controls, the average myelin sheath length was 10.6 +/- 1.5µm and 9.6 +/- 2.2µm in TetTx treated animals (student's two-tailed t-test $p = 0.20$).

Overall, the myelin extent, the average length of myelin sheaths multiplied by the number of myelin sheaths, per oligodendrocyte 6 hours after first sheath formation was significantly reduced in TetTx treated animals. In controls, the average myelin extent was 101.8 +/- 27.3 in controls and 66.5 +/- 24.2 in TetTx treated animals at 4dpf (two-tailed student's t-test $p = <0.003$).

In summary, in the absence of synaptic vesicle release, oligodendrocytes extended their exploratory processes in search for axons to myelinate and were able to form their myelin sheaths without delay, within approximately 6 hours after first sheath formation. However, oligodendrocytes in TetTx treated animals established fewer axon-OL contacts in this time period. Of the axon-OL contacts formed in TetTx treated animals, a smaller proportion converted to nascent myelin sheaths, however, this decrease was very subtle. Together, this lead to fewer myelin sheaths >5µm formed per oligodendrocytes in the absence of synaptic vesicle release in comparison to control oligodendrocytes. Once the myelin sheath >5µm was established, the

number of retractions or the formation of small axon-OL contacts <5µm per cell was not different to control oligodendrocytes. However, the number of oligodendrocytes analysed in time-lapse movies was relatively low (control n = 13; TetTx n = 11), and a subtle phenotype in the number of sheath retractions might only reveal itself with higher number of oligodendrocytes analysed (see discussion).

From the timelapse analysis, I can conclude that the reduction of myelin sheath number per oligodendrocyte is caused by a reduction of initially formed myelin sheaths. This reduction in initial myelin sheath formation is partly caused by a decrease in axon-OL contacts and furthermore, a lower conversion rate of axon-OL contacts to stable myelin sheaths. This suggests that the initial myelin sheath formation is at least partly dependent on synaptic vesicle release. The successful conversion of axon-OL contacts to myelin sheaths even in the absence of synaptic vesicle release, albeit reduced, indicates that there might be a second mechanism regulating myelin sheath formation, independently of neuronal activity.

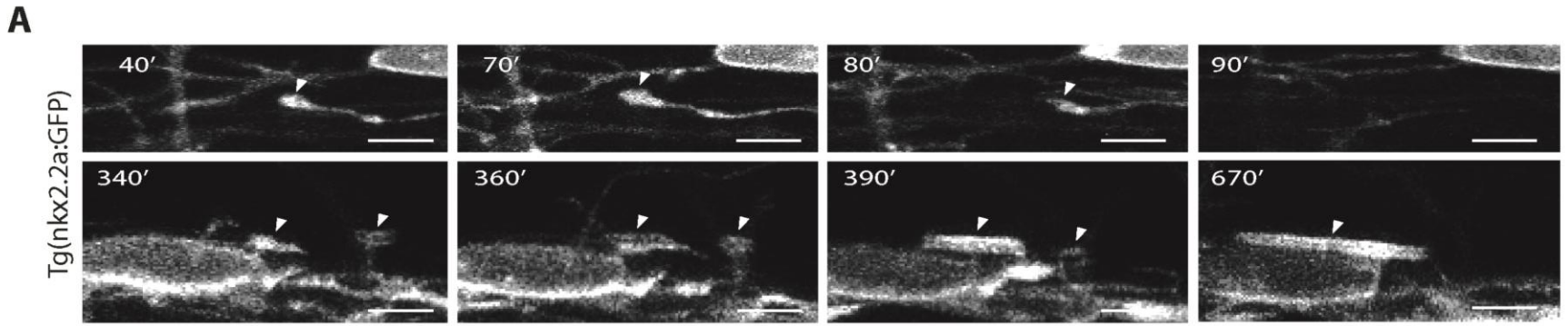

Figure 4.12: Putative axon-glial contact can lead to process retraction or ensheathment. (A) During the initial myelination stage, exploratory cell processes are extended from the oligodendrocyte cell body and form putative axo-glial contacts <5µm. These contacts can lead to the formation of myelin sheaths (bottom, left) or the retraction of the oligodendrocyte process (top and bottom, right) (scale bars = 5um).

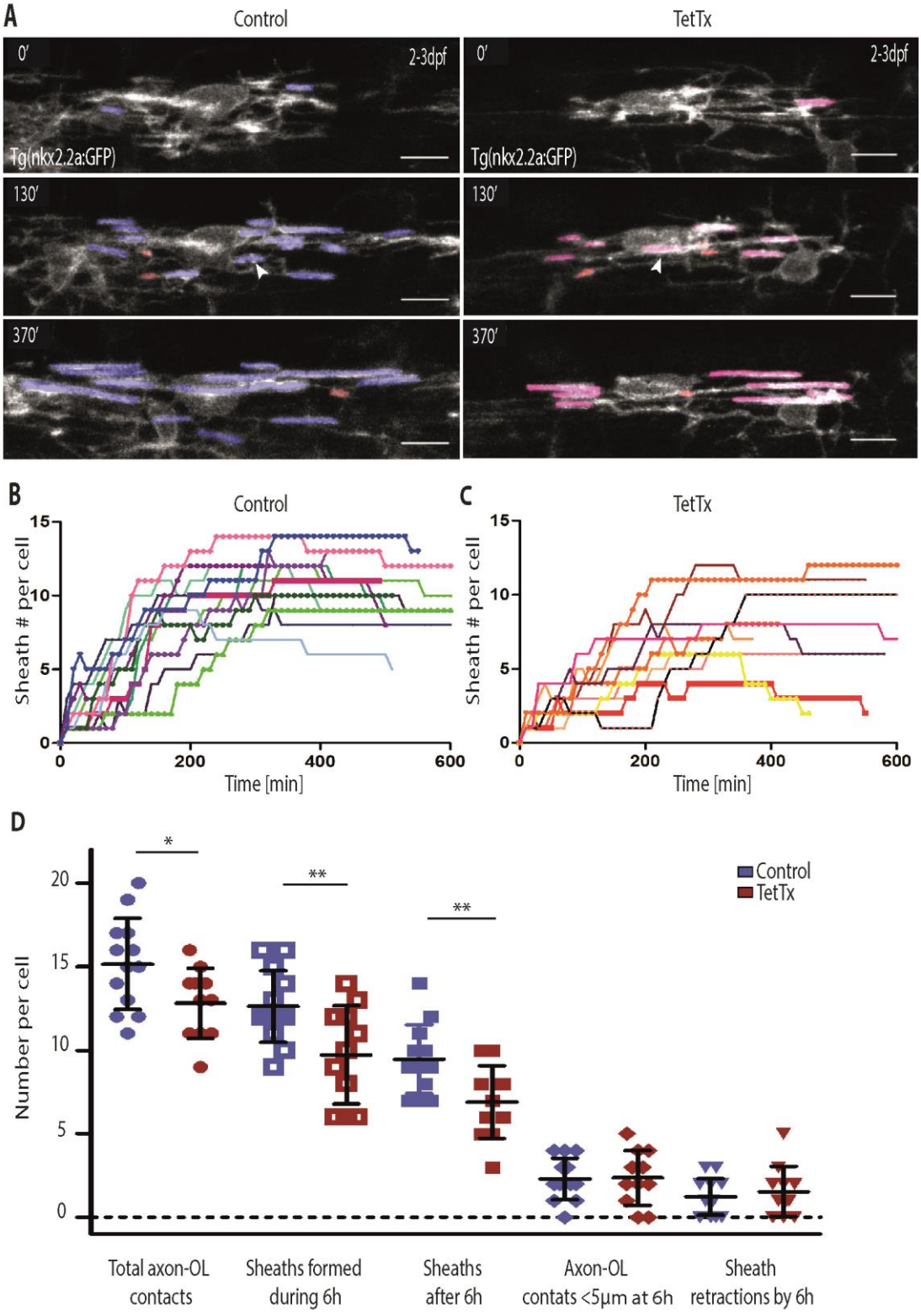
A
Control
TetTx
0'
2-3dpf
Tg(nkx2.2a:GFP)
130'
370'
B
Control
C
TetTx
Sheath # per cell
Time [min]
D
Control
TetTx
Number per cell
*
**
**
Total axon-OL contacts
Sheaths formed during 6h
Sheaths after 6h
Axon-OL contats <5µm at 6h
Sheath retractions by 6h

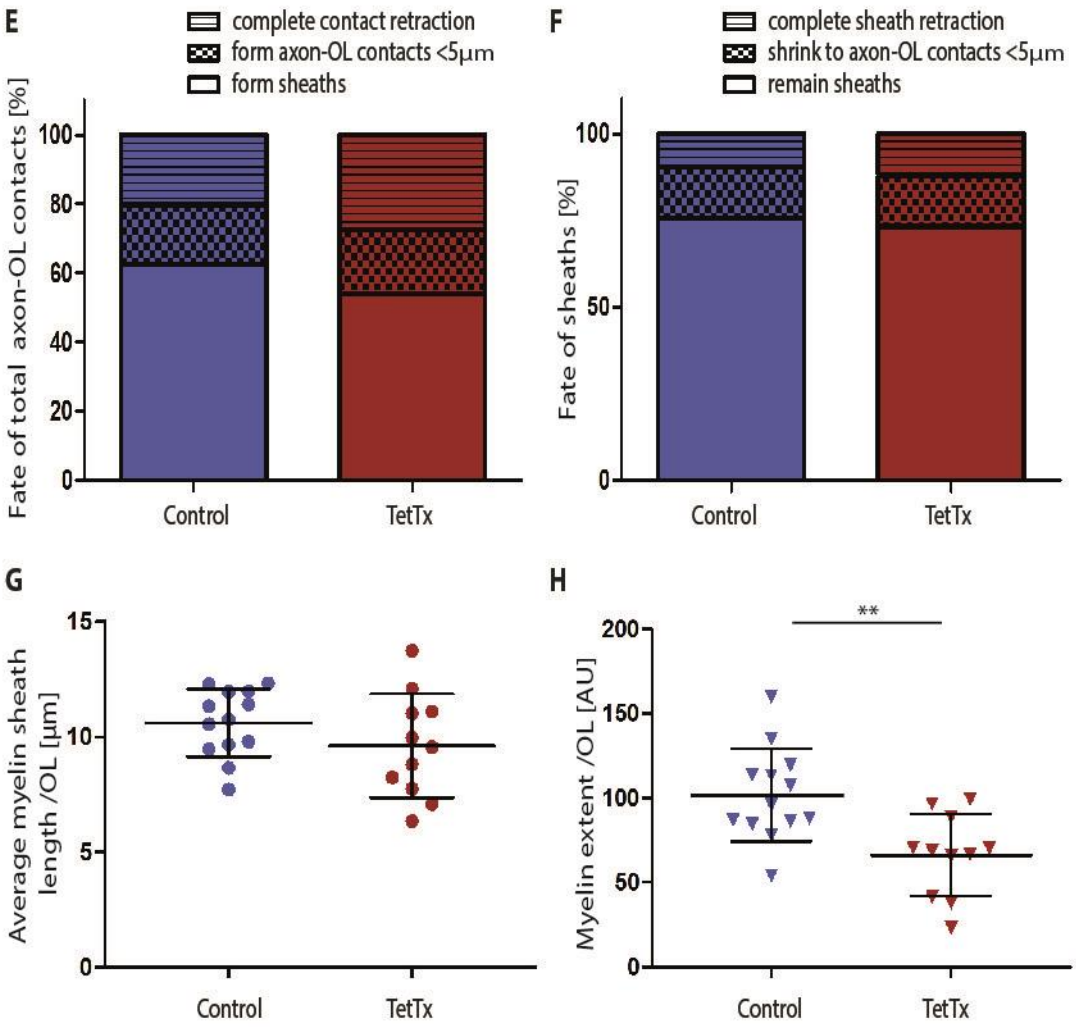

Figure 4.13: Synaptic vesicle release regulates myelin sheath number per oligodendrocyte. (A) Timelapse images of an oligodendrocyte in a control animal (left, scale bar = 10µm) and TetTx treated animal (right, scale bar = 10µm). All axon-oligodendrocyte contacts of this oligodendrocyte that form myelin sheaths are labelled in blue (control) and pink (TetTx). The colours used for the labelling of the myelin sheaths represents the respective oligodendrocytes traces shown in B and C. Axon-OL contacts <5µm that do not convert to stable myelin sheaths >5µm are labelled in red. Myelin sheaths >5µm that were retracted during the movie are indicated by arrows. (B) Myelin sheath number per cell over time. Each trace represents one control oligodendrocyte (oligodendrocyte n = 13, one cell per animal). (C) Myelin sheath number per cell over time. Each trace represents one TetTx oligodendrocyte (oligodendrocyte n = 11, one cell per animal). (D) Quantification of cellular processes during initial myelination, 6 hours after first sheath formation (control n = 13, TetTx n = 11, one cell per animal). The average number of total axon-OL contacts per oligodendrocyte was 15.2 +/- 2.7 in controls and 12.8 +/- 2.1 in TetTx treated animals (student's two-tailed t-test, p= 0.03), the average number of sheaths formed during the 6 hours was 12.6 +/- 2.2 in controls and 9.7 +/- 2.7 in

TetTx treated animals (student's two-tailed t-test p = 0.009), the average number of stable sheaths 6 hours after the first sheath formation was 9.5 +/- 2.0 in controls and 6.9 +/- 2.2 in TetTx treated animals (student's two-tailed t-test p = 0.007) , the average number of axon-OL contacts <5µm 6 hours after first sheath formation was 2.6 +/- 1.9 in controls and 2.4 +/- 1.6 in TetTx treated animals (student's two-tailed t-test p = 0.74) and the average number of sheath retractions during the 6 hours after first sheath formation was 3.1 +/- 1.2 in controls and 3.5 +/- 1.2 in TetTx treated animals (student's two-tailed t-test p = 0.36). (E) Fate of axon-OL contacts 6 hours after first sheath formation. The percentage of axon-OL contacts that turn to myelin sheaths >5µm was 62.4% in controls and 53.9% in TetTx treated animals. The percentage of axon-OL contacts that turn to small axon-oligodendrocyte contacts <5µm was 17.3% in controls and 18.4% in TetTx treated animals. The percentage of axon-OL contacts that retract was 20.3% in controls and 27.7% in TetTx treated animals. (F) Fate of myelin sheaths >5µm within 6 hours after first sheath formation. The percentage of myelin sheaths >5µm that remain stable myelin sheaths >5µm was 83.2% in controls and 71.0% in TetTx treated animals. The percentage of myelin sheaths >5µm that turn to small axon-oligodendrocyte contacts <5µm was 14.6% in controls and 13.1% in TetTx treated animals. The percentage of myelin sheaths >5µm that completely retract was 9.7% in controls and 15.9% in TetTx treated animals. (G) Quantification of the average myelin sheath length 6 hours after first sheath formation per oligodendrocyte. The average sheath length was 10.6 +/- 1.5µm in controls and 9.6 +/- 2.2µm in TetTx treated animals (student's two-tailed t-test p = 0.20). (H) Quantification of the overall myelin extent per oligodendrocyte 6 hours after first sheath formation, measured in the average length of myelin sheath per cell multiplied by the number of myelin sheaths per cell. The average myelin extent was 101.8 +/- 27.3 in controls and 66.5 +/- 24.2 in TetTx treated animals at 4dpf (two-tailed student's t-test p = <0.003).

4.2.7 Individual myelin sheaths show a dynamic range of diverse growth behaviours

In myelinated axons, action potentials propagate through saltatory conduction by passively jumping between nodes of Ranvier (Tasaki, 1982). The longitudinal length of myelin sheaths is therefore an important factor in determining conduction velocity. Another possible role for neuronal activity during myelination is the regulation of longitudinal myelin sheath growth.

If local neurotransmitter release, mediated through synaptic vesicle release, might be regulating myelin sheath growth, individual myelin sheaths could grow with different rates, dependent on the synaptic input they receive from their axons. In order to investigate whether synaptic vesicle release might influence the dynamic growth of myelin sheaths, I first characterized the normal sheath growth behaviour of myelin sheaths in controls in vivo. When comparing myelin sheath growth dynamics

between individual sheaths, all sheaths were analysed for 6 hours after their formation to ensure that each sheath was analysed for the same length of time. For this, I defined a myelin sheath as longitudinal structure >5µm, as described above, but only analysed the myelin sheaths that showed continuous sheath growth during the 6 hours of analysis after first sheath formation.

While some myelin sheaths showed very fast sheath growth, which resulted in a long sheath within 6 hours after ensheathment (Figure 4.14, A and B, colour coded in dark green in A and B), other myelin sheaths made by the same oligodendrocyte exhibited slower growth, which resulted in comparatively shorter sheaths in the same time span (Figure 4.14, C, colour coded in light green in A and C). Other myelin sheaths were formed for only a short time period and then retracted (Figure 4.14, D, colour coded in red in A and D). The differences in growth between the individual myelin sheaths made by individual oligodendrocytes are best illustrated by plotting the myelin sheath length against the time after each sheath was formed (Figure 4.14, A'). The fast growing myelin sheath shows a steeper growth slope (Figure 4.14, B'), compared to the slow growing sheath (Figure 4.14, C') and the retracted sheath (Figure 4.14, D').

The distinct dynamic growth of individual myelin sheaths could indicate an underlying regulation of myelin sheath growth by local axonal signals.

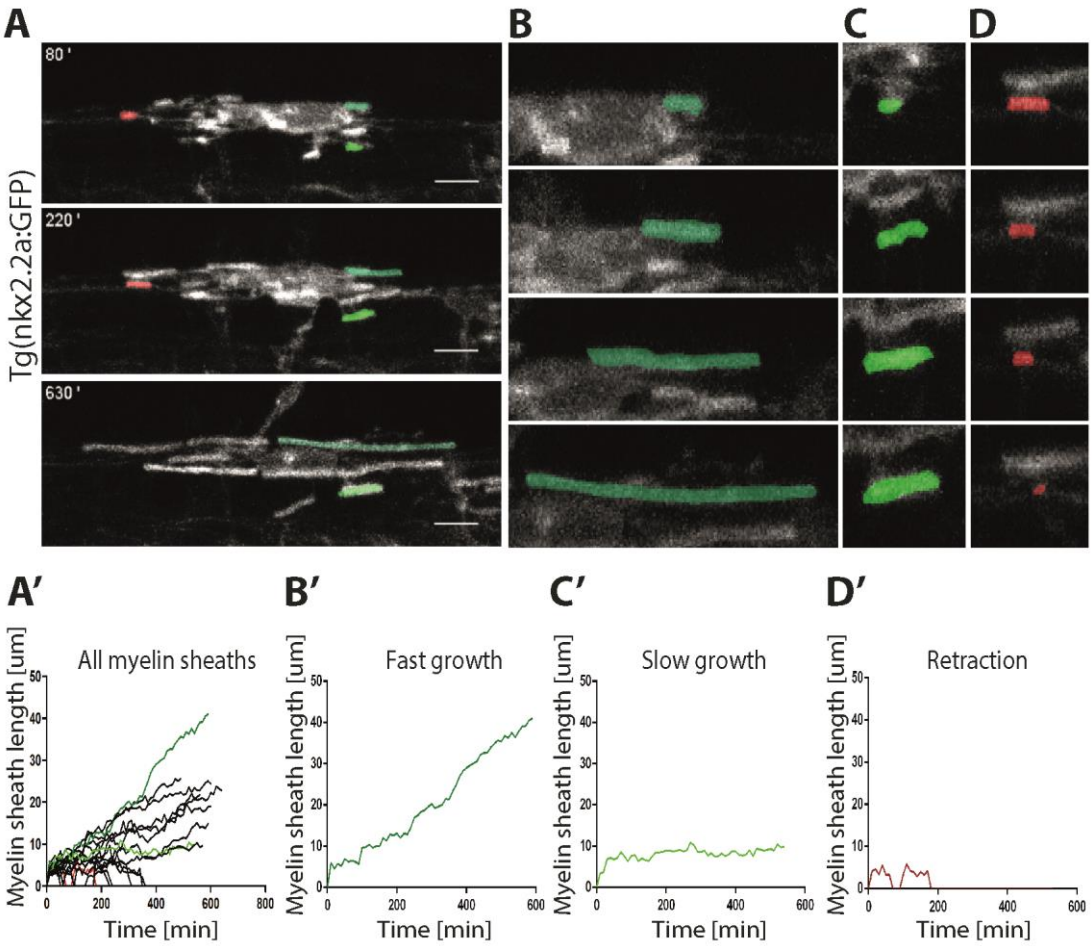

Figure 4.14: Myelin sheaths show dynamic growth. (A) Timelapse analysis reveals the dynamic growth of individual myelin sheaths made by the same oligodendrocyte during the onset of myelination, varying from fast growing sheaths (dark green) (B), slow growing sheath (light green) (C) and sheath retraction (red) (D). (A') Myelin sheath length over time of all myelin sheaths formed by the oligodendrocyte shown in A. (B') The fast growing myelin sheath shows a steeper growth slope, compared to the slow growing sheath (C') and the retracted sheath (D').

4.2.8 The dynamic behaviour of individual myelin sheaths is not exclusively regulated by limited space along axons

One possible explanation for the dynamic differences in the myelin sheath growth of individual myelin sheaths is that there might be neighbouring myelin sheaths along the same axon, not labelled in the Tg(nkx2.2a:GFP), which could limit the sheath growths of individual sheaths in length. One advantage in using the Tg(nkx2.2a:GFP) line to image individual cells is that the line only labels a subset of all OPCs and myelinating oligodendrocytes in the zebrafish spinal cord, allowing precise analysis of a single cell. However, unlabelled myelin sheaths next to the sheaths analysed might confound the analysis of their growth. For example, slow growing myelin sheaths might have a limited amount of free, unmyelinated space along the axon to grow in length, while sheaths exhibiting fast growth might ensheath axons with no neighbouring myelin sheaths nearby and therefore can grow longer in length in the same time frame as the slow growing sheath. If so, the dynamic growth of each myelin sheath could be regulated by the amount of free space along the to be myelinated axon.

In order to test whether the slower sheath growth observed in some of the sheaths in the timelapse movies could be due to limited free space along the axon, I used two transgenic reporter lines, Tg(nkx2.2a:GFP) that labelled individual oligodendrocytes and Tg(sox10:mRFP) that labelled, amongst other cell types, all myelinating oligodendrocytes in the spinal cord. In doing so, I could observe the sheath growth of individual sheaths in the single oligodendrocyte, labelled with GFP and mRFP, in the context of the neighbouring myelin sheaths, labelled with mRFP, formed by the other oligodendrocytes in the spinal cord. I imaged single oligodendrocytes and their neighbouring oligodendrocytes in double transgenic fish once a day before the onset of myelination at 2dpf until the initial myelination period is over at 4dpf. At 2dpf, no myelin sheaths are yet visible in the dorsal spinal cord, suggesting that these cells are still OPCs (Figure 4.15, A, top). By 3dpf, the same cell has differentiated to a myelinating oligodendrocyte and formed myelin sheaths of different lengths (Figure 4.15, A, middle, arrows). Note that while some sheaths vary almost three-fold in length, there are no immediate neighbouring myelin sheaths visible labelled by mRFP expression only, which would limit the sheath growth. By 4dpf, one of the

axons myelinated by that oligodendrocyte, presumably an ascending CoPA axon (see chapter 3) is fully myelinated, potentially limiting the growth rate of the individual myelin sheaths (Figure 4.15, A, bottom, arrows). Other sheaths by the same oligodendrocyte however, are not limited in their length by neighbouring myelin sheaths (Figure 4.15, A, bottom, stars) at this time point. In order to further investigate the influence of neighbouring myelin sheaths as a limiting factor for myelin sheath growth at later time points, I also labelled individual myelinating oligodendrocytes using a mosaic expression of mbp:mCherry-caax in a Tg(mbp:GFP-caax) background. Using this set-up, I can illustrate the amount of free space along the myelinated axons at later time points during myelination (Figure 4.15, B). While the axons in the dorsal tract are fully myelinated by 3dpf, there are still unmyelinated areas next to the myelin sheaths that ensheath an ascending axons, presumably belonging to a CiD interneurons (see chapter 3) (Figure 4.15, B, top, arrows).

By 4dpf, the space along the putative CiD axon is slowly filled by myelin sheaths (Figure 4.15, B, middle, arrows), while at 5dpf there are no visible gaps along what are likely the individual myelinated axons (Figure 4.15, B, bottom, arrows).

Also, note the myelin sheaths, which are completely retracted over multiple days (Figure 4.15, B, stars). The time course data suggests that at the onset of myelination in zebrafish between 2-3dpf, there are typically few neighbouring myelin sheaths in sufficient proximity to significantly limit longitudinal myelin sheath growth. Between 3-4dpf, more myelin sheath are formed and some axons such as the CoPA axon shown (Figure 4.15, A) can be fully myelinated by 4dpf, while other axons are not fully myelinated until 5dpf (Figure 4.15, B). Free axonal space and neighbouring myelin sheaths will more likely influence the myelin sheath growth rate of individual sheaths along such axons. However, the time course data between 2dpf and 3dpf indicates that the majority myelin sheaths are not restricted by neighbouring myelin sheaths (Figure 4.15, A). Therefore, I restricted my timelapse analysis to oligodendrocytes at 2-3dpf in anterior regions, or 3-4dpf in posterior regions, where the onset of myelination is delayed approximately 24hours in comparison to the anterior spinal cord due to the anterior-posterior gradient in myelination (Schwab and

Schnell, 1989). Thus, we can conclude that neighbouring myelin sheaths are not a limitation to dynamic sheath growth at these time points.

This indicates that the differences in dynamic myelin sheath growth could be regulated by local axonal signals, which promote the fast growth of individual myelin sheaths. Myelin sheaths growing independently of neuronal activity might be limited to a basal, slow growth, while myelin sheaths that receive additional axonal signal exhibit faster growth.

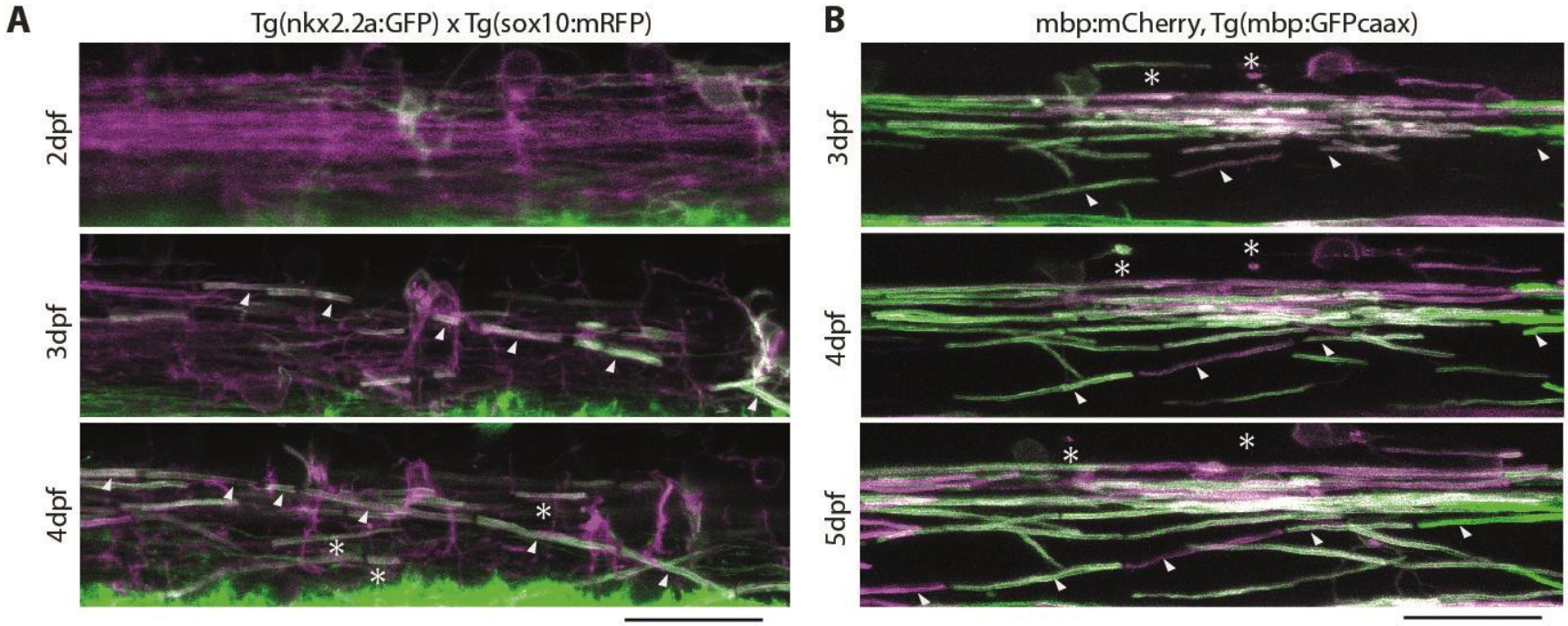

Figure 4.15: Myelination occurs during multiple days. (A) Labelling of oligodendrocytes from precursor stages to myelinating oligodendrocytes with Tg(nkx2.2a:GFP) in a Tg(sox10:mRFP) background shows that myelin sheaths are formed from 2dpf. The axons of neurons fated to be myelinated are ensheathed by myelin sheaths between 2 to 3 days (scale bar = 15um). (B) Labelling of individual myelinating oligodendrocytes (Tg(mbp:mCherry-caax)) in a Tg(mbp:GFP-caax) background shows robust myelin sheath formation at 3dpf and occasionally complete sheath retraction over a multiple days (scale bar = 15um).

4.2.9 *Reduction of synaptic vesicle release changes the dynamic growth of myelin sheaths*

Individual myelin sheaths in control animals showed a range of different growth rates during initial myelination, suggesting that local axonal signals promote the fast growth of individual sheaths, while slow growing myelin sheaths might receive less or no axonal signal. In order to investigate whether synaptic vesicle release might regulate fast growth in individual myelin sheaths, we observed the dynamic growth of myelin sheaths during initial myelination in TetTx treated animals using the time lapse settings described above.

During the first 6 hours after each myelin sheath was formed, oligodendrocytes in controls showed a variety of sheath lengths and growth speeds (Figure 4.16, A, left), as described above (Figure 4.14). The myelin sheath colour coded in light blue exhibits slow growth while the myelin sheath colour coded in light green shows fast growth. The axon-OL contacts colour coded in red never grew into a myelin sheath but remained as a small axon-OL <5µm and were not retracted during the 6 hours of analysis.

The majority of oligodendrocytes in TetTx treated animals analysed, however, only exhibited myelin sheaths with slow growth speed (Figure 4.16, A, right). One of the myelin sheaths exhibiting slow growth in this oligodendrocyte is colour coded in pink, the axon-OL contact colour coded in red never grew into a myelin sheath but remained as a small axon-OL <5µm and were not retracted during the 6 hours of analysis.

The difference in myelin sheath behaviour between controls and TetTx treated animals is best illustrated by plotting the length of each myelin sheath per oligodendrocyte against time (Figure 4.16, B and C, the line colour in plots corresponds to the colour code in A). While the majority of myelin sheaths in the control oligodendrocyte grow at a slow rate, some myelin sheaths show a steep growth slope representing fast sheath growth (Figure 4.16, B). The myelin sheaths in the oligodendrocyte in the TetTx treated animal only showed low growth slopes (Figure 4.16, C). On average, myelin sheaths in controls grew significantly faster with an average growth rate of 1.3µm/h, while myelin sheaths in TetTx treated animals grew with an average growth rate of 0.93µm/h (control n = 13, TetTx n =

11; student's two-tailed t-test p = 0.0006) (Figure 4.16, D). In order to quantify the reduction in fast growing myelin sheaths in TetTx, we defined fast sheath growth as 2µm/h or above, while slow sheath growth was defined as below 2µm/h. With this definition for fast and slow sheath growth, the majority of all sheaths per oligodendrocyte in both controls and TetTx treated animals grew at a slow speed (<2µm/h), with 79.3 +/- 19.3% in controls and 90 +/- 18.8% in TetTx treated animals. However, 20.7 +/- 19.3% of all sheaths per oligodendrocyte in control animals exhibited fast growth (22 out of 103 sheaths analysed), while only 9.9 +/- 18.8% of all sheaths per oligodendrocyte in TetTx treated animals exhibit fast growth (4 sheaths out of 59 sheaths analysed) (Figure 4.16, E). On a cellular level, 10 out of 13 oligodendrocytes used in this analysis had at least one fast growing myelin sheath per oligodendrocyte, whereas only 4 out of 11 oligodendrocytes in TetTx treated animals had at least one fast growing myelin sheath per oligodendrocyte.

The myelin sheaths of every oligodendrocyte recorded during the timelapse imaging of control and TetTx treated animals showed a wide range of different growth rates.

To give an overview of the differences between myelin sheath growth in controls and TetTx treated animals, I plotted the length of each myelin sheath per oligodendrocyte over time for all oligodendrocytes used in the analysis (controls n = 13, Figure 4.17, A, TetTx n = 11, Figure 4.17, B). Comparing the sheath length plotted again time graphs of oligodendrocytes in controls and TetTx treated animals visualizes that the majority of myelin sheaths in both control and TetTx treated animals grows at a slow, basal rate. However, the majority of cells in controls have one or more myelin sheaths growing at a steep slope, representing fast growth, while only few cells in TetTx treated animals show myelin sheaths growing at a steep slope.

The different growth rates in myelin sheaths formed by a control oligodendrocyte suggest that local axonal signals might regulate the dynamic growth of individual myelin sheaths. The reduction in fast growing myelin sheaths in TetTx treated animals further indicates that synaptic vesicle release can promote fast myelin sheath growth. Together, these findings imply that myelin sheaths growing at a slow rate can do so in an activity independent mechanism in the absence of synaptic vesicle release, whereas fast myelin sheath growth is regulated by the addition of local axonal signals released by synaptic vesicles.

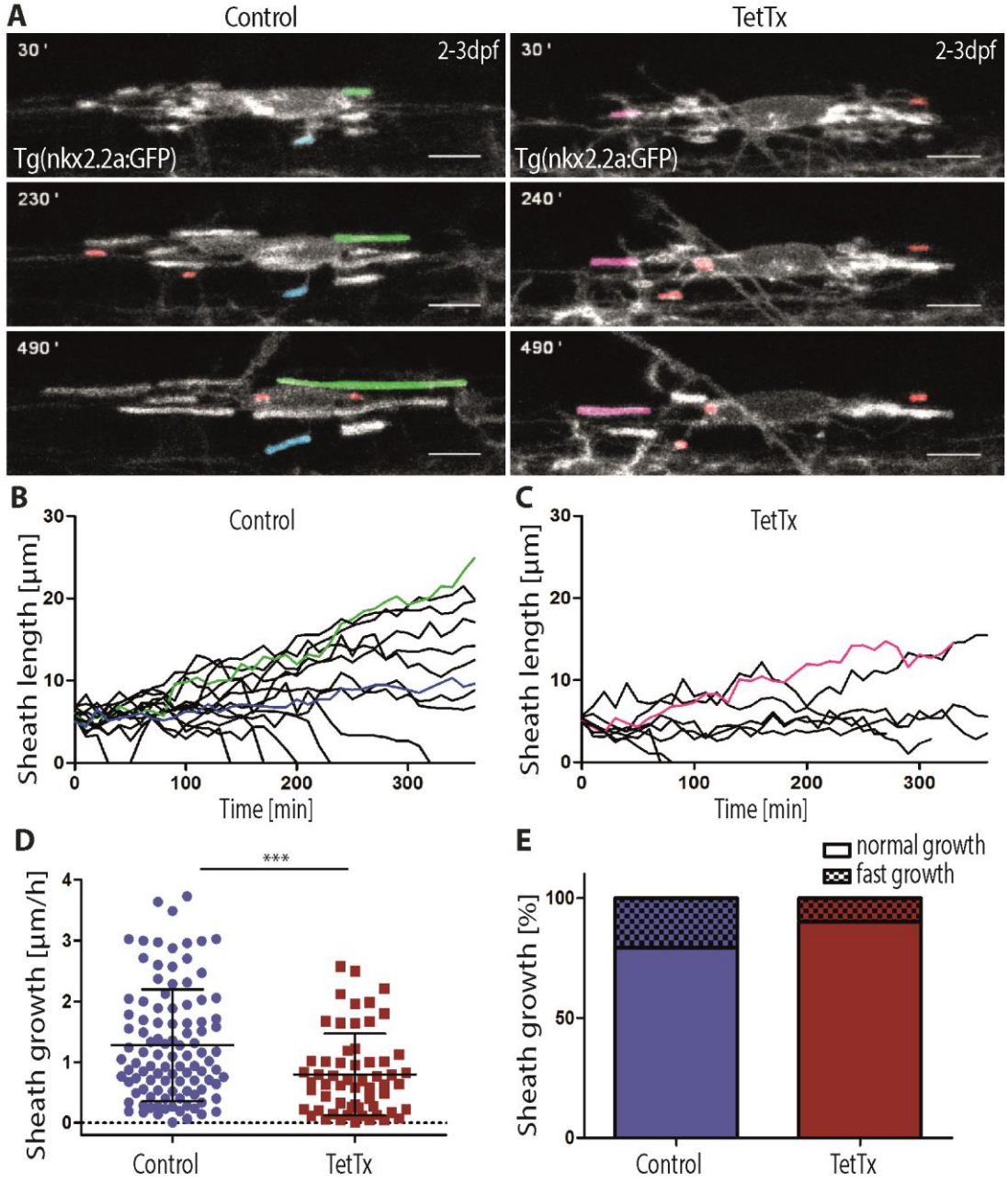

Figure 4.16: Reduction of synaptic vesicle release changes the dynamic growth of myelin sheaths

(A) Time-lapse images of an oligodendrocyte in a control (left) and TetTx treated animal (right) (Scale bar=10µm). Colour coded myelin sheaths represent the traces in B and C. Axon-OL contacts <5µm are colour coded in red. (B) Myelin sheath length plotted over time of all myelin sheaths >5µm formed by the control oligodendrocyte shown in A. (C) Myelin sheath length plotted over time of all myelin sheaths >5µm formed by the TetTx oligodendrocyte shown in A. (D) Myelin sheath growth of individual myelin sheaths within 6 hours after each sheath was formed in controls and TetTx treated animals. The average myelin sheath growth rate was 1.3µm/h in controls and 0.93µm/h in TetTx

treated animals (control n = 13, TetTx n = 11; student's two-tailed t-test p = 0.0006). (E) Percentage of fast growing (>2µm/h) and slow growing myelin sheaths (<2µm/h) in controls and TetTx treated animals. The percentage of myelin sheath that grew at a slow speed (<2µm/h) was 79.3 +/- 19.3% in controls and 90 +/- 18.8% in TetTx treated animals. The percentage of myelin sheath that grew at a fast speed (>2µm/h) was 20.7 +/- 19.3% in controls and 9.9 +/- 18.8% in TetTx treated animals.
Retracting myelin sheaths and myelin sheaths that were <5µm after 6 hours of individual sheath growth were excluded from analysis in D and E.

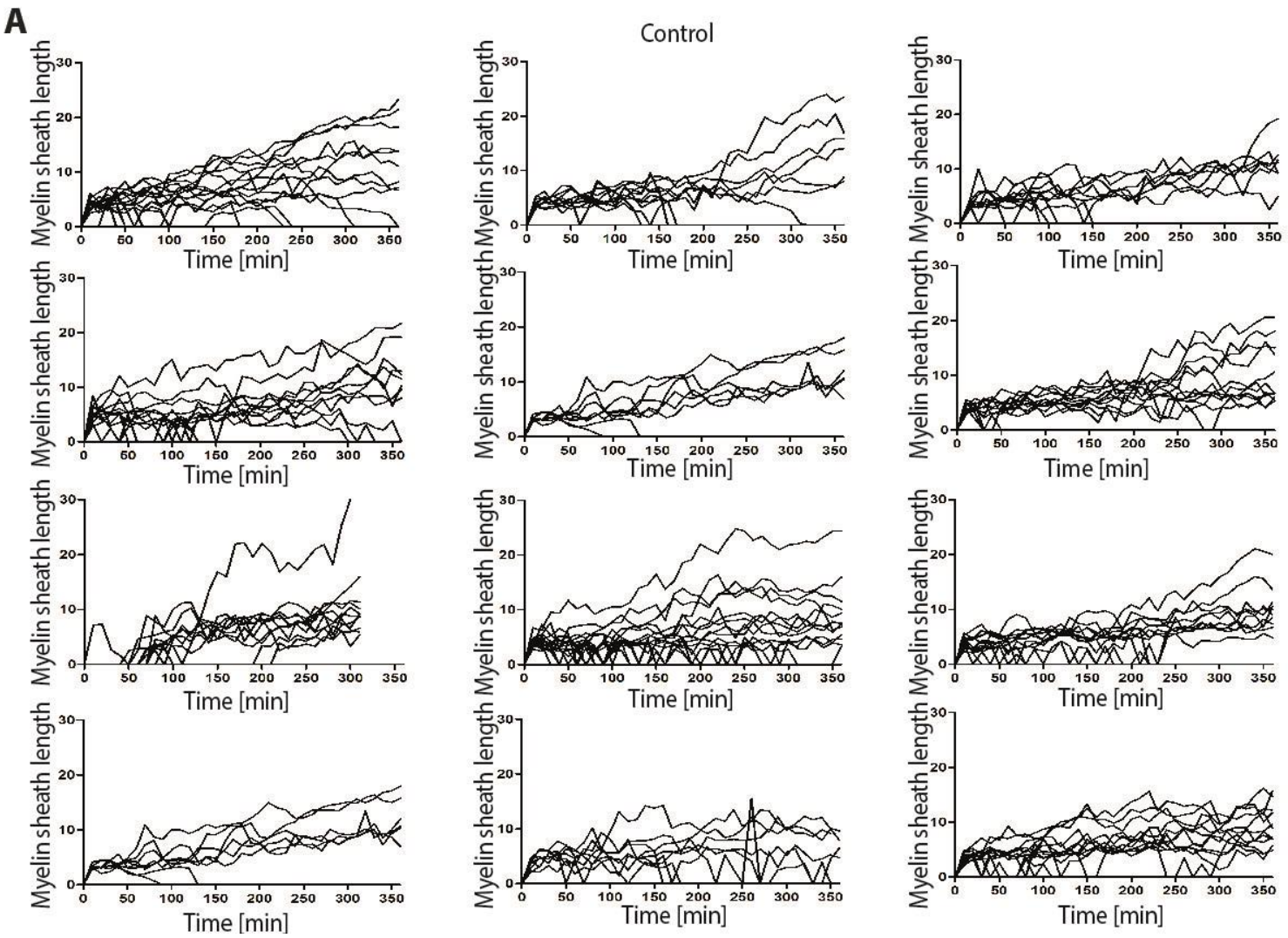
A
Control
Myelin sheath length
Time [min]
0
10
20
30
0
50
100
150
200
250
300
350

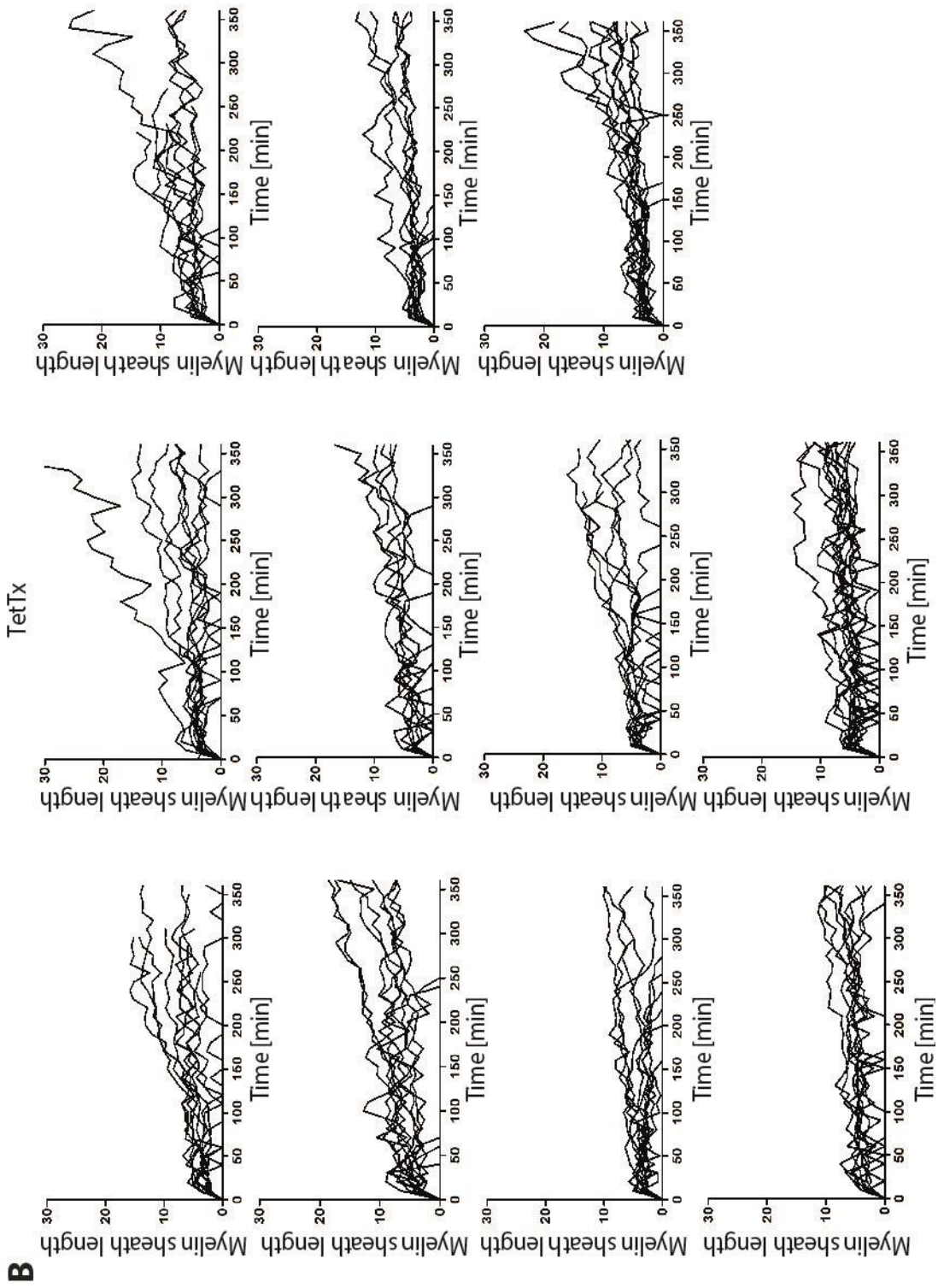

Figure 4.17: Myelin sheath growth over time traces. (A) Myelin sheath length over time in control animals. (B) Myelin sheath length over time traces in TetTx treated animals. Each graph represents one oligodendrocyte; each trace represents one myelin sheath.

4.2.9 Conclusion

Overall, in the absence of synaptic vesicle release, we found a reduction of 42% in the number of myelinated axons at 4dpf, which is accounted for by a 10% decrease in the number of myelinating oligodendrocytes and a 30% reduction of myelin sheath formed per oligodendrocyte. This 30% reduction of myelin sheath per oligodendrocyte stems from a decreased capability of oligodendrocytes to form a normal myelin sheath number during initial myelination. My preliminary timelapse analysis revealed that the decrease in myelin sheaths initially formed per oligodendrocyte in TetTx treated animals is partly caused by a reduction in axon-OL contacts prior to ensheathment and partly by a decrease in the number of axon-OL contacts that transform into myelin sheaths. Synaptic vesicle release is therefore important for the regulation of myelin sheath number per oligodendrocyte. Furthermore, individual myelin sheaths formed by the same oligodendrocyte showed a wide range of different growth dynamics, which was reduced to a more basal, slow growth in the absence of synaptic transmission (Figure 4.18).

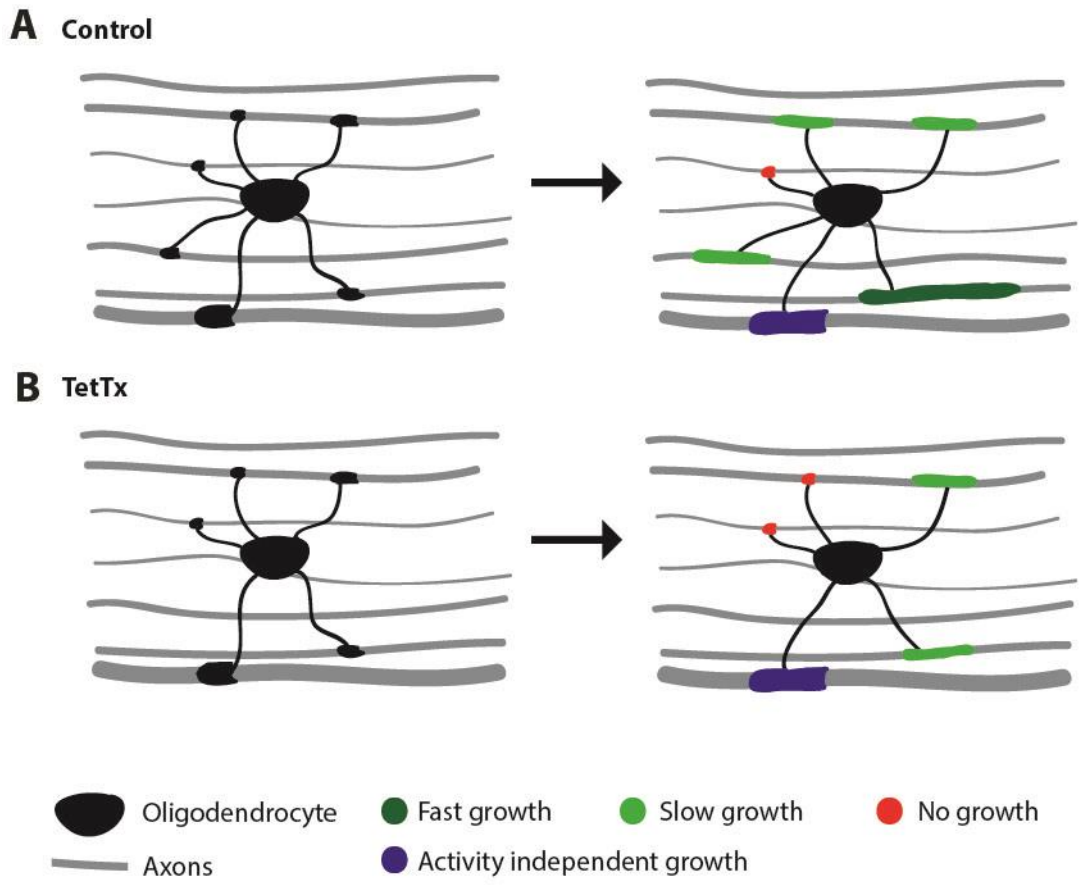

Figure 4.18: Model of synaptic vesicle release regulated myelination. (A) In control situations with normal synaptic vesicle release the majority of initial axon-OL contacts per oligodendrocyte (short black structures on left) grow into myelin sheaths on axon of large (blue) and intermediate calibre (green), above a certain size (approximately 0.3µm). Most myelin sheaths grow with a basal, slow speed (light green), while other can grow more quickly (dark green) up to three times the basal growth. **(**B) In absence of synaptic vesicle release the total number of axon-OL contacts is reduced. However, the myelination of the largest calibre axons is not severely affected (blue), while the myelination of intermediate calibre axons is reduced (red) and fewer myelin sheaths are formed per oligodendrocyte. Furthermore, the majority of myelin sheaths grow at a slow, uniform rate in the absence of synaptic vesicle release (light green).

4.3 Discussion

TetTx as a tool to inhibit synaptic vesicle release

Neuronal activity has been implicated in regulating oligodendrocyte proliferation and myelination in the past (for review see Barres and Raff, 1994, Fields, 2005, Zalc and Fields, 2000). The cellular mechanisms behind this process, however, have not been elucidated to date and it is unclear whether axonal signals released by synaptic vesicle transmission can induce myelinating oligodendrocytes to form myelin sheaths. In order to investigate how neuronal activity could influence myelinated axon formation, I reduced axonal synaptic vesicle release during initial myelination by TetTx expression.

I demonstrated that TetTx expression is sufficient to reduce synaptic transmission in the zebrafish spinal cord by patch-clamp recordings of the membrane potential of individual spinal cord neurons after extracellular stimulation in vivo. Even though previous studies used TetTx expression to inhibit synaptic vesicle release (Fredj et al., 2010), they did not specifically test the required TetTx concentration or examine the toxin effect by electrophysiology. While some of the patched TetTx expressing neurons showed a small response to the extracellular stimulation, none of them showed the typical fictive swimming behavior normally seen after extracellular stimulation in this experimental set-up. Furthermore, the TetTx treatment did not appear to cause developmental defects in zebrafish between injection of the TetTx mRNA at the one cell stage and 4dpf, apart from the development of heart edemas at 4dpf. Neuronal loss or a delay in the onset of myelination due to the TetTx treatment was also not detected. This indicates that the TetTx expression does not have an adverse influence on zebrafish development itself, which could have led to a falsely positive effect of the lack of neuronal activity on myelination. Overall, TetTx expression appears to be a solid technique to inhibit synaptic vesicle release and to ultimately reduce axonal electrical activity, preferable to TTX application due to the lack of specificity of pharmacological treatments, which made some of the previous in vitro and in vivo experiments applying TTX to reduce neuronal electrical activity questionable. However, the global TetTx expression is not without its drawbacks. TetTx inhibits synaptic vesicle release through cleavage of the synaptic vesicle protein VAMP-2 / synaptobrevin (Schiavo et al., 1992; Link etal., 1992; Pellizzari et

al., 1999; for review see Schiavo et al., 2000), which hinders the exocytosis of the synaptic vesicle content and effectively inhibits the release of neurotransmitters (Gerst, 1999; Gaisano, 2000; Mochida, 1989).

In the single neuron analysis, the axon morphology and calibre of RS and CiD neurons in TetTx treated animals was not different to control neurons, and there was no decrease in the number of axons with a calibre between 0.3 and 1.9µm quantified in the electron micrographs of TetTx treated animals, indicating that the TetTx treatment did not have adverse effects on neuronal development and morphology. In accordance with that, neither overexpression of VAMP2 in vitro (Zhou et al., 2000), nor TetTx mediated cleavage of VAMP2 in vitro (Harms and Graigs, 2005; Alberts et al., 2006) and in vivo (Fredj et al., 2010) has led to increase or impairment of axon size and morphology, indicating that VAMP2 activity has no influence on neuronal morphology.

However, TetTx has also been shown to cleave VAMP3 / cellubrevin (McMahon et al., 1993; Schiavo et al., 2000), which is a vesicle protein involved in membrane trafficking, the transport of signaling molecules and membrane proteins in membrane vesicles from the Golgi body to their secretion side within eukaryotic cells (Jan and Scheller, 2006; as reviewed in Cai et al., 2007). Cleavage of VAMP3 has been shown to affect integrin-dependent cell adhesion and cell migration in epithelial cells (Proux-Gillardeaux et al., 2005). TetTx expression might therefore affect the correct transport and integration of cell adhesion molecules and other signaling molecules that might be involved in axon-oligodendrocyte interactions in the axonal membrane. The recorded reduction in myelin might therefore be due to a decrease in axonal adhesion or signaling molecules presented at the axonal membrane through VAMP3 mediated membrane vesicle release. However, membrane trafficking during neurite outgrowth in hippocampal and cortical neurons in vitro has been shown to be mediated by the TetTx insensitive VAMP7 and was therefore unimpaired by TetTx expression (Alberts et al., 2006). Furthermore, axon arborization, including the complexity and stabilization of axon branches, was unimpaired in the tectum of zebrafish larvae with global TetTx expression (Fredj et al., 2010). Together these data suggest that membrane trafficking and cellular processes involving cell-adhesion molecules are unimpaired in TetTx treated animals.

Another aspect of the global TetTx treatment in this thesis that should be considered is that the TetTx expression is not exclusively restricted to neurons and other cell types, such as oligodendrocytes, also express the toxin.

If the myelin inducing effect of neuronal activity is indeed mediated through astrocytes responding to axonal ATP release as it has been suggested (Ishibashi et al., 2006), the astrocytes might be affected by the TetTx expression as VAMP2 and VAMP3 are expressed and functional in hippocampal astrocytes (Crippa et al., 2006; Bowser and Khakh, 2007).

Furthermore, VAMP2 and VAMP3 are expressed in oligodendrocytes (Madison et al., 199; Feldmann et al., 2009). Although the exact function for VAMP2 expression in oligodendrocytes is unknown (Madison et al. 1999), VAMP3 is presumed to take part in oligodendorcyte membrane trafficking during myelination, based on its upregulation during oligodendrocyte maturation and differentiation to a myelinating oligodendrocyte (Feldmann et al., 2009). Proteolipid protein (PLP), myelin-associated glycoprotein (MAG) and myelin-oligodendrocyte glycoprotein (MOG) have been shown to be co-localized with VAMP3 and VAMP7 positive endocytic vesicles (Krämer et al., 2001; Trajkovic et al., 2006; Winterstein et al., 2008). Genetic ablation of VAMP3 and VAMP7 in oligodendrocyte-neuron co-cultures has been shown to interfere with PLP transport to the myelin membrane (Feldmann et al., 2011). Together these data suggest that these myelin proteins are recycled through membrane trafficking via endocytic compartments and thereby contribute to myelin biogenesis, whereby VAMP3 mediates the membrane fusion of vesicles originating from the Golgi body to the oligodendrocyte plasma membrane, while VAMP7 mediates the transport of membrane proteins to the myelin membrane (Feldmann et al., 2011; as reviewed in White and Kramer-Albers, 2014). In vivo, however, mice deficient of VAMP3 show no myelin impairment as quantified by immuno-staining and western-blot analysis of myelin proteins, and only VAMP7 deficient mice showed a small decrease in the expression of PLP, MBP and MOG (Feldmann et al., 2011), suggesting that the function of VAMP3 in oligodendrocyte membrane trafficking can be compensated for and is not required for myelin biogenesis in vivo.

Disruption of VAMP2 function in purified oligodendrocytes in vitro, however, has been suggested to cause impaired oligodendrocyte morphology with smaller

processes and reduced branching (Sloane and Vartanian, 2007). In order to exclude the possibility that disruption of VAMP2 in oligodendrocytes in vivo would have the same effect in oligodendrocytes in TetTx treated animals, Dr. Marion Baraban (Lyons group) created genetic chimeras and transplanted oligodendrocytes from TetTx treated animals to control animals and from control animals into TetTx treated animals. TetTx expressing oligodendrocytes in a control environment with normal synaptic vesicle release, generated a normal number of myelin sheaths at 4dpf (an average of 11.4 sheaths per cell compared to the 11.7 sheath per cell I measured in controls), while control oligodendrocytes in the TetTx treated animals with absent synaptic vesicle release generated a reduced number of myelin sheaths at 4dpf (an average of 8.5 sheaths per cell compared to the 8.2 sheaths per cell I measured in TetTx treated animals). These findings indicate that the myelin phenotype in the TetTx treated animals does not result from the TetTx expression in oligodendrocyte.

Overall, I could show that global TetTx expression can successfully inhibit synaptic transmission without causing developmental defects in neuronal morphology and a delay in the onset of myelination. Furthermore, the transplant experiments performed by Dr. Marion Baraban demonstrated that the myelin phenotype in absence of synaptic vesicle release is caused independently of TetTx expression in oligodendrocytes.

Synaptic vesicle release as modulatory mechanism to regulate the extent of myelination

Increased neuronal activity has been shown to induce myelination in vivo (Gibson et al., 2014), while reduction of neuronal activity through social deprivation has been shown to lead to myelin defects (Liu et al., 2012; Makinodan et al., 2012). However, social isolation only indirectly implies a reduction in neuronal activity and cannot clarify to what extent neuronal activity had been reduced and what cellular aspects are involved during the neuronal activity dependent myelination.

Using TetTx, I demonstrated that reducing synaptic vesicle release in vivo leads to a reduction of myelinated axons in the zebrafish spinal cord. Using electron micrographs of transverse sections through the spinal cord at somite area 15, I quantified the number of myelinated axons and unmyelinated axons with an axon

calibre large enough to be myelinated. The smallest myelinated axons I found in the electron micrographs in the spinal cord had an axon calibre of approximately 0.3µm and subsequently, all axons with a calibre of 0.3µm or above were measured. The electron micrographs show a 40% reduction in myelinated axons per hemi spinal cord in TetTx treated animals compared to controls. This demonstrates that the absence of synaptic transmission affects the myelination of CNS axons in vivo and is in accordance with previous studies indicating a correlation between neuronal activity and myelination (Demerens et al., 1996; Wake et al., 2011; Liu et al., 2013; Makinodan et al., 2013; Gibson et al., 2014). Correspondingly, the number of unmyelinated axons increased by approximately 40% in the TetTx treated animals, indicating that the reduction of myelinated axons is not due to loss of axons with appropriate axon calibre. The average axon calibre of TetTx axons is, in fact, not affected by the TetTx treatment. The proportional distribution of myelinated as well as unmyelinated axons with an axon calibre above 0.3µm in TetTx treated animals is very similar to the controls, both exhibiting a Gaussian distribution from 0.3µm to 1.9µm. The Mauthner axon was excluded from the axon calibre measurements as it is a multifold larger than the other axons in the zebrafish spinal cord.

The 40% reduction in myelinated axons in TetTx treated animals indicates that synaptic activity influences myelination.

However, oligodendrocytes differentiated and formed robust myelin, even in the absence of synaptic vesicle release in the TetTx treated animals. This is very interesting, as previous in vitro findings showed that oligodendrocytes can differentiate (Knapp et al., 1987) and initiate myelination without axonal signaling per se by myelinating paraformaldehyde fixed axons (Rosenberg et al., 2008). Cultured oligodendrocytes even have been shown to form myelin around synthetic axon-like polystyrene fibres in complete absence of axonal signals (Lee et al., 2012). Together, these results indicate that neuronal activity is not required for CNS myelination per se and that there must be an activity independent mechanism regulating myelination. However, given the 40% reduction in myelinated axon number in absence of synaptic vesicle release indicates that neuronal activity does influence myelination in vivo. From an evolutionary perspective, multiple mechanisms regulating myelination would be the best strategy to ensure functional

central nervous system function. It is conceivable that there is more than one mechanism regulating myelination and that there is an activity dependent and an activity independent mode of myelination. It is therefore possible that neuronal activity has a modulatory rather than an absolute role in myelination and is regulating the extent of CNS myelination.

On a cellular level, a modulatory role for neuronal activity during myelination might be the regulation of the myelin extent formed per oligodendrocyte. Myelin extent, the average sheath length multiplied by the sheath number per oligodendrocyte as a proxy of the total amount of myelin, is generally very variable in oligodendrocytes. However, a recent study has demonstrated that oligodendrocytes are able to generate additional myelin sheaths in response to supernumery large calibre axons without reducing the sheath length of their other myelin sheaths (Almeida et al., 2011). In this case, the axonal signals provided by the supernumery axons resulted in the increase of myelin extent per oligodendrocyte. In the absence of synaptic vesicle release, the myelin extent per oligodendrocyte was significantly reduced. This was the case during initial myelination as well as after the initial myelination at 3dpf and 4dpf. Together, these observations suggest that the myelin extent that each oligodendrocyte produces might be influenced by axonal input through synaptic vesicle release.

Alternatively, it is also possible that only the myelination of particular circuits is dependent on neuronal activity. Those neuronal circuits might be required to adapt and coordinate their signaling speeds more than other circuits and therefore increase their plasticity through neuronal activity dependent myelin changes. Further analysis is needed to determine whether only the myelination of particular circuits can be regulated by neuronal activity or whether neuronal activity is a general mechanism to regulate the extent of overall myelination. The single neuron analysis, in which I investigated the myelination of RS and CiD neurons in TetTx treated animals, revealed that myelin ensheathment is reduced along axons of both neuron types in TetTx treated animals. This suggests that the extent of myelination is generally affected in all neurons rather than only in a subset of specific neurons, which are not myelinated at all, as I will discuss in more detail below. Nonetheless, it would be interesting to map the circuitry of the axons whose myelination is affected in the

absence of neuronal activity in order to further elucidate the myelin dependent mechanisms behind adaptive changes in neuronal circuits. Future experiments should inhibit synaptic vesicle release specifically in a subset of neurons, e.g. a known circuitry network such as the escape circuit in zebrafish (Kimmel et al., 1974; as reviewed in Eaton et al., 2001), perhaps using the expression of a plasmid containing UAS:TetTx-GFP, and characterize the onset and myelin ensheathment of these axons.

Synaptic vesicle release should also be inhibited in different CNS regions and other model organisms in order to exclude the possibility that the reduction in myelin extent seen in the absence of synaptic vesicle release in the spinal cord is region specific or different in other vertebrates.

Axon calibre as a regulatory mechanism influencing myelination

In the PNS, myelination is strictly correlated to axon calibre. Axons of a calibre above approximately 1μm^2 are myelinated, while smaller calibre axons remain unmyelinated (reviewed in Sherman and Brophy, 2005). Interestingly, myelination in the PNS can be experimentally induced when axon calibre is enlarged in axons which normally are not myelinated (Voyvodic, 1989). In the CNS, as I show here, small axons with a calibre as small as 0.3µm can be myelinated. Interestingly, I found that while small calibre axons can be myelinated in the CNS, the majority of myelinated axons were of relatively large calibre.

Target size alone has been shown to play a role in the initiation of myelination in in vitro experiments in which inert polystyrene fibres were ensheathed by oligodendrocytes if they had a certain calibre (Lee et al., 2012). If the calibre of the inert fibres was above 0.4µm, they were readily ensheathed, while fibres of a smaller calibre never were. In an elegant in vivo experiment utilizing supernumery large calibre axons in the CNS, Almeida et al. showed that the largest calibre axon, the Mauthner axon is always myelinated first. Furthermore, these experiments showed that individual oligodendrocytes are plastic and can produce more myelin sheaths than normal to myelinate the supernumery large calibre axons, indicating that large calibre axons can regulate oligodendrocyte behavior (Almeida et al., 2011).

The myelination of large calibre axons > 0.9µm was less severely affected by the inhibition of synaptic vesicle release than the myelination of axons with small to intermediate calibre between 0.3-0.9µm. This indicates that the reduction of synaptic vesicle release has more impact in the myelination of smaller calibre axons as a higher percentage of axons with large calibre axons were still myelinated in the TetTx treated animals and the largest calibre axons, such as the Mauthner axon, were always myelinated, even in the absence of synaptic transmission. This is another indication that there might be an activity independent mechanism regulating myelination in addition to the activity dependent mechanism.

The myelin ensheathment independent of axonal synaptic vesicles might be intrinsic to oligodendrocytes. It is possible, that the cellular cytoskeleton composition within oligodendrocyte processes facilitates the movement around axons above a certain calibre size more easily than the ensheathment of small calibre axons, which might require a less rigid cytoskeleton composition. Interestingly, tyrosine kinase Fyn has been shown to regulate the stability of the cellular cytoskeleton (Kraemer-Albers & White, 2011) and a loss of function of the non-receptor tyrosine kinase Fyn leads to hypomyelination in small calibre axons, but not in axons of larger calibre (Umemori et al. 1994), indicating that the myelination of smaller axons might require more cytoskeletal flexibility than the myelination of larger calibre axons. The ensheathment of larger calibre axons might therefore be facilitated by the physical property of a large calibre, whereas the ensheathment of smaller calibre axons might require additional axonal signals, such as neurotransmitter release or the expression of axonal signaling molecules. The hypothesis that local axonal signals might play a more prominent role in the regulation of small calibre axons rather than axons with large calibre would be in concordance with findings demonstrating that the axon calibre threshold at which axons are myelinated in the CNS can be manipulated from smaller to higher diameter by disruption of the extracellular matrix molecule beta1 integrin (Camara et al., 2009).

However, the reduction of myelinated axons in the electron micrographs of TetTx treated animals was not exclusively restricted to small calibre axons. Even though the myelination of small calibre axons was more affected by the reduction of synaptic vesicle release, the number of larger calibre axons was also decreased, with the

exception of the Mauthner axon, which was always myelinated. This indicates that axon calibre alone is not sufficient to induce the myelination of all axons, or at least the timely onset of myelination, in absence of synaptic vesicle release. Other axonal properties or axon-oligodendrocyte signaling might influence myelination in addition to axon calibre and synaptic vesicle release and I will discuss candidate signaling molecules in a separate section below.

Overall, my findings suggest that axon calibre as well as synaptic vesicle release influence axon selection, to some extent, during myelination. It remains unknown, whether the myelination of larger calibre axons is due to the physical size of the axons or an increase in axonal signal expression that is correlated with axon calibre, such as the increased expression of NRG-1 type III on large calibre PNS axons (Taveggia et al., 2005). Further studies are needed in order to elucidate whether axon calibre in the CNS can induce myelination in the absence of axonal signals in vivo and if so, whether this effect stems from the physical size of the axons itself or an increase in signal expression that correlates with axon calibre. The experimental increase of the axon calibre of an unmyelinated axon, not fated for myelination in the CNS, might lead to myelin ensheathment of the previously unmyelinated axon and change its myelination fate. Potential signaling molecules that are up-regulated with the increased calibre could then be individually tested in their ability to regulate the extent of myelination. Axon calibre of unmyelinated axons might be experimentally increased by limiting the number of nerves innervating a certain target tissue in the CNS, as it was done in the PNS by Voyvodic et al. (1989) by dissection of one of the sympathetic nerves innervating the submandibular duct, which led to an increase in axon calibre of the remaining sympathetic neurons in adult mice (Voyvodic et al. 1989).

The myelination of all axons with a potential to be myelinated is affected in the absence of synaptic vesicle release

Throughout the different species studied, during early myelination, specific axons and axonal tracts in the CNS are first to be myelinated while others are myelinated at later developmental stages or remain unmyelinated (Schreyer and Jones, 1982;

Remahl and Hildebrand, 1982; Schwab and Schnell, 1989; Baumann and Pham-Dinh, 2001 and Almeida et al., 2011).

This was verified by the analysis of the myelin ensheathment along axons of individual neurons, such as RS and CiD neurons, which have been shown to be myelinated while other neurons remained unmyelinated in wildtype animals (see chapter 3). In the absence of synaptic vesicle release, CiD and RS neurons showed a reduction of myelin ensheathment along the axon by approximately 30% as a result of the reduction of myelinating oligodendrocytes and myelin sheaths made per oligodendrocytes. This indicates that the reduction of myelinated axons in electron micrographs of the hemi spinal cord in TetTx treated animals is not due to specific axons that are normally myelinated but are not myelinated at all in the absence of synaptic vesicle release but rather that the myelin ensheathment along the axon of most axons with the potential to be myelinated is reduced in the absence of synaptic vesicle release. It is therefore likely, that all axons fated for myelination are affected in the absence of synaptic vesicle release. Given that the myelination of smaller calibre axons are more affected in TetTx treated animals than larger calibre axons, as discussed in the previous section, it is possible that the reduction in myelin ensheathment along the axon in absence of synaptic vesicle release varies according to axon calibre. However, axon calibre of CiD neurons is much smaller than the axon calibre of RS neurons and the reduction in average myelin ensheathment was not higher in CiD axons compared to RS axons. This somewhat surprising result might be due to an artefact in the data collection described in the results. The onset of myelination begins from approximately 3dpf (Almeida et al., 2011) and oligodendrocyte maturation and myelination occurs according to a distinct anterior-posterior gradient (Schwab and Schnell, 1989 as reviewed in Jessel, 2000; Baumann and Pham-Dinh, 2001 and Rowitch, 2004). The axon area in which the myelin ensheathment of RS axons was measured and the location of CiD neurons selected for measurement, however, varied along the spinal cord. Depending on the somite number in which CiD neurons were located and in which RS axons were measured at 4dpf, the amount of myelin ensheathment would have varied, as indicated by the large standard deviations. The same artefact occurred in both control and TetTx treated groups and therefore the reduced myelin ensheathment of RS and CiD

neurons in absence of myelination is still a valid result. However, due to the artefact in the myelin ensheathment measurements in the fluorescent images RS and CiD neurons in the TetTx treated animals, a subtle phenotype such as the higher reduction of myelinated axon of small axon calibre compared to axons of larger calibre observed in the electron micrographs might not have been detected. In order to avoid any location specific effects that might influence the amount of myelin along axons, it will be interesting to investigate the myelin ensheathment of large calibre and small calibre axon areas of the same axon. RS axons have a proximal-distal gradient in axon calibre along the axon, whereby axon areas proximal to the cell body are larger in calibre than axon areas distal to the cell body (see chapter 1 Introduction and chapter 3).

Quantifying the relative amount of myelin ensheathment in large and small areas along RS axons in absence of synaptic vesicle release might elucidate the role of axon calibre in axon selection during myelination in the absence of synaptic vesicle release.

Synaptic vesicle release has only a relatively small effect on oligodendrocyte differentiation

The 40% reduction of myelinated axons shown in the electron micrographs in absence of synaptic vesicle release demonstrates a role of neuronal activity in myelinated axon formation in vivo. Since the loss of myelinated axons is not due to loss of axons with the potential to be myelinated as shown in the quantification of axons above 0.3µm diameter, it must correlate with a reduction in myelin itself. A reduction in myelin could either stem from a reduction of myelinating oligodendrocytes in the absence of synaptic vesicle release or a reduction of myelin sheaths formed per oligodendrocyte.

Quantification of the mbp expressing cells showed that there is a 10% reduction of myelinating oligodendrocytes in the spinal cord of TetTx treated animals. The small decrease in myelinating oligodendrocytes may partly account for the 40% reduction in myelinated axons in TetTx treated animals as 10% fewer myelinating oligodendrocytes would also result in fewer myelin sheaths being formed along the axons. As the sheath length per oligodendrocyte measured in the single cell analysis

did not show an increase in sheath length, the remaining oligodendrocytes did not compensate for the loss of myelinating oligodendrocytes by increased longitudinal growth.

The 10% loss of myelinating oligodendrocytes might be caused either by a decrease in OPC formation, a decreased rate of OPC proliferation, an increase in OPC death or an inhibition in oligodendrocyte differentiation (for a review in oligodendrocyte development see Boulanger & Messier, 2014).

In the embryonic zebrafish spinal cord, OPCs emerge from the pMN domain, migrate and undergo only relatively few rounds of cell proliferation before differentiating to become myelinating oligodendrocytes. These different stages during oligodendrocyte development are extremely dynamic, but it is unknown to what extent neuronal activity could guide them. OPCs have been shown to retract upon contact with neighbouring OPC processes and migrate or proliferate to re-populate an area where OPCs have been experimentally ablated in order to secure an even OPC distribution throughout the CNS during development (Kirby et al., 2006) and in adults (Hughes et al., 2013). This tiling mechanism, however, indicates repulsive cell-cell interactions between OPC processes rather than cell-cell interactions between neurons and OPCs. OPC proliferation and oligodendrocyte differentiation have both been suggested to be regulated by neuronal activity (refs), but to somewhat conflicting ends. Neuronal innervation through axon-OPC synapses has been shown to inhibit OPC proliferation and promote OPC migration (Mangin et al., Gallo et al.), while oligodendrocyte proliferation and differentiation has been shown to be promoted by neuronal activity (Cavalliere et al., 2012; Gibson et al., 2014).

However, as shown here, approximately 90% of myelinating oligodendrocytes can differentiate in TetTx treated animals, indicating that the role of synaptic activity during OPC proliferation and differentiation is small and not essential for the majority of CNS myelination in vivo. This finding is in agreement with previous in vitro studies in which oligodendrocytes were shown to be able to differentiate in the absence of axons by an oligodendrocyte intrinsic default mechanism (Knapp et al., 1987; Bradel and Prince, 1983). On the other hand, studies in the rodent CNS have indicated that neuronal activity can influence OPC proliferation and differentiation

(Barres and Raff, 1993; Stevens et al., 2002; Mangin et al., 2012; Gibson et al., 2014). Unlike the rodent CNS, OPCs undergo only few cell divisions in the zebrafish spinal cord before the OPCs start to differentiate, due to the relatively small size of the spinal cord at early developmental stages (Park et al., 2007). The difference between the rodent studies and the relatively subtle decrease in oligodendrocyte number in TetTx treated animals might simply result from the fact that only a small number of OPC divisions could be influenced by the lack of synaptic vesicle release. As there are only a few rounds of OPC proliferation, during which neuronal activity might influence during early development, the decrease in oligodendrocyte number observed here might be subtle at 4dpf, but could be more striking at later developmental stages or in other areas of the CNS.

It is possible that an increased rate of OPC proliferation in response to lack of neuronal activity (Mangin et al., 2012) could have partly compensated for a potential decrease in oligodendrocyte differentiation rate in order to ensure an even distribution of myelinating oligodendrocytes even in the absence of synaptic activity.

Further characterization of the oligodendrocyte development, particularly of OPC development, are needed in order to elucidate whether OPC proliferation or differentiation is influenced by synaptic activity to account for the 10% decrease in myelinating oligodendrocytes in TetTx treated animals. In a future experiment, the number of OPCs and their differentiation rate should be quantified in the spinal cord and other CNS regions of TetTx treated animals, for example, by using the transgenic lines Tg(sox10:mRFP) and Tg(olig2:GFP) to label OPCs in high resolution time-lapse imaging. This experiment would reveal whether synaptic vesicle release can regulate OPC proliferation or differentiation and whether the effect of synaptic vesicle release is greater in other CNS areas where OPCs undergo many cell divisions before differentiating.

The number of myelin sheaths formed per oligodendrocyte is regulated by synaptic vesicle release

The 10% decrease in myelinating oligodendrocytes may partly account for the 40% reduction in myelinated axons seen in the electron micrographs of TetTx treated animals, but could not account for the total reduction in myelinated axon number.

As the majority of the myelinating oligodendrocyte population remains in the TetTx treated animals, the loss of myelinated axons could either stem from smaller myelin sheaths formed per oligodendrocyte or fewer myelin sheaths formed per oligodendrocyte.

Single cell analysis of individual myelinating oligodendrocytes using mosaic expression of mbp:mCherry revealed a decrease in myelin sheath number per oligodendrocyte of approximately 30%. Together with the 10% reduction in myelinating oligodendrocytes, this can account for the 40% loss of myelinated axons in the electron micrographs as fewer myelin sheaths made per oligodendrocyte would result in a reduction of myelinated areas along the axon. Synaptic vesicle release can, therefore, influence the number of myelinating oligodendrocytes, albeit to a small degree, and regulate the extent of myelin sheaths made per oligodendrocyte.

The single cell analysis also revealed that the average length of myelin sheaths is not significantly reduced in the absence of synaptic vesicle release, either at 3dpf or 4dpf. The fact that the average length of myelin sheaths in not significantly reduced might be another indication that the myelin sheaths formed in the absence of synaptic vesicle release are regulated by an activity independent mode of myelination. However, even though the average myelin sheath length was the same in oligodendrocytes in controls and TetTx treated animals, there was a trend to smaller myelin sheath length in oligodendrocytes in TetTx treated animals by 4dpf, indicating that the longitudinal growths of the myelin sheaths that can grow in the absence of synaptic vesicle release might be slower compared to controls. This could indicate that synaptic transmission might have a second regulatory function during myelination. As the length of myelin sheaths and spacing of nodes of Ranvier along the axons is an important factor determining signal conduction velocity, myelin sheath growth could be influenced locally by axonal activity. Axonal synaptic vesicle release might therefore regulate the longitudinal growth and length of myelin sheaths as I will discuss in a separate section below.

Post-migratory oligodendrocytes are very dynamic in the transition from OPC to myelinating oligodendrocyte, during which they repeatedly extend and retract exploratory processes in search for axons to myelinate. However, the selection process by which an oligodendrocyte selects the axons it is going to myelinate while

refraining to myelinate other axons in its proximity is unknown. One possible cellular mechanism underlying the selection process might be the stochastic generation of nascent myelin sheaths around numerous axons and the subsequent pruning of the myelin sheaths ensheathing the incorrect axons. However, Czopka et al. showed that, at a time-point when the majority of axons in the embryonic zebrafish spinal cord are unmyelinated, only approximately 25% of all myelin sheath per oligodendrocyte are retracted within 2 days after the first sheath formation, leaving 75% of myelin sheath stable and maintained long-term. If the initial axon selection was indeed stochastic, a higher percentage of all nascent myelin sheaths initially formed per oligodendrocyte would have to be retracted. This suggests that oligodendrocytes do not indiscriminately ensheath axons. It is likely that multiple factors interact to ensure the correct timing and axonal selection during myelination. Synaptic activity might be one of them, regulating the extent of myelination, e.g. the myelination of axons that might need additional axonal signals in order to be myelinated, such as small calibre axons. The axonal signals, presumably neurotransmitters released through synaptic vesicle release, might be required for the axonal selection prior to myelin ensheathment or the stabilization of nascent myelin sheaths. In the first case, oligodendrocytes in TetTx treated animals would form approximately 30% fewer myelin sheaths initially, in the latter case they would form a normal number of myelin sheaths but retract approximately 30% of the nascent myelin sheaths that are not stable.

My timelapse analysis of the initial myelination showed a 28% of decrease in the number of initially formed myelin sheaths per oligodendrocyte in the absence of synaptic vesicle release. This 28% reduction of initially formed myelin sheaths can indeed almost entirely account for the 30% loss of myelin sheath per oligodendrocytes seen at later stage during oligodendrocyte development. This finding suggests that synaptic vesicle release plays an important role in the axonal selection process during myelination.

In accordance with that, no significant increase in myelin sheath retractions were seen in TetTx treated animals during the first 6 hours of initial myelination. As the number of average myelin sheaths per oligodendrocyte is also 30% decreased in TetTx treated animals at later time points during oligodendrocyte development, this

indicates that synaptic vesicle release is not essential for the maintenance of stable myelin sheaths.

Oligodendrocytes only have a short critical time window during which the majority of myelin sheaths are being formed and after which the number of myelin sheaths per oligodendrocyte remains stable (Czopka et al. 2013). This has also been shown in a mammalian co-culture system, in which rodent oligodendrocytes make all their myelin sheaths within a short time period of 12 hours (Watkins et al., 2008). The reduction in myelin sheath number per oligodendrocytes in TetTx treated animals might be a reflection of a slower formation of myelin sheaths over time and they might form myelin sheaths for a longer period of time. However, there was no significant difference in the time window with which the oligodendrocytes formed their sheaths in TetTx treated animals compared to controls and the majority of myelin sheaths were formed within the critical 6 hour period, indicating that the timing of myelin sheath formation is regulated independently of synaptic vesicle release.

Given that the oligodendrocytes in TetTx treated animals form fewer myelin sheaths initially, synaptic activity is either required for the formation of stable myelin sheaths or for the formation of axon-oligodendrocyte contacts. If synaptic activity is involved prior to ensheathment, myelin sheath formation might be regulated by local axonal signals. Indeed, the number of axon-oligodendrocyte contacts after first sheath formation were significantly reduced in TetTx treated animals, indicating that local axonal signals, such as neurotransmitters, released through exocytosis of synaptic vesicles might attract oligodendrocyte processes to make contact with axons prior to ensheathment. Even though a lot of axon-oligodendrocyte contacts are established in the absence of synaptic vesicle release, the decrease in this contacts indicates that one of the mechanisms by which myelinating oligodendrocytes choose the axons they myelinate might be synaptic vesicle mediated signaling. The axonal signaling could either be extra-synaptic or synaptic, or a combination of both. If extra-synaptic, the axonal signal would be released through exocytosis of synaptic vesicles into the extracellular environment around the active axon, bind to the exploratory processes of pre-myelinating oligodendrocytes and guide them to ensheath the active axon. If the axon-oligodendrocyte interactions prior to ensheathment are synaptic, the axonal

signal would be released locally and bind directly to the pre-myelinating oligodendrocyte process prior to ensheathment. It is also conceivable that the extra-synaptic axonal signal might attract the exploratory oligodendrocyte process towards the active axon, where a synaptic connection is established during axon-oligodendrocyte contact.

Since the axon-oligodendrocyte contact to myelin sheath conversion rate was decreased in TetTx treated animals, fewer axon-oligodendrocyte contacts that were established transformed into myelin sheaths. This suggests that the axonal signal released through synaptic vesicles might also be important for the actual ensheathment of axons by oligodendrocyte processes. It is tempting to speculate that, after axon-oligodendrocyte contact has been established, axonal signals mediated through the described axon-oligodendrocyte synapse might induce the ensheathment of the axon. However, the expression of neurotransmitter receptors on OPCs, which have been correlated with the axon-oligodendrocyte synapse, are down-regulated as OPCs differentiate into myelinating oligodendrocytes and the excitatory postsynaptic currents recorded at early postnatal stages in OPCs is therefore subsequently reduced in myelinating oligodendrocytes (Kukley et al., 2010, De Biase et al., 2010). This suggests that the potential function of synaptic connections between axons and oligodendrocytes occurs prior to myelin ensheathment. The role of axon-oligodendrocyte synapses during myelination is discussed in more detail below.

The fate of small axon-oligodendrocyte contacts that remain after initial myelination

The small axon-oligodendrocyte contacts <5µm that remained after initial myelination, 6 hours after first myelin sheath formation, were either nascent myelin sheaths that are in the process of being retracted or are contacts that never form myelin sheaths. Myelin sheath retractions occur normally in wildtype oligodendrocytes and might be part of myelin remodeling or even myelin turn-over during which individual myelin sheaths would be retracted and replaced over time, as a recent in vivo study showed that CNS myelination remains plastic and susceptible to myelin changes throughout life (Young et al., 2013). During the initial phase of myelination, short sheaths are retracted within minutes, while the retraction process, sometimes called pruning, occurs more slowly in later stages of the oligodendrocyte

cell life and can take up to 1-2 days (Czopka et al., 2013). After that, the remaining myelin sheaths formed per oligodendrocyte are remarkably stable (Czopka et al., 2013).

As described above, only a relatively small number of axons are myelinated in the spinal cord during early development (approximately 200 out of several thousand axons) and the proportion of retractions is low in number compared to the number of ensheathment made. It is therefore unlikely that oligodendrocytes randomly ensheath axons without the right axon-oligodendrocyte interactions to guide the ensheathment. The retractions seen during the timelapses and the small axon-oligodendrocyte contacts might be accidental ensheathments made around "incorrect" axons. "Incorrect" axons might be axons that do not offer the right axonal signal to be myelinated or even release a negative, repressive signal in order to not be myelinated. Interestingly, there was no significant difference in the number of small axon-oligodendrocyte contacts <5µm between controls and TetTx at the end of initial myelination but there was a significant increase of these contacts in TetTx treated animals at 3dpf and 4dpf. At these time-points, the majority of cells would have had at least a few hours after the critical initial myelination period to grow their sheaths or retract unstable nascent sheaths. The small axon-oligodendrocyte contacts seen at the end of initial myelination might have grown into myelin sheaths >5µm by 3dpf and 4dpf in controls but failed to do so in the absence of synaptic vesicle release in TetTx treated animals. This would indicate that synaptic activity could induce the growth of nascent myelin sheaths after initial axon-oligodendrocyte contact. Axonal synaptic vesicle release might therefore also influence the myelin sheath growth itself, in addition to regulating the number of myelin sheaths per oligodendrocyte, which I will discuss in the section below.

It is also possible that the increase in short axon-oligodendrocyte contacts <5µm in TetTx treated animals stems from an increase of nascent sheath retractions. However, as the average number of myelin sheaths per oligodendrocyte in TetTx treated animals does not decrease over time between the end of the timelapse movie after the initial myelination (average sheath number per cell 6.9) and 3dpf (average sheath number per cell 9.0) as well as 4dpf (average sheath number per cell 8.8), it seems unlikely that this is the case.

Alternatively, the small axon-oligodendrocyte contacts <5µm might have been retracted in controls between the end of timelapse analysis after the initial myelination and 3dpf as well as 4dpf, while they were not retracted in TetTx treated animals. Given that synaptic vesicle release is inhibited in TetTx treated animals, this could suggest that the retractions of small axon-oligodendrocyte contacts, and perhaps even ensheathments, is based on the exocytosis of negative axonal signals released by axons. Axonal selection prior to myelin ensheathment would therefore be regulated by positive and negative cues released through synaptic vesicles along axons. In this case, the "incorrect" axon might belong to a certain neuronal subtype, which does not release the right axonal signal (or not enough of the axonal signal) and is therefore not usually myelinated (see Chapter 3, small axon-oligodendrocyte contacts around Rohon Beard axons). However, timelapse movies in Czopka et al. show that retractions of individual myelin sheaths are sometimes made from axons that are ensheathed by several stable myelin sheaths (Czopka et al. 2013), suggesting that sheath retractions are not always due to the ensheathment of "incorrect" axon.

There might even be a competitive mechanism amongst the myelin sheaths along myelinated axons regulating whether myelin sheaths remain stable or whether they are retracted. As the myelin sheaths that are retracted during the initial myelination are mainly relatively small, it is tempting to speculate whether smaller sheaths might be out-competed over longer sheaths along the same axon. In this case, positive and negative signals released along the same axon might create a competitive environment between myelin sheaths and thereby regulate which sheaths will be stable and which will be retracted.

Further in vivo studies of live oligodendrocyte behaviour during myelination are needed in order to elucidate the dynamic mechanisms behind myelin sheath retraction. In order to elucidate the fate of the small axon-oligodendrocyte contacts <5µm under normal conditions and in absence of synaptic vesicle release, a time-course analysis of the same individual oligodendrocyte between initial myelination until multiple hours after initial myelination at 3dpf and 4dpf should be carried out. This analysis will reveal whether the small axon-oligodendrocyte contacts after initial myelination will grow into full myelin sheath or whether they are retracted. The time-course of individual oligodendrocyte in TetTx treated animals will reveal

whether the growth of myelin sheath or their retraction is influenced by synaptic vesicle release.

The dynamic behavior of individual myelin sheaths is influenced by synaptic vesicle release

Effective signal conduction is crucial for normal nervous system function. Signal conduction in myelinated axons is not only determined by axon calibre but also by the spacing between the nodes of Ranvier. The precise regulation of the length of the internodes, the myelin sheaths, is therefore essential for rapid conduction velocity and the timed arrival of signals in neuronal circuits (Fields, 2005; Baumann and Pham-Dinh, 2001). During the timelapse analyses, different myelin sheaths often showed great diversity in longitudinal growth during the timelapse analyses in control animals. Even myelin sheaths made by the same oligodendrocyte showed a dynamic range of growth speeds, some of the sheaths growing three-fold in lengths compared to other sheaths by the same oligodendrocyte but around different axons. This observation suggests that the longitudinal elongation of different myelin sheaths might be regulated individually, by local axonal signals. Each axon might release varying amounts of the same axonal signal, such as neurotransmitters, which results in different growth rates of individual myelin sheaths per axon. The local regulation of myelin sheath growth per axon could be one mechanism to ensure the correct myelin sheath length and node of Ranvier spacing along the axon, whereby signal conduction is regulated optimally for each axon. Neuronal activity might therefore play an important role in the regulation of myelin sheath length and activity dependent local axonal signals might be behind the different growth rates of individual myelin sheaths. In accordance with that, oligodendrocytes in TetTx treated animals show a significant decrease in myelin sheath growth rate, with more slow growing myelin sheaths compared to controls. The increase in slow growing myelin sheath is in accordance with the trend towards smaller myelin sheaths per oligodendrocyte in TetTx treated animals seen in the single cell analysis at 3dpf and 4dpf. These observations indicate that the local axonal signals regulating individual sheath growth might be released by synaptic vesicle release.

Of course, myelin sheaths in TetTx treated animals grow even in the absence of synaptic vesicle release, indicating that this aspect of neuronal activity is not essential for the formation of all myelin sheaths. As discussed above, it is likely that there is a second mechanism regulating myelin sheath formation and that synaptic activity is has a modulatory effect on myelination. However, the increase in slow growth of myelin sheaths that can grow in TetTx treated animals indicates that synaptic activity might modulate the growth of myelin sheaths. It is possible, that myelin sheaths could grow at a slow, basal rate without the synaptic input of axonal signals as shown in TetTx treated animals. And local axonal signals could then induce fast growth of myelin sheaths. The adjustment of myelin sheath growth to the activity of individual axons might, therefore, be another modulatory mechanism by which neuronal activity can regulate myelin sheath growth.

Axon glial synapse as a potential mechanism behind activity dependent myelination

Oligodendrocytes can myelinate different axons of varying sizes, type and functional state. The process by which oligodendrocytes select the axons they myelinate, however, is unknown. Synaptic connections between OPCs and unmyelinated axons have been reported (Bergles et al. 2000, Kukley et al., 2007, Ziskin et al., 2007), through which axonal activity was shown to influence OPC behavior in vivo (Mangin et al., 2012). Axon-glial synapses might directly influence the behavior of oligodendrocyte processes during myelination in vivo. Glutamate and GABA receptor mediated calcium signaling in oligodendrocytes might regulate oligodendrocyte process behavior, similar to the way that activation of postsynaptic calcium signaling can influence dendrite extensions and retractions (Kennedy et al., 2005, Geer and Greenberg, 2008, Flavell and Greenberg, 2008). Local calcium signaling in OPC processes activated through glutamate release has also recently been implicated to regulate myelination in vitro (Wake et al., 2011). Synaptic activity has been demonstrated to influence various stages during axon-dendrite synapse formation, including its morphology, maintenance and function (Greer and Greenberg, 2008, Cohen and Greenberg, 2008, and West and Greenberg, 2011). If the axon-oligodendroglial synapse is similar to the axon-dendrite synapse, then synaptic activity might have a modulatory function in regulating the formation and

maintenance of the axon-oligodendroglial synapse. However, so far no effect of axon-glial synaptic interaction directly regulating myelination has been demonstrated in vivo. Here, we show that in the absence of synaptic vesicle release, oligodendrocytes form a reduced number of axon-oligodendrocyte contacts compared to controls. The absence of synaptic vesicle release might cause disturbances in the formation or function of the axon-glial synapse, which might lead to the reduced number of axon-oligodendrocyte contacts seen in the TetTx treated animals. In this case, the synaptic connection between axons and oligodendrocytes might be very transient and the axon-oligodendrocyte contacts are not fully established in its absence.

A possible disruption of the axon-oligodendrocyte synapse might also explain the trend towards a decrease in initial ensheathments per oligodendrocyte seen in the TetTx treated animals. After the axon-oligodendrocyte contact is established, axon-oligodendrocyte synapse mediated cell-cell interactions might initiate the ensheathment of the axon by the premyelinating oligodendrocyte process.

The axon-oligodendrocyte synapse might even play a crucial role in myelin sheath maintenance as myelination has been shown to be very plastic and new myelin sheaths are intercalated between existing myelin sheath or replace old sheaths throughout development (Young et al., 2013). However, an active role of the axon-oligodendrocyte synapse after initial ensheathment would indicate a more long-term role in the formation of a stable myelin sheath. Such a mechanism would rely on the continued maintenance and function of the axon-oligodendrocyte synapse during OPC differentiation and the formation of stable myelin sheath. Neurotransmitter receptor expression and excitatory postsynaptic currents recorded at early postnatal stages (Kukley et al., 2008, Ge et al., 2009), however, are reduced as OPCs differentiate into myelinating oligodendrocytes (Kukley et al., 2010, De Biase et al., 2010). Whether the axon-glial synapse functions only during OPC transition to myelinating oligodendrocyte or also during the formation of a stable myelin sheath has yet to be determined. Preliminary data using calcium imaging to observe transient calcium currents in oligodendrocytes and particularly the myelin sheaths, however, have revealed local calcium currents occurring in the nascent myelin sheaths surrounding active axons (data not shown). This might suggest that the role

of the axon-oligodendrocyte synapse might not be limited only to oligodendrocyte processes prior to myelination, but that the axon-oligodendrocyte synapse might mediate local axonal signals along the nascent myelin sheath, which might regulate its growth. In order to elucidate the precise role of axon-oligodendrocyte synapses during myelination in vivo, individual axon-glial synapses will need to be labelled and observed during oligodendrocyte development and myelin sheath formation. This will help to understand whether axon-glial synapses are lost in the transition between OPC and myelinating oligodendrocyte or whether they are preserved and functional during myelin sheath formation and maintenance. If indeed they are functional during myelin sheath formation and maintenance, inhibition of synaptic vesicle release would cause a reduction of neurotransmitter mediated calcium currents in nascent myelin sheaths, which would result in the reduction of axon-oligodendrocyte contacts and myelin sheath formation seen in TetTx treated animals. Calcium currents can be visualized by genetically encoded calcium indicators, such as GCaMP. GCaMP is a fusion protein consisting of a permuted GFP, calmodulin (CaM) and the M13 domain of a myosin light chain kinase. In the absence of calcium, the chromophore structure of the permuted GFP is disrupted and therefore only allows dim fluorescence. If Calcium binds to CaM, it undergoes conformational changes that are, together with M13, engineered to close the chromophore structure of the GFP in a hinge-like mechanism, which leads to increased GFP fluorescence. This successfully enables monitoring of calcium currents in cells expressing GCaMPs in their membranes (Akerboom et al., 2012; Tallini et al., 2006; Tian et al., 2009; Del Bene et al., 2010). Further analysis using GCaMP calcium imaging will reveal whether the calcium currents recorded in nascent myelin sheaths during the ensheathment in wildtype animals is indeed also reduced in TetTx treated animals as a consequence of inhibited synaptic vesicle release.

Candidate neurotransmitters that might be involved in the activity dependent regulation of myelination

In this chapter, I could show that inhibition of synaptic vesicle release reduces the myelin extent formed per oligodendrocyte and decreases the growth rate of myelin sheaths on axons. The inhibition of synaptic vesicle exocytosis reliably hinders the

release of synaptic vesicle content and thereby effectively inhibits the release of neurotransmitters (Gerst, 1999; Gaisano, 2000; Mochida, 2000). As the exocytosis of all neurotransmitters is inhibited, it is impossible to discern which of the neurotransmitters is involved in the activity dependent regulation of myelination. However, some of the known neurotransmitters have previously been implied in regulating myelinated axon formation and I will briefly discuss them below. The most promising candidate neurotransmitter is glutamate, which has been proposed to activate local mbp translation in vitro after binding to oligodendrocyte NMDA receptors and activating downstream signaling pathways involving tyrosine Fyn kinase (Wake et al., 2011). The in vivo relevance of glutamate mediated NMDA receptor activation during myelination, though, remains unclear as the genetic ablation of the functional NMDA receptor subunit in vivo did not lead to an obvious myelin defect (De Biase et al., 2011). Myelination in this study was assessed by g-ratios and myelin protein expression by western blots as well as immuno staining in the rostral and caudal forebrain and a subtle decrease in the number of myelin sheaths formed per oligodendrocyte might not have been detected in these analyses as the level of mbp expressed in the oligodendrocytes does. Glutamate mediated NMDA receptor activation might, therefore, still have a modulatory effect in regulating the extent or timing of myelination in the CNS in vivo. Apart from just regulating the extent of myelination, glutamate might also regulate OPC behaviour prior to myelination, as OPCs have been shown to receive glutamatergic synapses from axons in different CNS regions (Bergles et al., 2000; Kukley et al., 2007; Kukley et al., 2007, Ziskin et al., 2007; Lin et al., 2005; Karatodir et al.,2008; Mueller et al., 2009; Li et al., 2012). These glutamatergic axon-oligodendrocyte synapses are thought to influence OPC proliferation, migration and differentiation (Gallo et al., 1996; Gudz et al., 2006; Mangin et al., 2012). GABA is another neurotransmitter that has been shown to form synapses with OPCs and elicit excitatory postsynaptic currents after the stimulation of GABAergic neurons. The neural evoked excitation of these axon-oligodendrocyte synapses may be one mechanism by which neuronal activity might regulate oligodendrogenesis and myelination, although the precise role of the glutamatergic axon-OPC synapse remains to be elucidated (as reviewed in Gallo, 2008; Almeida and Lyons, 2013).

Another neurotransmitter that has previously been implicated to influence myelination is ATP and its derivative adenosine, which has been shown to inhibit proliferation of OPCs and thereby stimulate their differentiation into myelinating oligodendrocytes, thus increasing myelination in vitro (Steven et al., 1998; Stevens et al., 2002, as reviewed in Steven and Fields, 2000). Although the effect that the neurotransmitter on myelination might not be mediated through direct axon-oligodendrocyte interactions as ATP from electrically stimulated axons was found to activate the release of the cytokine leukemia inhibitory factor (LIF) from astrocytes in vitro (Scolding et al., 1989; Stankoff et al., 2002). LIF is known to promote myelination in mature oligodendrocytes and ATP might therefore not directly affect oligodendrocyte behaviour and myelination. Of course, other neurotransmitters that have not been previously investigated in promoting myelination might be mediating the activity dependent mode of myelination.

As shown in chapter 3, myelination is not restricted to neurons of a specific neurotransmitter, as I found glutamatergic (RS, CoPA, CiD) as well as glycinergic neurons (CoLA) that are fated for myelination while other glutamatergic (CoBL) and glycinergic (CoBL, CiA) (Higashijima et al., 2004) remained unmyelinated during the early zebrafish development. Glutamate or GABA released through synaptic vesicles might activate downstream signaling pathways in oligodendrocytes through NMDA receptor or GABA receptor binding, which in case of glutamate has been shown to induce myelin sheath formation as described above (Wake et al., 2011). The myelination of glutamatergic or GABAergic neurons might therefore be more affected in the absence of synaptic vesicle release. Both, RS and CiD neurons are glutamatergic and show a reduction in myelin ensheathment along their axons in the absence of synaptic vesicle release, indicating that glutamate release might activate downstream signaling pathways in oligodendrocytes that can regulate the extent of myelination along glutamatergic neurons.

So far, it is unclear whether neurons of other neurotransmitter types are equally affected or whether only the myelin extent of glutamatergic neurons can be regulated by synaptic vesicle release. Further analysis of the myelination status of individual neurons of different neurotransmitter types, such as the glycinergic CoLA neuron,

under normal condition and in the absence of synaptic vesicle release will reveal the neurotransmitters involved in the activity dependent regulation of myelination.
If only the myelination of glutamatergic neurons is reduced in the absence of synaptic vesicle release that would demonstrate axonal glutamate release as an important factor in axon-oligodendrocyte interactions regulating myelination. Furthermore, pharmacological application of the different neurotransmitters in the Ca^{2+} imaging set up described above, whereby GCaMP is expressed in oligodendrocyte processes and myelin sheaths, will be an ideal assay to screen for the neurotransmitter involved in the activity dependent mode of myelination.

Other neuronal signals that might have a modulatory function during myelination
As described above, although the myelination of small calibre axons was more affected in the TetTx treated animals, large calibre axons were also affected and axon calibre alone might therefore not be sufficient to regulate myelination, or at least the timely onset of myelination, in the absence of synaptic vesicle release. It is therefore likely that other signaling molecules might influence myelination through axon-oligodendrocyte interactions in addition to axon calibre and synaptic activity. Several candidate signaling molecules have been investigated previously, but none were solely required to induce CNS myelination, indicating that they, too, have a modulatory role during myelination. Candidate axon-oligodendrocyte signaling molecules include NRG-1 type III, which has been shown to have a small effect on CNS myelination, depending on region and developmental stage investigated (Brinkmann et al., 2008; Taveggia et al., 2008; Makinodan et al., 2012). Other axon-oligodendrocyte signals that have been shown to influence myelination, either regulate the extent of myelination by regulating the myelination of small rather than large calibre axon in case of beta1 integrin (Camara et al., 2009), or negatively influence the onset of myelination, such as PSA-CAM (Charles et al., 2009) and Jagged-1 to Notch1 signalling (Wang et al., 1998; Zhang et al., 2009; as reviewed in Taveggia et al., 2010). Numerous other signals have also been found to have a positive effect on the extent of myelination such as tyrosine Fyn kinase (Wake et al., 2011; Czopka et al., 2013) or the onset of myelination, such as Wnt-β-catenin (Fancy et al., 2009), or a negative regulatory effect on the onset of myelination, such as

GPR17 (Chen et al., 2009), and LINGO-1 (Mi et al., 2005). As none of these candidate molecules are essential for myelination per se, it will be interesting to elucidate the respective roles of the different axonal properties, synaptic vesicle release, axon calibre and axon-oligodendrocyte signalling molecules, in their modulatory roles in axon selection during myelination. In order to investigate the relative importance of the different signalling molecules described above during myelination in the absence of synaptic vesicle release, further high-resolution analyses at a cellular level are needed to test the precise role that these factors have in the selection of different axons of a particular type, calibre or functional state during myelination. Furthermore, in chemical screens using TetTx expressing fish new axon-oligodendrocyte signalling molecules might be identified that might regulate myelination independently of neuronal activity.

Conclusion

This investigation aimed to characterize oligodendrocyte behavior during myelination in the absence of synaptic vesicle release. I showed that, overall, there is a 40% decrease in the number of myelinated axons in the spinal cord of TetTx expressing zebrafish. This is partly correlated to a 10% reduction in oligodendrocyte differentiation and approximately 30% reduction of myelin sheaths initially formed per oligodendrocyte. We can therefore conclude that, synaptic vesicle release can, to some extent, influence oligodendrocyte differentiation and that it is important for regulating the number of myelin sheaths made by individual oligodendrocytes in vivo. As myelin sheaths are still formed even in the absence of synaptic vesicle release, the role of neuronal synaptic transmission in regulating myelination might be more modulatory rather than mandatory. Given the overall reduction in myelin ensheathment along axons of neurons fated for myelination, such as RS and CiD neurons, synaptic activity might simply amplify the overall myelinating potential of oligodendrocytes and increase the myelin extent they produce.

Furthermore, synaptic vesicle release has a second mechanism by which it regulates myelination. Myelin sheaths appear to be dynamically regulated by local axonal signals, as synaptic transmission has the potential to change the sheath growth rate from a basal, slow growth intrinsic to oligodendrocytes to a faster growth rate.

It is possible that the synapses that have been described between axons and the processes of oligodendrocyte precursor cells can directly guide the oligodendrocyte process to ensheath active axons and provide the signal to convert the oligodendrocyte process into a myelin sheath. Alternatively, the role of neuronal activity during myelination might be extra-synaptic and influence oligodendrocyte processes through axonal signals released into the cytoplasm.

Future analyses of the synaptic vesicle mediated axon-oligodendrocyte interactions before and after myelin ensheathment will reveal the role that the axon-oligodendrocyte synapse might play during myelination. Furthermore, an in depth characterization of the myelination of single axons of different neuronal types and axon calibre, will further elucidate the cellular mechanism by which neuronal activity can regulate myelinated axon formation.

Overall, I could show that synaptic vesicle release can regulate the extent of myelination by regulating the number of myelin sheaths formed per oligodendrocyte and provided evidence that synaptic activity is involved in axonal selection during myelination.

5. Discussion

5.1 Axonal selection during myelination is regulated by axonal properties such as axon calibre and synaptic activity

Myelination occurs in different areas of the CNS at different times during development and is extremely complex. In all CNS areas, oligodendrocytes are presented with a large variety of axons of different axon calibres, axon branching, neurotransmitter types and states of activity (Hildebrand and Hahn, 1978; Hildebrand, 1993; Murray and Blakemore, 1980; Baumann and Pham-Dinh, 2001). It is possible that oligodendrocytes are able to recognize their target axons by particular axonal properties, which could guide the oligodendrocyte process and establish the axon-oligodendrocyte contact and subsequent myelin ensheathment around the axons fated for myelination. Alternatively, oligodendrocyte contact and myelin ensheathment might influence axon properties, such as axon calibre and axon branching, and might therefore create the large variety of different axon morphologies in the CNS. In order to elucidate whether axonal properties influence axon selection during myelination or whether myelin ensheathment changes axonal properties, the myelination status of individual neurons during normal development and in absence of oligodendrocytes and myelin ensheathment was investigated in this thesis.

In accordance with previous studies (Matthews and Duncan, 1971; Waxman and Bennett, 1972; Remahl and Hildebrand, 1982; Hildebrand et al., 1993), I found that, while almost all large calibre axons with a calibre above 0.9µm are myelinated in the zebrafish spinal cord, myelinated as well as unmyelinated axons are found in the axon calibre range between 0.3µm and 0.9µm. These observations indicate that the physical size of axons above 0.9µm may be a factor in the axonal selection during myelination, but other axonal properties must also be involved in the myelination of axons of 0.3-0.9µm axon calibre. Alternatively, axon calibre of the myelinated axons >0.9µm might have been induced by axon-oligodendrocyte interactions mediated by myelin ensheathment, as it has been suggested by previous in vivo studies (Colello et al., Sanchez et al., 1996, 2000). In this case, myelinated axons with a calibre between 0.3-0.9µm might simply be in the process of expanding their calibre after myelin ensheathment.

In order to investigate whether axons selected for myelination have different axonal properties than axons that remain unmyelinated prior to myelination or whether the differences in axon morphology occur after myelination, I described the axon calibre in relation to the myelination fate of 3 spinal cord neurons that are fated for myelination, RS, CoPA and CiD neurons, and 3 spinal cord neurons that are not fated for myelination in the early zebrafish development, RB, CoBL and CiA neurons. Prior to myelination, the average axon calibre of all neurons was relatively uniform and axon calibre of most neurons did not increase after the onset of myelination. The axon calibre of the RS axon, however, did increase dramatically after the onset of myelination, indicating that the axon calibre of some neurons might be increased by myelin ensheathment. However, somewhat surprisingly, axon calibre of the largest axons in the spinal cord, including RS neurons, was unimpaired in the absence of all oligodendrocyte lineage cells, demonstrating that axons can grow independently from extrinsic signals secreted by oligodendrocytes or myelin ensheathment.

This also suggests that the myelinated axons with a calibre >0.9μm were likely to be selected for myelination due to their calibre size as their calibre did not increase with myelin ensheathment, indicating that axon calibre can influence axon selection during myelination. This is in accordance with in vitro findings that oligodendrocyte can even ensheath inert polystyrene fibres, in the complete absence of axonal signals, when the fibres was above a calibre of 0.4μm (Lee et al., 2012). In vivo, however, there is no strict threshold above which an axon is myelinated in the CNS and the axons with a calibre between 0.3-0.9μm likely require additional axonal signals in order to be myelinated.

Importantly, the functional state of these axons fated for myelination might be different from the axons that remain unmyelinated, e.g. RS, CoPA and CiD axons might fire action potentials more frequently during the onset of myelination than RB, CoBL and CiA axons.

As one main function of myelin is the rapid signal conduction of action potentials, I hypothesised that neuronal activity might be one of the axonal properties that influence axon selection during myelination. Indeed, in the absence of synaptic vesicle release in the TetTx treated zebrafish, there is a reduction in the number of myelinated axons, demonstrating that synaptic vesicle release can promote

myelination in vivo. Interestingly, small calibre axon in the range between 0.3 and 0.9µm were more affected than the larger calibre axons above 0.9µm, providing experimental evidence that axon calibre can influence the axon selection during myelination and that the myelination of smaller calibre axons is more dependent on additional axonal signal, such as synaptic activity. However, not only small calibre axons were affected by the loss of synaptic activity but also the myelination of large calibre axons above 0.9µm was reduced, indicating that either the onset of myelination in the absence of synaptic vesicle release might be delayed or that there are more factors controlling myelination than axon calibre and synaptic activity.

Other axon-oligodendrocyte interactions have been identified that can influence myelination in the CNS, one of them is the NRG1-ErbB signalling, although genetic ablation of NRG1-III expression in axons causes little or no myelin defects depending on the CNS region and developmental stage investigated (Brinkmann et al., 2008; Taveggia et al., 2008; Makinodan et al., 2012). More axon-oligodendorcyte signals have been identified that can influence myelination, however, they also either regulate the extent of myelination by regulating the myelination of small rather than large calibre axon in case of beta1 integrin (Camara et al., 2009), or negatively influence the onset of myelination, such as Jagged-1 to Notch1 signalling (Wang et al., 1998; Zhang et al., 2009; as reviewed in Taveggia et al., 2010) and axonal expression of PSA-CAM (Charles et al., 2009). However, none of these candidate molecules are essential for myelination per se. Further high-resolution analyses at a cellular level are needed in order to elucidate the precise role that these factors have in the selection of different axons of a particular type, calibre or functional state during myelination.

Together, my data indicate that axon selection during myelination is based on axonal properties and that axon calibre as well as synaptic activity are axon properties that influence myelination. It will be intriguing to further characterize the individual neurons fated for myelination according to their neurotransmitter type and functional state. I could show that there are both myelinated and unmyelinated glutamatergic and glycinergic neurons, however other neurotransmitter, such as the inhibitory neurotransmitter GABA, might play different roles in axonal selection during myelination. The functional state of individual neurons could be inferred by

monitoring their firing rates using the genetically encoded calcium indicator GCaMP, which increases its GFP fluorescence when calcium binds to it (Akerboom et al., 2012; Tallini et al., 2006; Tian et al., 2009; Del Bene et al., 2010). Action potential firing at different frequencies has been shown to have different effects on myelination in Schwann cells (Itoh et al, 1995; Stevens et al. 1998) and profiling the individual firing rates of myelinated axons will provide an insight into the mechanism by neuronal activity can influence axon selection during myelination.

Additionally, experimental manipulation of axonal properties of neurons not normally fated for myelination, such as increasing the axon firing rate (by optogenetic stimulation) might change the myelination fate of these neurons and would provide a better understanding of the axonal properties involved in axon selection during myelination.

Manipulating the firing rate of individual neurons might also reveal the myelin independent mechanism behind axon calibre growth. As the axon calibre of RS neurons grows tremendously, even in the absence of myelin ensheathment, during the early zebrafish development, it is possible that it receives increased synaptic input during this time compared to other neurons whose axon calibre remains relatively stable.

My findings suggest that axon calibre in the CNS is regulated either by a mechanism intrinsic to neurons as an inherent property or by the input of other neurons in the same circuit as an emergent property of the neuronal network.

As the axon calibre of RS neurons grows tremendously, even in the absence of myelin ensheathment, during the early zebrafish development, it is possible that it is regulated by a neuron intrinsic programme, input from other neurons in the same circuit, or feedback from its own synaptic targets. Global reduction of synaptic activity by TetTx has no influence on axon calibre growth in the spinal cord, as shown here, and axon branch growth has also been shown to be unimpaired by global expression of TetTx (Fredj et al., 2010). However, when synaptic vesicle release was only reduced in single neurons, axon branching was significantly decreased (Fredj et al. 2010), indicating that axonal phenotypes might only emerge in an activity competitive environment. It will be interesting to investigate the total number of synapses in the individual neurons fated for myelination and those that remain

unmyelinated with their axon calibre and myelination status in order to elucidate whether their functional activity correlates with these axonal features. Co-labeling of pre- and postsynaptic sides could be achieved by using the synaptophysin-GFP (Koester and Fraser, 2001; Meyer and Smith, 2006) and psd95-gfp (Arnold and Clapham, 1999; Niell et al., 2004) fusion proteins. If there is a functional correlation with axon calibre, it would be intriguing to manipulate the firing rate of specific axonal circuits that have been characterized, either by decrease of synaptic input by TetTx mosaic expression or by optogenetic stimulation of these circuits, and monitor the respective axon calibre of the neurons in these circuits. These manipulations will reveal whether the calibre of an axon is an inherent property of individual neurons or an emergent property of the neuronal network.

5.2 The mechanism by which synaptic activity can regulate the extent of myelination in vivo

High resolution imaging of live CNS myelin formation is beginning to elucidate the cellular mechanism behind myelination (Almeida et al., 2011; Czopka etal., 2013). Oligodendrocytes have been shown to repeatedly extend and retract their processes searching for axons to myelinate, but initiate formation of all of their sheaths within a short time period of only a few hours after the formation of the first myelin sheath (Czopka et al., 2013). Furthermore, the experimental addition of supernumery large calibre Mauthner axons in the zebrafish spinal cord showed that oligodendrocytes can form an increased number of myelin sheaths per cell (Almeida et al., 2011), demonstrating that the myelinating potential of oligodendrocytes is plastic and that their myelinating potential can be influenced by axonal cues. In the absence of synaptic vesicle release, oligodendrocytes form fewer myelin sheaths per cell, indicating that just as oligodendrocyte can be induced to form more myelin sheaths per cell in the presence of supernumery axons (Almeida et al., 2011), they form fewer myelin sheath in the absence of synaptic vesicle release. These findings indicate that the extent of myelin sheaths produced per oligodendrocytes can be influenced by axonal cues and that axonal synaptic vesicle release is one of the axonal cues.

Furthermore, I could show that the cellular mechanism by which synaptic activity can regulate the extent of myelination is the reduction of axon-oligodendrocyte contacts prior to myelin ensheathment. The initial reduction in axon-oligodendrocyte contacts in TetTx treated animals indicates that one of the mechanisms by which myelinating oligodendrocytes choose the axons they myelinate might be the synaptic vesicle mediated release of neurotransmitters.

It will be intriguing to elucidate the precise cellular mechanism behind the synaptic vesicle mediated axon choice during myelination, e.g. how the synaptic vesicle mediated neurotransmitter release can induce the axon-oligodendrocyte contact that leads to axon ensheathment. Oligodendroglial have been found to receive functional glutamatergic synapses (Bergles et al. 2010, De Biase et al. 2010, Ge et al., 2009; Kukley et al. 2008 and 2010) and GABAergic synapses (Lin & Bergles, 2003) from axons, which can elicit excitatory postsynaptic currents in OPCs in response to spontaneous and evoked activity from glutamatergic neurons (Bergles et al., 2000 Kukley et al., 2007 Ziskin et al., 2007 Lin et al., 2005; Karatodir et al.,2008 Li et al., 2012) and GABAergic neurons (Lin and Bergles, 2003, Jabs et al., 2005). Thus, the neurotransmitter mediated mechanism by which myelinating oligodendrocytes choose the axons they myelinate could either be synaptic or extra-synaptic, or a combination of both. If extra-synaptic, the role of the neurotransmitters released through synaptic vesicle exocytosis into the extracellular space might be the guidance of the exploratory oligodendrocyte process to the active axon prior to axon-oligodendrocyte contact and axon ensheathment. Synaptic axon-oligodendroglial interactions mediated by synaptic neurotransmitter release, on the other hand, might facilitate prolonged axon-oligodendrocyte contact and the actual axon ensheathment. Of course, it is also conceivable that the extra-synaptic neurotransmitter release might attract the exploratory oligodendrocyte process towards the active axon, where a synaptic connection is established prior to or during axon ensheathment. The time and pixel resolution of my time-lapse analysis was limited and unfortunately did not allow a conclusion whether axon-oligodendrocyte contact was reduced in the absence of synaptic vesicle release due to a decrease in exploratory process extension towards axons or due to a decrease in potential synaptic connections established prior to ensheathment. Future analysis will include high resolution live imaging of calcium

currents throughout the oligodendrocyte lineage using the genetically encoded calcium indicator GCaMP (Akerboom et al., 2012; Tallini et al., 2006; Tian et al., 2009; Del Bene et al., 2010) and co-labeling of pre- and postsynaptic sides using the synaptophysin-GFP (Koster and Fraser, 2001; Mayer and Smith, 2006) and psd95-gfp (Arnold and Clapham, 1999; Niell et al., 2004) fusion proteins, respectively, in order to label axon-oligodendroglial synapse when it occurs throughout the oligodendrocyte lineage. This might reveal whether synaptic vesicle release is required for the exploratory process extension prior to axon-oligodendrocyte contact or for the establishment of a synaptic axon-oligodendroglia connections leading to prolonged axon-oligodendrocyte contact and axon ensheathment. Furthermore, such analyses would allow investigation of whether the function of the axon-oligodendroglia synapse is limited to the period prior to or during initial axonal contact and ensheathment or whether functional vesicle release mediated axon-oligodendrocyte interactions underlie myelin sheath growth after ensheathment. Live calcium imaging in oligodendrocytes will also be extremely useful in pharmacological assays in which the oligodendrocyte response to the application of different neurotransmitters will be assessed during axon selection and myelin sheath formation. A candidate neurotransmitter that has been implied in regulating the extent of myelin sheath formation is glutamate. Glutamate has been shown to bind to the NMDA receptor in oligodendrocytes and thereby activate downstream signalling pathways involving tyrosine Fyn kinase, resulting in increased local translation of mbp (Wake et al., 2011). However, the functional relevance of NMDA receptor mediated signalling in vivo is unclear as the genetic ablation of the functional subunit of the NMDA receptor did not lead to a defect in the onset or extent of myelination (De Biase et al., 2011). It is possible that AMPA receptor signalling could have compensated for the loss of function of NMDA receptors during oligodendrocyte lineage progression. Other neurotransmitters, such as glycine, GABA, serotonin and dopamine, could also be involved during axon-oligodendrocyte interactions and it will be intriguing to identify which of the different neurotransmitters might play a role in the axon selection during myelination and to elucidate whether they perform different functions in this mechanism.

Overall, further analyses are needed in order to identify the neurotransmitter involved during the synaptic vesicle dependent regulation of myelin sheath formation and elucidate the underlying molecular mechanisms.

5.3 Concluding remarks and general future directions

In my thesis, I could demonstrate that axon calibre growth in the zebrafish spinal cord occurs independently of extrinsic signals provided by oligodendrocytes and myelin ensheathment and must therefore either be regulated by a neuron intrinsic programme, input from other neurons in the same circuit, or indeed feedback from its own synaptic targets. Furthermore, I described some of the axon properties in myelinated and unmyelinated axons and established that axon calibre as well as synaptic activity are axon properties that influence axon selection during myelination. I could also show that synaptic activity can regulate the extent of myelination by determining the number of myelin sheaths formed per oligodendrocyte and is therefore one of the factors regulating the myelinating capacity of oligodendrocytes. And lastly, I could show that myelin sheath growth is influenced by axonal synaptic vesicle release, indicating that myelin sheath growth can be regulated by local axonal signals.

It remains to be elucidated whether the myelin extent per oligodendrocyte could be increased by neuronal activity. Manipulations, such as the optogenetic stimulation of specific neuronal circuits as described above that might induce the myelination of previously unmyelinated neurons or induce hypermyelination in neurons normally fated for myelination, will reveal whether neuronal activity can also positively regulate the myelinating capacity of oligodendrocytes. Zebrafish are an ideal model system to study the effects of increased neuronal activity on oligodendrocyte behaviour at a cellular resolution, due to their rapid, external development and transparency during larval stages (Kimmel et al., 1990; Nuesslein-Volhard and Dahm, 2002). Furthermore, optogenetic manipulation of specific circuits has already been successfully applied in zebrafish and motor function has either been stimulated by the expression of the light gated channel LiGluR (Wyart et al., 2009) as well as channelrhodopsin (Douglass et al., 2008; Arrenberg et al., 2009; Schoonheim et al., 2010) or has been silenced by expression of halorhodopsin (Arrenberg et al., 2009)

(as reviewed in Baier and Scott, 2009; Del Bene and Wyart, 2012). If increasing neuronal activity and thereby synaptic vesicle release will increase the extent of myelin sheaths per oligodendrocytes as well as the myelin sheath growth over time, this could have important implications for clinical research. Future myelin repair strategies in demyelinating diseases might exploit the myelin inducing properties of synaptic vesicle release.

Furthermore, the axon-oligodendrocyte signalling pathways activated by local synaptic vesicle release also remain to be clarified. Another important experiment in the future will be to identify the neurotransmitter involved through monitoring calcium currents in oligodendrocytes by GCaMP imaging during pharmacological application of candidate neurotransmitters. This will help to elucidate the down-stream signalling pathway in oligodendrocytes during the activity dependent mode of myelination in future research.

Additionally, future experiments will include genetic and chemical screens in zebrafish in order to identify other axonal signals involved in the axon-oligodendrocyte signalling during myelination. Such screens, using forward genetic approaches or targeted reverse genetics might identify novel axon-oligodendrocyte signals that regulate axonal selection during myelination in the absence of synaptic vesicle release. The Lyons group is currently using a forward genetic screen to identify unknown axon-oligodendrocyte signals that might also modulate, or is perhaps even essential for, CNS myelination. These signals will perhaps elucidate the axon-oligodendrocyte interactions behind the activity independent mode of myelination in the absence of synaptic vesicle release.

Findings from the above described experiments could then be extrapolated and applied to mammalian systems, as myelin structure and oligodendrocyte behaviour is highly conserved between zebrafish and mammals. Thus, conclusions about axonal selection during myelination and factors involved drawn from zebrafish experiments will help to refine the targeted experimental design in rodent models.

6. References

Aggarwal, S., L. Yurlova and M. Simons. "Central Nervous System Myelin: Structure, Synthesis and Assembly." *Trends Cell Biol* 21, no. 10 (2011): 585-93.

Aguayo, A. J., L. Charron and G. M. Bray. "Potential of Schwann Cells from Unmyelinated Nerves to Produce Myelin: A Quantitative Ultrastructural and Radiographic Study." *J Neurocytol* 5, no. 8 (1976): 565-73.

Aguirre, A., J. L. Dupree, J. M. Mangin and V. Gallo. "A Functional Role for Egfr Signaling in Myelination and Remyelination." *Nat Neurosci* 10, no. 8 (2007): 990-1002.

Akerboom, J., T. W. Chen, T. J. Wardill, L. Tian, J. S. Marvin, S. Mutlu, N. C. Calderon, F. Esposti, B. G. Borghuis, X. R. Sun, A. Gordus, M. B. Orger, R. Portugues, F. Engert, J. J. Macklin, A. Filosa, A. Aggarwal, R. A. Kerr, R. Takagi, S. Kracun, E. Shigetomi, B. S. Khakh, H. Baier, L. Lagnado, S. S. Wang, C. I. Bargmann, B. E. Kimmel, V. Jayaraman, K. Svoboda, D. S. Kim, E. R. Schreiter and L. L. Looger. "Optimization of a Gcamp Calcium Indicator for Neural Activity Imaging." *J Neurosci* 32, no. 40 (2012): 13819-40.

Alberts, P., R. Rudge, T. Irinopoulou, L. Danglot, C. Gauthier-Rouviere and T. Galli. "Cdc42 and Actin Control Polarized Expression of Ti-Vamp Vesicles to Neuronal Growth Cones and Their Fusion with the Plasma Membrane." *Mol Biol Cell* 17, no. 3 (2006): 1194-203.

Almeida, R. G., T. Czopka, C. Ffrench-Constant and D. A. Lyons. "Individual Axons Regulate the Myelinating Potential of Single Oligodendrocytes in Vivo." *Development* 138, no. 20 (2011): 4443-50.

Almeida, R. G. and D. A. Lyons. "On the Resemblance of Synapse Formation and Cns Myelination." *Neuroscience*, (2013).

Althaus, H. H., H. Montz, V. Neuhoff and P. Schwartz. "Isolation and Cultivation of Mature Oligodendroglial Cells." *Naturwissenschaften* 71, no. 6 (1984): 309-15.

Altman, J. and Bayer, S. A. " Development of the Cerebellar System: In Relation to Its Evolution, Structure and Functions." *Boca Raton, FL: CRC Press.* , (1997).

Arnold, D. B. and D. E. Clapham. "Molecular Determinants for Subcellular Localization of Psd-95 with an Interacting K+ Channel." *Neuron* 23, no. 1 (1999): 149-57.

Arrenberg, A. B., F. Del Bene and H. Baier. "Optical Control of Zebrafish Behavior with Halorhodopsin." *Proc Natl Acad Sci U S A* 106, no. 42 (2009): 17968-73.

Arroyo, E. J. and S. S. Scherer. "On the Molecular Architecture of Myelinated Fibers." *Histochem Cell Biol* 113, no. 1 (2000): 1-18.

Asakawa, K. and K. Kawakami. "Targeted Gene Expression by the Gal4-Uas System in Zebrafish." *Dev Growth Differ* 50, no. 6 (2008): 391-9.

Auman, H. J., H. Coleman, H. E. Riley, F. Olale, H. J. Tsai and D. Yelon. "Functional Modulation of Cardiac Form through Regionally Confined Cell Shape Changes." *PLoS Biol* 5, no. 3 (2007): e53.

Baier, H. and E. K. Scott. "Genetic and Optical Targeting of Neural Circuits and Behavior--Zebrafish in the Spotlight." *Curr Opin Neurobiol* 19, no. 5 (2009): 553-60.

Balm, Paul H. M. and Diet GrÖNeveld. "The Melanin-Concentrating Hormone System in Fisha." *Annals of the New York Academy of Sciences* 839, no. 1 (1998): 205-209.

Barnett, M. W. and P. M. Larkman. "The Action Potential." *Pract Neurol* 7, no. 3 (2007): 192-7.

Barres, B. A. and M. C. Raff. "Proliferation of Oligodendrocyte Precursor Cells Depends on Electrical Activity in Axons." *Nature* 361, no. 6409 (1993): 258-260.

Barros, C. S., T. Nguyen, K. S. Spencer, A. Nishiyama, H. Colognato and U. Muller. "Beta1 Integrins Are Required for Normal Cns Myelination and Promote Akt-Dependent Myelin Outgrowth." *Development* 136, no. 16 (2009): 2717-24.

Barry, D. M., W. Stevenson, B. G. Bober, P. J. Wiese, J. M. Dale, G. S. Barry, N. S. Byers, J. D. Strope, R. Chang, D. J. Schulz, S. Shah, N. A. Calcutt, Y. Gebremichael and M. L. Garcia. "Expansion of Neurofilament Medium C Terminus Increases Axonal Diameter Independent of Increases in Conduction Velocity or Myelin Thickness." *J Neurosci* 32, no. 18 (2012): 6209-19.

Bartsch, S., D. Montag, M. Schachner and U. Bartsch. "Increased Number of Unmyelinated Axons in Optic Nerves of Adult Mice Deficient in the Myelin-Associated Glycoprotein (Mag)." *Brain Res* 762, no. 1-2 (1997): 231-4.

Basser, P. J., J. Mattiello and D. LeBihan. "Mr Diffusion Tensor Spectroscopy and Imaging." *Biophys J* 66, no. 1 (1994): 259-67.

Bastmeyer, M. and D. D. O'Leary. "Dynamics of Target Recognition by Interstitial Axon Branching Along Developing Cortical Axons." *J Neurosci* 16, no. 4 (1996): 1450-9.

Bauer, N. G., C. Richter-Landsberg and C. Ffrench-Constant. "Role of the Oligodendroglial Cytoskeleton in Differentiation and Myelination." *Glia* 57, no. 16 (2009): 1691-705.

Baumann, N. and D. Pham-Dinh. "Biology of Oligodendrocyte and Myelin in the Mammalian Central Nervous System." *Physiol Rev* 81, no. 2 (2001): 871-927.

Beaulieu, C. "The Basis of Anisotropic Water Diffusion in the Nervous System - a Technical Review." *NMR Biomed* 15, no. 7-8 (2002): 435-55.

Ben Fredj, N., S. Hammond, H. Otsuna, C. B. Chien, J. Burrone and M. P. Meyer. "Synaptic Activity and Activity-Dependent Competition Regulates Axon Arbor Maturation, Growth Arrest, and Territory in the Retinotectal Projection." *J Neurosci* 30, no. 32 (2010): 10939-51.

Bengtsson, S. L., Z. Nagy, S. Skare, L. Forsman, H. Forssberg and F. Ullen. "Extensive Piano Practicing Has Regionally Specific Effects on White Matter Development." *Nat Neurosci* 8, no. 9 (2005): 1148-50.

Bergles, D. E., R. Jabs and C. Steinhauser. "Neuron-Glia Synapses in the Brain." *Brain Res Rev* 63, no. 1-2 (2010): 130-7.

Bergles, D. E., J. D. Roberts, P. Somogyi and C. E. Jahr. "Glutamatergic Synapses on Oligodendrocyte Precursor Cells in the Hippocampus." *Nature* 405, no. 6783 (2000): 187-91.

Bernhardt, R. R., A. B. Chitnis, L. Lindamer and J. Y. Kuwada. "Identification of Spinal Neurons in the Embryonic and Larval Zebrafish." *J Comp Neurol* 302, no. 3 (1990): 603-16.

Berry, M. "Post-Injury Myelin-Breakdown Products Inhibit Axonal Growth: An Hypothesis to Explain the Failure of Axonal Regeneration in the Mammalian Central Nervous System." *Bibl Anat*, no. 23 (1982): 1-11.

Berthold, C. H. and M. Rydmark. "Electron Microscopic Serial Section Analysis of Nodes of Ranvier in Lumbosacral Spinal Roots of the Cat: Ultrastructural Organization of Nodal Compartments in Fibres of Different Sizes." *J Neurocytol* 12, no. 3 (1983): 475-505.

Bierman, H. S., S. J. Zottoli and M. E. Hale. "Evolution of the Mauthner Axon Cap." *Brain Behav Evol* 73, no. 3 (2009): 174-87.

Bilimoria, P. M. and A. Bonni. "Molecular Control of Axon Branching." *Neuroscientist* 19, no. 1 (2013): 16-24.

Boggs, J. M. "Myelin Basic Protein: A Multifunctional Protein." *Cell Mol Life Sci* 63, no. 17 (2006): 1945-61.

Boiko, T., A. Van Wart, J. H. Caldwell, S. R. Levinson, J. S. Trimmer and G. Matthews. "Functional Specialization of the Axon Initial Segment by Isoform-Specific Sodium Channel Targeting." *J Neurosci* 23, no. 6 (2003): 2306-13.

Boulanger, J. J. and C. Messier. "From Precursors to Myelinating Oligodendrocytes: Contribution of Intrinsic and Extrinsic Factors to White Matter Plasticity in the Adult Brain." *Neuroscience* 269, (2014): 343-66.

Bowser, D. N. and B. S. Khakh. "Two Forms of Single-Vesicle Astrocyte Exocytosis Imaged with Total Internal Reflection Fluorescence Microscopy." *Proc Natl Acad Sci U S A* 104, no. 10 (2007): 4212-7.

Bradel, E. J. and F. P. Prince. "Cultured Neonatal Rat Oligodendrocytes Elaborate Myelin Membrane in the Absence of Neurons." *J Neurosci Res* 9, no. 4 (1983): 381-92.

Brinkmann, B. G., A. Agarwal, M. W. Sereda, A. N. Garratt, T. Muller, H. Wende, R. M. Stassart, S. Nawaz, C. Humml, V. Velanac, K. Radyushkin, S. Goebbels, T. M. Fischer, R. J. Franklin, C. Lai, H. Ehrenreich, C. Birchmeier, M. H. Schwab and K. A. Nave. "Neuregulin-1/Erbb Signaling Serves Distinct Functions in Myelination of the Peripheral and Central Nervous System." *Neuron* 59, no. 4 (2008): 581-95.

Briscoe, J., A. Pierani, T. M. Jessell and J. Ericson. "A Homeodomain Protein Code Specifies Progenitor Cell Identity and Neuronal Fate in the Ventral Neural Tube." *Cell* 101, no. 4 (2000): 435-45.

Brosamle, C. and M. E. Halpern. "Characterization of Myelination in the Developing Zebrafish." *Glia* 39, no. 1 (2002): 47-57.

Buckley, C. E., A. Marguerie, W. K. Alderton and R. J. Franklin. "Temporal Dynamics of Myelination in the Zebrafish Spinal Cord." *Glia* 58, no. 7 (2010): 802-12.

Bujalka, H., M. Koenning, S. Jackson, V. M. Perreau, B. Pope, C. M. Hay, S. Mitew, A. F. Hill, Q. R. Lu, M. Wegner, R. Srinivasan, J. Svaren, M. Willingham, B. A. Barres and B. Emery. "Myrf Is a Membrane-Associated Transcription Factor That Autoproteolytically Cleaves to Directly Activate Myelin Genes." *PLoS Biol* 11, no. 8 (2013): e1001625.

Bunge, M. B., R. P. Bunge and G. D. Pappas. "Electron Microscopic Demonstration of Connections between Glia and Myelin Sheaths in the Developing Mammalian Central Nervous System." *J Cell Biol* 12, (1962): 448-53.

Bunge, M.B.; Bunge, R.P. and Ris H. "Ultrastructural Study of Remyelination in an Experimental Lesion in Adult Cat Spinal Cord." *J Biophys Biochem Cytol*, no. 10 (1961): 67–94.

Bunge, R. P. "Glial Cells and the Central Myelin Sheath." *Physiol Rev* 48, no. 1 (1968): 197-251.

Cahoy, J. D., B. Emery, A. Kaushal, L. C. Foo, J. L. Zamanian, K. S. Christopherson, Y. Xing, J. L. Lubischer, P. A. Krieg, S. A. Krupenko, W. J. Thompson and B. A. Barres. "A Transcriptome Database for Astrocytes, Neurons, and Oligodendrocytes: A New Resource for Understanding Brain Development and Function." *J Neurosci* 28, no. 1 (2008): 264-78.

Cai, H., K. Reinisch and S. Ferro-Novick. "Coats, Tethers, Rabs, and Snares Work Together to Mediate the Intracellular Destination of a Transport Vesicle." *Dev Cell* 12, no. 5 (2007): 671-82.

Camara, J., Z. Wang, C. Nunes-Fonseca, H. C. Friedman, M. Grove, D. L. Sherman, N. H. Komiyama, S. G. Grant, P. J. Brophy, A. Peterson and C. ffrench-Constant. "Integrin-Mediated Axoglial Interactions Initiate Myelination in the Central Nervous System." *J Cell Biol* 185, no. 4 (2009): 699-712.

Caroni, P. and M. E. Schwab. "Two Membrane Protein Fractions from Rat Central Myelin with Inhibitory Properties for Neurite Growth and Fibroblast Spreading." *J Cell Biol* 106, no. 4 (1988): 1281-8.

Catterall, W. A. "The Molecular Basis of Neuronal Excitability." *Science* 223, no. 4637 (1984): 653-61.

Cavaliere, F., M. Benito-Munoz, M. Panicker and C. Matute. "Nmda Modulates Oligodendrocyte Differentiation of Subventricular Zone Cells through Pkc Activation." *Front Cell Neurosci* 7, (2013): 261.

Cavaliere, F., O. Urra, E. Alberdi and C. Matute. "Oligodendrocyte Differentiation from Adult Multipotent Stem Cells Is Modulated by Glutamate." *Cell Death Dis* 3, (2012): e268.

Chan, J. R., T. A. Watkins, J. M. Cosgaya, C. Zhang, L. Chen, L. F. Reichardt, E. M. Shooter and B. A. Barres. "Ngf Controls Axonal Receptivity to Myelination by Schwann Cells or Oligodendrocytes." *Neuron* 43, no. 2 (2004): 183-91.

Charles, P., R. Reynolds, D. Seilhean, G. Rougon, M. S. Aigrot, A. Niezgoda, B. Zalc and C. Lubetzki. "Re-Expression of Psa-Ncam by Demyelinated Axons: An Inhibitor of Remyelination in Multiple Sclerosis?" *Brain* 125, no. Pt 9 (2002): 1972-9.

Chen, M. S., A. B. Huber, M. E. van der Haar, M. Frank, L. Schnell, A. A. Spillmann, F. Christ and M. E. Schwab. "Nogo-a Is a Myelin-Associated Neurite Outgrowth Inhibitor and an Antigen for Monoclonal Antibody in-1." *Nature* 403, no. 6768 (2000): 434-9.

Chen, S., C. Hall and J. T. Barbieri. "Substrate Recognition of Vamp-2 by Botulinum Neurotoxin B and Tetanus Neurotoxin." *J Biol Chem* 283, no. 30 (2008): 21153-9.

Chen, T. W., T. J. Wardill, Y. Sun, S. R. Pulver, S. L. Renninger, A. Baohan, E. R. Schreiter, R. A. Kerr, M. B. Orger, V. Jayaraman, L. L. Looger, K. Svoboda and D. S. Kim. "Ultrasensitive Fluorescent Proteins for Imaging Neuronal Activity." *Nature* 499, no. 7458 (2013): 295-300.

Chen, Y., H. Wu, S. Wang, H. Koito, J. Li, F. Ye, J. Hoang, S. S. Escobar, A. Gow, H. A. Arnett, B. D. Trapp, N. J. Karandikar, J. Hsieh and Q. R. Lu. "The Oligodendrocyte-Specific G Protein-Coupled Receptor Gpr17 Is a Cell-Intrinsic Timer of Myelination." *Nat Neurosci* 12, no. 11 (2009): 1398-406.

Ching, W., G. Zanazzi, S. R. Levinson and J. L. Salzer. "Clustering of Neuronal Sodium Channels Requires Contact with Myelinating Schwann Cells." *J Neurocytol* 28, no. 4-5 (1999): 295-301.

Chong, S. Y., S. S. Rosenberg, S. P. Fancy, C. Zhao, Y. A. Shen, A. T. Hahn, A. W. McGee, X. Xu, B. Zheng, L. I. Zhang, D. H. Rowitch, R. J. Franklin, Q. R. Lu and J. R. Chan. "Neurite Outgrowth Inhibitor Nogo-a Establishes Spatial Segregation and Extent of Oligodendrocyte Myelination." *Proc Natl Acad Sci U S A* 109, no. 4 (2012): 1299-304.

Clarke, J. D., B. P. Hayes, S. P. Hunt and A. Roberts. "Sensory Physiology, Anatomy and Immunohistochemistry of Rohon-Beard Neurones in Embryos of Xenopus Laevis." *J Physiol* 348, (1984): 511-25.

Cohen, S. and M. E. Greenberg. "Communication between the Synapse and the Nucleus in Neuronal Development, Plasticity, and Disease." *Annu Rev Cell Dev Biol* 24, (2008): 183-209.

Cole, J. S., A. Messing, J. Q. Trojanowski and V. M. Lee. "Modulation of Axon Diameter and Neurofilaments by Hypomyelinating Schwann Cells in Transgenic Mice." *J Neurosci* 14, no. 11 Pt 2 (1994): 6956-66.

Colello, R. J., L. R. Devey, E. Imperato and U. Pott. "The Chronology of Oligodendrocyte Differentiation in the Rat Optic Nerve: Evidence for a Signaling Step Initiating Myelination in the Cns." *J Neurosci* 15, no. 11 (1995): 7665-72.

Colello, R. J., U. Pott and M. E. Schwab. "The Role of Oligodendrocytes and Myelin on Axon Maturation in the Developing Rat Retinofugal Pathway." *J Neurosci* 14, no. 5 Pt 1 (1994): 2594-605.

Colello, R. J. and M. E. Schwab. "A Role for Oligodendrocytes in the Stabilization of Optic Axon Numbers." *J Neurosci* 14, no. 11 Pt 1 (1994): 6446-52.

Colman, D. R., G. Kreibich, A. B. Frey and D. D. Sabatini. "Synthesis and Incorporation of Myelin Polypeptides into Cns Myelin." *J Cell Biol* 95, no. 2 Pt 1 (1982): 598-608.

Crippa, D., U. Schenk, M. Francolini, P. Rosa, C. Verderio, M. Zonta, T. Pozzan, M. Matteoli and G. Carmignoto. "Synaptobrevin2-Expressing Vesicles in Rat Astrocytes: Insights into Molecular Characterization, Dynamics and Exocytosis." *J Physiol* 570, no. Pt 3 (2006): 567-82.

Czopka, T., C. Ffrench-Constant and D. A. Lyons. "Individual Oligodendrocytes Have Only a Few Hours in Which to Generate New Myelin Sheaths in Vivo." *Dev Cell* 25, no. 6 (2013): 599-609.

Czopka, T. and D. A. Lyons. "Dissecting Mechanisms of Myelinated Axon Formation Using Zebrafish." *Methods Cell Biol* 105, (2011): 25-62.

Dangata, Y. Y. and M. H. Kaufman. "Morphometric Analysis of the Postnatal Mouse Optic Nerve Following Prenatal Exposure to Alcohol." *J Anat* 191 (Pt 1), (1997): 49-56.

Davis, J. Q., S. Lambert and V. Bennett. "Molecular Composition of the Node of Ranvier: Identification of Ankyrin-Binding Cell Adhesion Molecules Neurofascin (Mucin+/Third Fniii Domain-) and Nrcam at Nodal Axon Segments." *J Cell Biol* 135, no. 5 (1996): 1355-67.

De Biase, L. M., S. H. Kang, E. G. Baxi, M. Fukaya, M. L. Pucak, M. Mishina, P. A. Calabresi and D. E. Bergles. "Nmda Receptor Signaling in Oligodendrocyte Progenitors Is Not Required for Oligodendrogenesis and Myelination." *J Neurosci* 31, no. 35 (2011): 12650-62.

De Biase, L. M., A. Nishiyama and D. E. Bergles. "Excitability and Synaptic Communication within the Oligodendrocyte Lineage." *J Neurosci* 30, no. 10 (2010): 3600-11.

de Waegh, S. and S. T. Brady. "Altered Slow Axonal Transport and Regeneration in a Myelin-Deficient Mutant Mouse: The Trembler as an in Vivo Model for Schwann Cell-Axon Interactions." *J Neurosci* 10, no. 6 (1990): 1855-65.

de Waegh, S. M., V. M. Lee and S. T. Brady. "Local Modulation of Neurofilament Phosphorylation, Axonal Caliber, and Slow Axonal Transport by Myelinating Schwann Cells." *Cell* 68, no. 3 (1992): 451-63.

Del Bene, F. and C. Wyart. "Optogenetics: A New Enlightenment Age for Zebrafish Neurobiology." *Dev Neurobiol* 72, no. 3 (2012): 404-14.

Del Bene, F., C. Wyart, E. Robles, A. Tran, L. Looger, E. K. Scott, E. Y. Isacoff and H. Baier. "Filtering of Visual Information in the Tectum by an Identified Neural Circuit." *Science* 330, no. 6004 (2010): 669-73.

Demerens, C., B. Stankoff, M. Logak, P. Anglade, B. Allinquant, F. Couraud, B. Zalc and C. Lubetzki. "Induction of Myelination in the Central Nervous System by Electrical Activity." *Proc Natl Acad Sci U S A* 93, no. 18 (1996): 9887-92.

Dougherty, K. D., C. F. Dreyfus and I. B. Black. "Brain-Derived Neurotrophic Factor in Astrocytes, Oligodendrocytes, and Microglia/Macrophages after Spinal Cord Injury." *Neurobiol Dis* 7, no. 6 Pt B (2000): 574-85.

Douglass, A. D., S. Kraves, K. Deisseroth, A. F. Schier and F. Engert. "Escape Behavior Elicited by Single, Channelrhodopsin-2-Evoked Spikes in Zebrafish Somatosensory Neurons." *Curr Biol* 18, no. 15 (2008): 1133-7.

Duncan, D. "The Importance of Diameter as a Factor in Myelination." *Science* 79, no. 2051 (1934): 363.

Dupree, J. L., Girault, J. A. and Popko, B. "Axo-Glial Interactions Regulate the Localization of Axonal Paranodal Proteins." *J. Cell Biol.*, no. 147 (1999): 1145–1152.

Eaton, R. C., R. K. Lee and M. B. Foreman. "The Mauthner Cell and Other Identified Neurons of the Brainstem Escape Network of Fish." *Prog Neurobiol* 63, no. 4 (2001): 467-85.

Elder, G. A., V. L. Friedrich, Jr., P. Bosco, C. Kang, A. Gourov, P. H. Tu, V. M. Lee and R. A. Lazzarini. "Absence of the Mid-Sized Neurofilament Subunit Decreases Axonal Calibers, Levels of Light Neurofilament (Nf-L), and Neurofilament Content." *J Cell Biol* 141, no. 3 (1998): 727-39.

Elder, G. A., V. L. Friedrich, Jr., C. Kang, P. Bosco, A. Gourov, P. H. Tu, B. Zhang, V. M. Lee and R. A. Lazzarini. "Requirement of Heavy Neurofilament Subunit in the Development of Axons with Large Calibers." *J Cell Biol* 143, no. 1 (1998): 195-205.

Elder, G. A., V. L. Friedrich, Jr. and R. A. Lazzarini. "Schwann Cells and Oligodendrocytes Read Distinct Signals in Establishing Myelin Sheath Thickness." *J Neurosci Res* 65, no. 6 (2001): 493-9.

Elmore, S. "Apoptosis: A Review of Programmed Cell Death." *Toxicol Pathol* 35, no. 4 (2007): 495-516.

Emery, B. "Regulation of Oligodendrocyte Differentiation and Myelination." *Science* 330, no. 6005 (2010): 779-82.

Emery, B., D. Agalliu, J. D. Cahoy, T. A. Watkins, J. C. Dugas, S. B. Mulinyawe, A. Ibrahim, K. L. Ligon, D. H. Rowitch and B. A. Barres. "Myelin Gene Regulatory Factor Is a Critical Transcriptional Regulator Required for Cns Myelination." *Cell* 138, no. 1 (2009): 172-85.

Falk, J., C. Bonnon, J. A. Girault and C. Faivre-Sarrailh. "F3/Contactin, a Neuronal Cell Adhesion Molecule Implicated in Axogenesis and Myelination." *Biol Cell* 94, no. 6 (2002): 327-34.

Fancy, S. P., S. E. Baranzini, C. Zhao, D. I. Yuk, K. A. Irvine, S. Kaing, N. Sanai, R. J. Franklin and D. H. Rowitch. "Dysregulation of the Wnt Pathway Inhibits Timely Myelination and Remyelination in the Mammalian Cns." *Genes Dev* 23, no. 13 (2009): 1571-85.

Feldmann, A., J. Amphornrat, M. Schonherr, C. Winterstein, W. Mobius, T. Ruhwedel, L. Danglot, K. A. Nave, T. Galli, D. Bruns, J. Trotter and E. M. Kramer-Albers. "Transport of the Major Myelin Proteolipid Protein Is Directed by Vamp3 and Vamp7." *J Neurosci* 31, no. 15 (2011): 5659-72.

Feldmann, A., C. Winterstein, R. White, J. Trotter and E. M. Kramer-Albers. "Comprehensive Analysis of Expression, Subcellular Localization, and Cognate Pairing of Snare Proteins in Oligodendrocytes." *J Neurosci Res* 87, no. 8 (2009): 1760-72.

Fetcho, J. R. and S. Higashijima. "Optical and Genetic Approaches toward Understanding Neuronal Circuits in Zebrafish." *Integr Comp Biol* 44, no. 1 (2004): 57-70.

Fields, R. D. "Myelination: An Overlooked Mechanism of Synaptic Plasticity?" *Neuroscientist* 11, no. 6 (2005): 528-31.

Fields, R. D. "Myelin Formation and Remodeling." *Cell* 156, no. 1-2 (2014): 15-7.

Fields, R. D. "Neuroscience. Myelin--More Than Insulation." *Science* 344, no. 6181 (2014): 264-6.

Fields, R. D. and Y. Ni. "Nonsynaptic Communication through Atp Release from Volume-Activated Anion Channels in Axons." *Sci Signal* 3, no. 142 (2010): ra73.

Filbin, M. T. "Myelin-Associated Inhibitors of Axonal Regeneration in the Adult Mammalian Cns." *Nat Rev Neurosci* 4, no. 9 (2003): 703-13.

Flynn, K. C., C. W. Pak, A. E. Shaw, F. Bradke and J. R. Bamburg. "Growth Cone-Like Waves Transport Actin and Promote Axonogenesis and Neurite Branching." *Dev Neurobiol* 69, no. 12 (2009): 761-79.

Friede, R. L. "Control of Myelin Formation by Axon Caliber (with a Model of the Control Mechanism)." *J Comp Neurol* 144, no. 2 (1972): 233-52.

Friede, R. L., J. Brzoska and U. Hartmann. "Changes in Myelin Sheath Thickness and Internode Geometry in the Rabbit Phrenic Nerve During Growth." *J Anat* 143, (1985): 103-13.

Friede, R. L. and T. Samorajski. "Myelin Formation in the Sciatic Nerve of the Rat. A Quantitative Electron Microscopic, Histochemical and Radioautographic Study." *J Neuropathol Exp Neurol* 27, no. 4 (1968): 546-70.

Friede, R. L. and T. Samorajski. "Axon Caliber Related to Neurofilaments and Microtubules in Sciatic Nerve Fibers of Rats and Mice." *Anat Rec* 167, no. 4 (1970): 379-87.

Fruhbeis, C., D. Frohlich, W. P. Kuo, J. Amphornrat, S. Thilemann, A. S. Saab, F. Kirchhoff, W. Mobius, S. Goebbels, K. A. Nave, A. Schneider, M. Simons, M. Klugmann, J. Trotter and E. M. Kramer-Albers. "Neurotransmitter-Triggered Transfer of Exosomes Mediates Oligodendrocyte-Neuron Communication." *PLoS Biol* 11, no. 7 (2013): e1001604.

Fukui, Y., S. Hayasaka, K. S. Bedi, H. S. Ozaki and Y. Takeuchi. "Quantitative Study of the Development of the Optic Nerve in Rats Reared in the Dark During Early Postnatal Life." *J Anat* 174, (1991): 37-47.

Funch, P. G., S. L. Kinsman, D. S. Faber, E. Koenig and S. J. Zottoli. "Mauthner Axon Diameter and Impulse Conduction Velocity Decrease with Growth of Goldfish." *Neurosci Lett* 27, no. 2 (1981): 159-64.

Funfschilling, U., L. M. Supplie, D. Mahad, S. Boretius, A. S. Saab, J. Edgar, B. G. Brinkmann, C. M. Kassmann, I. D. Tzvetanova, W. Mobius, F. Diaz, D. Meijer, U. Suter, B. Hamprecht, M. W. Sereda, C. T. Moraes, J. Frahm, S. Goebbels and K. A. Nave. "Glycolytic Oligodendrocytes Maintain Myelin and Long-Term Axonal Integrity." *Nature* 485, no. 7399 (2012): 517-21.

Gainey, M. A., J. R. Hurvitz-Wolff, M. E. Lambo and G. G. Turrigiano. "Synaptic Scaling Requires the Glur2 Subunit of the Ampa Receptor." *J Neurosci* 29, no. 20 (2009): 6479-89.

Gaisano, H. Y. "A Hypothesis: Snare-Ing the Mechanisms of Regulated Exocytosis and Pathologic Membrane Fusions in the Pancreatic Acinar Cell." *Pancreas* 20, no. 3 (2000): 217-26.

Gallo, G. "The Cytoskeletal and Signaling Mechanisms of Axon Collateral Branching." *Dev Neurobiol* 71, no. 3 (2011): 201-20.

Gallo, V., J. M. Mangin, M. Kukley and D. Dietrich. "Synapses on Ng2-Expressing Progenitors in the Brain: Multiple Functions?" *J Physiol* 586, no. 16 (2008): 3767-81.

Gallo, V., J. M. Zhou, C. J. McBain, P. Wright, P. L. Knutson and R. C. Armstrong. "Oligodendrocyte Progenitor Cell Proliferation and Lineage Progression Are Regulated by Glutamate Receptor-Mediated K+ Channel Block." *J Neurosci* 16, no. 8 (1996): 2659-70.

Gao, F. B., B. Durand and M. Raff. "Oligodendrocyte Precursor Cells Count Time but Not Cell Divisions before Differentiation." *Curr Biol* 7, no. 2 (1997): 152-5.

Garcia, M. L., C. S. Lobsiger, S. B. Shah, T. J. Deerinck, J. Crum, D. Young, C. M. Ward, T. O. Crawford, T. Gotow, Y. Uchiyama, M. H. Ellisman, N. A. Calcutt and D. W. Cleveland. "Nf-M Is an Essential Target for the Myelin-Directed "Outside-in" Signaling Cascade That Mediates Radial Axonal Growth." *J Cell Biol* 163, no. 5 (2003): 1011-20.

Garcia, M. L., M. V. Rao, J. Fujimoto, V. B. Garcia, S. B. Shah, J. Crum, T. Gotow, Y. Uchiyama, M. Ellisman, N. A. Calcutt and D. W. Cleveland. "Phosphorylation of Highly Conserved Neurofilament Medium Ksp Repeats Is Not Required for Myelin-Dependent Radial Axonal Growth." *J Neurosci* 29, no. 5 (2009): 1277-84.

Gary, D. S., M. Malone, P. Capestany, T. Houdayer and J. W. McDonald. "Electrical Stimulation Promotes the Survival of Oligodendrocytes in Mixed Cortical Cultures." *J Neurosci Res* 90, no. 1 (2012): 72-83.

Ge, W. P., W. Zhou, Q. Luo, L. Y. Jan and Y. N. Jan. "Dividing Glial Cells Maintain Differentiated Properties Including Complex Morphology and Functional Synapses." *Proc Natl Acad Sci U S A* 106, no. 1 (2009): 328-33.

Geren, B.B., and Schmitt, F.O. "The Structure of the Schwann Cell and Its Relation to the Axon in Certain Invertebrate Nerve Fibers." *Proceedings of the National Academy of Sciences of the United States of America*, no. 40 (1954): 863-870.

Gerst, J. E. "Snares and Snare Regulators in Membrane Fusion and Exocytosis." *Cell Mol Life Sci* 55, no. 5 (1999): 707-34.

Gibson, D. A. and L. Ma. "Developmental Regulation of Axon Branching in the Vertebrate Nervous System." *Development* 138, no. 2 (2011): 183-95.

Gibson, E. M., D. Purger, C. W. Mount, A. K. Goldstein, G. L. Lin, L. S. Wood, I. Inema, S. E. Miller, G. Bieri, J. B. Zuchero, B. A. Barres, P. J. Woo, H. Vogel and M. Monje. "Neuronal Activity Promotes Oligodendrogenesis and Adaptive Myelination in the Mammalian Brain." *Science* 344, no. 6183 (2014): 1252304.

Givogri, M. I., R. M. Costa, V. Schonmann, A. J. Silva, A. T. Campagnoni and E. R. Bongarzone. "Central Nervous System Myelination in Mice with Deficient Expression of Notch1 Receptor." *J Neurosci Res* 67, no. 3 (2002): 309-20.

Greer, P. L. and M. E. Greenberg. "From Synapse to Nucleus: Calcium-Dependent Gene Transcription in the Control of Synapse Development and Function." *Neuron* 59, no. 6 (2008): 846-60.

Griffiths, I. R., I. D. Duncan and M. McCulloch. "Shaking Pups: A Disorder of Central Myelination in the Spaniel Dog. Ii. Ultrastructural Observations on the White Matter of the Cervical Spinal Cord." *J Neurocytol* 10, no. 5 (1981): 847-58.

Groeschel, S., B. Vollmer, M. D. King and A. Connelly. "Developmental Changes in Cerebral Grey and White Matter Volume from Infancy to Adulthood." *Int J Dev Neurosci* 28, no. 6 (2010): 481-9.

Gudz, T. I., H. Komuro and W. B. Macklin. "Glutamate Stimulates Oligodendrocyte Progenitor Migration Mediated Via an Alphav Integrin/Myelin Proteolipid Protein Complex." *J Neurosci* 26, no. 9 (2006): 2458-66.

Guo, F., Y. Maeda, E. M. Ko, M. Delgado, M. Horiuchi, A. Soulika, L. Miers, T. Burns, T. Itoh, H. Shen, E. Lee, J. Sohn and D. Pleasure. "Disruption of Nmda Receptors in Oligodendroglial Lineage Cells Does Not Alter Their Susceptibility to Experimental Autoimmune Encephalomyelitis or Their Normal Development." *J Neurosci* 32, no. 2 (2012): 639-45.

Gyllensten, L. "Postnatal Development of the Visual Cortex Is Darkness (Mice)." *Acta Morphol Neerl Scand* 2, (1959): 331-45.

Gyllensten, L. and T. Malmfors. "Myelinization of the Optic Nerve and Its Dependence on Visual Function--a Quantitative Investigation in Mice." *J Embryol Exp Morphol* 11, (1963): 255-66.

Haenisch, C., H. Diekmann, M. Klinger, G. Gennarini, J. Y. Kuwada and C. A. Stuermer. "The Neuronal Growth and Regeneration Associated Cntn1 (F3/F11/Contactin) Gene Is Duplicated in Fish: Expression During Development and Retinal Axon Regeneration." *Mol Cell Neurosci* 28, no. 2 (2005): 361-74.

Hale, M. E., D. A. Ritter and J. R. Fetcho. "A Confocal Study of Spinal Interneurons in Living Larval Zebrafish." *J Comp Neurol* 437, no. 1 (2001): 1-16.

Hall, A. M. and E. D. Roberson. "Mouse Models of Alzheimer's Disease." *Brain Res Bull* 88, no. 1 (2012): 3-12.

Halloran, M. C. and K. Kalil. "Dynamic Behaviors of Growth Cones Extending in the Corpus Callosum of Living Cortical Brain Slices Observed with Video Microscopy." *J Neurosci* 14, no. 4 (1994): 2161-77.

Hammarstrom, A. K. and P. W. Gage. "Oxygen-Sensing Persistent Sodium Channels in Rat Hippocampus." *J Physiol* 529 Pt 1, (2000): 107-18.

Hao, J., C. H. Williams, M. E. Webb and C. C. Hong. "Large Scale Zebrafish-Based in Vivo Small Molecule Screen." *J Vis Exp*, no. 46 (2010).

Hardy, R. and R. Reynolds. "Neuron-Oligodendroglial Interactions During Central Nervous System Development." *J Neurosci Res* 36, no. 2 (1993): 121-6.

Harms, K. J. and A. M. Craig. "Synapse Composition and Organization Following Chronic Activity Blockade in Cultured Hippocampal Neurons." *J Comp Neurol* 490, no. 1 (2005): 72-84.

Hartline, D. K. and D. R. Colman. "Rapid Conduction and the Evolution of Giant Axons and Myelinated Fibers." *Curr Biol* 17, no. 1 (2007): R29-35.

Hayes, W. P. and R. L. Meyer. "Impulse Blockade by Intraocular Tetrodotoxin During Optic Regeneration in Goldfish: Hrp-Em Evidence That the Formation of Normal Numbers of Optic Synapses and the Elimination of Exuberant Optic Fibers Is Activity Independent." *J Neurosci* 9, no. 4 (1989): 1414-23.

He, L. and Q. R. Lu. "Coordinated Control of Oligodendrocyte Development by Extrinsic and Intrinsic Signaling Cues." *Neurosci Bull* 29, no. 2 (2013): 129-43.

Hess, A. and J. Z. Young. "The Nodes of Ranvier." *Proc R Soc Lond B Biol Sci* 140, no. 900 (1952): 301-20.

Higashijima, S., G. Mandel and J. R. Fetcho. "Distribution of Prospective Glutamatergic, Glycinergic, and Gabaergic Neurons in Embryonic and Larval Zebrafish." *J Comp Neurol* 480, no. 1 (2004): 1-18.

Higashijima, S., M. A. Masino, G. Mandel and J. R. Fetcho. "Imaging Neuronal Activity During Zebrafish Behavior with a Genetically Encoded Calcium Indicator." *J Neurophysiol* 90, no. 6 (2003): 3986-97.

Higashijima, S., M. Schaefer and J. R. Fetcho. "Neurotransmitter Properties of Spinal Interneurons in Embryonic and Larval Zebrafish." *J Comp Neurol* 480, no. 1 (2004): 19-37.

Hildebrand, C. and R. Hahn. "Relation between Myelin Sheath Thickness and Axon Size in Spinal Cord White Matter of Some Vertebrate Species." *J Neurol Sci* 38, no. 3 (1978): 421-34.

Hildebrand, C., S. Remahl, H. Persson and C. Bjartmar. "Myelinated Nerve Fibres in the Cns." *Prog Neurobiol* 40, no. 3 (1993): 319-84.

Hildebrand, C., S. Remahl and S. G. Waxman. "Axo-Glial Relations in the Retina-Optic Nerve Junction of the Adult Rat: Electron-Microscopic Observations." *J Neurocytol* 14, no. 4 (1985): 597-617.

Hoffman, P. N. and R. J. Lasek. "The Slow Component of Axonal Transport. Identification of Major Structural Polypeptides of the Axon and Their Generality among Mammalian Neurons." *J Cell Biol* 66, no. 2 (1975): 351-66.

Hoffman, P. N., R. J. Lasek, J. W. Griffin and D. L. Price. "Slowing of the Axonal Transport of Neurofilament Proteins During Development." *J Neurosci* 3, no. 8 (1983): 1694-700.

Hoffman, P. N., G. W. Thompson, J. W. Griffin and D. L. Price. "Changes in Neurofilament Transport Coincide Temporally with Alterations in the Caliber of Axons in Regenerating Motor Fibers." *J Cell Biol* 101, no. 4 (1985): 1332-40.

Hong, C. C. "Large-Scale Small-Molecule Screen Using Zebrafish Embryos." *Methods Mol Biol* 486, (2009): 43-55.

Howarth, C., P. Gleeson and D. Attwell. "Updated Energy Budgets for Neural Computation in the Neocortex and Cerebellum." *J Cereb Blood Flow Metab* 32, no. 7 (2012): 1222-32.

Hu, X., C. W. Hicks, W. He, P. Wong, W. B. Macklin, B. D. Trapp and R. Yan. "Bace1 Modulates Myelination in the Central and Peripheral Nervous System." *Nat Neurosci* 9, no. 12 (2006): 1520-5.

Huang, C. J., C. T. Tu, C. D. Hsiao, F. J. Hsieh and H. J. Tsai. "Germ-Line Transmission of a Myocardium-Specific Gfp Transgene Reveals Critical Regulatory Elements in the Cardiac Myosin Light Chain 2 Promoter of Zebrafish." *Dev Dyn* 228, no. 1 (2003): 30-40.

Hughes, E. G., S. H. Kang, M. Fukaya and D. E. Bergles. "Oligodendrocyte Progenitors Balance Growth with Self-Repulsion to Achieve Homeostasis in the Adult Brain." *Nat Neurosci* 16, no. 6 (2013): 668-76.

Hursh, J. B. "Conduction Velocity and Diameter of Nerve Fibers." *Am. J. Physiol.*, no. 127 (1939): 131-139.

Hwang, W. Y., Y. Fu, D. Reyon, M. L. Maeder, S. Q. Tsai, J. D. Sander, R. T. Peterson, J. R. Yeh and J. K. Joung. "Efficient Genome Editing in Zebrafish Using a Crispr-Cas System." *Nat Biotechnol* 31, no. 3 (2013): 227-9.

Inder, T. E. and P. S. Huppi. "In Vivo Studies of Brain Development by Magnetic Resonance Techniques." *Ment Retard Dev Disabil Res Rev* 6, no. 1 (2000): 59-67.

Innocenti, G. M., A. Vercelli and R. Caminiti. "The Diameter of Cortical Axons Depends Both on the Area of Origin and Target." *Cereb Cortex* 24, no. 8 (2014): 2178-88.

Ishibashi, T., K. A. Dakin, B. Stevens, P. R. Lee, S. V. Kozlov, C. L. Stewart and R. D. Fields. "Astrocytes Promote Myelination in Response to Electrical Impulses." *Neuron* 49, no. 6 (2006): 823-32.

Itoh, K., B. Stevens, M. Schachner and R. D. Fields. "Regulated Expression of the Neural Cell Adhesion Molecule L1 by Specific Patterns of Neural Impulses." *Science* 270, no. 5240 (1995): 1369-72.

Jabs, R., T. Pivneva, K. Huttmann, A. Wyczynski, C. Nolte, H. Kettenmann and C. Steinhauser. "Synaptic Transmission onto Hippocampal Glial Cells with Hgfap Promoter Activity." *J Cell Sci* 118, no. Pt 16 (2005): 3791-803.

Jahn, O., S. Tenzer and H. B. Werner. "Myelin Proteomics: Molecular Anatomy of an Insulating Sheath." *Mol Neurobiol* 40, no. 1 (2009): 55-72.

Jahn, R. and R. H. Scheller. "Snares--Engines for Membrane Fusion." *Nat Rev Mol Cell Biol* 7, no. 9 (2006): 631-43.

Jarjour, A. A., H. Zhang, N. Bauer, C. Ffrench-Constant and A. Williams. "In Vitro Modeling of Central Nervous System Myelination and Remyelination." *Glia* 60, no. 1 (2012): 1-12.

Jessell, T. M. "Neuronal Specification in the Spinal Cord: Inductive Signals and Transcriptional Codes." *Nat Rev Genet* 1, no. 1 (2000): 20-9.

Jessen, K. R. and R. Mirsky. "The Origin and Development of Glial Cells in Peripheral Nerves." *Nat Rev Neurosci* 6, no. 9 (2005): 671-82.

Johansen-Berg, H., V. Della-Maggiore, T. E. Behrens, S. M. Smith and T. Paus. "Integrity of White Matter in the Corpus Callosum Correlates with Bimanual Co-Ordination Skills." *Neuroimage* 36 Suppl 2, (2007): T16-21.

Johnson, D. and R. H. Quarles. "Deposition of the Myelin-Associated Glycoprotein in Specific Regions of the Developing Rat Central Nervous System." *Brain Res* 393, no. 2 (1986): 263-6.

Jontes, J. D., J. Buchanan and S. J. Smith. "Growth Cone and Dendrite Dynamics in Zebrafish Embryos: Early Events in Synaptogenesis Imaged in Vivo." *Nat Neurosci* 3, no. 3 (2000): 231-7.

Jung, D. W., E. S. Oh, S. H. Park, Y. T. Chang, C. H. Kim, S. Y. Choi and D. R. Williams. "A Novel Zebrafish Human Tumor Xenograft Model Validated for Anti-Cancer Drug Screening." *Mol Biosyst* 8, no. 7 (2012): 1930-9.

Jung, S. H., S. Kim, A. Y. Chung, H. T. Kim, J. H. So, J. Ryu, H. C. Park and C. H. Kim. "Visualization of Myelination in Gfp-Transgenic Zebrafish." *Dev Dyn* 239, no. 2 (2010): 592-7.

Kachar, B., T. Behar and M. Dubois-Dalcq. "Cell Shape and Motility of Oligodendrocytes Cultured without Neurons." *Cell Tissue Res* 244, no. 1 (1986): 27-38.

Kalaria, R. N., R. Akinyemi and M. Ihara. "Does Vascular Pathology Contribute to Alzheimer Changes?" *J Neurol Sci* 322, no. 1-2 (2012): 141-7.

Kalil, K. and E. W. Dent. "Branch Management: Mechanisms of Axon Branching in the Developing Vertebrate Cns." *Nat Rev Neurosci* 15, no. 1 (2014): 7-18.

Kaplan, M. R., A. Meyer-Franke, S. Lambert, V. Bennett, I. D. Duncan, S. R. Levinson and B. A. Barres. "Induction of Sodium Channel Clustering by Oligodendrocytes." *Nature* 386, no. 6626 (1997): 724-8.

Karadottir, R., P. Cavelier, L. H. Bergersen and D. Attwell. "Nmda Receptors Are Expressed in Oligodendrocytes and Activated in Ischaemia." *Nature* 438, no. 7071 (2005): 1162-6.

Karadottir, R., N. B. Hamilton, Y. Bakiri and D. Attwell. "Spiking and Nonspiking Classes of Oligodendrocyte Precursor Glia in Cns White Matter." *Nat Neurosci* 11, no. 4 (2008): 450-6.

Kim, E. and M. Sheng. "Pdz Domain Proteins of Synapses." *Nat Rev Neurosci* 5, no. 10 (2004): 771-81.

Kimmel, C. B., W. W. Ballard, S. R. Kimmel, B. Ullmann and T. F. Schilling. "Stages of Embryonic Development of the Zebrafish." *Dev Dyn* 203, no. 3 (1995): 253-310.

Kimmel, C. B., J. Patterson and R. O. Kimmel. "The Development and Behavioral Characteristics of the Startle Response in the Zebra Fish." *Dev Psychobiol* 7, no. 1 (1974): 47-60.

Kimmel, C. B., S. L. Powell and W. K. Metcalfe. "Brain Neurons Which Project to the Spinal Cord in Young Larvae of the Zebrafish." *J Comp Neurol* 205, no. 2 (1982): 112-27.

Kimmel, C. B., R. M. Warga and T. F. Schilling. "Origin and Organization of the Zebrafish Fate Map." *Development* 108, no. 4 (1990): 581-94.

Kirby, B. B., N. Takada, A. J. Latimer, J. Shin, T. J. Carney, R. N. Kelsh and B. Appel. "In Vivo Time-Lapse Imaging Shows Dynamic Oligodendrocyte Progenitor Behavior During Zebrafish Development." *Nat Neurosci* 9, no. 12 (2006): 1506-11.

Kirschner, D.A. and A.E. Blaurock. "Organization, Phylogenetic Variations and Dynamic Transitions of Myelin Structure." *Myelin: biology and chemistry (Martenson RE, ed*, (1992): 3–78.

Kirschner, D. A., H. Inouye, A. L. Ganser and V. Mann. "Myelin Membrane Structure and Composition Correlated: A Phylogenetic Study." *J Neurochem* 53, no. 5 (1989): 1599-609.

Knapp, P. E., W. P. Bartlett and R. P. Skoff. "Cultured Oligodendrocytes Mimic in Vivo Phenotypic Characteristics: Cell Shape, Expression of Myelin-Specific Antigens, and Membrane Production." *Dev Biol* 120, no. 2 (1987): 356-65.

Kocsis, J. D. and S. G. Waxman. "Absence of Potassium Conductance in Central Myelinated Axons." *Nature* 287, no. 5780 (1980): 348-9.

Koester, J. "Functional Consequences of Passive Membrane Properties of the Neuron. ." *Principles of Neural Science. Elsevier: New York*, (1985a): 66-86.

Koester, J. "Nongated Channels and Passive Membrane Properties of the Neuron." *Principles of Neural Science. Elsevier: New York*, (1985b): 58-65.

Kohashi, T. and Y. Oda. "Initiation of Mauthner- or Non-Mauthner-Mediated Fast Escape Evoked by Different Modes of Sensory Input." *J Neurosci* 28, no. 42 (2008): 10641-53.

Kolodziejczyk, K., A. S. Saab, K. A. Nave and D. Attwell. "Why Do Oligodendrocyte Lineage Cells Express Glutamate Receptors?" *F1000 Biol Rep* 2, (2010): 57.

Korn, H. and D. S. Faber. "The Mauthner Cell Half a Century Later: A Neurobiological Model for Decision-Making?" *Neuron* 47, no. 1 (2005): 13-28.

Koster, R. W. and S. E. Fraser. "Tracing Transgene Expression in Living Zebrafish Embryos." *Dev Biol* 233, no. 2 (2001): 329-46.

Kramer, E. M., A. Schardt and K. A. Nave. "Membrane Traffic in Myelinating Oligodendrocytes." *Microsc Res Tech* 52, no. 6 (2001): 656-71.

Kramer-Albers, E. M. and R. White. "From Axon-Glial Signalling to Myelination: The Integrating Role of Oligodendroglial Fyn Kinase." *Cell Mol Life Sci* 68, no. 12 (2011): 2003-12.

Kucenas, S., H. Snell and B. Appel. "Nkx2.2a Promotes Specification and Differentiation of a Myelinating Subset of Oligodendrocyte Lineage Cells in Zebrafish." *Neuron Glia Biol* 4, no. 2 (2008): 71-81.

Kukley, M., E. Capetillo-Zarate and D. Dietrich. "Vesicular Glutamate Release from Axons in White Matter." *Nat Neurosci* 10, no. 3 (2007): 311-20.

Kukley, M., A. Nishiyama and D. Dietrich. "The Fate of Synaptic Input to Ng2 Glial Cells: Neurons Specifically Downregulate Transmitter Release onto Differentiating Oligodendroglial Cells." *J Neurosci* 30, no. 24 (2010): 8320-31.

Kuwada, J. Y., R. R. Bernhardt and N. Nguyen. "Development of Spinal Neurons and Tracts in the Zebrafish Embryo." *J Comp Neurol* 302, no. 3 (1990): 617-28.

Kwan, K. M., E. Fujimoto, C. Grabher, B. D. Mangum, M. E. Hardy, D. S. Campbell, J. M. Parant, H. J. Yost, J. P. Kanki and C. B. Chien. "The Tol2kit: A Multisite Gateway-Based Construction Kit for Tol2 Transposon Transgenesis Constructs." *Dev Dyn* 236, no. 11 (2007): 3088-99.

Lamborghini, J. E. "Disappearance of Rohon-Beard Neurons from the Spinal Cord of Larval Xenopus Laevis." *J Comp Neurol* 264, no. 1 (1987): 47-55.

Lander, A. D. "Understanding the Molecules of Neural Cell Contacts: Emerging Patterns of Structure and Function." *Trends Neurosci* 12, no. 5 (1989): 189-95.

Lappe-Siefke, C., S. Goebbels, M. Gravel, E. Nicksch, J. Lee, P. E. Braun, I. R. Griffiths and K. A. Nave. "Disruption of Cnp1 Uncouples Oligodendroglial Functions in Axonal Support and Myelination." *Nat Genet* 33, no. 3 (2003): 366-74.

Lasek, R. J., L. Phillips, M. J. Katz and L. Autilio-Gambetti. "Function and Evolution of Neurofilament Proteins." *Ann N Y Acad Sci* 455, (1985): 462-78.

Lassmann, H., W. Bruck, C. Lucchinetti and M. Rodriguez. "Remyelination in Multiple Sclerosis." *Mult Scler* 3, no. 2 (1997): 133-6.

Lee, K. K., Y. de Repentigny, R. Saulnier, P. Rippstein, W. B. Macklin and R. Kothary. "Dominant-Negative Beta1 Integrin Mice Have Region-Specific Myelin Defects Accompanied by Alterations in Mapk Activity." *Glia* 53, no. 8 (2006): 836-44.

Lee, S., M. K. Leach, S. A. Redmond, S. Y. Chong, S. H. Mellon, S. J. Tuck, Z. Q. Feng, J. M. Corey and J. R. Chan. "A Culture System to Study Oligodendrocyte Myelination Processes Using Engineered Nanofibers." *Nat Methods* 9, no. 9 (2012): 917-22.

Levine, J. M. and R. Reynolds. "Activation and Proliferation of Endogenous Oligodendrocyte Precursor Cells During Ethidium Bromide-Induced Demyelination." *Exp Neurol* 160, no. 2 (1999): 333-47.

Levine, J. M., F. Stincone and Y. S. Lee. "Development and Differentiation of Glial Precursor Cells in the Rat Cerebellum." *Glia* 7, no. 4 (1993): 307-21.

Lewis, K. E., J. Bates and J. S. Eisen. "Regulation of Iro3 Expression in the Zebrafish Spinal Cord." *Dev Dyn* 232, no. 1 (2005): 140-8.

Lewis, K. E. and J. S. Eisen. "From Cells to Circuits: Development of the Zebrafish Spinal Cord." *Prog Neurobiol* 69, no. 6 (2003): 419-49.

Li, H., J. P. de Faria, P. Andrew, J. Nitarska and W. D. Richardson. "Phosphorylation Regulates Olig2 Cofactor Choice and the Motor Neuron-Oligodendrocyte Fate Switch." *Neuron* 69, no. 5 (2011): 918-29.

Li, H., Y. Lu, H. K. Smith and W. D. Richardson. "Olig1 and Sox10 Interact Synergistically to Drive Myelin Basic Protein Transcription in Oligodendrocytes." *J Neurosci* 27, no. 52 (2007): 14375-82.

Li, H. and W. D. Richardson. "The Evolution of Olig Genes and Their Roles in Myelination." *Neuron Glia Biol* 4, no. 2 (2008): 129-35.

Li, Q., M. Brus-Ramer, J. H. Martin and J. W. McDonald. "Electrical Stimulation of the Medullary Pyramid Promotes Proliferation and Differentiation of Oligodendrocyte Progenitor Cells in the Corticospinal Tract of the Adult Rat." *Neurosci Lett* 479, no. 2 (2010): 128-33.

Ligon, K. L., S. Kesari, M. Kitada, T. Sun, H. A. Arnett, J. A. Alberta, D. J. Anderson, C. D. Stiles and D. H. Rowitch. "Development of Ng2 Neural Progenitor Cells Requires Olig Gene Function." *Proc Natl Acad Sci U S A* 103, no. 20 (2006): 7853-8.

Lim, D. A. and A. Alvarez-Buylla. "Interaction between Astrocytes and Adult Subventricular Zone Precursors Stimulates Neurogenesis." *Proc Natl Acad Sci U S A* 96, no. 13 (1999): 7526-31.

Lin, S. C. and D. E. Bergles. "Synaptic Signaling between Gabaergic Interneurons and Oligodendrocyte Precursor Cells in the Hippocampus." *Nat Neurosci* 7, no. 1 (2004): 24-32.

Lin, S. C., J. H. Huck, J. D. Roberts, W. B. Macklin, P. Somogyi and D. E. Bergles. "Climbing Fiber Innervation of Ng2-Expressing Glia in the Mammalian Cerebellum." *Neuron* 46, no. 5 (2005): 773-85.

Link, E., L. Edelmann, J. H. Chou, T. Binz, S. Yamasaki, U. Eisel, M. Baumert, T. C. Sudhof, H. Niemann and R. Jahn. "Tetanus Toxin Action: Inhibition of Neurotransmitter Release Linked to Synaptobrevin Proteolysis." *Biochem Biophys Res Commun* 189, no. 2 (1992): 1017-23.

Liu, J., K. Dietz, J. M. DeLoyht, X. Pedre, D. Kelkar, J. Kaur, V. Vialou, M. K. Lobo, D. M. Dietz, E. J. Nestler, J. Dupree and P. Casaccia. "Impaired Adult Myelination in the Prefrontal Cortex of Socially Isolated Mice." *Nat Neurosci* 15, no. 12 (2012): 1621-3.

Liu, X., R. Bates, D. M. Yin, C. Shen, F. Wang, N. Su, S. A. Kirov, Y. Luo, J. Z. Wang, W. C. Xiong and L. Mei. "Specific Regulation of Nrg1 Isoform Expression by Neuronal Activity." *J Neurosci* 31, no. 23 (2011): 8491-501.

Lu, Q. R., T. Sun, Z. Zhu, N. Ma, M. Garcia, C. D. Stiles and D. H. Rowitch. "Common Developmental Requirement for Olig Function Indicates a Motor Neuron/Oligodendrocyte Connection." *Cell* 109, no. 1 (2002): 75-86.

Lu, Q. R., D. Yuk, J. A. Alberta, Z. Zhu, I. Pawlitzky, J. Chan, A. P. McMahon, C. D. Stiles and D. H. Rowitch. "Sonic Hedgehog--Regulated Oligodendrocyte Lineage Genes Encoding Bhlh Proteins in the Mammalian Central Nervous System." *Neuron* 25, no. 2 (2000): 317-29.

Lubetzki, C., C. Demerens and B. Zalc. "Signaux Axonaux Et Myélinogenèse Dans Le Système Nerveux Central." *Medecine/sciences* 13, (1997): 1097-1105.

Lumsden, A. and R. Krumlauf. "Patterning the Vertebrate Neuraxis." *Science* 274, no. 5290 (1996): 1109-15.

Lundgaard, I., A. Luzhynskaya, J. H. Stockley, Z. Wang, K. A. Evans, M. Swire, K. Volbracht, H. O. Gautier, R. J. Franklin, Ffrench-Constant Charles, D. Attwell and R. T. Karadottir. "Neuregulin and Bdnf Induce a Switch to Nmda Receptor-Dependent Myelination by Oligodendrocytes." *PLoS Biol* 11, no. 12 (2013): e1001743.

Lyons, D. A., S. G. Naylor, A. Scholze and W. S. Talbot. "Kif1b Is Essential for Mrna Localization in Oligodendrocytes and Development of Myelinated Axons." *Nat Genet* 41, no. 7 (2009): 854-8.

Lyons, D. A., H. M. Pogoda, M. G. Voas, I. G. Woods, B. Diamond, R. Nix, N. Arana, J. Jacobs and W. S. Talbot. "Erbb3 and Erbb2 Are Essential for Schwann Cell Migration and Myelination in Zebrafish." *Curr Biol* 15, no. 6 (2005): 513-24.

Madison, D. L., W. H. Krueger, D. Cheng, B. D. Trapp and S. E. Pfeiffer. "Snare Complex Proteins, Including the Cognate Pair Vamp-2 and Syntaxin-4, Are Expressed in Cultured Oligodendrocytes." *J Neurochem* 72, no. 3 (1999): 988-98.

Makinodan, M., K. M. Rosen, S. Ito and G. Corfas. "A Critical Period for Social Experience-Dependent Oligodendrocyte Maturation and Myelination." *Science* 337, no. 6100 (2012): 1357-60.

Mangin, J. M., P. Li, J. Scafidi and V. Gallo. "Experience-Dependent Regulation of Ng2 Progenitors in the Developing Barrel Cortex." *Nat Neurosci* 15, no. 9 (2012): 1192-4.

Marti, E., R. Takada, D. A. Bumcrot, H. Sasaki and A. P. McMahon. "Distribution of Sonic Hedgehog Peptides in the Developing Chick and Mouse Embryo." *Development* 121, no. 8 (1995): 2537-47.

Matthews, M. A. and D. Duncan. "A Quantitative Study of Morphological Changes Accompanying the Initiation and Progress of Myelin Production in the Dorsal Funiculus of the Rat Spinal Cord." *J Comp Neurol* 142, no. 1 (1971): 1-22.

McDonald, W. I. and G. D. Ohlrich. "Quantitative Anatomical Measurements on Single Isolated Fibres from the Cat Spinal Cord." *J Anat* 110, no. Pt 2 (1971): 191-202.

McKerracher, L., S. David, D. L. Jackson, V. Kottis, R. J. Dunn and P. E. Braun. "Identification of Myelin-Associated Glycoprotein as a Major Myelin-Derived Inhibitor of Neurite Growth." *Neuron* 13, no. 4 (1994): 805-11.

McMahon, H. T., Y. A. Ushkaryov, L. Edelmann, E. Link, T. Binz, H. Niemann, R. Jahn and T. C. Sudhof. "Cellubrevin Is a Ubiquitous Tetanus-Toxin Substrate Homologous to a Putative Synaptic Vesicle Fusion Protein." *Nature* 364, no. 6435 (1993): 346-9.

Mendelson, B. "Development of Reticulospinal Neurons of the Zebrafish. Ii. Early Axonal Outgrowth and Cell Body Position." *J Comp Neurol* 251, no. 2 (1986): 172-84.

Menn, B., J. M. Garcia-Verdugo, C. Yaschine, O. Gonzalez-Perez, D. Rowitch and A. Alvarez-Buylla. "Origin of Oligodendrocytes in the Subventricular Zone of the Adult Brain." *J Neurosci* 26, no. 30 (2006): 7907-18.

Messing, A., R. R. Behringer, J. P. Hammang, R. D. Palmiter, R. L. Brinster and G. Lemke. "P0 Promoter Directs Expression of Reporter and Toxin Genes to Schwann Cells of Transgenic Mice." *Neuron* 8, no. 3 (1992): 507-20.

Meyer, M. P. and S. J. Smith. "Evidence from in Vivo Imaging That Synaptogenesis Guides the Growth and Branching of Axonal Arbors by Two Distinct Mechanisms." *J Neurosci* 26, no. 13 (2006): 3604-14.

Mi, S., R. H. Miller, X. Lee, M. L. Scott, S. Shulag-Morskaya, Z. Shao, J. Chang, G. Thill, M. Levesque, M. Zhang, C. Hession, D. Sah, B. Trapp, Z. He, V. Jung, J. M. McCoy and R. B. Pepinsky. "Lingo-1 Negatively Regulates Myelination by Oligodendrocytes." *Nat Neurosci* 8, no. 6 (2005): 745-51.

Michailov, G. V., M. W. Sereda, B. G. Brinkmann, T. M. Fischer, B. Haug, C. Birchmeier, L. Role, C. Lai, M. H. Schwab and K. A. Nave. "Axonal Neuregulin-1 Regulates Myelin Sheath Thickness." *Science* 304, no. 5671 (2004): 700-3.

Miller, D. J., T. Duka, C. D. Stimpson, S. J. Schapiro, W. B. Baze, M. J. McArthur, A. J. Fobbs, A. M. Sousa, N. Sestan, D. E. Wildman, L. Lipovich, C. W. Kuzawa, P. R. Hof and C. C. Sherwood. "Prolonged Myelination in Human Neocortical Evolution." *Proc Natl Acad Sci U S A* 109, no. 41 (2012): 16480-5.

Miller, R. H. "Regulation of Oligodendrocyte Development in the Vertebrate Cns." *Prog Neurobiol* 67, no. 6 (2002): 451-67.

Mochida, S., B. Poulain, U. Weller, E. Habermann and L. Tauc. "Light Chain of Tetanus Toxin Intracellularly Inhibits Acetylcholine Release at Neuro-Neuronal Synapses, and Its Internalization Is Mediated by Heavy Chain." *FEBS Lett* 253, no. 1-2 (1989): 47-51.

Mogha, A., A. E. Benesh, C. Patra, F. B. Engel, T. Schoneberg, I. Liebscher and K. R. Monk. "Gpr126 Functions in Schwann Cells to Control Differentiation and Myelination Via G-Protein Activation." *J Neurosci* 33, no. 46 (2013): 17976-85.

Monk, K. R., S. G. Naylor, T. D. Glenn, S. Mercurio, J. R. Perlin, C. Dominguez, C. B. Moens and W. S. Talbot. "A G Protein-Coupled Receptor Is Essential for Schwann Cells to Initiate Myelination." *Science* 325, no. 5946 (2009): 1402-5.

Monk, K. R., K. Oshima, S. Jors, S. Heller and W. S. Talbot. "Gpr126 Is Essential for Peripheral Nerve Development and Myelination in Mammals." *Development* 138, no. 13 (2011): 2673-80.

Moore, C. L., R. Kalil and W. Richards. "Development of Myelination in Optic Tract of the Cat." *J Comp Neurol* 165, no. 2 (1976): 125-36.

Mukhopadhyay, G., P. Doherty, F. S. Walsh, P. R. Crocker and M. T. Filbin. "A Novel Role for Myelin-Associated Glycoprotein as an Inhibitor of Axonal Regeneration." *Neuron* 13, no. 3 (1994): 757-67.

Muller, J., D. Reyes-Haro, T. Pivneva, C. Nolte, R. Schaette, J. Lubke and H. Kettenmann. "The Principal Neurons of the Medial Nucleus of the Trapezoid Body and Ng2(+) Glial Cells Receive Coordinated Excitatory Synaptic Input." *J Gen Physiol* 134, no. 2 (2009): 115-27.

Murray, J. A. and Blakemore, W. F. "The Relationship between Internodal Length and Fibre Diameter in the Spinal Cord of the Cat." *J. neurol. Sci.*, no. 45 (1980): 29-41.

Nave, K. A. "Neurological Mouse Mutants and the Genes of Myelin." *J Neurosci Res* 38, no. 6 (1994): 607-12.

Nave, K. A., C. Lai, F. E. Bloom and R. J. Milner. "Splice Site Selection in the Proteolipid Protein (Plp) Gene Transcript and Primary Structure of the Dm-20 Protein of Central Nervous System Myelin." *Proc Natl Acad Sci U S A* 84, no. 16 (1987): 5665-9.

Nave, K. A. and J. L. Salzer. "Axonal Regulation of Myelination by Neuregulin 1." *Curr Opin Neurobiol* 16, no. 5 (2006): 492-500.

Niell, C. M., M. P. Meyer and S. J. Smith. "In Vivo Imaging of Synapse Formation on a Growing Dendritic Arbor." *Nat Neurosci* 7, no. 3 (2004): 254-60.

Nishiyama, A., M. Watanabe, Z. Yang and J. Bu. "Identity, Distribution, and Development of Polydendrocytes: Ng2-Expressing Glial Cells." *J Neurocytol* 31, no. 6-7 (2002): 437-55.

Nixon, R. A. "The Slow Axonal Transport of Cytoskeletal Proteins." *Curr Opin Cell Biol* 10, no. 1 (1998): 87-92.

Nixon, R. A., P. A. Paskevich, R. K. Sihag and C. Y. Thayer. "Phosphorylation on Carboxyl Terminus Domains of Neurofilament Proteins in Retinal Ganglion Cell Neurons in Vivo: Influences on Regional Neurofilament Accumulation, Interneurofilament Spacing, and Axon Caliber." *J Cell Biol* 126, no. 4 (1994): 1031-46.

Novitch, B. G., A. I. Chen and T. M. Jessell. "Coordinate Regulation of Motor Neuron Subtype Identity and Pan-Neuronal Properties by the Bhlh Repressor Olig2." *Neuron* 31, no. 5 (2001): 773-89.

Nüsslein-Volhard, C. and Dahm, R. "Zebrafish: A Practical Approach." *Oxford University Press*, (2002).

O'Brien, R. J., S. Kamboj, M. D. Ehlers, K. R. Rosen, G. D. Fischbach and R. L. Huganir. "Activity-Dependent Modulation of Synaptic Ampa Receptor Accumulation." *Neuron* 21, no. 5 (1998): 1067-78.

O'Leary, D. D., A. R. Bicknese, J. A. De Carlos, C. D. Heffner, S. E. Koester, L. J. Kutka and T. Terashima. "Target Selection by Cortical Axons: Alternative Mechanisms to Establish Axonal Connections in the Developing Brain." *Cold Spring Harb Symp Quant Biol* 55, (1990): 453-68.

O'Meara, R. W., J. P. Michalski and R. Kothary. "Integrin Signaling in Oligodendrocytes and Its Importance in Cns Myelination." *J Signal Transduct* 2011, (2011): 354091.

Omlin, F. X. "Optic Disc and Optic Nerve of the Blind Cape Mole-Rat (Georychus Capensis): A Proposed Model for Naturally Occurring Reactive Gliosis." *Brain Res Bull* 44, no. 5 (1997): 627-32.

Orentas, D. M., J. E. Hayes, K. L. Dyer and R. H. Miller. "Sonic Hedgehog Signaling Is Required During the Appearance of Spinal Cord Oligodendrocyte Precursors." *Development* 126, no. 11 (1999): 2419-29.

Padfield, P. J. "A Tetanus Toxin Sensitive Protein Other Than Vamp 2 Is Required for Exocytosis in the Pancreatic Acinar Cell." *FEBS Lett* 484, no. 2 (2000): 129-32.

Pajevic, S., P. J. Basser and R. D. Fields. "Role of Myelin Plasticity in Oscillations and Synchrony of Neuronal Activity." *Neuroscience*, (2013).

Park, H. C., A. Mehta, J. S. Richardson and B. Appel. "Olig2 Is Required for Zebrafish Primary Motor Neuron and Oligodendrocyte Development." *Dev Biol* 248, no. 2 (2002): 356-68.

Park, H. C., J. Shin, R. K. Roberts and B. Appel. "An Olig2 Reporter Gene Marks Oligodendrocyte Precursors in the Postembryonic Spinal Cord of Zebrafish." *Dev Dyn* 236, no. 12 (2007): 3402-7.

Parrish, J. Z., P. Xu, C. C. Kim, L. Y. Jan and Y. N. Jan. "The Microrna Bantam Functions in Epithelial Cells to Regulate Scaling Growth of Dendrite Arbors in Drosophila Sensory Neurons." *Neuron* 63, no. 6 (2009): 788-802.

Pedraza, L., J. K. Huang and D. Colman. "Disposition of Axonal Caspr with Respect to Glial Cell Membranes: Implications for the Process of Myelination." *J Neurosci Res* 87, no. 15 (2009): 3480-91.

Peles, E. and J. L. Salzer. "Molecular Domains of Myelinated Axons." *Curr Opin Neurobiol* 10, no. 5 (2000): 558-65.

Pellizzari, R., O. Rossetto, G. Schiavo and C. Montecucco. "Tetanus and Botulinum Neurotoxins: Mechanism of Action and Therapeutic Uses." *Philos Trans R Soc Lond B Biol Sci* 354, no. 1381 (1999): 259-68.

Perge, J. A., J. E. Niven, E. Mugnaini, V. Balasubramanian and P. Sterling. "Why Do Axons Differ in Caliber?" *J Neurosci* 32, no. 2 (2012): 626-38.

Perkins, C. S., A. J. Aguayo and G. M. Bray. "Schwann Cell Multiplication in Trembler Mice." *Neuropathol Appl Neurobiol* 7, no. 2 (1981): 115-26.

Perry, V. H., M. C. Brown and E. R. Lunn. "Very Slow Retrograde and Wallerian Degeneration in the Cns of C57bl/Ola Mice." *Eur J Neurosci* 3, no. 1 (1991): 102-5.

Peters, A. Palay, S. and Webster H. de F. "The Fine Structure of the Nervous System: The Neuron and the Supporting Cells." *Oxford Univ. Press.*, (1991).

Pfeiffer, S.E., Warrington, A.E., and Bansal, R. "The Oligodendrocyte and Its Many Cellular Processes." *Trends in cell biology*, no. 3 (1993): 191-197.

Pogoda, H. M., N. Sternheim, D. A. Lyons, B. Diamond, T. A. Hawkins, I. G. Woods, D. H. Bhatt, C. Franzini-Armstrong, C. Dominguez, N. Arana, J. Jacobs, R. Nix, J. R. Fetcho and W. S. Talbot. "A Genetic Screen Identifies Genes Essential for Development of Myelinated Axons in Zebrafish." *Dev Biol* 298, no. 1 (2006): 118-31.

Poliak, S. and E. Peles. "The Local Differentiation of Myelinated Axons at Nodes of Ranvier." *Nat Rev Neurosci* 4, no. 12 (2003): 968-80.

Pollard, J. D. and J. G. McLeod. "Nerve Grafts in the Trembler Mouse. An Electrophysiological and Histological Study." *J Neurol Sci* 46, no. 3 (1980): 373-83.

Poncet, C., C. Soula, F. Trousse, P. Kan, E. Hirsinger, O. Pourquie, A. M. Duprat and P. Cochard. "Induction of Oligodendrocyte Progenitors in the Trunk Neural Tube by Ventralizing Signals: Effects of Notochord and Floor Plate Grafts, and of Sonic Hedgehog." *Mech Dev* 60, no. 1 (1996): 13-32.

Popko, B., C. Puckett, E. Lai, H. D. Shine, C. Readhead, N. Takahashi, S. W. Hunt, 3rd, R. L. Sidman and L. Hood. "Myelin Deficient Mice: Expression of Myelin Basic Protein and Generation of Mice with Varying Levels of Myelin." *Cell* 48, no. 4 (1987): 713-21.

Portugues, R., K. E. Severi, C. Wyart and M. B. Ahrens. "Optogenetics in a Transparent Animal: Circuit Function in the Larval Zebrafish." *Curr Opin Neurobiol* 23, no. 1 (2013): 119-26.

Proux-Gillardeaux, V., R. Rudge and T. Galli. "The Tetanus Neurotoxin-Sensitive and Insensitive Routes to and from the Plasma Membrane: Fast and Slow Pathways?" *Traffic* 6, no. 5 (2005): 366-73.

Puelles, L. and J. L. Rubenstein. "Forebrain Gene Expression Domains and the Evolving Prosomeric Model." *Trends Neurosci* 26, no. 9 (2003): 469-76.

Qi, Y., J. Cai, Y. Wu, R. Wu, J. Lee, H. Fu, M. Rao, L. Sussel, J. Rubenstein and M. Qiu. "Control of Oligodendrocyte Differentiation by the Nkx2.2 Homeodomain Transcription Factor." *Development* 128, no. 14 (2001): 2723-33.

Quarles, R. H. "Myelin-Associated Glycoprotein (Mag): Past, Present and Beyond." *J Neurochem* 100, no. 6 (2007): 1431-48.

Raff, M. C., E. R. Abney and J. Fok-Seang. "Reconstitution of a Developmental Clock in Vitro: A Critical Role for Astrocytes in the Timing of Oligodendrocyte Differentiation." *Cell* 42, no. 1 (1985): 61-9.

Ranvier, L. " Leçons Sur L'histologie Du Système Nerveux." *Paris, Savy*, (1878b).

Rao, M. V., J. Campbell, A. Yuan, A. Kumar, T. Gotow, Y. Uchiyama and R. A. Nixon. "The Neurofilament Middle Molecular Mass Subunit Carboxyl-Terminal Tail Domains Is Essential for the Radial Growth and Cytoskeletal Architecture of Axons but Not for Regulating Neurofilament Transport Rate." *J Cell Biol* 163, no. 5 (2003): 1021-31.

Raper, J. and C. Mason. "Cellular Strategies of Axonal Pathfinding." *Cold Spring Harb Perspect Biol* 2, no. 9 (2010): a001933.

Rasband, M. N., J. S. Trimmer, E. Peles, S. R. Levinson and P. Shrager. "K+ Channel Distribution and Clustering in Developing and Hypomyelinated Axons of the Optic Nerve." *J Neurocytol* 28, no. 4-5 (1999): 319-31.

Readhead, C. and L. Hood. "The Dysmyelinating Mouse Mutations Shiverer (Shi) and Myelin Deficient (Shimld)." *Behav Genet* 20, no. 2 (1990): 213-34.

Readhead, C., B. Popko, N. Takahashi, H. D. Shine, R. A. Saavedra, R. L. Sidman and L. Hood. "Expression of a Myelin Basic Protein Gene in Transgenic Shiverer Mice: Correction of the Dysmyelinating Phenotype." *Cell* 48, no. 4 (1987): 703-12.

Remahl, S. and C. Hildebrand. "Changing Relation between Onset of Myelination and Axon Diameter Range in Developing Feline White Matter." *J Neurol Sci* 54, no. 1 (1982): 33-45.

Remahl, S. and C. Hildebrand. "Myelinated Non-Axonal Neuronal Elements in the Feline Olfactory Bulb Lack Sites with a Nodal Structural Differentiation." *Brain Res* 325, no. 1-2 (1985): 1-11.

Remahl, S. and C. Hildebrand. "Relations between Axons and Oligodendroglial Cells During Initial Myelination. Ii. The Individual Axon." *J Neurocytol* 19, no. 6 (1990): 883-98.

Richardson, W. D., N. Kessaris and N. Pringle. "Oligodendrocyte Wars." *Nat Rev Neurosci* 7, no. 1 (2006): 11-8.

Richardson, W. D., N. Pringle, M. J. Mosley, B. Westermark and M. Dubois-Dalcq. "A Role for Platelet-Derived Growth Factor in Normal Gliogenesis in the Central Nervous System." *Cell* 53, no. 2 (1988): 309-19.

Rio Hortega, D.P. "Histogenesis Y Evolucion Normal; Exodo Y Distribucion Regional De La Microglia." *Memor Real Soc Esp Hist Nat* 11, (1921): 213–268.

Rio Hortega, D.P. "Tercera Aportacion Al Conocimiento Morfologico E Interpretacion Funcional De La Oligodendroglia." *Memor Real Soc Esp Hist Nat*, no. 14 (1928): 5–122.

Ritchie, J. M. "On the Relation between Fibre Diameter and Conduction Velocity in Myelinated Nerve Fibres." *Proc R Soc Lond B Biol Sci* 217, no. 1206 (1982): 29-35.

Ritchie, J.M. "Physiological Basis of Conduction in Myelinated Nerve Fibres." *Myelin, Plenum press*, (1984): 117-146.

Rivers, L. E., K. M. Young, M. Rizzi, F. Jamen, K. Psachoulia, A. Wade, N. Kessaris and W. D. Richardson. "Pdgfra/Ng2 Glia Generate Myelinating Oligodendrocytes and Piriform Projection Neurons in Adult Mice." *Nat Neurosci* 11, no. 12 (2008): 1392-401.

Rosenberg, S. S., E. E. Kelland, E. Tokar, A. R. De la Torre and J. R. Chan. "The Geometric and Spatial Constraints of the Microenvironment Induce Oligodendrocyte Differentiation." *Proc Natl Acad Sci U S A* 105, no. 38 (2008): 14662-7.

Rosenberg, S. S., B. L. Powell and J. R. Chan. "Receiving Mixed Signals: Uncoupling Oligodendrocyte Differentiation and Myelination." *Cell Mol Life Sci* 64, no. 23 (2007): 3059-68.

Rosenbluth, J. "Peripheral Myelin in the Mouse Mutant Shiverer." *J Comp Neurol* 193, no. 3 (1980): 729-39.

Rowitch, D. H. "Glial Specification in the Vertebrate Neural Tube." *Nat Rev Neurosci* 5, no. 5 (2004): 409-19.

Rowitch, D. H. and A. R. Kriegstein. "Developmental Genetics of Vertebrate Glial-Cell Specification." *Nature* 468, no. 7321 (2010): 214-22.

Rushton, W. A. "A Theory of the Effects of Fibre Size in Medullated Nerve." *J Physiol* 115, no. 1 (1951): 101-22.

Sakai, T., A. Mikami, M. Tomonaga, M. Matsui, J. Suzuki, Y. Hamada, M. Tanaka, T. Miyabe-Nishiwaki, H. Makishima, M. Nakatsukasa and T. Matsuzawa. "Differential Prefrontal White Matter Development in Chimpanzees and Humans." *Curr Biol* 21, no. 16 (2011): 1397-402.

Sakamoto, Y., K. Kitamura, K. Yoshimura, T. Nishijima and K. Uyemura. "Complete Amino Acid Sequence of Po Protein in Bovine Peripheral Nerve Myelin." *J Biol Chem* 262, no. 9 (1987): 4208-14.

Sakurai, T., M. Lustig, M. Nativ, J. J. Hemperly, J. Schlessinger, E. Peles and M. Grumet. "Induction of Neurite Outgrowth through Contactin and Nr-Cam by Extracellular Regions of Glial Receptor Tyrosine Phosphatase Beta." *J Cell Biol* 136, no. 4 (1997): 907-18.

Salzer, J. L. "Clustering Sodium Channels at the Node of Ranvier: Close Encounters of the Axon-Glia Kind." *Neuron* 18, no. 6 (1997): 843-6.

Salzer, J. L. "Polarized Domains of Myelinated Axons." *Neuron* 40, no. 2 (2003): 297-318.

Samorajski, T. and R. L. Friede. "A Quantitative Electron Microscopic Study of Myelination in the Pyramidal Tract of Rat." *J Comp Neurol* 134, no. 3 (1968): 323-38.

Samorajski, T. and R. L. Friede. "Size-Dependent Distribution of Axoplasm, Schwann Cell Cytoplasm, and Mitochondri in the Peripheral Nerve Fibers of Mouse." *Anat Rec* 161, no. 3 (1968): 281-92.

Sanchez, I., L. Hassinger, P. A. Paskevich, H. D. Shine and R. A. Nixon. "Oligodendroglia Regulate the Regional Expansion of Axon Caliber and Local Accumulation of Neurofilaments During Development Independently of Myelin Formation." *J Neurosci* 16, no. 16 (1996): 5095-105.

Sanchez, I., L. Hassinger, R. K. Sihag, D. W. Cleveland, P. Mohan and R. A. Nixon. "Local Control of Neurofilament Accumulation During Radial Growth of Myelinating Axons in Vivo. Selective Role of Site-Specific Phosphorylation." *J Cell Biol* 151, no. 5 (2000): 1013-24.

Schebesta, M. and F. C. Serluca. "Olig1 Expression Identifies Developing Oligodendrocytes in Zebrafish and Requires Hedgehog and Notch Signaling." *Dev Dyn* 238, no. 4 (2009): 887-98.

Scherer, S. S., D. Y. Wang, R. Kuhn, G. Lemke, L. Wrabetz and J. Kamholz. "Axons Regulate Schwann Cell Expression of the Pou Transcription Factor Scip." *J Neurosci* 14, no. 4 (1994): 1930-42.

Schiavo, G., F. Benfenati, B. Poulain, O. Rossetto, P. Polverino de Laureto, B. R. DasGupta and C. Montecucco. "Tetanus and Botulinum-B Neurotoxins Block Neurotransmitter Release by Proteolytic Cleavage of Synaptobrevin." *Nature* 359, no. 6398 (1992): 832-5.

Schiavo, G., M. Matteoli and C. Montecucco. "Neurotoxins Affecting Neuroexocytosis." *Physiol Rev* 80, no. 2 (2000): 717-66.

Schmithorst, V. J., M. Wilke, B. J. Dardzinski and S. K. Holland. "Cognitive Functions Correlate with White Matter Architecture in a Normal Pediatric Population: A Diffusion Tensor Mri Study." *Hum Brain Mapp* 26, no. 2 (2005): 139-47.

Schnell, L. and M. E. Schwab. "Axonal Regeneration in the Rat Spinal Cord Produced by an Antibody against Myelin-Associated Neurite Growth Inhibitors." *Nature* 343, no. 6255 (1990): 269-72.

Schoonheim, P. J., A. B. Arrenberg, F. Del Bene and H. Baier. "Optogenetic Localization and Genetic Perturbation of Saccade-Generating Neurons in Zebrafish." *J Neurosci* 30, no. 20 (2010): 7111-20.

Schreyer, D. J. and E. G. Jones. "Growth and Target Finding by Axons of the Corticospinal Tract in Prenatal and Postnatal Rats." *Neuroscience* 7, no. 8 (1982): 1837-53.

Schwab, M. E. and L. Schnell. "Region-Specific Appearance of Myelin Constituents in the Developing Rat Spinal Cord." *J Neurocytol* 18, no. 2 (1989): 161-9.

Schweitzer, J., T. Becker, M. Schachner, K. A. Nave and H. Werner. "Evolution of Myelin Proteolipid Proteins: Gene Duplication in Teleosts and Expression Pattern Divergence." *Mol Cell Neurosci* 31, no. 1 (2006): 161-77.

Scott, E. K., L. Mason, A. B. Arrenberg, L. Ziv, N. J. Gosse, T. Xiao, N. C. Chi, K. Asakawa, K. Kawakami and H. Baier. "Targeting Neural Circuitry in Zebrafish Using Gal4 Enhancer Trapping." *Nat Methods* 4, no. 4 (2007): 323-6.

Sherman, D. L. and P. J. Brophy. "Mechanisms of Axon Ensheathment and Myelin Growth." *Nat Rev Neurosci* 6, no. 9 (2005): 683-90.

Sherman, D. L., M. Krols, L. M. Wu, M. Grove, K. A. Nave, Y. G. Gangloff and P. J. Brophy. "Arrest of Myelination and Reduced Axon Growth When Schwann Cells Lack Mtor." *J Neurosci* 32, no. 5 (2012): 1817-25.

Shrager, P. and S. D. Novakovic. "Control of Myelination, Axonal Growth, and Synapse Formation in Spinal Cord Explants by Ion Channels and Electrical Activity." *Brain Res Dev Brain Res* 88, no. 1 (1995): 68-78.

Simons, M. and D. A. Lyons. "Axonal Selection and Myelin Sheath Generation in the Central Nervous System." *Curr Opin Cell Biol* 25, no. 4 (2013): 512-9.

Simons, M. and J. Trotter. "Wrapping It Up: The Cell Biology of Myelination." *Curr Opin Neurobiol* 17, no. 5 (2007): 533-40.

Sloane, J. A. and T. K. Vartanian. "Myosin Va Controls Oligodendrocyte Morphogenesis and Myelination." *J Neurosci* 27, no. 42 (2007): 11366-75.

Snaidero, N., W. Mobius, T. Czopka, L. H. Hekking, C. Mathisen, D. Verkleij, S. Goebbels, J. Edgar, D. Merkler, D. A. Lyons, K. A. Nave and M. Simons. "Myelin Membrane Wrapping of Cns Axons by Pi(3,4,5)P3-Dependent Polarized Growth at the Inner Tongue." *Cell* 156, no. 1-2 (2014): 277-90.

Snaidero, N. and M. Simons. "Myelination at a Glance." *J Cell Sci* 127, no. Pt 14 (2014): 2999-3004.

Snider, J., A. Pillai and C. F. Stevens. "A Universal Property of Axonal and Dendritic Arbors." *Neuron* 66, no. 1 (2010): 45-56.

Sobottka, B., Ziegler, U., Kaech, A., Becher, B., and Goebels, N. "Cns Live Imaging Reveals a New Mechanism of Myelination: The Liquid Croissant Model." *Glia*, no. 59 (2011): 1841-1849.

Stankoff, B., M. S. Aigrot, F. Noel, A. Wattilliaux, B. Zalc and C. Lubetzki. "Ciliary Neurotrophic Factor (Cntf) Enhances Myelin Formation: A Novel Role for Cntf and Cntf-Related Molecules." *J Neurosci* 22, no. 21 (2002): 9221-7.

Stevens, B. "Response of Schwann Cells to Action Potentials in Development." *Science* 287, no. 5461 (2000): 2267-2271.

Stevens, B. and R. D. Fields. "Response of Schwann Cells to Action Potentials in Development." *Science* 287, no. 5461 (2000): 2267-71.

Stevens, B., T. Ishibashi, J. F. Chen and R. D. Fields. "Adenosine: An Activity-Dependent Axonal Signal Regulating Map Kinase and Proliferation in Developing Schwann Cells." *Neuron Glia Biol* 1, no. 1 (2004): 23-34.

Stevens, B., S. Porta, L. L. Haak, V. Gallo and R. D. Fields. "Adenosine: A Neuron-Glial Transmitter Promoting Myelination in the Cns in Response to Action Potentials." *Neuron* 36, no. 5 (2002): 855-68.

Stevens, B., S. Tanner and R. D. Fields. "Control of Myelination by Specific Patterns of Neural Impulses." *J Neurosci* 18, no. 22 (1998): 9303-11.

Stevens, C. F. "Neurotransmitter Release at Central Synapses." *Neuron* 40, no. 2 (2003): 381-8.

Stolt, C. C., S. Rehberg, M. Ader, P. Lommes, D. Riethmacher, M. Schachner, U. Bartsch and M. Wegner. "Terminal Differentiation of Myelin-Forming Oligodendrocytes Depends on the Transcription Factor Sox10." *Genes Dev* 16, no. 2 (2002): 165-70.

Sturrock, R. R. "Gliogenesis in the Prenatal Rabbit Spinal Cord." *J Anat* 134, no. Pt 4 (1982): 771-93.

Sugihara, I., E. J. Lang and R. Llinas. "Uniform Olivocerebellar Conduction Time Underlies Purkinje Cell Complex Spike Synchronicity in the Rat Cerebellum." *J Physiol* 470, (1993): 243-71.

Sun, Y., D. H. Meijer, J. A. Alberta, S. Mehta, M. F. Kane, A. C. Tien, H. Fu, M. A. Petryniak, G. B. Potter, Z. Liu, J. F. Powers, I. S. Runquist, D. H. Rowitch and C. D. Stiles. "Phosphorylation State of Olig2 Regulates Proliferation of Neural Progenitors." *Neuron* 69, no. 5 (2011): 906-17.

Susuki, K., K. J. Chang, D. R. Zollinger, Y. Liu, Y. Ogawa, Y. Eshed-Eisenbach, M. T. Dours-Zimmermann, J. A. Oses-Prieto, A. L. Burlingame, C. I. Seidenbecher, D. R. Zimmermann, T. Oohashi, E. Peles and M. N. Rasband. "Three Mechanisms Assemble Central Nervous System Nodes of Ranvier." *Neuron* 78, no. 3 (2013): 469-82.

Suter, U., A. A. Welcher, T. Ozcelik, G. J. Snipes, B. Kosaras, U. Francke, S. Billings-Gagliardi, R. L. Sidman and E. M. Shooter. "Trembler Mouse Carries a Point Mutation in a Myelin Gene." *Nature* 356, no. 6366 (1992): 241-4.

Takada, N., S. Kucenas and B. Appel. "Sox10 Is Necessary for Oligodendrocyte Survival Following Axon Wrapping." *Glia* 58, no. 8 (2010): 996-1006.

Tallini, Y. N., M. Ohkura, B. R. Choi, G. Ji, K. Imoto, R. Doran, J. Lee, P. Plan, J. Wilson, H. B. Xin, A. Sanbe, J. Gulick, J. Mathai, J. Robbins, G. Salama, J. Nakai and M. I. Kotlikoff. "Imaging Cellular Signals in the Heart in Vivo: Cardiac Expression of the High-Signal Ca2+ Indicator Gcamp2." *Proc Natl Acad Sci U S A* 103, no. 12 (2006): 4753-8.

Tasaki, I. "Physiology and Electrochemistry of Nerve Fibers." *Academic Press: New York,* (1982).

Tauber, H., T. V. Waehneldt and V. Neuhoff. "Myelination in Rabbit Optic Nerves Is Accelerated by Artificial Eye Opening." *Neurosci Lett* 16, no. 3 (1980): 235-8.

Taveggia, C., P. Thaker, A. Petrylak, G. L. Caporaso, A. Toews, D. L. Falls, S. Einheber and J. L. Salzer. "Type Iii Neuregulin-1 Promotes Oligodendrocyte Myelination." *Glia* 56, no. 3 (2008): 284-93.

Taveggia, C., G. Zanazzi, A. Petrylak, H. Yano, J. Rosenbluth, S. Einheber, X. Xu, R. M. Esper, J. A. Loeb, P. Shrager, M. V. Chao, D. L. Falls, L. Role and J. L. Salzer. "Neuregulin-1 Type Iii Determines the Ensheathment Fate of Axons." *Neuron* 47, no. 5 (2005): 681-94.

Thomas, J. L., N. Spassky, E. M. Perez Villegas, C. Olivier, I. Cobos, C. Goujet-Zalc, S. Martinez and B. Zalc. "Spatiotemporal Development of Oligodendrocytes in the Embryonic Brain." *J Neurosci Res* 59, no. 4 (2000): 471-6.

Tian, L., S. A. Hires, T. Mao, D. Huber, M. E. Chiappe, S. H. Chalasani, L. Petreanu, J. Akerboom, S. A. McKinney, E. R. Schreiter, C. I. Bargmann, V. Jayaraman, K. Svoboda and L. L. Looger. "Imaging Neural Activity in Worms, Flies and Mice with Improved Gcamp Calcium Indicators." *Nat Methods* 6, no. 12 (2009): 875-81.

Tomasi, S., R. Caminiti and G. M. Innocenti. "Areal Differences in Diameter and Length of Corticofugal Projections." *Cereb Cortex* 22, no. 6 (2012): 1463-72.

Turnley, A. M. and P. F. Bartlett. "Mag and Mog Enhance Neurite Outgrowth of Embryonic Mouse Spinal Cord Neurons." *Neuroreport* 9, no. 9 (1998): 1987-90.

Turrigiano, G. G. "The Self-Tuning Neuron: Synaptic Scaling of Excitatory Synapses." *Cell* 135, no. 3 (2008): 422-35.

Umemori, H., S. Sato, T. Yagi, S. Aizawa and T. Yamamoto. "Initial Events of Myelination Involve Fyn Tyrosine Kinase Signalling." *Nature* 367, no. 6463 (1994): 572-6.

Vabnick, I., J. S. Trimmer, T. L. Schwarz, S. R. Levinson, D. Risal and P. Shrager. "Dynamic Potassium Channel Distributions During Axonal Development Prevent Aberrant Firing Patterns." *J Neurosci* 19, no. 2 (1999): 747-58.

Virchow, R. "Ueber Das Ausgebreitete Vorkommen Einer Dem Nervenmark Analogen Substanz in Den Tierischen Geweben." *Virchows Arch. Pathol. Anat.* 6, (1854): 562.

Voyvodic, J. T. "Target Size Regulates Calibre and Myelination of Sympathetic Axons." *Nature* 342, no. 6248 (1989): 430-3.

Waehneldt, T. V. "Phylogeny of Myelin Proteins." *Ann N Y Acad Sci* 605, (1990): 15-28.

Wake, H., P. R. Lee and R. D. Fields. "Control of Local Protein Synthesis and Initial Events in Myelination by Action Potentials." *Science* 333, no. 6049 (2011): 1647-51.

Wang, S., A. D. Sdrulla, G. diSibio, G. Bush, D. Nofziger, C. Hicks, G. Weinmaster and B. A. Barres. "Notch Receptor Activation Inhibits Oligodendrocyte Differentiation." *Neuron* 21, no. 1 (1998): 63-75.

Warf, B. C., J. Fok-Seang and R. H. Miller. "Evidence for the Ventral Origin of Oligodendrocyte Precursors in the Rat Spinal Cord." *J Neurosci* 11, no. 8 (1991): 2477-88.

Watkins, T. A., B. Emery, S. Mulinyawe and B. A. Barres. "Distinct Stages of Myelination Regulated by Gamma-Secretase and Astrocytes in a Rapidly Myelinating Cns Coculture System." *Neuron* 60, no. 4 (2008): 555-69.

Waxman, S. G. "Determinants of Conduction Velocity in Myelinated Nerve Fibers." *Muscle Nerve* 3, no. 2 (1980): 141-50.

Waxman, S. G. "Axon-Glia Interactions: Building a Smart Nerve Fiber." *Curr Biol* 7, no. 7 (1997): R406-10.

Waxman, S. G. and M. V. Bennett. "Relative Conduction Velocities of Small Myelinated and Non-Myelinated Fibres in the Central Nervous System." *Nat New Biol* 238, no. 85 (1972): 217-9.

Welch, M. J., J. R. Purkiss and K. A. Foster. "Sensitivity of Embryonic Rat Dorsal Root Ganglia Neurons to Clostridium Botulinum Neurotoxins." *Toxicon* 38, no. 2 (2000): 245-58.

Werner, H. B. "Do We Have to Reconsider the Evolutionary Emergence of Myelin?" *Front Cell Neurosci* 7, (2013): 217.

West, A. E. and M. E. Greenberg. "Neuronal Activity-Regulated Gene Transcription in Synapse Development and Cognitive Function." *Cold Spring Harb Perspect Biol* 3, no. 6 (2011).

Westerfield, M. "The Zebrafish Book: A Guide for the Laboratory Use of Zebrafish (Danio Rerio)." (2007).

White, R. and E. M. Kramer-Albers. "Axon-Glia Interaction and Membrane Traffic in Myelin Formation." *Front Cell Neurosci* 7, (2014): 284.

Wilkins, A., S. Chandran and A. Compston. "A Role for Oligodendrocyte-Derived Igf-1 in Trophic Support of Cortical Neurons." *Glia* 36, no. 1 (2001): 48-57.

Wilkins, A., H. Majed, R. Layfield, A. Compston and S. Chandran. "Oligodendrocytes Promote Neuronal Survival and Axonal Length by Distinct Intracellular Mechanisms: A Novel Role for Oligodendrocyte-Derived Glial Cell Line-Derived Neurotrophic Factor." *J Neurosci* 23, no. 12 (2003): 4967-74.

Willard, M. and C. Simon. "Modulations of Neurofilament Axonal Transport During the Development of Rabbit Retinal Ganglion Cells." *Cell* 35, no. 2 Pt 1 (1983): 551-9.

Williams, J. A., A. Barrios, C. Gatchalian, L. Rubin, S. W. Wilson and N. Holder. "Programmed Cell Death in Zebrafish Rohon Beard Neurons Is Influenced by Trkc1/Nt-3 Signaling." *Dev Biol* 226, no. 2 (2000): 220-30.

Windebank, A. J., P. Wood, R. P. Bunge and P. J. Dyck. "Myelination Determines the Caliber of Dorsal Root Ganglion Neurons in Culture." *J Neurosci* 5, no. 6 (1985): 1563-9.

Winterstein, C., J. Trotter and E. M. Kramer-Albers. "Distinct Endocytic Recycling of Myelin Proteins Promotes Oligodendroglial Membrane Remodeling." *J Cell Sci* 121, no. Pt 6 (2008): 834-42.

Woodruff, R. H., M. Fruttiger, W. D. Richardson and R. J. Franklin. "Platelet-Derived Growth Factor Regulates Oligodendrocyte Progenitor Numbers in Adult Cns and Their Response Following Cns Demyelination." *Mol Cell Neurosci* 25, no. 2 (2004): 252-62.

Woods, I. G., D. A. Lyons, M. G. Voas, H. M. Pogoda and W. S. Talbot. "Nsf Is Essential for Organization of Myelinated Axons in Zebrafish." *Curr Biol* 16, no. 7 (2006): 636-48.

Wyart, C., F. Del Bene, E. Warp, E. K. Scott, D. Trauner, H. Baier and E. Y. Isacoff. "Optogenetic Dissection of a Behavioural Module in the Vertebrate Spinal Cord." *Nature* 461, no. 7262 (2009): 407-10.

Xiao, J., A. W. Wong, M. M. Willingham, M. van den Buuse, T. J. Kilpatrick and S. S. Murray. "Brain-Derived Neurotrophic Factor Promotes Central Nervous System Myelination Via a Direct Effect Upon Oligodendrocytes." *Neurosignals* 18, no. 3 (2010): 186-202.

Xin, M., T. Yue, Z. Ma, F. F. Wu, A. Gow and Q. R. Lu. "Myelinogenesis and Axonal Recognition by Oligodendrocytes in Brain Are Uncoupled in Olig1-Null Mice." *J Neurosci* 25, no. 6 (2005): 1354-65.

Yakovlev, P.I. and Lecours, A.R. "The Myelinogenic Cycles of Regional Maturation of the Brain." *Regional Development of the Brain in Early Life*, (1966): 3-70.

Yamasaki, H., G. S. Bennett, C. Itakura and M. Mizutani. "Defective Expression of Neurofilament Protein Subunits in Hereditary Hypotrophic Axonopathy of Quail." *Lab Invest* 66, no. 6 (1992): 734-43.

Yin, X., T. O. Crawford, J. W. Griffin, Ph Tu, V. M. Lee, C. Li, J. Roder and B. D. Trapp. "Myelin-Associated Glycoprotein Is a Myelin Signal That Modulates the Caliber of Myelinated Axons." *J Neurosci* 18, no. 6 (1998): 1953-62.

Yiu, G. and Z. He. "Glial Inhibition of Cns Axon Regeneration." *Nat Rev Neurosci* 7, no. 8 (2006): 617-27.

Yoshida, M. and D. R. Colman. "Parallel Evolution and Coexpression of the Proteolipid Proteins and Protein Zero in Vertebrate Myelin." *Neuron* 16, no. 6 (1996): 1115-26.

Young, K. M., K. Psachoulia, R. B. Tripathi, S. J. Dunn, L. Cossell, D. Attwell, K. Tohyama and W. D. Richardson. "Oligodendrocyte Dynamics in the Healthy Adult Cns: Evidence for Myelin Remodeling." *Neuron* 77, no. 5 (2013): 873-85.

Yuan, X., A. M. Eisen, C. J. McBain and V. Gallo. "A Role for Glutamate and Its Receptors in the Regulation of Oligodendrocyte Development in Cerebellar Tissue Slices." *Development* 125, no. 15 (1998): 2901-14.

Zalc, B. and D. R. Colman. "Origins of Vertebrate Success." *Science* 288, no. 5464 (2000): 271-2.

Zalc, B. and R. D. Fields. "Do Action Potentials Regulate Myelination?" *Neuroscientist* 6, no. 1 (2000): 5-13.

Zannino, D. A. and B. Appel. "Olig2+ Precursors Produce Abducens Motor Neurons and Oligodendrocytes in the Zebrafish Hindbrain." *J Neurosci* 29, no. 8 (2009): 2322-33.

Zhang, X., J. Q. Davis, S. Carpenter and V. Bennett. "Structural Requirements for Association of Neurofascin with Ankyrin." *J Biol Chem* 273, no. 46 (1998): 30785-94.

Zhang, Y., Y. Bekku, Y. Dzhashiashvili, S. Armenti, X. Meng, Y. Sasaki, J. Milbrandt and J. L. Salzer. "Assembly and Maintenance of Nodes of Ranvier Rely on Distinct Sources of Proteins and Targeting Mechanisms." *Neuron* 73, no. 1 (2012): 92-107.

Zhou, Q. and D. J. Anderson. "The Bhlh Transcription Factors Olig2 and Olig1 Couple Neuronal and Glial Subtype Specification." *Cell* 109, no. 1 (2002): 61-73.

Zhou, Q., G. Choi and D. J. Anderson. "The Bhlh Transcription Factor Olig2 Promotes Oligodendrocyte Differentiation in Collaboration with Nkx2.2." *Neuron* 31, no. 5 (2001): 791-807.

Zhou, Q., S. Wang and D. J. Anderson. "Identification of a Novel Family of Oligodendrocyte Lineage-Specific Basic Helix-Loop-Helix Transcription Factors." *Neuron* 25, no. 2 (2000): 331-43.

Zhu, Q., S. Couillard-Despres and J. P. Julien. "Delayed Maturation of Regenerating Myelinated Axons in Mice Lacking Neurofilaments." *Exp Neurol* 148, no. 1 (1997): 299-316.

Zhu, X., D. E. Bergles and A. Nishiyama. "Ng2 Cells Generate Both Oligodendrocytes and Gray Matter Astrocytes." *Development* 135, no. 1 (2008): 145-57.

Ziskin, J. L., A. Nishiyama, M. Rubio, M. Fukaya and D. E. Bergles. "Vesicular Release of Glutamate from Unmyelinated Axons in White Matter." *Nat Neurosci* 10, no. 3 (2007): 321-30.

Zonta, B., S. Tait, S. Melrose, H. Anderson, S. Harroch, J. Higginson, D. L. Sherman and P. J. Brophy. "Glial and Neuronal Isoforms of Neurofascin Have Distinct Roles in the Assembly of Nodes of Ranvier in the Central Nervous System." *J Cell Biol* 181, no. 7 (2008): 1169-77.

Zuchero, J. B. and B. A. Barres. "Intrinsic and Extrinsic Control of Oligodendrocyte Development." *Curr Opin Neurobiol* 23, no. 6 (2013): 914-20.